FOR REFERENCE ONLY

28 APR 2005

LCN = 10379088

41 0657318 3



ProQuest Number: 10182975

All rights reserved

INFORMATION TO ALL USERS
The quality of this reproduction is dependent upon the quality of the copy submitted.

In the unlikely event that the author did not send a complete manuscript
and there are missing pages, these will be noted. Also, if material had to be removed,
a note will indicate the deletion.



ProQuest 10182975

Published by ProQuest LLC (2017). Copyright of the Dissertation is held by the Author.

All rights reserved.
This work is protected against unauthorized copying under Title 17, United States Code
Microform Edition © ProQuest LLC.

ProQuest LLC.
789 East Eisenhower Parkway
P.O. Box 1346
Ann Arbor, MI 48106 – 1346

Tissue transglutaminase:

a novel cell adhesion protein

Dilek Telci

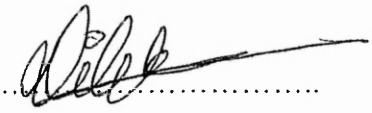
A thesis submitted in partial fulfilment of the requirements of the Nottingham Trent University for the degree of Doctor of Philosophy

September 2004

Declaration

This work has not been accepted in substance for any other degree, and is not concurrently being submitted in candidature for any other degree.

This is to certify that the work was carried out by the candidate herself. Due acknowledgement has been made of all assistance received.

Signed 

(Candidate)

Signed 

(Director of Studies)

Abstract

When purified tissue transglutaminase (tTG) is immobilised on plasma fibronectin it forms an extracellular complex (FN-tTG), which partially restores attachment and spreading of human osteoblast cells and mouse Swiss 3T3 fibroblasts when the integrin mediated direct binding to FN is impaired using Arg-Gly-Asp (RGD) containing peptides. However, the molecular mechanism(s) and the physiological importance of this RGD-independent cell adhesion process, are not fully understood. The role of the FN-bound tTG complex in mediating the RGD-independent cell adhesion was investigated by characterisation of the FN-tTG matrix and the intracellular signals that lead to changes in protein phosphorylation during this process. The FN-tTG matrix compensated for the RGD inhibition of cell adhesion in different cell types, which was independent of the endogenous ECM protein synthesis. A physiological matrix composed of cell-assembled FN with increased levels of bound cell-secreted tTG supported RGD-independent cell adhesion of Swiss 3T3 fibroblasts. tTG bound to tissue culture plastic or N-terminal FN fragments, which contain a putative high affinity binding site for tTG, was not sufficient to sustain the RGD-independent cell adhesion, suggesting a requirement for the association of tTG with the entire FN molecule. The compensatory effect of the FN-tTG complex for the RGD-inhibition of cell adhesion did not require transamidating activity of tTG, or the binding of tTG to $\alpha_4\beta_1$ integrins, but was dependent on the interaction of tTG with cell-surface heparan sulphate chains and the activity of PKC-α. The RGD-independent cell adhesion to FN-tTG was linked to the activation of cell survival focal adhesion kinase, extracellular signal-regulated kinase and c-Jun-NH_2-terminal kinase and also required the Raf-1 kinase activity. Apoptosis of tTG-null mouse dermal fibroblasts induced by inhibition of integrin function by RGD peptide (anoikis) could be rescued in response to FN-tTG, suggesting an extracellular survival role for tTG. The correlation between the externalisation and binding of tTG to FN in situations of cell stress and wounding supports the idea that extracellular tTG in complex with FN acts as a pro-survival adhesion factor for anchorage-dependent cells.

Acknowledgments

I would like to thank Prof. Martin Griffin for his support and advice throughout my research period. To work in his guidance in this project was very valuable. I also wish to express my gratitude to Dr. Elisabetta Verderio Edwards for offering me her assistance throughout the my Ph.D.

I am also indebted to my lecturers from Middle East Technical University and Brunel University for equipping me with all the valuable knowledge, throughout my university years.

I would like to express my appreciation to my colleagues; Zita Balklava, Panos Kotsakis, Emma Storey, Richard Parsons, David Chau, Shakthi Dookie, Cansin Turkaslan, Dr.XioLing Li, Dr. Joan Cortez, Dr. Richard Jones, and Dr. Russell Collighan, for making the biochemistry lab a great place to be.

I would also like to thank my friends, Amanda Miles, Asan Bacak, Asli Ugun, Bahar Sogutmaz Ozdemir, Erika Parkinson, Hulya and Senay Sakaoglu, Lauren Schewitz, and Matthew James Bell for being present as many times as I needed and for their kindness.

My deepest gratitude goes to my parents and grandmother. I am grateful to my father for his incredible emotional and financial support; you were there whenever I needed you daddy. I am thankful to my mother for her trust and confidence in me. Special thanks to the teacher of my life, my grandmother, who sacrificed the best years of her life to look after me. I will never forget your advice and doctrine.

Publications

Papers

Verderio, E.A., Telci, D., Okoye, A., Melino, G., and Griffin, M (2003). A novel RGD-independent cell adhesion pathway mediated by fibronectin-bound tissue transglutaminase rescues cells from anoikis. *J. Biol. Chem.*, **278**, 42604-42614

Abstracts

Verderio, E., Telci, D., Okoye, A., Baccarini, M., and Griffin M (2002). A tissue transglutaminase FN complex supports a novel RGD independent cell adhesion. The poster was presented at the BSCB Annual Spring Meeting on Cell Regulation through Molecular Machines.

Telci, D., Verderio, E.A., Baccarini, M., and Griffin, M (2002). Importance of tissue transglutaminase cell adhesion complex in signalling pathways. The poster was presented at 6th International conference on transglutaminase and protein cross-linking, September 14-17, Ferrara, Italy. The abstract was published in the Minerva Biotechnologica, **14:** 210

Verderio, E.A., Telci, D., Okoye, A., Melino, G., and Griffin, M (2002) Fibronectin-bound tissue transglutaminase rescues cells from anoikis. 6th International conference on transglutaminase and protein cross-linking, September 14-17, Ferrara, Italy. The abstract was published in the Minerva Biotechnologica, **14:** 210-211.

Verderio, E.A., Telci, D., and Griffin, M. (2003). Are HSPGs (heparan sulfate proteoglycans) cell-surface receptors for matrix tissue transglutaminase? 8th International Congress on Amino Acids and Proteins, 5-9 September, Roma, Italy.

Verderio, E., Telci, D.; Li, X., Dookie, S., Jones, R., Melino, G., and M. Griffin. (2004). Heterotypic association of extracellular matrix fibronectin with tissue transglutaminase mediates RGD-independent cell signalling and protects cells from anoikis. COST Action 844 meeting, 9-11 May, Bertinoro (Forli), Italy.

List of Abbreviations

ADP	Adenosine-5′-diphosphate
ATP	Adenosine-5′-triphosphate
BSA	Bovine serum albumin
BTC	Biotin-X-cadaverine; 5(((N-(Biotinoyl)amino)hexanoyl) amino) pentylamine trifluoroacetate salt
Ca^{2+}	Free calcium ion
cDNA	Complementary deoxyribonucleic acid
DMEM	Dulbecco's modified Eagle's medium
DMSO	Dimethyl sulphoxide
DNA	Deoxyribonucleic acid
DTT	Dithiothreitol
dUTP	2'-Deoxyuridine, 5'-Triphosphate
FAK	Focal Adhesion Kinase
ECL	Enhanced chemiluminescence
ECM	Extracellular matrix
EDTA	Ethylene diamine tetraacetic acid
ELISA	Enzyme linked immunoabsorbant assay
ERK	Extracellular signal-regulated kinases
EXAP	Extravidine peroxidase
FCS	Foetal calf serum
FITC	Fluorescein isothiocyanate
FN	Fibronectin
GDP	Guanosine-5′-diphosphate
gpl tTG	Guinea pig liver transglutaminase
GTP	Guanosine-5′-triphosphate
GTPase	Guanosine-5′-triphosphatase
HRP	Horseradish peroxidase
IgG	Immunoglobulin
JNK	c-Jun-NH_2-terminal kinase
kDa	Kilodaltons
LTBP-1	Latent TGF-β1 binding protein-1
M	Molar
MAPK	Mitogen-activated protein kinase
MEK	MAPK kinase 1
MKK	MAPK kinase
MKKK	MAPK kinase kinase
ml	Milliliters
mM	Millimolar
μ	Micro
μl	Microlitres
μM	Micromolar
mRNA	Messenger ribonucleic acid
nM	Nanomolar
nM	Nanomolar
PAGE	Polyacrylamide gel electrophoresis

PBS	Phophate buffered saline
pH	Negative log of hydrogen ion concentration
PKCα	Protein Kinase Cα
PMSF	Phenyl methyl sulfonyl fluoride
RT	Room temperature
SD	Standard deviation
SDS	Sodium dodecyl sulphate
TdT	Terminal deoxynucleotidyl transferase
TEMED	N,N,N,N′-tetramethylene diamine
TG	Transglutaminase
tTG	Tissue transglutaminase
TGF-β1	Transforming growth factor β1
TMB	3,3′,5,5′-tetramethylbenzidine
TNF	Tumour necrosis factor
Tris	Tris(hydroxymethyl)-aminoethane
Triton X-100	t-Ocylphenoxypolyethoxyethanol
TUNEL	terminal deoxynucleotidyl transferase-uridine nucleotide nick-end labelling
XTT	Sodium 3'-[1-(phenylamino-carbonyl)-3,4-tetrazolium}-bis (4-methoxy-6-nitor) benzene sulfonic acid hydrate

Table of Contents

Chapter 1: Introduction 1

1.1 Transglutaminases 2
1.2 Different forms of transglutaminase enzymes in mammals 4
1.3 Factor XIII 7
1.4 Keratinocyte Transglutaminase 10
1.5 Epidermal Transglutaminase 11
1.6 Prostate Transglutaminase 12
1.7 Erythrocyte Band 4.2 13
1.8 Transglutaminases X, Y, and Z 14
1.9 Tissue Transglutaminase 15
1.9.1 Structure of tissue transglutaminase 15
1.9.2 Regulation of tissue transglutaminase 18
1.9.3 Physiological functions of tissue transglutaminase 20
1.9.3.1 Role of tissue transglutaminase in cell growth and differentiation 21
1.9.3.2 Tissue transglutaminase in receptor mediated endocytosis 22
1.9.3.3 Tissue transglutaminase involvement in Ca^{+2}-mediated stimulus secretion coupling 22
1.9.3.4 Involvement of tissue transglutaminase in cell death 23
1.9.4 Human diseases associated with tissue transglutaminase 25
1.9.4.1 Tissue transglutaminase and coeliac disease 25
1.9.4.2 Tissue transglutaminase and fibrosis 26
1.9.4.3 Tissue transglutaminase and cancer 27
1.9.4.4 Tissue transglutaminase and neurodegenerative diseases 29
1.9.5 Tissue transglutaminase in extracellular environment 30
1.9.5.1 Fibronectin 35
1.9.6 The cell surface tTG and cell adhesion 40
1.9.7 Tissue transglutaminase in wound healing 46
1.10 Aims 49

Chapter 2: Materials and Methods 50

2.1 Materials 50
2.1.1 Chemicals 50
2.1.2 Materials 51
2.1.3 Equipment 52
2.2 Methods 54
2.2.1 Methods in cell culture 54
2.2.1.1 Cells and culture conditions 54
2.2.1.2 Isolation of primary mouse dermal fibroblast 55
2.2.1.3 Cell passaging 56
2.2.1.4 Determination of cell number 56
2.2.1.5 Cryopreservation of the cell lines 57

2.2.1.6 Cell defrosting from storage 57
2.2.2 Preparation of a physiological extracellular matrix 57
2.2.2.1 Coating of plates with fibronectin and fibronectin fragments 57
2.2.2.2 Immobilisation of tissue transglutaminase on FN matrices 58
2.2.2.3 Formation of a native cell assembled extracellular matrix 58
2.2.3 Detection of relative levels of tTG in matrices 59
2.2.3.1. Detection of tTG antigen by ELISA 59
2.2.3.2 Measurement of tTG activity by biotin-X-cadaverine incorporation 60
2.2.4 Visualisation of FN-tTG matrix with double immuno-fluorescent staining 61
2.2.5 Cell adhesion assay 61
2.2.5.1 Inhibition of RGD-mediated cell adhesion 61
2.2.5.2 Cell fixation and permeablisation 62
2.2.5.3 May-Grunwald and Giemsa co-staining 62
2.2.5.4 Quantification of cell adhesion 63
2.2.6 Preparation of total cell lysates 63
2.2.7 Determination of protein concentration by Lowry Method 64
2.2.8 Sodium Dodecyl-Sulphate Polyacrylamide Gel Electrophoresis 64
2.2.9 Western Blotting of proteins from polyacrylamide gels 66
2.2.10 Immuno-development of Western Blots 67
2.2.11 Densitometric analysis of blots 68
2.2.12 Analysis of Protein Kinase C-α Translocation to Membrane 68
2.2.13 Immuno-fluorescence visualisation of tyrosine phosphorylation levels 69
2.2.14 The measurement of cell viability 70
2.2.15 The detection of caspase-3 catalytic activity 70
2.2.16 Analysis of Anoikis by Flow Cytometry and Fluorescent Microscopy 71
2.2.17 Statistical analysis 72

Chapter 3: Characterisation of fibronectin bound tissue transglutaminase complex 73

3.1 Introduction 73
3.2 Methods 75
3.2.1 Detection of relative levels of tTG in cell assembled extracellular matrix 75
3.2.2 Measurement of immobilised tTG activity 75
3.2.3 The inhibition of FN-bound tTG activity 76
3.2.4 The detection of relative levels of FN after blocking FN-tTG matrix with Cub7402 and the control antibody IgG1k 76
3.3 Results 78
3.3.1 Immobilisation and detection of FN-bound tTG 78
3.3.2 Analysis of a native cell assembled extracellular matrix 78
3.3.3 Measurement of tTG bound to amino-terminal FN fragments 82
3.3.4 The measurement of tTG cross-linking activity in culture medium 84
3.3.5 Inhibition of the cross-linking activity of FN-bound tTG 87
3.3.6 The availability of FN after blocking the FN-tTG matrix 87
3.3.7 The three dimensional detection of FN-tTG matrix 87
3.4 Discusssion 93

Chapter 4: The role of fibronectin bound tissue transglutaminase in RGD-independent cell adhesion 97

4.1 Introduction 97
4.2 Methods 100
4.2.1 Inhibition of protein synthesis 100
4.2.2 The inhibition of RGD-mediated cell adhesion of Swiss 3T3 fibroblasts to the physiological cell assembled matrix 100
4.2.3 The inhibition of FN-bound tTG in cell adhesion assay 101
4.3 Results 102
4.3.1.1 The FN-tTG matrix compensates for RGD inhibition of cell adhesion independently from endogenous ECM protein synthesis 102
4.3.1.2 The fibronectin bound tTG supports RGD independent cell adhesion in different cell types 112
4.3.1.3 A cell assembled matrix of FN and tTG restores RGD inhibition of cell attachment 132
4.3.2 tTG can support the RGD-independent cell adhesion only in complex with full length FN 137
4.3.2.1 The importance of tTG bound to FN to mediate RGD-independent cell adhesion 137
4.3.2.2 tTG immobilisation on amino-terminal FN fragments is not sufficient to support RGD-independent adhesion 142
4.3.3 tTG cross-linking activity is not required to restore impaired cell adhesion 145
4.3.4 Evidence for a direct role of FN-associated tTG in RGD-independent binding to cells 148
4.4 Discusssion 151

Chapter 5: The characterisation of intracellular signalling in the RGD-independent cell adhesion pathway 156

5.1 Introduction 156
5.2 Methods 160
5.2.1 Inhibition of $\alpha_4\beta_1$ integrin mediated cell adhesion 160
5.3 Results 162
5.3.1 RGD-independent cell adhesion does not require the activation of $\alpha_4\beta_1$ integrin 162
5.3.2 The digestion of cell-surface heparan sulphate chains abolish RGD-independent cell adhesion 167
5.3.3 The activation of PKC-α is necessary for RGD-independent cell adhesion 170
5.3.3.1 The RGD-independent cell adhesion in response to FN-tTG is blocked by the PKC-α inhibitor 170
5.3.3.2 Evidence for the translocation of PKC-α to membranes during

RGD-independent cell adhesion 173
5.3.4 The intracellular level of tyrosine phosphorylation is increased by FN-tTG matrix 176
5.3.5 FN-tTG signalling activates focal adhesion kinase 179
5.3.6 The role of PKC-α in the tyrosine phosphorylation of FAK 183
5.3.7 The characterisation of cell survival signalling pathway induced during RGD-independent cell adhesion 187
5.3.7.1 The loss of Raf-1 impairs the restoration of cell adhesion by FN-tTG complex 187
5.3.7.2 Role of the MEK-ERK pathway in FN-tTG mediated signalling 190
5.3.7.3 The RGD-independent cell signalling is linked to JNK1/2 kinase 194
5.3.8 FN-bound tTG rescues primary dermal fibroblast from anoikis 198
5.3.8.1 Caspase-3 is activated in MDFTg2-/- cells undergoing anoikis by inhibition of RGD-independent integrin function 200
5.3.8.2 The inhibition of RGD-independent integrin function results in nuclear fragmentation 200
4.4 Discusssion 206

Chapter 6: Discussion 213

References 226

List of Tables

Table 1.1 Transglutaminase nomenclature 5
Table 2.1 The recipe for the preparations of various percentages of polyacrylamide gels 65

List of Figures

Figure 1.1 Reactions catalysed by transglutaminases 3
Figure 1.2 Schematic structure and functional domains of tissue transglutaminase 17
Figure 1.3 Domain structure of fibronectin 37
Figure 1.4 A model for fibronectin assembly 39
Figure 1.5 Schematic presentation of molecular mechanisms in cell-matrix adhesions 43
Figure 1.6 The Mitogen-activated kinase modules 45
Figure 3.3.1 The ELISA detection of the relative levels of tTG bound to FN and plastic 79
Figure 3.3.2a ELISA analysis of the relative levels of tTG in the physiological cell assembled matrix 80
Figure 3.3.2b ELSA analysis of the relative levels of tTG in the physiological cell assembled matrix 81
Figure 3.3.3 ELISA detection of the relative levels of tTG bound to the amino-terminal FN fragments 83
Figure 3.3.4 The measurement of FN-bound tTG activity 85
Figure 3.3.5 The measurement of tTG activity in physiological cell assembled matrix 86
Figure 3.3.6 Inhibition of FN-bound tTG activity by R283 88
Figure 3.3.7 ELISA detection of FN levels after blocking the FN-tTG matrix with antibodies 89
Figure 3.3.8 The immuno-staining of FN and FN-bound tTG in the presence and absence of cell attachment 91
Figure 4.3.1a Visualisation of cycloheximide treated HOB cells on FN and FN-tTG matrices in the presence and absence of the RGD peptide 104
Figure 4.3.1b Effect of RAD peptide on the cell adhesion of cycloheximide treated HOB cells to FN and FN-tTG matrices 105
Figure 4.3.1c Effect of RGD peptide on the cell adhesion of cycloheximide treated HOB cells to FN and FN-tTG matrices 106
Figure 4.3.2a Visualisation of cycloheximide treated Swiss3T3 fibroblasts on FN and FN-tTG matrices in the presence and absence of the RGD peptide 109
Figure 4.3.2b Effect of RAD peptide on the cell adhesion of cycloheximide treated Swiss3T3 fibroblasts to FN and FN-tTG matrices 110
Figure 4.3.2c Effect of RGD peptide on the cell adhesion of cycloheximide treated Swiss3T3 fibroblasts to FN and FN-tTG matrices 111
Figure 4.3.3a Visualisation of ECV304 cells on FN and FN-tTG matrices in the presence and absence of the RGD peptide 114
Figure 4.3.3b Effect of RAD peptide on the cell adhesion of ECV304 cells to FN and FN-tTG matrices 115
Figure 4.3.3c Effect of RGD peptide on the cell adhesion of ECV304 cells to FN and FN-tTG matrices 116

Figure 4.3.4a Visualisation of Human Dermal Fibroblasts on FN and FN-tTG matrices in the presence and absence of the RGD peptide **119**

Figure 4.3.4b Effect of RAD peptide on the cell adhesion of Human Dermal Fibroblasts to FN and FN-tTG matrices **120**

Figure 4.3.4c Effect of RGD peptide on the cell adhesion of Human Dermal Fibroblasts to FN and FN-tTG matrices **121**

Figure 4.3.5a Visualisation of MDFTg2+/+ cells on FN and FN-tTG matrices in the presence and absence of the RGD peptide **124**

Figure 4.3.5b Effect of RAD peptide on the cell adhesion of MDFTg2+/+ cells to FN and FN-tTG matrices **125**

Figure 4.3.5c Effect of RGD peptide on the cell adhesion of MDFTg2+/+ cells to FN and FN-tTG matrices **126**

Figure 4.3.6a Visualisation of MDFTg2-/- cells on FN and FN-tTG matrices in the presence and absence of the RGD peptide **129**

Figure 4.3.6b Effect of RAD peptide on the cell adhesion of MDFTg2-/- cells to FN and FN-tTG matrices **130**

Figure 4.3.6c Effect of RGD peptide on the cell adhesion of MDFTg2-/- cells to FN and FN-tTG matrices **131**

Figure 4.3.7 Adhesion of Swiss 3T3 fibroblasts to the cell assembled matrix **134**

Figure 4.3.8 RGD-independent cell adhesion of Swiss 3T3 fibroblasts to the cell assembled matrix **136**

Figure 4.3.9 Comparison of the RGD-independent cell adhesion of HOB cells to unblocked and marvel-blocked FN-tTG matrices **139**

Figure 4.3.10 Comparison of RGD-independent cell adhesion of HOB cells to FN-tTG and TCP-tTG matrices **141**

Figure 4.3.11 The RGD-inhibition of HOB cell adhesion on amino terminal FN fragments with and without immobilised tTG **144**

Figure 4.3.12 The RGD-independent cell adhesion of HOB cells to FN-tTG following inactivation of tTG **147**

Figure 4.3.13 The importance of tTG in the support of the RGD-independent cell adhesion when immobilised on FN **150**

Figure 5.3.1 Importance of a4b1 integrin function in the support of the RGD-independent cell adhesion of Swiss 3T3 fibroblasts **164**

Figure 5.3.2 Effect of FN CS-1 fragment on the cell adhesion of Swiss 3T3 fibroblasts to FN and FN-tTG matrices **166**

Figure 5.3.3 Role of cell-surface heparan sulphate chains in the RGD-independent cell adhesion of HOB cells **169**

Figure 5.3.4 The involvement of PKC-α in adhesion of HOB cells to FN and FN-tTG matrices in the presence of RGD and RAD peptide **172**

Figure 5.3.5 Characterisation of PKC-α translocation during the RGD-independent cell-adhesion of HOB cells to FN –tTG matrix **175**

Figure 5.3.6 Visualisation of tyrosine phosphorylation levels by immuno-fluorescence during the adhesion of HOB cells to FN and FN-tTG matrices in the presence of RAD and RGD peptides **178**

Figure 5.3.7a Effect of RGD inhibition on the tyrosine phosphorylation levels of FAK during the adhesion of HOB cells to FN and FN-tTG matrix **181**

Figure 5.3.7b Effect of RGD inhibition on the total levels of FAK during the adhesion of HOB cells to FN and FN-tTG matrix **182**
Figure 5.3.8a Effect of PKC-α inhibitor Go6976 on the tyrosine phosphorylation FAK levels during the RGD-independent adhesion of HOB cells to FN-tTG matrix **185**
Figure 5.3.8b Effect of PKC-α inhibitor Go6976 on the total FAK levels during the RGD-independent adhesion of HOB cells to FN-tTG matrix **186**
Figure 5.3.9 Adhesion of Raf +/+ and Raf -/- fibroblasts to FN and FN-tTG matrices in the presence of RAD and RGD peptides **189**
Figure 5.3.10a Effect of RGD inhibition on the tyrosine phosphorylated ERK1/2 levels during the adhesion of HOB cells to FN and FN-tTG matrix **192**
Figure 5.3.10b Effect of RGD inhibition on the total ERK1/2 levels during the adhesion of HOB cells to FN and FN-tTG matrix **193**
Figure 5.3.11a Effect of RGD inhibition on the levels of phospho-tyrosine JNK1/2 during the adhesion of HOB cells to FN and FN-tTG matrix **196**
Figure 5.3.11b Effect of RGD inhibition on the levels of total JNK1/2 during the adhesion of HOB cells to FN and FN-tTG matrix **197**
Figure 5.3.12 Effect of RGD peptide on survival of MDFTg2-/- fibroblasts **199**
Figure 5.3.13 Analysis of Caspase-3 activity levels during RGD peptide-stimulated anoikis of MDFTg2-/- fibroblasts **201**
Figure 5.3.14a Flow cytometric analysis of apoptotic nuclei in MDFTg2-/- fibroblasts due to the RGD inhibition **203**
Figure 5.3.14b Quantification of mean number of apoptotic cells **203**
Figure 5.3.14c Immuno-fluorescence staining of fragmented nuclei of MDFTg2-/- fibroblasts undergoing anoikis **204**

Chapter 1: Introduction

Chapter 1: Introduction

Most cells reside in a protein network called the extracellular matrix (ECM), which they secrete and mould into the intercellular space. The associations between cells, their attachment to basement membranes, the migration of cells and the formation of cell projections, all require selective adhesion of cells either to one another and/or to the extracellular matrix. In recent years, advances in the understanding of the molecular basis of cell adhesion have revealed the existence of specific families of cell surface receptors. Molecular analyses of cell adhesion have revealed that adhesion has profound effects on cells that go far beyond merely sticking them together. The interaction of cell-surface adhesion receptors with the extracellular matrix components regulates various cellular functions, including differentiation, proliferation, and migration (Hynes, 1999). The specificity of cellular functions comes from the combinatorial expression and interactions between a large number of adhesion receptors. The major families of adhesion receptors, whose molecular functions are well defined at present, include the cadherins, selectins, integrins, and membrane-bound heparan proteoglycans such as syndecans, and glypicans (Petruzzelli *et.al.,* 1999; Tumova *et.al.,* 2000).

Adhesion to the extracellular matrix may also serve as a crucial survival signal for many anchorage dependent cells (Frisch and Screaton, 2001). A central component of the ECM which regulates adhesion dependent survival is the adhesive glycoprotein fibronectin (FN). Cell attachment to fibronectin mediates cell survival through interacting with cell surface receptors. One high affinity binding partner for FN, which also acts as a modulator of the fibronectin matrix is tissue-type transglutaminase (tTG, type II) (Aeschlimann and Thomazy, 2000), which belongs to a large family of calcium dependent transamidases. Accumulating evidence indicates that the tissue transglutaminase has a physiological role in cell adhesion and stabilisation of ECM. Due to the immensity of this area and to avoid the plethora of information, it is essential to summarise the present literature in the context of transglutaminases, the cell adhesion protein fibronectin, and cell surface receptors.

1.1 Transglutaminases

Transglutaminases (TGs) are a widely distributed family of proteins found in many tissues and body fluids of vertebrates as well as micro-organisms, plants and invertebrates. The first finding introducing an enzyme with transamidating activity from guinea pig liver was reported in 1957 by Clarke and co-workers (Clarke *et.al.,* 1957). To date many types of transglutaminases (Enzyme Commission System of Classification 2.3.2.13) have been characterised. Transglutaminases mediate post-translational modification of proteins by catalysing a wide range of aminolytic and hydrolytic reactions (Lorand and Conrad, 1984).

All mammalian transglutaminases catalyse a protein cross-linking reaction by mediating a calcium dependent acyl transfer reaction between the γ-carboxamide group of a polypeptide-bound glutamine (Gln) and the ε-amino group of a polypeptide bound lysine to form a ε-(γ-glutamyl)-lysine isopeptide bond (Pisano *et.al.,* 1968; Lorand and Graham, 2003; figure 1.1a). The binding of calcium is essential, as it induces a conformational change that exposes a cysteine residue in the active site domain. The reaction results in the release of ammonia and the formation of the covalently cross-linked molecules resistant to mechanical and proteolytic breakdown (Griffin and Wilson, 1984; Melino *et.al.,* 1994). The resulting supramolecular structure is a crucial component of important biological processes including blood coagulation, the differentiation of the epidermis of skin and ECM assembly (Griffin *et.al.,* 2002).

TGs can also use primary amines and polyamines, such as putrescine, spermine, and histamine, as substrates for amine incorporation (Birckbichler *et.al.,* 1977a; Folk and Finlayson, 1977; figure 1.1b). The reaction results in the formation of a (γ-glutamyl)-polyamine bond through incorporation of a primary amine into a polypeptide-bound glutamine.

TGs are known to hydrolyse esters such as nitrophenyl and thiocholine esters (Folk and Finlayson, 1977). Biochemical studies also indicate that certain TGs can form an ester bond between specific glutamine residue of proteins like involucrin

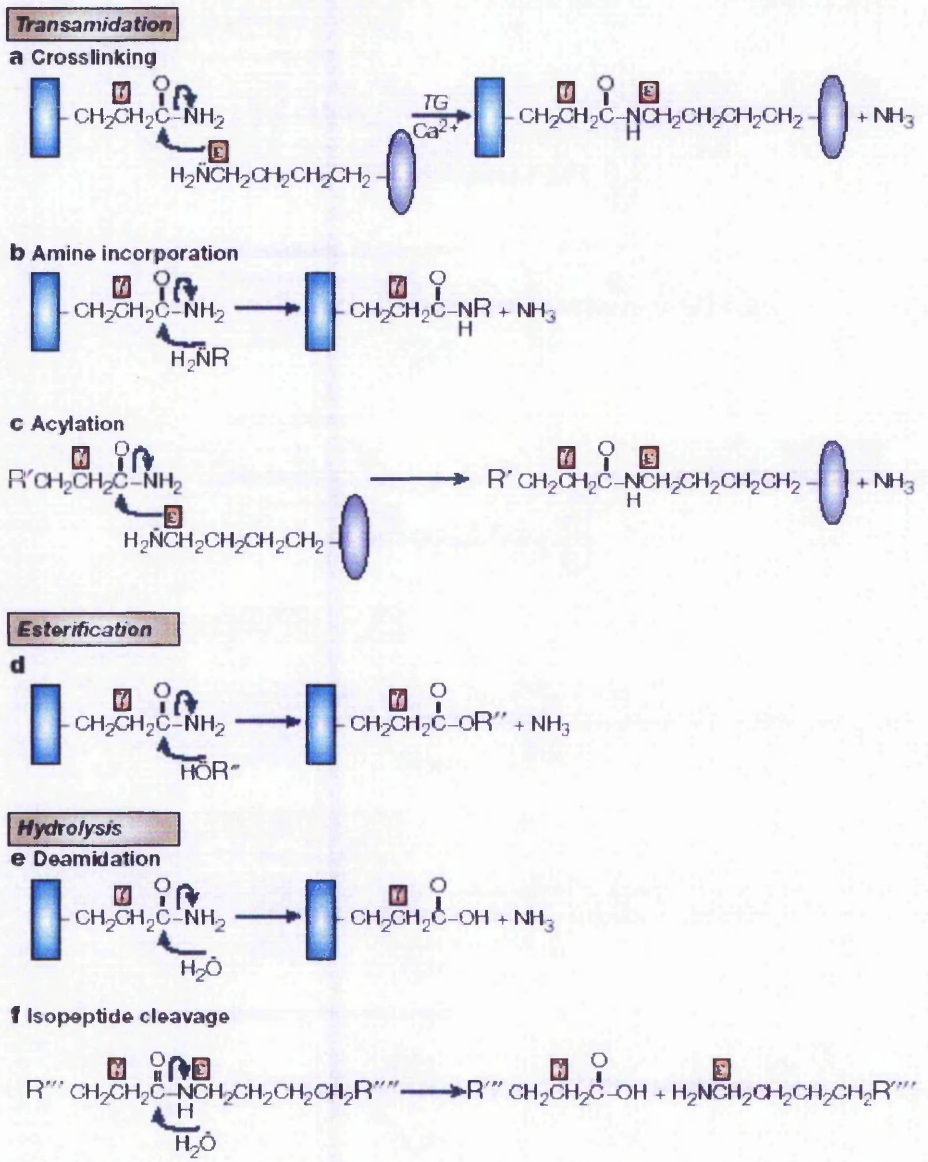


Figure 1.1 Reactions catalysed by transglutaminases

Schematic presentation of various post-translational reactions between the acceptor glutamine residue of one protein (blue rectangle) and **a,c** the lysine donor residue of another (purple ellipse); **b,** an amine (H_2NR); **d,** a ceramide (HOR''); **e,** water (H_2O). R' represents a Gln-containing peptide, R''' and R'''' represents the side chains in branched isopeptides (Lorand and Graham, 2003).

and a ceramide such as ω-hydroxyceramides (Nemes *et.al.,* 1999; figure 1.1d). The esterification of the protein bound glutamine residues plays an important role in the epidermal barrier formation.

It has been shown that transglutaminases can catalyse the hydrolysis (deamidation) of amide groups of protein- and peptide-bound glutamine residues (Mycek and Waelsch, 1960; Aleanzi *et.al.,* 2001; figure 1.1e). This selective deamidation of glutamine residues has been proposed to act as the main factor contributing to the onset of celiac disease (Ciccocioppo *et.al.,* 2003). Recent work has reported that TGs can break isopeptide linkages with high affinities for the γ-branched substrates (figure 1.1f). Tissue type transglutaminase and Factor XIIIa reportedly exhibit isopeptidase activity and hydrolyse the ε-(γ-glutamyl)-lysine isopeptide bond, suggesting a dynamic role for transglutaminases in cell biology by not only catalysing but also breaking of ε-(γ-glutamyl)-lysine bonds (Parameswaran *et.al.,* 1997).

Although the enzymatic reaction pathways of TGs can be outlined simply in figure 1.1, the actual mechanism is more complicated. After binding of the acceptor glutamine-containing substrate to the enzyme, the formation of a γ-glutamylthiolester takes place with the active-centre cysteine (Cys) residue of the TG, known as the acylenzyme intermediate. This results in the release of ammonia (figure1.1a-e). The acyl-enzyme complex then reacts with the donor amine substrate, which attacks the thiolester bond. As a result of this step, the active-centre Cys residue reverts back into its original form, allowing the enzyme to participate in another cycle of catalysis. Depending on the nature of the donor substrate various products are generated at the end of the reaction (Lorand and Graham, 2003; Griffin *et.al.,* 2002; figure 1.1).

1.2 Different forms of transglutaminase enzymes in mammals

There is accumulating evidence to support the notion that several transglutaminases can be expressed in the same tissue and perform different functions (Aeschlimann*et.al.,* 1998; Grenard *et.al.,* 2001; Griffin *et.al.,* 2002). To date, nine

Gene	Protein	Synonyms	Tissue Expression	Function
F13A1	Factor XIIIa subunit	Fibrin-stabilising factor, Laki-Lorand factor, Pro-fibrinoligase, plasma pro-TG	Platelets, astrocytes, dermal dendritic cells, chondrocytes, placenta, synovial fluid	Blood coagulation, bone growth, ECM stabilisation
TGM1	TG1	TG_K, keratinocyte TG, particulate TG	Keratinocytes, brain	Cell-envelope formation
TGM2	TG2	TG_C, tissue TG, endothelial-, erythrocyte-, TG, Gh, Ghα	Ubiquitous	Multiple
TGM3	TG3	TG_E, epidermal TG, callus-, hair follicle-, bovine snout TG	Squamous epithelium, brain	Cell-envelope formation
TGM4	TG4	TG_P, prostate TG, vesiculase, dorsal prostate protein 1, major androgen-regulated prostate secretory protein	Prostate	Semen Coagulation
TGM5	TG5	TG_X	Ubiquitous expression except for the CNS and lymphatic system	Unknown
TGM6	TG6	TG_Y	Unknown	Unknown
TGM7	TG7	TG_Z	Ubiquitous	Unknown
EPB42	Band 4.2	ATP-binding erythrocyte membrane protein band 4.2	Erythrocytes, bone marrow, fetal liver and spleen	Membrane skeletal component

Table 1.1 Transglutaminase nomenclature (Lorand and Graham, 2003).

distinct TG forms have been identified at the genomic level in humans (Grenard *et.al.,* 2001). As shown in table 1.1, the transglutaminase family includes, the circulating zymogen factor XIII (FXIII), the keratinocyte transglutaminase (TG1), the ubiquitous tissue transglutaminase (TG2), the epidermal transglutaminase (TG3), prostate transglutaminase (TG4), erythrocyte band 4.2, and the recently discovered transglutaminase X, Y and Z (TG5, TG6, TG7) (Aeschlimann *et.al.,* 1998; Grenard *et.al.,* 2001).

Transglutaminases are encoded by a family of closely related genes that have a high degree of sequence similarity. All of the TG genes seem to be organised in a similar way with a notable conservation of intron distribution and splice sites (Grenard *et.al.,* 2001). Alternative splice variants have been detected for several TGs, including TG2, TG4, TG5, and erythrocyte band 4.2 protein (Fraij and Gonzales, 1996; Monsonego *et.al.,* 1997; Aeschlimann *et.al.,* 1998; Candi *et.al.,* 2001; Citron *et.al.,* 2001). Phylogenetic studies indicate that evolution of TG genes has taken place in two different lineages upon an early-gene duplication event. The first lineage comprises TG2, TG3, and erythrocyte band 4.2, while the second one consists of FXIIIa and TG1 (Polakowska *et.al.,* 1992; Grenard *et.al.,* 2001).

All members of transglutaminase family share a common amino acid sequence of Tyrosine-Glycine-Glutamine-Cysteine-Tryptophan-Valine at the active site (Ikura *et.al.,* 1988; Gentile *et.al.,* 1991). The TGs do not undergo carbohydrate modification despite the presence of several potential sites for N-linked glycosylation. Although sequence analysis of TGs revealed many Cys residues, no formation of intra-molecular disulphide bonds have been detected so far (Lorand and Graham, 2003). TGs, even those that are secreted, lack an amino-terminal hydrophobic leader sequence, which is characteristic of a secreted protein. Most transglutaminase enzymes are post-translationally modified by the removal of the initiator methionine residue, followed by N-acetylation.

TGs have been implicated to be involved in several human pathological states such as neurodegenerative diseases (Lesort *et.al.,* 2000; Karpuj *et.al.,* 2002; Selkoe, 2002), autoimmune diseases (Piacentini and Colizzi, 1999; Aleanzi *et.al.,* 2001), cancer (Birckbichler *et.al.,* 1977b; Barnes *et.al.,* 1985), and tissue fibrosis (Griffin *et.al.,* 1979; Mirza *et.al.,* 1997; Johnson *et.al.,* 1997 and 2003).

1.3 Factor XIII

Factor XIII is the final zymogen in the blood coagulation cascade, which is converted to the active transglutaminase enzyme (Factor XIIIa) by thrombin cleavage (Takagi and Doolittle, 1974; Lorand *et.al.,* 1980). FXIII of plasma is a tetramer consisting of two types of globular A subunits surrounded by two long thin flexible strand-like B subunits (A_2B_2), while cellular FXIII exists as a homodimer of potentially active A subunits (A_2) in platelets, macrophages and other cells (Schwartz *et.al.,* 1973; Takagi and Doolittle, 1974; Carnell *et.al.,* 1989). The subunit structure and complete amino acid sequence of plasma FXIII has been established by electron microscopy and a combination of cDNA cloning and amino acid sequence analysis (Ichinose *et.al.,* 1986; Grundmann *et.al.,* 1986; Carnell *et.al.,* 1989). The mRNA of FXIIIa is 3.9 kb in size, consisting of 2.2 kb of open reading frame for 731 amino acids with a molecular mass of approximately 83 kDa (Grundmann *et.al.,* 1986; Ichinose *et.al.,* 1986). Despite of its presence in the blood plasma, no hydrophobic leader sequence was identified in the primary structure of FXIIIa (Grundmann *et.al.,* 1986). The mature molecule has six potential sites for glycosylation; however, no carbohydrate residue was detected (Takashi *et.al.,* 1986; Greenberg *et.al.,* 1991). Gene studies for FXIIIa localised the thrombin cleavage site to exons 2 and 12, active site region to exon 7, and two putative calcium binding regions to exons 6 and 11 (Ichinose *et.al.,* 1988; Hettasch and Greenberg, 1994; Hettasch *et.al.,* 1997).

The FXIIIA subunit is present in hematopoetic cells such as monocytes, machrophages, megakaryocytes, platelets (Weisberg *et.al.,* 1987; Kiesselbach and Wagner, 1972; Lopaciuk *et.al.,* 1976). FXIIIA has also been identified in the placenta, uterus, prostate and liver (Greenberg *et.al.,* 1991; Adany, 1996). The molecular mechanisms of FXIIIA release into the plasma and the extracellular matrix is not clear, however, recent data suggests that FXIIIA is released form cells of hematopoetic origin during cell destruction and is thought to unite with FXIIIB in the circulation (Kaetsu *et.al.,* 1996; Nurminskaya *et.al.,* 1998).

The amino acid sequence of the human FXIIIB subunit was deduced from nucleic acid sequences of the cDNA clones isolated from the human liver library (Bottenus

et.al., 1990). The 2.2 kb mRNA of FXIIIB codes for a protein of 614 amino acids (Carnell *et.al.,* 1989). The mature FXIIIB is a typical mosaic glycoprotein containing 8.5% of charbohydrate and composed of 10 tandem repeats of 60 amino acids each with two disulfide bridges (Ichinose *et.al.,* 1990).

The gene coding for FXIIIB is mapped to chromosome 1q31-32.1 in linkage with the genes coding for complement factor H, peptidase C, and rennin (Bottenus *et.al.,* 1990; Muszbek *et.al.,* 1999). The 28 kb-gene consists of 12 exons, the first of which encodes for the leader sequence common for secretory proteins (Bottenus *et.al.,* 1990). While the last exon codes for the C-terminal region of the protein, the remaining exons (2-11) encodes for the 10 tandem repeats that demonstrate a high degree of internal homology and is likely to serve as a protein binding module (Aeschlimann and Paulsson., 1994).

The activation of FXIII occurs when thrombin cleaves the peptide bond near the N-terminus of the A subunit at Arg37-Gly38 (Takagi and Dolittle, 1974; Lorand, 1986). Consequently, the activation peptide consisting of 37 amino acid residues is separated from the N-terminal end of A subunits (Schwartz *et.al.,* 1973). Recently, radiocrystallographic analysis demonstrated that upon thrombin cleavage, the activation peptide remained attached to the molecule at its original position occluding the active-site cavity (Yee *et.al.,* 1995). In the presence of calcium ions, the B subunits dissociate from the tetramer, and the active-site cysteine originally buried within the catalytic core domain becomes unmasked (Hornyak *et.al.,* 1989; Hornyak and Shafer, 1991). The presence of fibrinogen accelerates the proteolytic separation of active peptide by approximately 100-fold (Greenberg *et.al.,* 1987). The cofactor activity of fibrinogen in this reaction can be attributed to the formation of a fibrin-plasma FXIII complex, which is processed by thrombin more efficiently (Naski *et.al.,* 1991). The FXIIIB subunit is believed to regulate and stabilise the tetramer structure during the activation of zymogen in plasma (Aeschlimann and Paulsson., 1994). The inhibitory effect of purified plasma FXIIIB on contact activation of blood coagulation suggests a novel feed-back inhibition mechanism of blood coagulation (Halkier and Magnusson, 1988).

The transglutamination reaction catalysed by FXIIIa leads to the cross-linking of γ-chains of two different fibrin molecules to form characteristic γ-chain dimers

followed by the polymerisation of the α-chains of fibrin (Schwartz *et.al.,* 1973). The activation of FXIII leads to the cross-linking of two types of proteins, including proteins of the coagulation and fibrinolytic system, and also adhesion proteins. Fibrin is the main physiological of substrate for FXIIIa. The cross-linking reaction catalysed by FXIIIa between fibrin molecules increases the strength of fibrin clots (Doolittle *et.al.,* 1979; Shainoff *et.al.,* 1991). FXIIIa can also cross-link fibrin to thrombospodin to anchor the blood clot to the site of injury (Bale and Mosher, 1986). The cross-linking of α_2 antiplasmin, the main physiological inactivator of plasmin, to fibrin by the FXIIIa was shown to increase the resistance of the clot to fibrinolysis by plasmin (Booth, 1999; Sakata and Aoki, 1980; Reed *et.al.,* 1991). The other coagulation substrates for FXIIIa include the blood coagulation factor V (Francis *et.al.,* 1986), fibrinogen (Dyr *et.al.,* 1989), von Willebrand factor (Hada *et.al.,* 1986), type-2 plasminogen activator inhibitor (Jensen *et.al.,* 1993; Ritchie *et.al.,* 2000), and plasminogen (Benxiden *et.al.,* 1993). Soluble fibronectin found in body fluids becomes cross-linked to fibrin and collagen during plasma clotting in a FXIIIa-catalysed reaction (Mosher and Schad, 1979). In addition, plasma fibronectin attached to the surface of fibroblasts, as well as fibronectin synthesised by these cells are both proposed to be cross-linked by FXIIIa at ECM sites, which is then incorporated into the assembling ECM (Barry and Mosher, 1988 and 1990).

The deficiency in FXIII activity have been likened to a variety of diseases in three major areas: haemostasis, wound healing and maintaining pregnancy. Severe bleeding diathesis of most patients who are deficient in FXIII demonstrated the presence and functional integrity of FXIII is essential for maintaining normal haemostasis (Kitchens and Newcomb, 1979). The importance of FXIII in wound healing has been demonstrated in patients and animals with FXIII deficiency, who presented impaired healing of wounds (Muszbeck *et.al,* 1999). Pregnant women who are homozygous for FXIII deficiency are destined to lose their foetus at the early stage of gestation by miscarriage (Lorand *et.al.,* 1980).

Recently FXIIIa has been reported to inhibit capillary tube formation in fibrin and mediate adhesion of endothelial cells in an integrin-dependent manner. The adhesive activity of FXIIIa was found not to be dependent on its transglutaminase

activity, and did not involve the FXIIIB subunits (Dallabrida *et.al.,* 2000). A following study has shown that endothelial cells bind to FXIIIa via their $\alpha_v\beta_3$ receptor, while FXIIIa binds platelet glycoprotein IIb/IIIa receptor. FXIIIa, therefore, mediates the interaction of platelets with endothelial cells, which may be relevant for wound repair after vascular injury in FXIII-deficient patients (Dardik *et.al.,* 2002).

1.4 Keratinocyte Transglutaminase

Transglutaminase type 1, the so- called "keratinocyte-type" transglutaminase (TG1) was identified and analysed as an intracellular enzyme in epidermal keratinocytes (Rice and Green, 1977; Thacher and Rice, 1985). The cDNA cloning of the TG1 from human and rat epidermal keratinocytes revealed the enzyme as the largest of all the transglutaminase family members with a molecular mass of 89-90 kDa (Phillips *et.al.,* 1990). The full length of the enzyme was later shown to be larger, running as a band of 106 kDa as recognised by antibody in Western Blots obtained from proliferating keratinocytes (Kim *et.al.,* 1994 and 1995).

Keratinocyte TG is primarily associated with the cytoplasmic side of the plasma membrane through fatty acylation at cysteine residues by thioester-linked palmitic and myristic acid (Chakravarty and Rice, 1989). Membrane-bound TG1 exists in two forms; a full-length inactive zymogen form of 106 kDa or a proteolytically processed form of 67/33/10 kDa with high activity. The cytosolic enzyme exists as the full-length inactive form, the 67 kDa fragment and the 67/33 kDa complex (Thacher and Rice, 1985; Kim *et.al.,* 1995). Keratinocyte TG is the major enzyme involved in the formation of the cornified envelope during terminal differentiation of the epidermis. This cornified envelope functions as the protective barrier in the skin and consists of a 10-20nm thick deposited layer of TG1 -catalysed highly cross-linked proteins on the intracellular surface of the plasma membrane (Ta *et.al.,* 1990). The main substrates for the keratinocyte TG includes loricrin (Hohl, 1993), involucrin (Simon and Green, 1988), cornifin (Marvin *et.al.,* 1992), keratin, filaggrin and elafin (Steinert and Marekov, 1995; Simon *et.al.,* 1996). Several mutations in the TG1 gene leading to a deficiency in the keratinocyte TG were

reported in some families with lamellar ichthyosis, an autosomal recessive skin disorder, which results in the thickening of epidermis with a high risk of sepsis and dehydration (Huber *et.al.,* 1995; Hennies *et.al.,* 1998). Recent studies with TG 1-deficient mice demonstrated the importance of keratinocyte enzyme in the development and the maturation of the stratum corneum as well as the neonatal adaptation to environment. The TG 1-/- mice had erythrodermic skin with abnormal keratinisation and impaired skin barrier function leading to an early neonatal stage death (Matsuki *et.al.,* 1998).

1.5 Epidermal Transglutaminase

Epidermal transglutaminase (TG3) was the first epidermal enzyme to be isolated and characterised. Early studies reported a soluble protein of about 50 kDa purified from human callus and cow snout epidermis (Buxman and Wuepper, 1976; Ogawa and Goldsmith, 1976). However, biochemical analyses later revealed that TG3 is in fact a proenzyme with a molecular weight of 77 kDa. TG3 activation requires proteolytic cleavage of zymogen into a catalytically active 50 kDa amino-terminal fragment and a 27 kDa carboxyl-terminal peptide (Kim *et.al.,* 1990). Although proteases responsible for the proteolytic activation of TG3 remain unknown, dispase, a protease from *Bacillus polymyxa*, is able to cleave the zymogen resulting in activation *in vitro* (Martinet *et.al.,* 1988; Hitomi *et.al.,* 1999).

Epidermal transglutaminase is believed to be involved in the formation of the cornified envelope of the epidermis during terminal differentiation (Buxman and Wuepper, 1975). For some substrates in the epidermis, TG3 favours intra-molecular cross-linking whereas TG1 prefers intermolecular reactions involving different lysine and glutamine residues (Kalinin *et.al.,* 2002). Immunohistochemical analysis using monoclonal antibodies located human TG3 to the cytoplasm of the cultured terminally differentiating keratinocytes in the outer layer of epidermis (Hitomi *et.al.,* 2003). In addition, TG3 is thought to be required for the cross-linking of the structural proteins trichohyalin and the keratin intermediate filaments to form a rigid structure within the inner root sheath cells during hair shaft formation (Lee *et.al.,* 1993).

Expression studies has shown that TG3 mRNA is expressed in a number of tissues besides epidermis including brain, testis, intestine, spleen, and kidney (Hitomi *et.al.,* 1999). The physiological importance of this wide expression is yet to be determined. Recently, autoimmune antibodies against TG3 have been detected as the dominant autoantigens in patients with dermatitis herpetiformis, a blistering skin disease characterised by granular IgA deposits in the papillary dermis (Sardy *et.al.,* 2002).

1.6 Prostate Transglutaminase

Prostate transglutaminase (TG4) was first purified and characterised in the dorsal prostate and coagulation gland of rats (Wilson and French, 1980; Seitz *et.al.,* 1990). Rat TG4 was reported to be highly glycosylated and to possess a lipid anchor which is retained during enzyme apocrine secretion. It is secreted as a homodimeric protein of 150 kDa with monomers consisting of a molecular weight around 75 kDa (Seitz *et.al.,* 1991). In rodents, TG4 is present in the coagulating gland secretion and responsible for the formation of the copulatory plug in the female genital tract after coitus (William-Ashman, 1984). An additional role of this enzyme has been suggested by investigating TG4-catalysed polymeric forms of seminal vesicle proteins in the masking of the antigenity of the male gamate, thereby suppressing an immune response in female genital tract against sperm cells (Mukherjee *et.al.,* 1983; Paonessa *et.al.,* 1984).

The fluorescence *in situ* hybridisation analysis mapped a human TG4 gene at the chromosome 3 within the interval 3p21.33-p22 (Gentile *et.al.,* 1995). Sequencing of cDNA-clones encoding the human TG4 showed a protein of 684 amino acids with a predicted molecular mass of 77 kDa (Dubbink *et.al.,* 1996). The expression of human TG4 gene is limited to the prostate, exclusively to the luminal epithelial cells (Dubbink *et.al.,* 1999). Although the expression and synthesis of the human TG4 is highly variable between individuals, it has been reported to be down regulated in most metastatic prostate cancer (An *et.al.,* 1999). Like rat TG4, the human TG4 is also implicated in suppressing the sperm surface antigenicity (Porta *et.al.,* 1986).

1.7 Erythrocyte Band 4.2

Erythrocyte Band 4.2, or pallidin, is a major component of the human erythrocyte membrane accounting for approximately 5% of the total membrane protein mass (Korsgren and Cohen, 1986). Molecular cloning of human erythrocyte Band 4.2 (Korsgren *et.al.,* 1990; Sung *et.al.,* 1990) and mouse erythrocyte Band 4.2 (Rybicki *et.al.,* 1994) showed that the Band 4.2 is a transglutaminase-like molecule in erythrocytes but lacks the essential active site cysteine for the cross-linking activity. The Band 4.2 gene is approximately 20 kilo bases long and encodes for a 77 kDa protein (Korsgren *et.al.,* 1990 and 1991).

Band 4.2 is associated with the cytoplasmic surface of the erythrocyte membrane through binding to the erythrocyte anion transport protein band 3 (Korsgren *et.al.,* 1986). It also binds to structural membrane protein ankyrin in solution and may associate with band 4.1 protein (Korsgren and Cohen, 1988). Recently work done on Rhesus null (Rh-) cells suggested that human Band 4.2 protein interacts with Rh membrane complex member CD47 and is involved in the skeleton linkage and/or membrane translocation of the Rh complex (Mouro-Chanteloup *et.al.,* 2003). It is therefore likely that Band 4.2 plays an important role in membrane function or structure. Band 4.2 protein has also been detected in a number of nonerythroid cell types (Korsgren *et.al.,* 1986; Friedrichs *et.al.,* 1989) mostly localised in the intracellular vesicles, suggesting its involvement in the formation of intracellular storage vesicles (Risinger *et.al.,* 1996).

Analysis of the amino acid sequence of human erythrocyte Band 4.2 revealed that Band 4.2 contains a nucleotide binding P-loop (Azim *et.al.,* 1996) and a penultimate glycine residue, the usual site for myristylation (Risinger *et.al.,* 1992). The nucleotide specificity of P-loop is restricted to ATP, however the functional significance of ATP binding is yet to be identified. A study of the myristylation of Band 4.2 protein showed that the process is required for the targeting of Band 4.2 to specific intracellular locations (Risinger *et.al.,* 1996).

Absence or deficiency of Band 4.2 results in haemolytic anaemia associated with spherocytic or elliptocytic erythrocytes (Kanzaki *et.al.,* 1996; Hayette *et.al.,* 1995). Protein Band 4.2 deficient -/- mice showed abnormal regulation of erythrocyte

cation transport and loss of normal erythrocyte membrane surface (Peters *et.al.,* 1999). These findings suggest that Band 4.2 has an essential role in the regulation of erythrocyte shape and maintenance of membrane stability.

1.8 Transglutaminases X, Y, and Z

Of all the transglutaminase enzymes, transglutaminase X (TG5), transglutaminase Y (TG6), and transglutaminase Z (TG7) were the last members of the family to be discovered. The physiological functions of TG5, TG6, and TG7 have not been well defined. Nevertheless, cDNA analysis revealed the structure and location of the genes encoding for these novel members of the transglutaminase family (Aeschlimann *et.al.,* 1998); Grenard *et.al.,* 2001).

The first finding on TG5 has come from expression analysis of transglutaminase forms in human keratinocytes. The enzyme consists of 720 amino acid residues with a molecular weight of approximately 81 kDa. Comparison of the deduced amino acid sequence of TG5 to the other members of the TG family showed that the catalytic domain structure and active site residues required for enzymatic activity are conserved with an overall sequence identity around 35% (Aeschlimann *et.al.,* 1998). The TG5 gene spans about 35 kb and encodes for four related transcripts with different length due to alternative splicing (Grenard *et.al.,* 2001; Candi *et.al.,* 2002). Detection of full length TG5 during the early stages of keratinocyte differentiation suggests that TG5 may play a role in this process in parallel to TG1 and TG3 (Candi *et.al.,* 2002). Recently, abnormal levels of TG5 have been linked with hyperkeratotic phenotype in ichthyosis and Darier's disease (Candi *et.al.,* 2002).

In attempt to sequence the chromosomal segments coding for tTG and TG3, a novel transglutaminase, called TG6, has been mapped on the 20q11 region of chromosome 20 (Grenard *et.al.,* 2001).

Expression studies carried out in human prostate carcinoma tissue revealed another novel transglutaminase, TG7, with a molecular mass of 80 kDa. The TG7 cDNA is approximately 2.3 kb long, and the resulting protein consists of 710 amino acids. Sequencing analysis revealed a number of aberrantly spliced gene products,

unlikely to be of physiological significance. The genes encoding for TG5 and TG7 have been localised in tandem with Band 4.2 gene on human chromosome 15. TG5 and TG7 showed widespread expression, which overlapped with the expression pattern of tTG and TG3 in some tissues (Grenard *et.al.,* 2001).

1.9 Tissue Transglutaminase

Tissue transglutaminase (tTG, or TG2) is a unique member of the transglutaminase family and is expressed in a wide variety of different cells and tissues including brain (Thomazy and Fesus, 1989). The tTG enzyme is a multifunctional protein with distinct and reciprocally regulated catalytic activities. The enzyme is localised in various parts of cell including cytosol, plasma, nucleus, nuclear membranes, cell surface and the extracellular matrix, which is the subject of this thesis.

Tissue transglutaminase is encoded by the TGM2 gene, which is 32.5 kb and contains 13 exons separated by 12 introns. Along with the gene for TG3, the TGM2 gene has been mapped to the chromosome 20 (Fraij *et.al.,* 1992; Gentile *et.al.,* 1994).The regulation of tTG gene expression can be controlled by retinoic acid (Moore *et.al.,* 1984; Gentile *et.al.,* 1991), as well as TNFα, IL-6 and TGFβ-1 (Lu *et.al.,* 1995; Aeschlimann and Thomazy, 2000). Analysis of the genomic organisation of the TG2 gene showed that the alternative splicing of tTG mRNA is possible. Two additional forms of tTG (TGH and TGH2) and an alternatively spliced short form of the enzyme lacking the GTP-binding site were observed in erythroleukemia cells (Fraij *et.al.,* 1992; Fraij and Gonzales, 1996) and in astrocytes (Monsonego *et.al.,* 1997), respectively.

1.9.1 Structure of tissue transglutaminase

Molecular cloning of tTG cDNA of human (Gentile *et.al.,* 1991), bovine (Nakanishi *et.al.,* 1991), mouse (Gentile *et.al.,* 1991), guinea pig (Ikura *et.al.,* 1988), and chicken (Weraarchakul-Boonmark *et.al.,* 1992) origin, revealed a monomeric protein of 685-691 amino acids with a molecular mass of 76-85 kDa (Aeschlimann and Paulsson, 1994).

Analysis of the deduced amino acid sequence of tTG has revealed an active site with a cysteine residue located at position 276 in guinea pig liver tTG (Ikura *et.al.,* 1988), and 277 in human tTG (Gentile *et.al.,* 1991). On the basis of the amino acid sequence from guinea pig liver, tTG molecule does not have any classical hydrophobic leader sequence and lacks carbohydrate glycosylation and disulphide bonds, despite the presence of six potential glycosylation sites and 17 cysteine residues, respectively (Ikura *et.al.,* 1998). During the post-translational modification of tTG, the initiator methionine is removed, followed by subsequent acetlylation of the penultimate alanine residue. This N-acetlylation does not affect the transglutaminase activity of tTG enzyme, and is suggested to serve as an alternate signal for protein secretion (Ikura *et.al.,* 1990; Muesh *et.al.,* 1990). The calcium-binding site thought be responsible for the regulation of the enzyme's transglutaminase activity, is located in two regions rich in glutamine residues around amino acids 450 and 470 (Ichinose *et.al.,* 1990).

The three dimensional structure of tTG has been derived from that of FXIII, and consists of a N-terminal β-sandwich domain (residues 1-138), followed by a large α/βcatalytic core (residues 139-471), and two C-terminal barrels (residues 472-686) (Lorand and Graham 2003; figure 1.2a; Chen and Mehta, 1999; figure 1.2b). This organisation of four domains is highly conserved during the evolution of TG isoforms, such that the crystal structure of red sea bream liver transglutaminase demonstrates similar overall and active site structures with FXIII (Noguchi *et.al.,* 2001; Griffin *et.al.,* 2002). The cysteine (C277), histidine (H335) and aspartic acid (D358) residues in the catalytic core are conserved among all enzymatically active members of the TG family (Griffin *et.al.,* 2002). The C277 in tTG is crucial for the formation of the thioester bond with a substrate bound glutamine (Folk and Cole, 1966; Lee *et.al.,* 1993). Expression studies carried out on different functional constructs have revealed that the catalytic core domain alone is not enough for the TG activity; hence the flanking domains also play a role in modulation of the transamidating activity of TG. The N-terminal β-sandwich domain to the catalytic core is essential for the TG activity, while the core domain is required for the hydrolysis of GTP and ATP (Iismaa *et.al.,* 1997). Point mutation analysis of

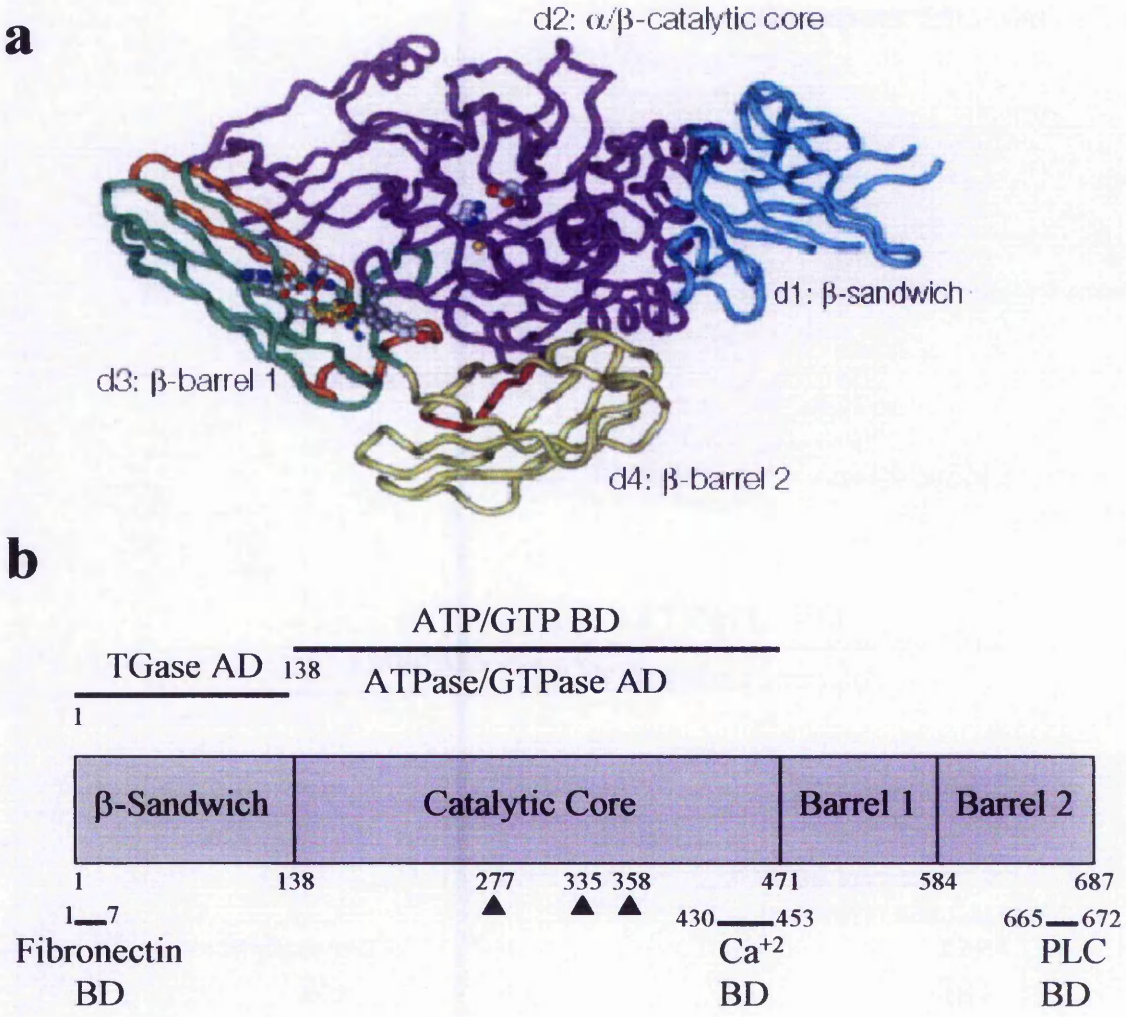


Figure 1.2 Schematic structure and functional domains of tissue transglutaminase

a, Three dimensional crystal structure of tTG (Lorand and Graham, 2003); **b,** Schematic presentation of various binding and functional domains in tTG protein. BD, binding domain; AD, activity domain; ▲ , active site triad involving Cys^{277}, His^{335}, and Asp^{358}; PLC, phospholipase C (Chen and Mehta, 1999).

tryptophan residues in the core domain revealed that tryp241 is essential for tTG cross-linking activity (Murthy *et.al.,* 2002). Recent work has localised the GTP-binding domain of tTG to a 15-amino acid segment between residues 159 and 173 in the core domain of tTG (Iismaa *et.al.,* 2000).

1.9.2 Regulation of tissue transglutaminase

Tissue transglutaminase catalyses both calcium dependent protein cross-linking and calcium-independent but magnesium-dependent GTP and ATP hydrolysis, implying that it could serve as a bi-functional enzyme (Lee *et.al.,* 1989). Early *in vitro* studies performed by Folk and co-workers and by Achyuthan and Greenberg reported the requirement of calcium as an activator of tTG, and the modulation of the cross-linking activity by guanosine nucleotides, respectively (Folk *et.al.,* 1967; Achyuthan and Greenberg, 1987).

The hydrolytic activity of tTG took on a new dimension when tTG was shown to be identical to a previously characterised GTP-binding protein, namely Ghα, which was co-purified with rat-liver α_1-adrenergic receptors (Nakaoka *et.al.,* 1984). De novo purification of Gh indicated that the 74 kDa α subunit (Ghα) is associated with a 50 kDa β subunit (Gh_β), which modulates the GTP binding and GTPase activity of Ghα (Baek *et.al.,* 1996). The sequence analysis of Ghα was shown to have high similarity to tTG. The tTG cross-linking activity in the cell is tightly controlled by local concentrations of calcium ions and guanosine nucleotides (Smethurst and Griffin, 1996). The inhibition of cross-linking activity of the enzyme by guanosine nucleotides is non-competitive, and is believed to cause a conformational change that reduces the affinity of tTG for calcium. The inhibitory effect of GTP, however, can be partially reversed by the addition of calcium ions (Achyuthan and Greenberg, 1987; Smethurst and Griffin, 1996). Inside the healthy cell tTG remains latent unless the depletion of intracellular GTP or enhancement of calcium influx (3-4 calcium ions/enzyme) takes place (Folk and Finlayson, 1977; Zhang *et.al.,* 1998).

As stated earlier, in addition to GTP, ATP has also been shown to be hydrolysed by tTG in a magnesium dependent manner (Lee *et.al.,* 1989; Lai *et.al.,* 1998). The

studies by Lai *et al.*. (1996 and 1998) have clearly established that magnesium (Mg^{2+})-nucleotide (GTP/ATP) complexes can modulate the protein cross-linking activity of tTG. Mg^{2+}-GTP reversibly binds to gpl tTG and inhibits the transamidating activity of tTG by inducing a conformational change that can be reversed by calcium ions. In contrast, the Mg^{2+}-ATP binding induces a conformational change in tTG that inhibits GTPase activity but has no effect on transamidating activity. In this sense, it is clear that the enzymatic activities of tTG are controlled by local concentrations of Mg^{2+}, Ca^{2+}, and nucleotides. Compared to the calcium activated form of tTG, the GTP-bound form of enzyme confers a resistance against proteolysis, suggesting that GTP-binding is important for the protection of tTG from intracellular proteases (Zhang *et.al.,* 1998).

As the physiological levels of Ca^{2+} are insufficient to reverse the inhibition by GTP, a mechanism must exist to control the intracellular cross-linking activity of the tTG. In support of this hypothesis, Lai *et al.* (1997) has reported that in the absence of GTP, the membrane lipid sphingosylphophocholine can serve as a potent activator of tTG cross-linking activity by reducing the calcium requirement for the activation of tTG. Recently, Lai *et al.* (2001) proposed an interesting interplay between nitric oxide (NO) and tTG involving nitrosylation of active site cysteine residues by NO donors. The S-nitrosylation of tTG resulted in a marked inhibition of cross-linking activity and an increased sensitivity to the inhibitory effects of GTP.

A recent study suggested that tTG has protein disulphide isomerase (PDI) activity and can convert completely reduced/denatured inactive RNase A molecule to the native active enzyme by catalysing the formation of correct disulphide bonds (Hasegawa *et.al.,* 2003). The PDI activity of tTG was found to be independent from its transamidating and hydrolytic activity since it did not require Ca^{+2} and was not inhibited by nucleotides.

A more recent report by Mishra and Murphy (2004) has proposed an intrinsic kinase activity for tTG. The tTG was detected in purified fractions of breast cancer cells containing insulin-like growth factor-binding protein-3 (IGFBP-3) kinase activity. The membrane fractions lost their IGFBP-3 activity when antisera to tTG was used to immunoprecipitate tTG from the membrane fractions. Moreover, the

incubation of the breast cancer cells with tTG inhibitors abolished the ability of cell membrane preparation to phosphorylate IGFBP-3, suggesting that tTG can function as an ectokinase in breast cancer cells.

The majority of tTG is found in the cytoplasm, where it could interact with membrane, cytoplasmic, and cytoskeletal proteins. Although tTG does not comprise a hydrophobic leader sequence, the presence of the enzyme is detected in the cell membrane fractions (Griffin *et.al.,* 1978; Barnes *et.al.,* 1985). Sub-cellular fractionation and electron microscopy studies revealed that tTG can exist as a membrane-associated protein, where it cross-links plasma membrane proteins to form sodium docecyl-insoluble aggregates (Slife *et.al.,* 1988; Juprelle-Soret *et.al.,* 1988; Tyrell *et.al.,* 1988a). Recent studies also placed tTG in the nucleus, both as a cross-linking enzyme and as a nuclear GTP-binding protein (Sigh *et.al.,* 1995; Lesort *et.al.,* 1998). As tTG has a high molecular weight, it is possible that enzyme is transported to the nucleus by importin-mediated nuclear transport (Kohler *et.al.,* 1997; Peng *et.al.,* 1999), where it may be involved in the modification of its nuclear substrates such as histones (Ballestar *et.al.,* 1996), retinoblastoma protein (Oliverio *et.al.,* 1997) and transcription factor SP1 (Han *et.al.,* 2000). Accumulating evidence over the past decade indicates tTG can be externalised from cells and deposited into the ECM. The mechanisms and the physiological importance of tTG in the ECM will be discussed in detail later on in the text.

1.9.3 Physiological functions of tissue transglutaminase

Although tTG was the first TG described (Clarke *et.al.,* 1957) and one of the most extensively studied transglutaminases, its precise physiological functions still remain elusive. Emerging evidence indicates that tTG may have roles in diverse biological functions including cell growth and differentiation, cell signalling, receptor mediated endocytosis, insulin-secretion, cell death, adhesion, and wound healing.

1.9.3.1 Role of tissue transglutaminase in cell growth and differentiation

Early investigations suggested a negative correlation between tTG activity and cell proliferation in different types of proliferating cells exhibiting low levels of tTG (Birckbichler and Patterson, 1978). Following studies using human fibroblasts, further demonstrated that treatment of cells with the non-specific tTG inhibitor cystamine, promoted cell growth (Birckbichler *et.al.,* 1981). However, other lines of evidence reported comparable growth rates by cell lines over-expressing tTG, suggesting that the growth inhibition of tTG observed previously, might have been due to non-specific effects of inhibitors (Johnson *et.al.,* 1994). Recent evidence has suggested that tTG may indirectly modulate cell growth through growth factors such as the potent growth inhibitor TGFβ, and hepatocyte growth factor (Kojima *et.al.,* 1993; Katoh *et.al.,* 1996). Findings showing the increase in tTG expression during maturation of human blood monocytes to macrophages, suggested the involvement of tTG in cell differentiation (Seiving *et.al.,* 1991).

In its capacity as a signal transducing G protein Ghα, tTG can mediate signal transduction similar to classical heterotrimeric G-proteins (Nakaoka *et.al.,* 1994; Im *et.al.,* 1997). The GDP-bound Ghα associates with the Ghβ protein to form the holoprotein Gh (Baek *et.al.,* 1996). The binding of Ghβ to Ghα, decreases the affinity of Ghα to GTP, and hence down-regulates the GTPase function of tTG (Baek *et.al.,* 1996; Feng *et.al.,* 1999). Tissue transglutaminase has been shown to interact with the oxytocin (Park *et.al.,* 1998), and thromboxane A_2 receptors (Vezza *et.al.,* 1999), as well as the α_{1B} and α_{1D} adrenergic receptors (Nakaoka *et.al.,* 1994; Chen *et.al.,* 1996). The latter interaction is responsible for the activation of phospholipase C (PLC) δ1 activation (Feng *et.al.,* 1996; Park *et.al.,* 1998), which can hydrolyse phosphatidylinositol diphosphate (PIP_2) to the second-messengers inositol triphosphate, a potent inducer of calcium release from intracellular pools, and diacylglycerol (DAG), activator of serine/threonine kinase protein kinase C. Although it is clear that tTG associates with these receptors and can activate PLC-δ1, the physiological contribution of tTG to these signalling pathways needs to be clarified.

1.9.3.2 Tissue transglutaminase in receptor mediated endocytosis

Several lines of evidence have implicated tTG as a participant in a process known as receptor mediated endocytosis; whereby receptor bound proteins are intaken into the cell in clathrin-coated pits and vesicles. When the aggregation of α2-macroglobulin and its subsequent endocytosis into fibroblasts, were found to be inhibited by a diverse group of tTG inhibitors, the potential involvement of tTG in cross-linking the ligand into its receptor or stabilising the membrane for receptor aggregation was suggested (Davies *et.al.,* 1980). However, later the authors showed that receptor mediated endocytosis was found to be normal in cells that are deficient in transglutaminases, suggesting that their previous observation might be due to the non-specific effects of the TG inhibitors used and that tTG is not obligatory for this process (Davies *et.al.,* 1984). Although the role of tTG in receptor mediated endocytosis of fibroblast remains notorious, in macrophages Schroff *et al.* (1981) showed a direct correlation between levels of transglutaminases and endocytosis. Furthermore, activated macrophages characterised by enhanced phagocytosis were reported to exhibit marked increases in tTG activity than their non-activated counterparts (Murtaugh *et.al.,* 1983). Recently, the endocytosis of immune complexes has also been reported to cause the activation of transglutaminases in mouse macrophages (Abe *et.al.,* 2000).

1.9.3.3 Tissue transglutaminase involvement in Ca^{+2}-mediated stimulus secretion coupling

tTG has also been implicated in stimulus secretion coupling of insulin. The endocrine release of insulin occurs by exocytotic fusion with the plasma membrane and is triggered by a rise in intracellular calcium (Matschinsky *et.al.,* 1996). Early studies proposed a functional role for tTG in calcium-dependent glucose-stimulated insulin release from pancreatic β cells (Sener *et.al.,* 1985; Bungay *et.al.,* 1986). Highly cross-linked transglutaminase-mediated polymeric aggregates have been detected in sedimented material of islet homogenates during investigations into the endogenous substrate proteins of islet transglutaminase (Bungay *et.al.,* 1986). Later

studies implicated tTG in insulin receptor aggregation, internalisation and intracellular processing, through cross-linking receptors in the area of clathrin-coated pits, thereby participating in the regulation of insulin action in target tissues (Baldwin *et.al.,* 1980; Haigler *et.al.,* 1980). Recently work carried out on tTG null mice (tTG-/-) reported that the tTG -/- mice phenotype resembles the MODY (maturity-onset diabetes of young) patients, in that they show glucose intolerance with hyperglycaemia due to impairment in glucose-stimulated insulin secretion (Bernassola *et.al.,* 2002).

1.9.3.4 Involvement of tissue transglutaminase in cell death

Apoptosis is one of the two mechanisms by which cell death occurs in an intrinsically programmed manner. Apoptosis is characterized by distinctive morphologic changes in the nucleus and cytoplasm, such as chromatin cleavage, and the packaging of the cellular contents into vesicles, which are phagocytosed by neighbouring cells or macrophages. This mode of cell death serves as a balance to mitosis in regulating the size of animal tissues and in mediating pathologic processes associated with tumour growth and tissue remodelling (Green and Reed, 1998). The initial report on tTG as a mediator of apoptosis came from Fesus *et al.* (1987), where the levels of tTG mRNA, protein, and tTG-catalysed isopeptides were found to be increased in cells undergoing apoptosis during the involution of lead nitrate-induced liver hyperplasia. The detection of tTG-dependent cross-linking in the detergent insoluble apoptotic bodies has been shown *in vivo* and *in vitro* apoptosis models (Fesus *et.al.,* 1989; Knight *et.al.,* 1993). The activation of tTG is thought to be responsible for the stabilising the apoptotic cells by cross-linking the cytoplasmic and membrane proteins, prior to their clearance by phagocytotic cells (Fesus, 1998). The human neuroblastoma cells transfected with a tTG cDNA showed a marked increase in cell death, conversely stable transfectants with an anti-sense tTG cDNA demonstrated a pronounced decrease in apoptosis, confirming the involvement of tTG in cell death (Melino *et.al.,* 1994). In another instance, however, over-expression of tTG in transfected fibroblasts under the control of inducible tetracycline regulatory system, did not lead to an

increased rate of cell death in these cells (Verderio *et.al.,* 1998). In addition, using tTG-/- mice, evidence has been obtained suggesting that tTG is not obligatory for the apoptotic mechanism, as these mice show no significant differences in induction of apoptosis (De Laurenzi and Melino, 2001; Nanda *et.al.,* 2001). Contradicting these results were the recent finding that the increased tTG expression may function to provide protection against apoptotic insults, thus ensuring cell survival by preventing apoptosis via a GTP-binding mechanism (Antonyak *et.al.,* 2001, 2002 and 2003). Together, these results indicate that tTG could be involved in apoptosis only in specific cell types, where it acts as a mediator for apoptosis. In other instances, the specific expression of tTG in dying cells seems to be an epiphenomenon due to disruption of calcium homeostasis.

The tTG enzyme has also been implicated in the pathological process of necrosis that occurs when the cell is deprived of its vital processes by physical or chemical lesions, induced by external factors such as acute physical or chemical damage. Necrosis results in loss of membrane integrity, swelling of the cell, and rupture release of the cellular contents into the extracellular environment inducing an intense inflammatory reaction. Gilad *et al.* (1985) reported an increase in the exogenous and endogenous tTG activity in sympathetic and sensory neurons during injury induced necrotic cell death. Later studies have implicated a correlation between elevated levels tTG-cross-linked proteins and liver cell necrosis (Zatloukal *et.al.,* 1992; Fukuda *et.al.,* 1993). Recently, using a model involving electroporation to cause necrotic cell death, tTG has been shown to lead the formation of highly cross-linked proteinaceous shells from intracellular proteins (Nicholas *et.al.,* 2003). Formation of these structures was found to be dependent on elevated levels of intracellular calcium, but was independent of intracellular proteases. In the same study, the authors demonstrated that mechanical wounding of cell monolayers by scratching led to the redistribution of tTG activity to the extracellular matrix. The modification of proteins in the intracellular and extracellular spaces by tTG may serve to stabilize tissues post-trauma, and thus contribute to the maintenance of tissue integrity.

1.9.4 Human diseases associated with tissue transglutaminase

In the past few decades, much attention has been focused on the potential role of tTG in the pathogenesis of several disease states. The inappropriate activation of tTG that leads to altered protein-cross-linking and GTPase/ATPase activity has been suggested to contribute to a number of different pathologies, including coeliac disease, fibrosis, cancer and neurodegenerative diseases in humans.

1.9.4.1 Tissue transglutaminase and coeliac disease

An increasing number of studies have been carried out in the last few years on the possible involvement of transglutaminase activity in coeliac disease (CD), which is an enteropathy caused by sensitivity to gliadin, the reactive component of wheat protein gluten. The disease is characterised by a T-cell mediated reaction to gliadin resulting in damage to the intestinal epithelium and ensuing effacement of villi to produce a flat mucosa (Trier, 1991). Consequently, patients with CD usually suffer from difficulty in absorption leading to malnutrition. Another factor that is always associated with CD is the presence of specific auto-reactive antibodies in the sera (Dieterich *et.al.,* 1997). Tissue transglutaminase is expressed at low levels in the healthy small intestine, however, tTG expression in jejunal biopsies of CD patients is shown to be elevated by nearly three fold suggesting that this activity could be responsible for CD (Bruce *et.al.,* 1985).

Since gliadin possesses a very large number of glutamine residues, it can acts as a good substrate to tTG. Porta *et al.* (1990) has shown that gliadin and its proteolytic fragments were capable of acting *in vitro* as substrates for guinea pig liver tTG. The enzyme catalysed the cross-linking reactions between glutamine endoresidues and either free amines or lysine endoresidues of gliadin. Thus, it is possible that tTG might cross-link itself with gliadin and act as a hapten for the formation of antibodies against gliadin. This hypothesis is plausible as previously detected specific auto-reactive antibodies were shown to be auto-antibodies targeted against tTG (Dieterich *et.al.,* 1997). It has also been reported that the high levels of anti-

tTG antibody titter is strictly dependent on the consumption of wheat products in the diet.

Based on a series of *in vitro* experiments, the possibility of deamidation of gliadin by tTG has been cited for generating neoepitopes of gliadin. The deamidation of gliadin can take place in the acidic environment of the stomach or alternatively can be catalysed by tTG in an environment bereft of amine donors. The *in vitro* deamidation of gliadin by tTG treatment significantly increases the ability of gliadin fragments to stimulate the proliferation of gliadin-specific T cells (Molberg *et.al.,* 1998; Van de Wal *et.al.,* 1998). From these findings, it is evident that tTG contributes to the development of coeliac disease on two levels. In the first of which, the enzyme forms immunoreactive complexes after forming a complex with gliadin initiating the T-cell and then B-cell responses. Alternatively, tTG mediates deamidation of glutamine residues in gliadin, which stimulates T-cell response against gliadin.

1.9.4.2 Tissue transglutaminase and fibrosis

Given that transglutaminases create covalent ε-(γ-glutamyl) lysine cross-links they are prime enzymes in the reconstitution of tissue integrity damaged by traumatic or other pathological injuries. In recent years, pioneering work indicated tTG to be involved in the extracellular matrix organisation which is important in cell-matrix interactions (Aeschlimann *et.al.,* 1991; Barsigian *et.al.,* 1991; Martinez *et.al.,* 1994). Perturbation in the formation of the extracellular matrix has been implicated in a number of pathological conditions including fibrosis, which is the production of fibrous connective tissue as a consequence of chronic inflammation or healing. Fibrosis replaces lost parenchymal tissue, resulting in scar formation. Recent evidence implicated tTG in fibrotic conditions of various tissues, such as the liver (Mirza *et.al.,* 1997; Piacentini *et.al.,* 1999; Grenard *et.al.,* 2001), heart (Small *et.al.,* 1999; Zhang *et.al.,* 2003), and kidney (Johnson *et.al.,* 1997, 1999 and 2003). The involvement of tTG in the fibrotic process was first reported in paraquat-induced pulmonary fibrosis with raised tTG levels (Griffin *et.al.,* 1979). It has been suggested that tTG may be involved in stabilizing the fibrotic lesions formed

during hepatic fibrogenesis, since an increase in tTG gene expression has been recorded during hepatic injury and fibrosis in rats (Mirza *et.al.,* 1997). Immunohistochemical analysis of fibrotic livers has demonstrated that transglutaminase-mediated cross-linking occurs in the liver extracellular matrix during the early and inflammatory stages of liver fibrosis (Grenard *et.al.,* 2001). In the heart, directed cardiac overexpression of Gh/tTG was shown to cause cardiac hypertrophy, diffuse interstitial fibrosis, and depressed ventricular function at rest (Small *et.al.,* 1999; Zhang *et.al.,* 2003). An association of tTG with fibrosis was further indicated by its upregulation in an experimental renal fibrosis model (Johnson *et.al.,* 1997). It was proposed that the enzyme had important physiologic functions in disease development by stabilizing the increased ECM by protein cross-linking. Later work by same authors demonstrated that the tubular cells were the major site of tTG synthesis, however, both mesangial and interstitial cells also contributed the elevated levels of tTG in chronic renal disease (Johnson *et.al.,* 1999 and 2003). In general, it is likely that the leakage of tTG into extracellular environment can contribute to the development of fibrotic conditions by increasing the resistance of deposited matrix to breakdown which in turn leads to the increased deposition of extensive scar tissue.

1.9.4.3 Tissue transglutaminase and cancer

Alterations of tTG expression levels could also contribute to the development of tumour progression and the malignant phenotype. A comparison of neoplastic cells with their normal counterparts has identified a decrease in transglutaminase activity, which is reflected as a reduction in ε-(γ-glutamyl) lysine isopeptide bonds in malignant cells (Birckbichler and Patterson, 1980). Indirect immunofluorescence studies correlated the changes in enzyme activity with the reduced amount of tTG antigen in the particulate-fraction of transformed cells. Similarly, induction of hepatocellularcarcinomas in rats by treatment with chemicals resulted in a reduction in transglutaminase activity, which was accompanied by redistribution of the enzyme to the particulate fraction of the cell (Barnes *et.al.,* 1985). A further decrease in tTG activity was detected in hamster osteosarcomas following their

metastasis, indicating a reduced ability of cells to cross-link the basal membranes and thus facilitating the invasion of vascular system. Another study noted that transglutaminase activity was reduced by some 65% in chemically induced rat hepatocellular carcinomas when compared to normal rat livers. The ratio of the activity of the cytosolic tTG enzyme to that of the membrane-bound enzyme was shown to be higher in normal liver (Hand *et.al.,* 1988). The inverse correlation between tTG activity and tumour metastatic potential, plus the redistribution of enzyme to the particulate fraction, has subsequently been confirmed by other workers (Delcros *et.al.,* 1986; Hand *et.al.,* 1990; Knight 1991; Beninati *et.al.,* 1993).

Considering the reduced expression of tTG in both murine and human tumours, Johnson *et al.* (1994) investigated the role of tTG in tumour progression using cDNA transfection technology. The highly malignant hamster fibrosarcoma cell line, Met B, was transfected with a human tTG cDNA construct and the transfected cells were then reintroduced into the animal. *In vitro*, transglutaminase transfected clones showed no significant difference in their growth rate, cell morphology or levels of spontaneous apoptosis. However, when compared to non-transfected and transfected control cells, the Met B clones expressing exogenous tTG exhibited a reduced incidence of primary tumour formation, which is accompanied by an increase in cell adhesion to tissue culture plastic and fibronectin coated surfaces. This finding supports the hypothesis that low tTG levels may make the ECM susceptible to mechanical and proteolytic degradation, and such a destabilisation of ECM might favour tumour cell invasion.

The decline of tTG activity in tumours could potentially act as a prognostic biomarker (Birckbichler *et.al.,* 2000); however, analysis of different tumour cell lines demonstrated no apparent correlation between tTG expression and the malignant potential of the cells (Takaku *et.al.,* 1995). The investigation of tTG expression levels in various tumour cell lines has suggested that tTG may not be a tumour related marker as it is expressed in high levels in tumour cells including the liver neoplastic nodules (Denk *et.al.,* 1984), and drug-resistant human breast carcinoma cells (Mehta, 1994). Given the conflicting evidence, the role of tTG in

tumour growth and progression is difficult to depict, yet, tTG might be important in certain aspects of the process depending on the type and stage of the neoplasm.

1.9.4.4 Tissue transglutaminase and neurodegenerative diseases

Evidence has been beginning to emerge that tTG may also be important in neurodegenerative diseases. To date, there are eight genetically inherited neurodegenerative diseases that have been characterised by a progressive impairment of coordination and motor neuron degeneration associated with the expansion in $(CAG)_n$ repeats. The CAG tri-nucleotide repeat expansion within the affected gene results in proteins with abnormal polyglutamine (Q_n) expansions. These proteins form insoluble intracellular and cytoplasmic inclusions which lead to neuronal death and progressive neurodegeneration (Kim *et.al.,* 2002). Peptides containing polyglutamine stretches have been shown to be potent substrates for tTG (Kahlem *et.al.,* 1996). Indeed, the ability of polyglutamines to act as a tTG substrate improves with the increasing polyglutamine length (Gentile *et.al.,* 1998). These findings may support the notion that the cross-linking and/or polyamination of Q_n domains by tTG is important in the cause of $(CAG)_n$ /(Q_n) expansion diseases.

The involvement of tTG in Huntington's disease (HD) has been suggested based on the demonstration of elevated tTG activity in affected regions of diseased brains (Lesort *et.al.,* 1999). HD is an autosomal dominant disease that is caused by CAG expansions in the relevant gene encoding for huntingtin protein (Lesort *et.al,* 2000). Huntingtin is found in the aggregates that characterise HD (Becher *et.al.,* 1998) and acts as a substrate for tTG *in vitro* (Kahlem *et.al.,* 1996). Karpuj *et al.* (1999) have proposed that tTG catalysed cross-linking of huntingtin protein may be involved in the formation of nonamyloidogenic nuclear inclusions found in the HD brain. Recent experiments on transgenic mice model of HD reported a prolonged survival and decreased abnormal movements in animals in response to the administration of the tTG inhibitor cystamine (Karpuj *et.al.,* 2002).

tTG has been found to be elevated in Alzheimer's disease, the most common age-related neurodegenerative disorder. Alzheimer's disease (AD) is characterised by

the presence of two types of protein aggregates; extracellular neuritic senile plaques, and intra-neuronal neurofibrillary tangles. As different isoforms of TGs are found to co-localise with the plaques and tangles in the brains of AD patients, it is likely that TGs contribute to the formation of these aggregates (Lesort *et.al.,* 1999). Later, this was confirmed by *in vitro* studies that have shown the components of plaques and tangles as the substrates for TGs. For example, tTG can utilise the β-amyloid, which is found in fibrillular from in plaques, in the formation of insoluble polymers (Rasmussen *et.al.,* 1994). In addition, tau the major component of neurofibrillary tangles was demonstrated to act as a substrate for tTG and form both filamentous and insoluble aggregates (Murthy *et.al,* 1998). These observations suggested that tTG might participate in the formation of plaques and tangles through cross-linking and/or polyamination, which in turn leads to the pathogenesis of AD.

With regard to the genetic basis of neurodegenerative disorders, it has been suggested that tTG, like many highly expressed genes in the central nervous system, undergoes alternative processing. The alternative splicing of tTG gene results in a short splice variant of tTG that encodes for a truncated enzyme lacking the GTP-binding site (Citron *et.al.,* 2001). The short isoform of tTG has an increased cross-linking activity as it is not negatively regulated by GTP. The elevated expression of tTG and transcription of short splice variants result in unregulated cross-liking and are associated with increased neuronal loss in affected regions in the demented brain (Citron *et.al.,* 2002). The full spectrum of tTG participation in neurodegeneration awaits further elucidation, however the alternative splicing might well be the critical transcriptional regulatory process that becomes disrupted in the early onset of the neurodegeneration.

1.9.5 Tissue transglutaminase in extracellular environment

Although tTG lacks the hydrophobic signal peptide which would indicate secretion by conventional endoplasmic reticulum and Golgi apparatus route, accumulating evidence points to its presence on the cell surface and in the ECM (Martinez *et.al.,* 1994; Aeschlimann and Paulson, 1994; Gaudry *et.al.,* 1999a, b; Akimov *et.al.,*

2000 and 2001; Balklava *et.al.,* 2002; Upchurch *et.al.,* 1987; Lorand *et.al.,* 1988; Aeschlimann *et.al.,* 1991; Nunes *et.al.,* 1997; Verderio *et.al.,* 1999).

The physiological implication of tTG in the extracellular environment was proposed to be mainly reconstruction and/or stabilisation of the fine structure of ECM. Battaglia and Shaprio (1988) has suggested for the first time that cell surface tTG is likely to play an important role in the stabilisation of extracellular material as the transglutaminase inhibitors disorganised the fertilisation envelope in sea urchin eggs. Since then a number of the major matrix proteins have been identified as *in vitro* glutaminyl substrates for tTG, including fibronectin (Tamaki and Aoki, 1981; Mosher *et.al.,* 1991), fibrinogen (Chen and Doolittle, 1971; Cottrell *et.al.,* 1979; Guadiz *et.al.,* 1997), osteonectin (Aeschlimann *et.al.,* 1995; Hohenadl *et.al.,* 1995), osteopontin (Prince *et.al.,* 1991; Sorensen *et.al.,* 1994), osteocalcin (Kaartinen *et.al.,* 1997), collagens (Mosher,1984; Juprelle-Soret *et.al.,* 1988, Kleman *et.al.,* 1995; Esterre *et.al.,* 1998), vitronectin (Sane *et.al.,* 1988), laminin-nidogen complex (Aeschlimann *et.al.,* 1991), and elafin (Nara *et.al.,* 1994). Although the extracellular space provides optimum conditions for tTG cross-linking activity such as high calcium concentration and low concentration of inhibitory factors such as GTP and zinc, it is not clear if all these potential substrates are cross-linked by tTG *in vivo*.

In a study by Aeschlimann and Paulsson (1991), the potential role of tTG transglutaminase in crosss-linking of laminin-nidogen complex was investigated using [^{3}H]-putrescine as the amine donor substrate. Laminin is the most abundant non-collagenous protein of basement membrane and is present in the tissue as an equimolar complex with the protein nidogen (Paulsson *et.al.,* 1987). A comparison of putrescine incorporation in nidogen and in tTG itself showed similar incorporation kinetics to that of N,N-dimethlycasein, the radioactive glutamyl donor substrate. The laminin-nidogen complex isolated from the basement membrane of the murine tumor was found to incorporate half as much amine as purified nidogen. SDS-PAGE analysis and electron microscopy of the reaction products showed that the covalently cross-linked aggregates formed by tTG treatment were organised in a head to head arrangement similar to that described for calcium-induced self-aggregation. Thus, it is likely that tTG action *in vivo* leads

to a covalently cross-linked laminin-nidogen complex and participates in the stabilisation of the basement membrane underlying the epidermis.

The extracellular tTG has also a potential role in tissue mineralisation, stabilisation of dermo-epidermal junctions, cell-matrix interactions that affect cell spreading and migration and wound healing. Furthermore, the secreted enzyme contributes to the covalent modification and activation of several growth factors including transforming growth factor-β_1 (TGF-β_1) in the ECM (Lorand and Graham, 2003).

The secretion of tTG into the ECM of skeletal tissues is strictly regulated and crucial for connective and bone tissue remodelling (Aeschlimann *et.al.,* 1996). For example, the chondrocyte differentiation and cartilage calcification in endochondral bone formation and in maturation of tracheal cartilage were found to be correlated with the expression and the externalisation of tTG (Aeschlimann *et.al.,* 1993). In the development of endochondral bones, tTG initially appears intracellullarly in the proliferation/maturation zone, and is then externalised from hypertrophic chondrocytes and participates in cross-linking prior to mineralisation. In trachea, maturation of cartilage due to minerilisation is accompanied by expression of tTG at the border of the hydroxyapatite deposits. The authors later detected the γ-glutamyl- ε-lysine cross-link reaction product using a cross-link specific antibody in cryosections of rat bone and cartilage (Aeschlimann *et.al.,* 1995). The incorporation of a synthetic transglutaminase substrate in cultured tracheal explants revealed enzyme activity in a ring-like pattern in the pericellular matrix of chondrocytes. The cross-linked osteonectin containing complexes from chondrocyte matrix revealed a similar molecular weight pattern to the *in vitro* cross-linking of osteonetin by tTG, suggesting the tTG-catalysed cross-linking, such as cross-linking of osteonectin *in situ*, is a physiological mechanism for cartilage and bone matrix stabilisation.

Elafin, a skin-derived inhibitor of serine proteases, contains a cementoin achoring sequence, which serve as a substrate for tTG *in vitro* and can be cross-linked to laminin. Nara *et al.* (1994) has reported the presence of covalently-cross-linked aggregates of cementoin-elafin in human trachea and in elastic fibres of various tissues. Given that elafin inhibits the elastase-mediated tissue proteolysis, the cross-linking of elafin by tTG is likely to protect the cartilage and elastic fibres from

undesirable protease attacks, and increase the mechanical strength of these tissues. The involvement of tTG in stabilisation of connective tissue was also reported by Kleman *et al.* (1995) using human rhabdomycosarcoma cell cultures. This cell line was characterised by synthesising a highly insoluble ECM matrix of collagen V/XI fibrils. However, when the cells were cultured in the presence of tTG inhibitors, a drastic increase in collagen solubility was observed. The irreversible cross-linking of collagen V/XI fibrils by tTG observed in cell culture suggests that tTG may play a role in stabilisation of extracellular matrices in the early steps of collagen fibrillogenesis.

Tissue transglutaminase appears to play an important role in the stability of dermo-epidermal junctions, a specialised structure that fortifies the attachment of epidermis to dermis. The integrity of the dermo-epidermal junction is largely guaranteed by anchoring fibrils (Burgeson, 1993). The characterisation of anchoring fibrils identified type VII collagen as the major if not the sole structural component of anchoring fibrils. Analysis of biopsies from patients receiving keratinocyte autographs showed that collagen VII in anchoring fibrils is a potential substrate for tTG. The occurrence of tissue transglutaminase cross-linking sites on anchoring fibrils coincided with the clinical stability of skin graft, suggesting its importance in the stability of dermo-epidermal junctions (Raghunath *et.al.,* 1996b). Tissue transglutaminase is operative at the dermo-epidermal junctions (Aeschlimann and Paulsson, 1991; Aeschlimann *et.al.,* 1995) and underlying dermal structures, particularly the elastic fibrillar apparatus (Raghunath *et.al.,* 1996a; Trask *et.al.,* 2001). The elastic fibers are composed of two morphologically distinct components; an amorphous core of elastin and a peripherial mantle of 10-12nm microfibrils (Qian and Glanville 1997). Microfibrils are found in many tissues and at dermo-epidermal junctions. In skin, microfibrils anchor the epidermal cells to elastic fibers in the dermis by forming a continuous link with the elastin-associated microfibrils (Davis, 1994). Microfibrillar proteins fibrillin-1, fibrillin-2 and micro-fibril-associated glycoprotein-1 (MAGP-1) have been identified as the constituents of microfibrils. The fibrillins are the major components of microfibrils and are characterised by an extended domain structure that includes blocks of epidermal-growth like repeats (Raghunath *et.al.,* 1996b).

The extraction of microfibrils from amniotic membranes revealed the presence of transglutaminase-derived γ-glutamyl- ε-lysine cross-links located at this extended domain structure, known to have a periodic pattern of amine acceptor sites (Oian and Glanville 1997). While these results established the presence of cross-linked homopolymers of fibrillins, the other component of microfibrils has also been shown to be a substrate of tTG. MAGP-1 is a small molecular weight protein associated with the extracellular matrix microfibrils. Biochemical studies have shown that MAGP-1 is a glutaminyl substrate for transglutaminase-catalysed cross-linking and forms high molecular weight aggregates, which are resistant to reduction or denaturation (Brown-Augsburger *et.al.,* 1994). The final evidence for the role of tTG cross-linking in tissue interphases has come from the analysis of cryosections from human and monkey eyes, which revealed that the stability of ocular connective tissue correlated with the transamidation of zonular fibers (Raghunath *et.al.,* 1999). In the light of these data it is likely that tTG may covalently stabilise the anchoring fibrils and microfibrils to form the dermo-epidermal junction that are resistant to mechanical and proteolytic break-down.

Recent experiments indicate that tTG might be involved in the activation of latent transforming growth factor-β (TGF-β). TGF-β plays a pivotal role in a diverse range of cellular responses, including proliferation, differentiation, migration, and death (Zhu and Burgess, 2000). The cytokine TGF-β is synthesised from cells as a biological inactive precursor protein consisting of the mature TGF-β associated with a propeptide called latency associated peptide (LAP), and a latent TGF-β binding protein (LTBP). This physiologically inactive complex is referred to as large latent TGF-β complex and it is unable to bind to TGF-β receptors (Massague, 1990). The dissociation of the mature enzyme from LAP is required for the release of activated form of TGF-β (Lyons *et.al.,* 1988). The LTBP is not necessary to render the growth factor latent; however, it plays an important role in targeting TGF-β into the ECM (Taipale *et.al.,* 1994). There are four members in the LTBP family that display characteristic EGF-like repeats, three protein domains containing eight conserved cysteine residues and a mixed domain (Zhu and Burgess, 2000). The structural similarity of LTBPs with microfibrillar proteins suggested the involvement of tTG in the storage and regulation of the extracellular

pool of latent TGF-β. The study on bovine endothelial cells revealed that the activation of cell-associated latent TGF-β was inhibited by seven different inhibitors of transglutaminase as well as a neutralising antibody against bovine tTG (Kojima *et.al.,* 1993). *In vitro* studies demonstrated that both large latent complex and LTBP-1 of large complex are substrates for tTG, and the inhibition of tTG severely attenuates the incorporation of LTBP-1 into the matrix. The amino terminal region of the LTBP-1 comprises the tTG reactive site and mediates its association with the extracellular matrix, whereas LAP interacts with the carboxy-terminal of LTBP-1 (Nunes *et.al.,* 1997). The direct evidence for tTG and LTBP-1 association came from a study which utilised a transfected cell system over-expressing the tTG. Immunohistochemical data revealed that induced expression of tTG was accompanied by an increased rate of LTBP-1 deposition into the ECM. The co-distribution of two proteins, particularly at the cell surface and the cell-cell contacts, was further confirmed by electron microscopy (Verderio *et.al.,* 1999). Recently, tTG was shown to participate in the incorporation of latent TGF-β into the extracellular matrix of aging chondrocytes (Le *et.al.,* 2001). These results suggest that tTG might play an important role in targeting the latent TGF-β complex to the ECM by cross-linking the LTBP of the latent complex to the matrix proteins. Accordingly, a pool of cytokine can accumulate in the ECM, from which it is released by proteolysis. In support of this hypothesis, Szondy *et al.* (2003) reported that tTG -/- mice show a deficiency in TGF-β activation leading to the development of splenomegaly and glomerulonephritis.

1.9.5.1 Fibronectin

Fibronectin (FN) is a well-known substrate for tTG, however the interaction between fibronectin and tTG has shown to be independent from the enzyme's cross-linking activity (Fesus *et.al.,* 1986). Fibronectin is a major protein of blood and tissues. Being a principal component of the extracellular matrix, it is now clear that FN influences a variety of physiological processes such as tissue remodelling during embryogenesis and wound healing (Mosher, 1984). Fibronectin is a glycoprotein that exists in a soluble protomeric form in micromolar concentration

in blood plasma and in an insoluble multimeric form in fibrillar extracellular structures and basement membranes of most tissues. Soluble fibronectin also exists in amniotic fluid, seminal fluid, joint fluid, and cerebrospinal fluid (Mosher, 1984). Fibronectin usually exists as a dimer, consisting of similar but not necessarily identical chains, each of which has a molecular size of 250 kDa. The FN dimer is formed by a pair of disulphide bonds that joins the carboxy terminal end of the chains. In each chain, there are about 30 intra-chain disulphide bonds as well as two sulfhydryl groups, which can participate in intermolecular disulphide bonding (Romberger, 1997). FN is a mosaic protein, which comprises a series of discrete repeating units of amino acid homology termed Type I, II, and III modules (figure 1.3). The domain structure of FN contains 12 type I modules, 2 type II, 15 to 17 (depending on splicing) type III, and a variable (V) sequence that is not homologous to other parts of fibronectin. These modules can be grouped into larger functional units that bind to cell surfaces, collagen, heparin, and fibrin. The 2 type III modules that undergo alternative splicing events are called ED-A (extradomain-A) and ED-B (Schwarzbauer, 1991). Cellular fibronectin is synthesised locally in tissues and contains variable amounts of either or both ED-A and ED-B. However, plasma fibronectin, synthesised by the liver hepatocytes, contains neither ED-A nor ED-B. Furthermore, the plasma dimers of fibronectin contain only one subunit with V region, whereas almost all cellular fibronectin subunits contain this region (Schwarzbauer, *et.al.,* 1989).

Fibronectin functions from within a fibrillar extracellular matrix. Most adherent cells continuously produce FN and deposit it to the ECM. The deposition and assembly of FN in the ECM is a cell-mediated multistep process that proceeds from initiation through elongation to stabilisation (Schwarzbauer and Sechler, 1999; figure 1.4). Each step is highly regulated requiring multiple fibronectin domains for binding to cells, to other fibronectin molecules, and other ECM components.

In the first step, FN binds to specific sites on the surface of substrate-attached cells, which have been termed the matrix assembly sites. This binding depends on interactions between amino-terminal 70 kDa region of the protein (matrix-assembly domain of fibronectin) and cell surface integrin receptors as the removal of any of

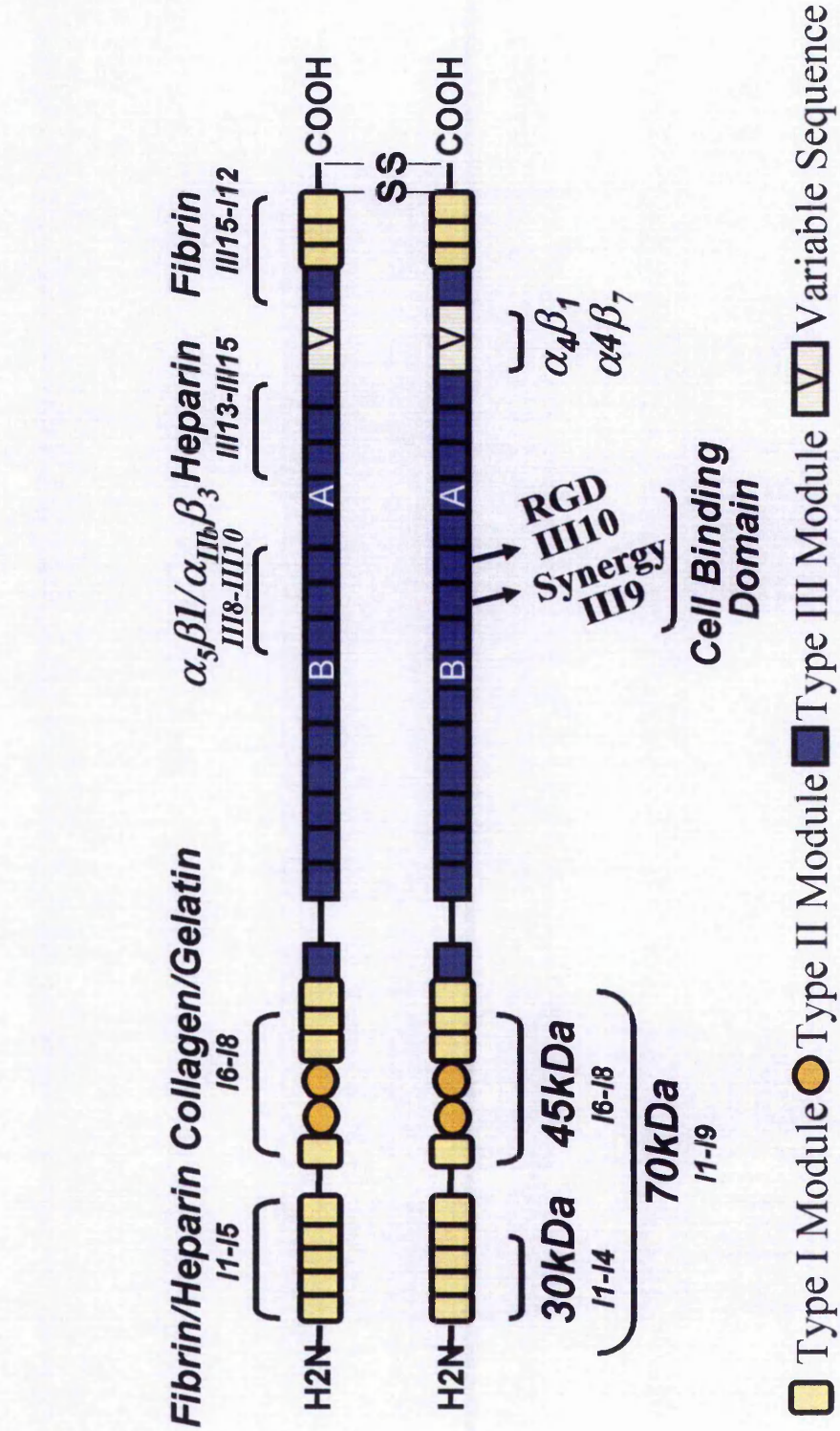


Figure 1.3 Domain structure of fibronectin

the modules at 70 kDa region or the monoclonal antibodies against integrins inhibit the assembly of FN (Sottile, 1991; Akiyama *et.al.,* 1989). Fibronectin binds to $\alpha_5\beta_1$ and $\alpha_{IIB}\beta_3$ integrins through a cell adhesive site comprising modules III8-III10 (Aota *et.al.,* 1991). Together the Arginine-Glycine-Aspartic acid (RGD) site in III10 and synergy site in III9 are the most critical sites in the integrin mediated matrix assembly (Schwarzbauer and Sechler, 1999). Recently, a novel RGD-independent fibronectin assembly pathway was shown to initiate in Ramos B lymphoma and CHO(B2) α4 cells. This novel pathway is initiated by $\alpha_4\beta_1$ integrin binding to the alternatively spliced V region of fibronectin (Sechler *et.al.,* 2000) . The fibronectin molecule also comprises adhesive sites for fibrin, heparin, collagen and $\alpha_4\beta_7$ integrins (figure 1.3). A glutamine residue close to amino-terminal site of FN serves as a transglutaminase site for activated plasma transglutaminase (FXIIIa). The cross-linking mediated by FXIIIa is important for the incorporation of fibronectin into fibrin clots during the blood clotting process (Muszbek *et.al.,* 1999).

The elongation step starts with integrin clustering and binding of additional fibronectin. Through interaction among or between fibronectin molecules, the cell-bound protomeric fibronectin is converted into disulphide-stabilised multimers (McKeown-Longo and Mosher, 1984; Chen and Mosher, 1996). Most of the fibronectin binding sites involved in fibril elongation have been mapped into amino-terminal repeats I1-5, the first two modules of type III repeat, and COOH-terminal heparin domain (Sottile *et.al.,* 1991; Chernousov *et.al.,* 1991; Bultmann *et.al.,* 1998).

In the final step, the binding site on the cell surface is regenerated as mature fibrils are gradually converted into a detergent-insoluble form, yielding stable matrix (McKeown-Longo and Mosher, 1983). It is likely that the protomeric form of soluble fibronectin, an inactivated state, is activated by integrin binding and that leads conformational changes allowing fibronectin self-association at cell surface (Schwarzbauer and Sechler, 1999).

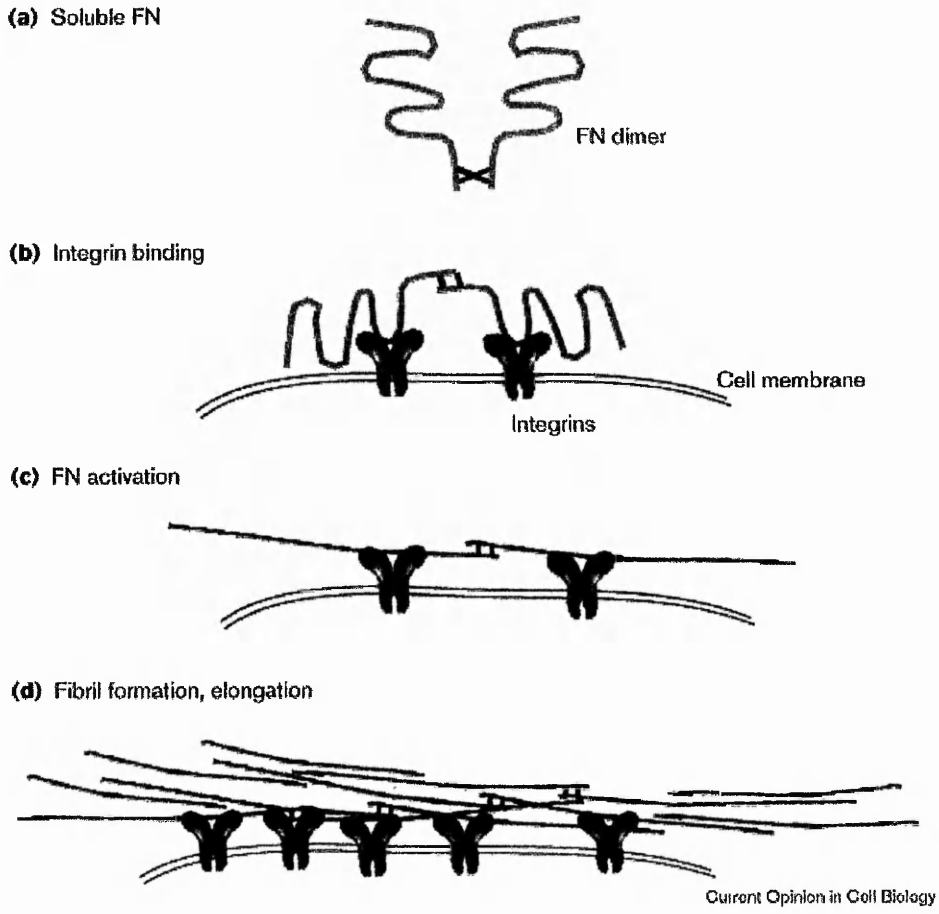


Figure 1.4 A model for fibronectin assembly

Illustration of the multistep process of fibronectin assembly proceeding from initiation (a,b), through elongation (c-d), and stabilisation (d) (Schwarzbauer and Sechler, 1999).

1.9.6 The cell surface tTG and cell adhesion

The mechanism of tTG secretion remains unknown, however, the enzyme appears to be secreted from the cells in a controlled manner (Gaudry *et.al.,* 1999a; Upchurch *et.al.,* 1987; Balklava *et.al.,* 2002). The N-terminal β-sandwich domain and the presence of a non-proline *cis* peptide bond at Tyr274 as well as an intact active site, Cys277, are important in the externalisation of tTG (Gaudry *et.al.,* 1999a; Balklava *et.al.,* 2002).

Preliminary indications of tTG on cell surface came from cell fractionation studies using lung and liver tissues (Griffin *et.al.,* 1979; Slife *et.al.,* 1986; Tyrrell *et.al.,* 1988). Homogenates from lung tissue showed that a large amount of enzyme is present in particulate fractions (Griffin *et.al.,* 1978 and 1979). The detergent-insoluble material isolated from confluent cultures of human lung fibroblasts also showed high amounts of tTG antigen and activity (Birckbichler and Patterson, 1980). Later, the constituent of tTG particulate fractions has been revealed by electron microscopy. The pelleted fraction of recovered enzyme was found to consist of large membrane sheets with associated extracellular matrix and free collagen fibres (Juprelle-Soret *et.al.,* 1988). The externalisation of tTG into extracellular matrix of lung has been shown to take place before the maturation of the organ, suggesting the contribution of tTG to lung development (Schittny *et.al.,* 1997). The liver is the organ where tTG was first isolated (Sarkar *et.al.,* 1957). Tissue homogenates from rat liver have shown that transglutaminase activity was predominantly associated with the plasma membrane fraction (Slife *et.al.,* 1985). In a following study the authors have shown that this plasma membrane fraction contained substrates for tTG and that the substrates are part of a large molecular weight complex which is not dissociated by SDS and disulphide reducing agents (Slife *et.al.,* 1986; Tyrrell 1988). Additional studies showed that the particulate tTG and the large molecular weight complex are specifically associated with membrane fragments derived from the lateral plasma membrane of the hepatocyte (Tyrrell *et.al.,* 1986). Since these fragments were also enriched in junctional elements which contain sites of cell to cell interaction, it has been proposed that tTG may

form covalently cross-linked protein matrices which can enhance the adhesiveness of the cells (Slife *et.al.,* 1986; Tyrrell 1986). Evidence of cell surface tTG co-ordinating the interaction between cells and ECM began to accumulate rapidly. Pioneer studies have shown that transglutaminase cross-linking of matrix proteins promoted cell adhesion (Fesus *et.al.,* 1986; Sane *et.al.,* 1991; Martinez *et.al.,* 1994), and the induction of tTG in several cultured cell lines led to an increase in cell adhesives (Cai *et.al.,* 1991; Gentile *et.al.,* 1992). For example, the cross-linking of substrate-immobilised fibronectin by cell associated tTG served to firmly anchor the endothelial cells to the basement membrane (Martinez *et.al.,* 1994). Furthermore, the tTG transfected fibroblasts cells exhibited an extended and much flattened morphology reflecting increased cell adhesion of cells to the substratum (Gentile *et.al.,* 1992).

Other studies examined the importance of tTG in cell adhesion by down-regulating tTG synthesis (Martinez *et.al.,* 1994; Jones *et.al.,* 1997). The culturing of endothelial cells in the presence of non-peptidyl inactivators specific for transglutaminases rendered the cells susceptible to trypsin-induced detachment from the substratum (Martinez *et.al.,* 1994). In a following study, Jones *et al.* (1997) clearly showed that induction of a decrease in tTG expression via transfecting a human umbilical endothelial cell line with an anti-sense RNA resulted in susceptibility to detachment by proteolytic enzymes and reduced cell spreading.

Recently, a close association of the cell-surface related tTG with β_1 and β_3 integrins has been shown to happen in focal adhesion sites, where fibronectin fibril assembly is taking place (Gaundry *et.al.,* 1999b; Akimov *et.al.,* 2000; Takahashi *et.al.,* 2001; Akimov and Belkin, 2001).

Integrins are the major cell-surface receptors that mediate cell-extracellular matrix contact. The interaction between cells and the ECM is important in a wide range of biological phenomena, including cell proliferation, suppression of apoptosis, cell migration, regulation of gene expression, differentiation, blood cloting, and wound healing (Critchley *et.al.,* 1999). Structurally defined adhesion sites between cultured cells and the ECM were described using interference-reflection microscopy and termed as focal contacts or focal adhesions (Izzard and Lochner,

1980). Focal contacts are elongated small regions along the ventral plasma membrane and associated with actin microfilaments at their cytoplasmic aspects. This association plays an important role in the regulation of actin organisation, thereby affecting cell spreading, morphogenesis and migration (Calderwood *et.al.,* 2000). Focal adhesions are complex structures containing large number of proteins that are involved in multiple signal transduction processes (Zamir and Geiger, 2001; figure 1.5).

The major transmembrane ECM receptors in these sites belong to the integrin family of cell surface glycoproteins (Damsky *et.al.,* 1985; Horwitz *et.al.,* 1986). Integrins are heterodimers composed of an α and β subunit, each of which has a large extracellular domain, and a shorter cytoplasmic domain (Petruzzelli *et.al.,* 1999). In vertebrates, there are at least 18 distinct α and 8 β subunits. The association of the α subunits (120 to 180 kDa) and β subunits (90 to 110 kDa) and the presence of divalent cations are essential for ligand binding (Gailit and Ruoslahti, 1988).

Most integrins bind a variety of large extracellular matrix proteins such as fibronectin, vitronectin, fibrinogen, laminin, collagen and the complement component iC3b (Etzioni, 1999). Integrins require activation to bind their physiological ligands. Activation is normally induced by the "inside-out" signalling pathway in which integrins undergo dynamic changes such as lateral mobility of subunits and conformational changes within domains (Detmers *et.al.,* 1987; Sims *et.al.,* 1991). This process can result in alterations in the affinity of integrin heterodimers or clustering of heterodimers into multimers. Once bound to a physiological ligand, integrins become clustered at focal contacts and transduce signals to cells through "outside-in" signalling pathway. Integrins transduce signals by associating with adapter proteins through their β-cytoplasmic tails (Giancotti and Ruoslahti, 1999).

In addition to integrins, other molecules such as proteoglycans (Woods and Couchman, 1994 and 1998, Zimmermann and David 1999; Woods *et.al,* 2000), and glycosaminoglycan receptors (Bono *et.al.,* 2001) were shown to localise to focal adhesions. The molecular inventory of focal contacts is very complex and still not well-defined. The abundant literature on the components of focal adhesion revealed

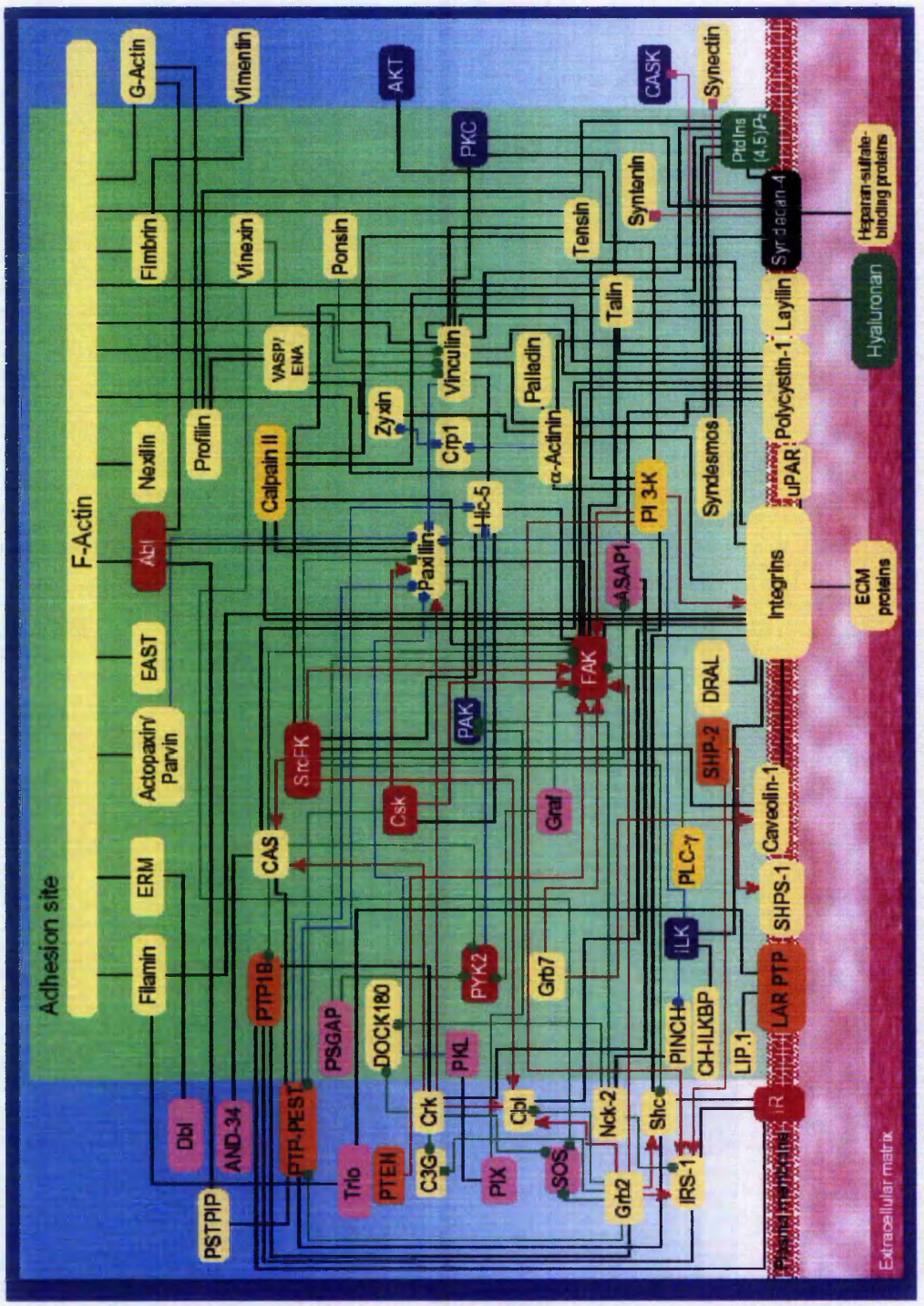


Figure 1.5 Schematic presentation of molecular mechanisms in cell-matrix adhesions

The summary of the molecular inventory of focal contacts (the internal green box) and additional selected proteins that affect matrix adhesions (external blue frame) (Zamir and Geiger, 2001).

cytoskeletal proteins (i.e. tensin, vinculin, paxillin, α-actinin, parvin/actopaxin and talin), tyrosine kinases (i.e. Src, FAK, PYK2, Csk and Abl), serine/threonine kinases (i.e. ILK, PKC and PAK), modulators of small GTPases (i.e. ASAP1, Graf, PKL and PSGAP), tyrosine phosphatases (i.e. SHP-2 and LAR PTP), and other enzymes such as PI-3 kinase and the protease calpain-II (Zamir and Geiger, 2001; figure 1.5). The induction of serine/threonine and tyrosine kinases activates the mitogen-activated protein (MAP) kinase pathways, which is involved in alternation of gene expression, cellular proliferation and differentiation (Giancotti and Ruoslahti, 1999). The MAP kinases are common participants in signal transduction pathways from the membrane to the nucleus. The basic assembly of MAPK pathway is a three-component module composed of a MAPK kinase kinase (MKKK), a MAPK kinase (MKK) and MAPK. The MAPK is a serine/threonine kinase and has the ability to phosphorylate other protein kinases, phospholipases, cytoskeleton associated proteins and transcription factors (Widmann, 1999). To date, 12 members of the MAPK family have been identified and grouped into 5 subfamilies on the basis of sequence homology and function. The first three subfamilies of MAPK family are composed of extracellular signal-regulated kinases (ERK) 1, 2, 3, 4, and 5 (Garrington and Johnson, 1999, figure 1.6). The ERKs are among the protein kinases most commonly activated in signal transduction pathways. They have been particularly linked to cell proliferation and differentiation (Boulton *et.al.,* 1991), but have important roles in many other events including long-term potentiation in neurons (Grewal *et.al.,* 1999), and cell migration (Howe *et.al.,* 2002). The next subfamily was distinguished by its ability to phosphorylate c-Jun transcription factor at the amino-terminal sites following exposure of cells to UV light (Hibi M, 1993). Hence, this particular MAPK was termed as the c-Jun-NH_2-terminal kinase, JNK. The JNK activity has been implicated in the response to cell stress, specifically apoptosis. Inhibition of JNK signalling showed that JNK is necessary for apoptosis in response to growth factor withdrawal stress, DNA damage, and ligation of Fas on the cell surface (Xia *et.al.*, 1995). On the other hand, several reports have suggested that JNK activation may act to promote survival and growth in several cell lines (Smith *et.al.,* 1997;

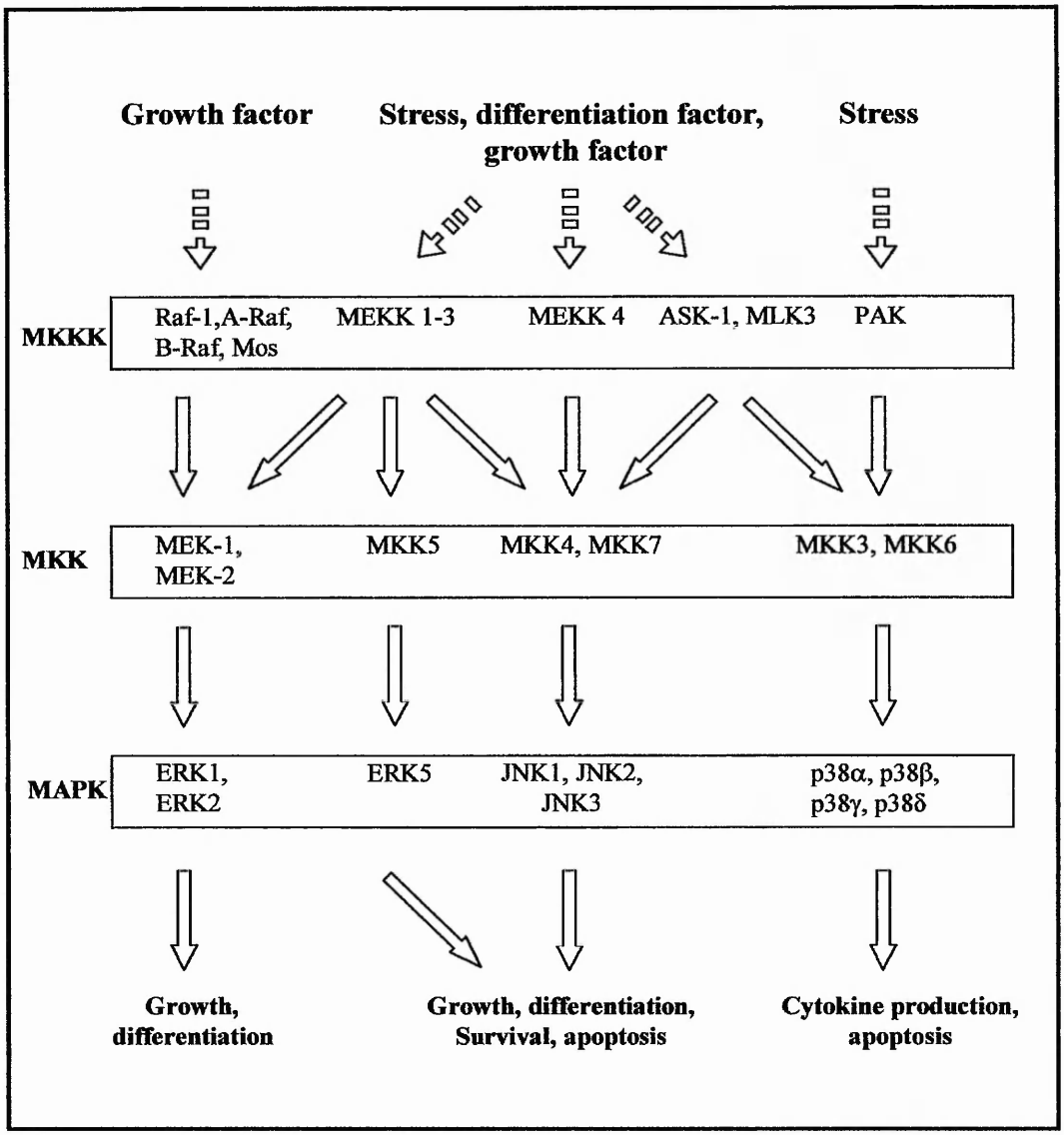


Figure 1.6 The Mitogen-activated kinase modules

The schematic representation of MKKK, MKK and MAPK subfamilies, their upstream regulators and their target cellular responses (Garrington and Johnson, 1999)

Potapova *et.al.,* 1997; Almeida *et.al,* 2000). The last subfamily MAPK family consists of four homologous proteins, termed as p38α, p38β, p38γ, and p38δ (Widmann, 1999). The p38 group was discovered as a lipopolysaccharide (LPS)-induced tyrosine phosphoprotein and as the target of a drug developed to inhibit LPS-induced tumour necrosis-factor-α biosynthesis. The inhibition of p38 kinase resulted in blockage of cytokines TNF-α and IL-2 in stimulated monocytes, suggesting that p38 is important for cytokine biosynthesis (Lee *et.al.,* 1994). Similar to JNKs, p38 enzymes are often activated by cellular stress such as UV irradiation, osmotic shock, heat shock and protein synthesis inhibitors; thus, they are referred to as stress-activated protein kinases (Widmann, 1999). The p38 MAPKs have also been implicated in death-receptor induced apoptosis as the inhibition of p38 activity impairs Fas-induced apoptosis in T cells (Brenner *et.al.,* 1997).

Current understanding on the adhesion-mediated signalling illustrates a complex and dynamic process. The cell adhesion and the formation of focal contacts are important for the structural stability of tissue architecture as well as induction of multiple signalling pathways that determine the cell's destiny.

1.9.7 Tissue transglutaminase in wound healing

Wound healing is a dynamic process involving a series overlapping events that take place in three phases: inflammation, tissue rebuilding/matrix deposition, and tissue remodelling. Tissue injury activates the blood clotting cascade, which results in platelet aggregation and the formation of a dense cross-linked network of fibrin and fibronectin called the provisional matrix. This matrix not only acts to prevent excessive blood loss but also re-establishes haemostasis and supports cell adhesion and migration (Midwood *et.al.,* 2004). Platelets within the thrombus release growth factors and adhesive proteins that stimulate the inflammatory response by the recruitment and activation of neutrophils, macrophages, and fibroblasts. The infiltrating neutrophils cleanse the wound area by solubilising cellular debris and pathogens, and macrophages phagocyte these remnants. Macrophages also serve to release growth factors and cytokines such as platelet-derived growth factor

(PDGF), vascular endothelial growth factor (VEGF), and TGF-β, which initiate the transition between inflammation to tissue rebuilding/matrix deposition (Singer and Clark, 1999). In cutaneous wounds, keratinocytes move into the damaged area to re-establish the epithelial barrier. The matrix remodelling is initiated by the combinatory action of several matrix metalloproteases (MMPs) and tissue inhibitors of MMPs (TIMPs) through degradation of the existing matrix in and around the wound edge to create a path for cell migration. Formation of new matrix in the wound space is carried out by fibroblast through gradual replacement of the provisional matrix with a granulation tissue composed of FN and collagen (McCawley and Matrisian, 2001). As endothelial cells at the wound margin begin to proliferate and re-vascularise, fibroblasts differentiate into myofibroblasts and contract the matrix to bring the edges of the wound together. In translation from the granulation to scar tissue, the architecture of the new tissue is re-modelled as collagen fibrils are bundled and cross-linked. Finally, many of the fibroblasts undergo apoptosis, leaving the collagen-rich scar tissue behind.

Given that transglutaminases can catalyse ε-(γ-glutamyl)-lysine cross-links in the ECM, it is not surprising that TGs have been associated with inflammation and wound healing. While FXIIIa is clearly involved in stabilisation of fibrin clot during blood coagulation and in the deposition of granulation tissues (Muszbek *et.al.,* 1999), the potential role of tTG in wound healing is confirmed by the observation that tTG -/- mice present delayed wound healing (Mearns *et.al.,* 2002). Increased tTG activity in wound healing was first implicated in herbicide-damaged rat lung during in an experimental model of pulmonary fibrosis (Griffin *et.al.,* 1979). In experiments with wounded rat dorsal skin, tTG activity and antigen levels have been shown to increase in all skin layers in the period of one to five days (Bowness *et.al.,* 1988). Other studies have reported that isopeptide linkage of aminopeptide of type III collagen, which occurs in wound healing (Bowness *et.al.,* 1987a), can be catalysed by liver transglutaminase (Bowness *et.al.,* 1987b). Upchurch *et al.* (1991) has shown that endogenous tTG is localised in ECM around the wound area following puncture wounding of a fibroblast cell monolayer. Following studies showed that there is a dramatic increase in levels of tTG deposition to the ECM during tissue repair and cellular stress (Raghunath *et.al.,*

1996b; Johnson *et.al.,* 1999; Haroon *et.al.,* 1999). Examination of the wound healing process in punch biopsy wounds on rats has revealed that the expression of tTG by endothelial, skeletal muscle cells and macrophages has resulted in an increase in tTG antigen and activity at sites of neovascularisation in the provisional fibrin matrix within the wound. The tTG expression occurred in association with TGF-β, TNF-α, IL-6, and VEGF production in the wound, which were shown to be present in the inflammation stage of wound healing. (Haroon *et.al.,* 1999). The up-regulation of tTG during inflammation plays an important role in regulation of enzyme phospholipase A2, which is responsible from the indirect initiation of local vasodilation by regulating the release of arachidonic acid from the cell membrane. tTG enhances the activity of phospholipase A2 through the formation of an isopeptide bond within the secretory isoforms of phospholipase A2 (sPLA2) or by polyamination of the sPLA2 (Cordella-Miele *et.al.,* 1990 and 1993). Consistent with this data, it was recently shown that *in vivo* application of transglutaminase inhibitors can inhibit tTG mediated modification of sPLA2 culminating in an anti-inflammatory effect (Sohn *et.al.,* 2003). The increase in tTG expression might also regulate the inflammatory response by reducing the leakage of intracellular contents of dying cells into the wound. In case of cellular damage, the Ca^{+2} influx will enable tTG to cross-link the intracellular proteins thereby preventing leakage of cellular components from the dying cells, which in turn helps to modulate prolonged inflammatory response (Nicholas *et.al.,* 2003).

Evidence for the involvement of tTG in wound healing has also been obtained from the analysis of biopsies from patients receiving keratinocyte autografts (Raghunath *et.al.,* 1996). The skin regenerating from keratinocyte autografts was found to be substantially cross-linked by tTG in a time-dependent fashion. The authors have speculated that the external application of purified tTG might accelerate the wound healing process. Haroon *et al.* (1999) showed that the topical application of recombinant tTG in an *in vivo* dorsal skin flap window chamber promoted angiogenesis in the wound and resulted in blood vessel length density. In support of this hypothesis, the use of tTG in experimental repair of rat optic nerves (Eitan *et.al.,* 1994) and articular cartilage (Jurgensen *et.al.,* 1997) has been reported. In the later study, tTG was shown to increase the adhesive strength at the cartilage-

cartilage interface when it was topically applied to the surface of cartilage-bone cylinders.

1.10 Aims

Initial studies showed that specific association of tTG with matrix FN results in the formation of an extracellular adhesion complex that can partially restore attachment and spreading of human osteoblast-like cells and mouse Swiss 3T3 fibroblasts when the integrin mediated direct binding to FN is impaired using Arg-Gly-Asp (RGD) containing peptides. In the following work, the first objective was to characterise this distinct FN-tTG extracellular adhesion complex and clarify the relative contributions of tTG and FN to the RGD-independent cell adhesion process. The second aim of this study was to investigate whether the RGD-independent cell adhesion could be mediated by a physiological matrix of cell-assembled FN and cell-secreted tTG and/or by tTG bound to N-terminal FN fragments, which contain putative high affinity binding site for tTG. A further part of this project was to investigate the potential role of FN-tTG matrix as a pro-survival adhesion factor in inducing intracellular signals that rescue anchorage-dependent cells undergoing a detachment-induced programmed cell death due to loss of RGD-dependent cell adhesion.

Chapter 2: Materials and Methods

Chapter 2: Materials and Methods

2.1 Materials

2.1.1 Chemicals

The deionised water (dH_2O) used in experiments was obtained from an Elgastat system 2 water purifier (ELGA Ltd, High Wycombe, UK) or Milli Q water purifier (Millipore/Waters, Watford, UK).

The general chemical reagents and cell culture media were purchased from Sigma – Aldrich Company Ltd, Dorset UK unless otherwise stated. Other chemicals and reagents were obtained from the following suppliers:

Amersham Pharmacia Biotech. UK Ltd, Little Chalfont, UK:

The full range rainbow molecular markers and ECL Chemiluminescence development kit

Bachem, Merseyside, UK:

The synthetic H-Gly-Arg-Gly-Asp-Thr-Pro-OH (GRGDTP) and H-Gly-Arg-Ala-Asp-Ser-Pro-OH (GRADSP) peptides

BD Transduction Laboratories, Oxford, UK:

Anti-phosphotyrosine rabbit polyclonal and mouse monoclonal antibody

Bio-Rad, Hemel Hempstead, UK:

Bio-Rad protein assay kit, and Bio-Rad 4-20% pre-cast gradient SDS-PAGE gel

Calbiochem, Nottingham, UK:

The synthetic H-Gly-Arg-Gly-Asp-Thr-Pro-OH (GRGDTP), H-Gly-Arg-Ala-Asp-Ser-Pro-OH (GRADSP) peptides, GO6976, and Fibroblast Growth Factor

Chemicon International Ltd, Harrow, UK:

Anti-integrin alpha-4 mouse monoclonal antibody

Dako A/S, Glostrop, Denmark:

Anti-mouse IgG -FITC, -TRITC and -HRP conjugates, anti-goat Immunoglubulins-HRP conjugate, and anti-rabbit IgG-TRITC conjugate

Molecular Probes, Eugene (OR), USA:

Biotin-X-cadaverine

Neomarkers, Fremont, USA:

Anti-tissue transglutaminase mouse monoclonal antibody Cub7402

New England Biolabs Ltd, Hertfordshire, UK:

Anti-phospho-Akt (Ser473) rabbit polyclonal and anti-Akt rabbit polyclonal antibodies

Promega, Southampton, UK:

CaspACE^{TM} Assay System , Colorimetric

Roche Diagnostic Ltd, East Sussex, UK:

Cell proliferation assay kit II (XTT), and TUNEL apoptosis kit

Santa Cruz Biotechnology Inc, Calne, UK:

Anti-phospho-ERK(E-4) mouse monoclonal antibody, anti-phospho-JNK(G-7) mouse monoclonal antibody, anti-PKCα(H-7) mouse monoclonal antibody, anti-phospho- PKCα(Ser657) rabbit polyclonal antibody, and anti-phospho-Syndecan-4(Ser 179) goat polyclonal antibody

Seikagaku Corporation, Tokyo, Japan:

Chondroitinase ABC lyase

Sigma – Aldrich Company Ltd, Dorset UK:

Human plasma fibronectin, fibronectin amino (N)-terminal fragments, guinea pig liver tTG, heparinase III (heparitinase) from *Flavobacterium heparinum*, protease inhibitor cocktail for mammalian tissues, phorbol-12-myristate-13-acetate (PMA), and extravidin-peroxidase

Upstate Ltd, Buckingham, UK:

Anti-phospho-FAK(Tyr397) and anti-phospho-FAK(Try576) rabbit polyclonal antibodies

Vecta Laboratories Inc, Peterborough, UK:

Vectashield fluorescence mounting medium

2.1.2 Materials

Amersham Pharmacia Biotech. UK Ltd, Little Chalfont, UK:

Electrode paper (grade 1F)

BDH Laboratories suppliers, Milton Keynes, UK:

Coverslips, microscope slides

Biosoft, Cambridge, UK:

Quantiscan densitometry analysis software

Genetic Research Instrumentation Ltd, Essex UK:

Nitrocellulose membranes

Improved Neubauer, Carlton, UK:

Haemocytometer

Lab-tek Brand Products, Naperville (IL), USA:

8- well glass chamber slides

Nalgenunc International, Rochester (NY), USA:

Cryovials

Sarstedt Ltd., Leicester, UK:

0.5-, 1.5- and 2- ml microcentrifuge tubes, 5 ml scintillation vial inserts and tops, 15- and 50- ml sterile centrifuge tubes, 10 and 5 ml sterile pipettes, automatic pipette fillers, pipette tips, and disposable filters (0.20 μm pore size)

Scientific Laboratory Supplies, Nottingham, UK:

Tissue culture flasks T25, T75, T150, 10-cm and 6-cm petri dishes, 6- and 96- well plates, and Genex Beta automatic pipettes

Whatman Ltd, Maidstone, UK:

Whatman electroblotting 3M filter paper

2.1.3 Equipment

Beckman Instrument (UK) Ltd, High Wycombe, UK:

Spectrophotometer Model DU-7, centrifuges Avanti J-30 I, MSE Centaur 2, GPKR, MSE Microcentaur, Optima TLX Tabletop ultracentrifuge and COULTER® EPICS® XL™ Flow Cytometer

Bio-Rad, Hemel Hempstead, UK:

Protean III Minigel Vertical Electrophoresis Apparatus and Western Blot wet transfer system

B&L Systems, Maarssen, The Netherlands:

Atto-minigel protein electrophoresis system

Corning, Staffs, UK:

pH meter, spectrophotometers

Flow Laboratories, High Wycombe, UK:

Laminar flow cabinet Gelaire BSB 4A

Grant Instruments, Cambridge, UK:

Water baths

Jouan, Tring Herts, UK:

CO_2 incubator Model IG150

Leica Lasertechnik, Heidelberg, Germany:

TCSNT confocal laser microscope

MSE Scientific Instruments, Cambridge, UK:

Sonicator Model Soniprep 150

Nikon Inc, Badhoevedorp, The Netherlands:

Inverted Phase Microscope model TMS-F

Olympus Optical Co (UK) Ltd, London, UK:

Inverted Phase Microscope model CK2 and BH2, OM4 Ti 35 mm camera and digital camera 3C JVC.

Sanyo Gallenkamp PLC, Loughborough, UK:

Harrier 18/80 refrigerated centrifuge, MCO-175M O_2/CO_2 Incubator

Tecan UK Ltd, Goring-on-Thames:

SpectraFluor 96-well ELISA plate reader and XFluor4 software

Walker Safety Cabinets Ltd, Derbyshire, UK:

Laminar flow class II series model 5142412

2.2 Methods

2.2.1 Methods in cell culture

2.2.1.1 Cells and culture conditions

The cells used in the project included primary human osteoblasts, Swiss Albino mouse embryo 3T3 fibroblast, human urinary bladder carcinoma cell line (ECV304), primary human dermal fibroblasts, Raf-1 wild type and knock out 3T3-like immortalised fibroblast cell lines. All cells were cultured in a humidified atmosphere at 37°C, 5% (v/v) CO_2, 95% (v/v) air.

The human osteoblast cell line (HOB), which was a kind gift by Dr. S. Anderson and Prof. S Downes (University of Nottingham, UK), was isolated from femoral heads of trabecular bone (DiSilvio *et.al.,* 1995) and spontaneously immortalised. HOB cells were cultured in Dulbecco's modified Eagle's medium (DMEM) supplemented with 10% (v/v) heat inactivated fetal calf serum (FCS), 2 mM L-glutamine, 1% (v/v) nonessential amino acids and penicillin/streptomycin (100 U/ml and 100 μg/ml, respectively) and used for experiments between passages 48-52.

Swiss 3T3 albino fibroblasts were obtained from American Type Culture Collection (ATCC, USA) and maintained in the same medium as human osteoblasts. Swiss 3T3 fibroblasts (clone TG3) stably transfected with the tissue transglutaminase cDNA under the control of a tetracycline-regulated inducible promoter (Gossen and Bujard, 1992; Verderio *et.al.,*1998) were grown in DMEM containing 10% (v/v) heat inactivated FCS, 2 mM L-glutamine, 100 U/ml penicillin, 100 μg/ml streptomycin, 400 μg/ml active G418, 250 μg/ml xanthine, 15 μg/ml hypoxanthine, 10 μg/ml thymine, 2 μg/ml aminopterin, 10 μg/ml mycophenolic acid, and 2 μg/ml tetracycline. Swiss 3T3 TG3 clone was cultured in tetracycline containing medium to express low endogenous levels of tissue transglutaminase. The medium was changed every 2 days and replaced with medium containing a fresh addition of tetracycline. To induce tTG expression, cells were grown in the absence of tetracycline for at least 72 hours. The wild type Swiss 3T3 fibroblast and clone TG3 were used for experiments between passages 7-15.

The human urinary bladder carcinoma cell line (ECV304), was obtained from the European Collection of Animal Cell Cultures (ECACC). The ECV304 were routinely cultured between passages 10-20 in DMEM containing the same supplements as the medium for human osteoblasts.

The primary human dermal fibroblasts were isolated from human foreskin by Panos Kotsakis (Nottingham Trent University, UK) and kindly donated to be used for experiments between passages 5-9. The cell line was maintained in DMEM containing 10% (v/v) heat inactivated FCS, 2 mM L-glutamine, 1% (v/v) nonessential amino acids, 100 U/ml penicillin, 100 µg/ml streptomycin.

Raf-1 wild-type and null 3T3-like immortalised fibroblast cell line was a kind gift from Dr. Baccarini (Institute of Microbiology and Genetics, Vienna, Austria) (Mikula M *et. al.*, 2001). The cells were cultured between passages 5-20 in DMEM supplemented with 10% (v/v) heat inactivated FCS, 2 mM L-glutamine, 1% (v/v) nonessential amino acids, 100 U/ml penicillin, and 100 µg/ml streptomycin.

2.2.1.2 Isolation of primary mouse dermal fibroblast

The mouse dermal fibroblasts (MDF) were isolated from wild type (Tg 2+/+) and knockout mice (Tg 2-/-) kindly donated by Prof. Melino and Dr. De Laurenzi (IDI-IRCCS, University Tor Vergata, Rome) (De Laurezi *et.al.*, 2001). The primary cultures of dermal fibroblast were prepared from mouse skin as follows. Adult animals were sacrificed by neck dislocation and shaved on the back. A region of pelt was removed from the back of animal under aseptic conditions and placed into medium containing 25% penicillin/streptomycin for 5 minutes. Following three washes with DMEM, the pelt was transferred to a sterile tissue culture 60 mm dish and cut into small pieces (approximately 3x8 mm) using a combination of forceps and a sharp scalpel. The skin pieces were then transferred into DMEM containing 0.2% Dispase and 100 U/ml penicillin, and 100 µg/ml streptomycin, and incubated at 4°C for 18 hours. Dispase ensures the removal of the epidermis from the underlying dermis by digesting the basal lamina.

After the overnight incubation, skin samples were washed three times with DMEM, and the inner-dermis was scraped from the epidermis. The dermis was then minced into smaller pieces (3x3 mm) in a 60 mm dish and three to four pieces were placed per well of a 6-well plate. Sterile coverslips were pressed-placed onto dermis pieces and 5 ml of growth medium were added into each well. The culture was finally placed in the incubator at 37°C in 5% CO_2, and incubated for one week in the same culture medium with regular checks for contamination. Any keratinocyte contamination was eliminated, as they do not persist in the culture for very long without regular feeding in the first week, leaving fibroblasts as the only cell type surviving. After one week, the medium was replaced with fresh growth medium every 3 days for three weeks. After examining the formation of colonies, the cells were harvested as described below (Section 2.2.1.3) and plated into T25 tissue culture flasks. The MDFTg2+/+ and -/- cells were maintained in the DMEM-F12 HAM medium supplemented with 10% (v/v) heat inactivated FCS, 2 mM L-glutamine, 1% (v/v) non essential amino acids up to passage 10.

2.2.1.3 Cell passaging

Cells were passaged when they reached approximately 90% confluency for immortalised cell lines and 70% confluency for primary cell lines. The cell monolayer was rinsed once with PBS (pH 7.4) prior to treatment with 0.25% (w/v) trypsin, 5 mM EDTA solution in PBS, pH 7.4 at 37°C. The detached cells were collected in medium containing 7- 8% (v/v) fetal calf serum to inactivate the trypsin and centrifuged at 300 x *g* for 10 minutes. Cells were resuspended in the growth medium and seeded in tissue culture flasks to the desired confluency.

2.2.1.4 Determination of cell number

Cells were trypsinised and centrifuged as described above (Section 2.2.1.3) and resuspended in DMEM. 10µl aliquots of the cell suspension were applied to a haemocytometer. The cells were counted in 4 separate fields using phase/contrast microscopy on an inverted light microscope (Olympus CK2). The cell number per

millilitre of cell suspension was calculated according to the formula "counted number of cells x dilution factor / mm^2 of counted area x chamber depth".

2.2.1.5 Cryopreservation of the cell lines

Cells were trypsinised, counted as described in Section 2.2.1.4 and resuspended in 10% (v/v) cell culture grade DMSO in heat inactivated FCS. Cells were then pipetted in 1 ml aliquots into cryogenic vials and slowly frozen at -70°C in a specialised cryogenic container overnight before transfer to a liquid nitrogen container for long-term storage.

2.2.1.6 Cell defrosting from storage

Cryogenic vials of cells stored in liquid nitrogen were removed and quickly placed in a water bath at 37°C. The cell suspension was carefully transferred into a sterile Falcon tube and 5 ml of serum supplemented growth medium was added drop wise, with mixing after each addition to ensure slow dilution. The diluted cell suspension was then centrifuged at 300 x *g* to eliminate the traces of DMSO present in the freezing mix. Cells were resuspended in the growth medium and transferred to a tissue culture flask. The medium was changed duringthe next 12-24 hours and cells were passaged at least once before using them in an experiment.

2.2.2 Preparation of a physiological extracellular matrix

2.2.2.1 Coating of plates with fibronectin and fibronectin fragments

The wells of a microtitre plate were coated with FN and amino-terminal FN fragments at concentrations previously optimised by an ELISA-based assay where polyclonal anti-FN antibody (Sigma-Aldrich, UK) was used in a stoichiometric excess (Verderio *et.al.,* 2000). The concentrations of the fibronectin and proteolytic fragments used were optimised as follows:

Full length FN	5 μg/ml
70-kDa amino-terminal fragment of FN	42 μg/ml
45-kDa amino-terminal fragment of FN	54 μg/ml
30-kDa amino-terminal fragment of FN	54 μg/ml

The FN and N-terminal fragments were diluted in 50 mM Tris-HCl, pH 7.4 and 50 μl/well used to coat the plate for either for one hour at 37°C or overnight at 4°C.

2.2.2.2 Immobilisation of tissue transglutaminase on FN matrices

The guinea pig liver tissue transglutaminase (gpl tTG) was purified and dialysed by Dr.Li (Leblanc *et.al.,* 1999) under Nottingham Trent University facilities or purchased from Sigma-Aldrich, UK. For immobilisation of the enzyme on FN and N-terminal fragments, wells were washed once in 50 mM Tris-HCl, pH 7.4. In some cases, the wells were blocked with 3% (w/v) Marvel in PBS, pH 7.4 for 30 minutes at 37 °C prior to tTG immobilisation. The 20 μg/ml tTG solution was prepared by dissolving the 1 mg/ml of gpl tTG in PBS containing 2 mM EDTA, pH 7.4 to inhibit Ca^{2+}-dependent activity of the enzyme. The tTG solution was then added to the tissue culture plastic (TCP), or TCP coated with FN, and FN fragment-matrices for 1 hour at 37°C.

2.2.2.3 Formation of a native cell assembled extracellular matrix

Swiss 3T3 TG3 cells were cultured to 90% confluency for four days under non-induced conditions. Cells were detached from the substratum with trypsin and seeded on 96-well plates at a density of $1x10^3$ cells/well. The non-induced cells were cultured in a specially conditioned medium (Section 2.2.1.1) with tetracycline, while the induced cells were cultured in the medium without tetracycline. The medium was changed every two days to ensure the induction or suppression of transglutaminase activity in desired wells. Cells were allowed to deposit a cell-assembled extracellular matrix on tissue culture plastic for 16 to 18 days. To further increase the levels of tTG in the deposited matrix, tTG was pre-activated in 5 mM dithiothreitol (DTT) on ice for one hour. The pre-activated tTG

was then diluted in the culture medium to 10 μg/ml reducing the DTT concentration to 0.05 mM, and 100 μl was added to the assigned wells. Cells were cultured in a humidified atmosphere at 37°C, 5% (v/v) CO_2, 95% (v/v) air for 16 hours. On the day of the experiment cells were detached from wells using 5 mM EDTA, PBS, pH 7.4 leaving the native cell assembled extracellular matrix laid on tissue culture plastic.

2.2.3 Detection of relative levels of tTG in matrices

2.2.3.1. Detection of tTG antigen by ELISA

The presence of tTG antigen on different substrata was detected by using a modified enzyme linked immunosorbent assay (Verderio *et.al.*, 1999).

After coating the 96-well plate with 50 μl of FN and N-terminal fragments as described above (Section 2.2.2.1), the wells were washed once in 50 mM Tris-HCl, pH 7.4 and then blocked with 50 μl of 3% (w/v) BSA in PBS, pH 7.4 for an hour at room temperature. The tTG solutions at different concentrations were prepared by dissolving 1 mg/ml of tTG in PBS, 2 mM EDTA, pH 7.4. The tTG solutions were then added to the tissue culture plastic or BSA-blocked FN and FN fragment matrices. After a one-hour incubation at 37°C, the tTG solutions were removed and wells were washed once with 100 μl of 50 mM Tris-HCl, pH 7.4. Prior to the incubation with anti-tTG monoclonal antibody Cub 7402 (Neomarkers, UK), wells were blocked with 5% (w/v) Marvel in PBS, pH 7.4 (blocking buffer) for 30 minutes at room temperature. After a two-hour incubation with Cub 7402 (200 ng/ml in blocking buffer) at room temperature, the wells were washed three times (final wash for 20 minutes) with blocking buffer. To detect the antigen-antibody complex, the wells were incubated with 100 ng/ml of peroxidase labelled anti-mouse IgG (Dako, Denmark) for two hours at room temperature. At the end of incubation, the wells were washed three times with blocking buffer and once with PBS, pH 7.4. The wells were then pre-equilibrated with the developing buffer, phosphate-citrate buffer with urea and hydrogen peroxide (Sigma-Aldrich, UK). Development of the reaction was performed by addition of developing buffer containing the substrate 7.5% (w/v) 3,3',5,5'-tetramethyl benzidine in DMSO

(TMB). The colour development was terminated by addition of 50 µl of 2.5M H_2SO_4 and the absorbance read at 450 nm using a Spectrafluor plate reader. Results were expressed as absorbance at 450 nm.

2.2.3.2 Measurement of tTG activity by biotin-X-cadaverine incorporation

The activity of matrix-bound tTG was measured with a TG activity assay based on biotin-X-cadaverine (BTC) incorporation into fibronectin (Jones *et.al.*, 1997). The linearity of FN-bound tTG activity has been shown previously by Verderio *et al.* (2000).

The wells of microtitre plate were coated with 50 µl of human plasma FN and blocked with 3% (w/v) BSA in PBS, pH 7.4 for 30 minutes at room temperature. After three washes with PBS, pH 7.4, the wells were incubated with 100 µl of tTG at a concentration of 20 µg/ml (dissolved in PBS, 2 mM EDTA, pH 7.4) for one hour at 37°C. In control wells, 100 µl of PBS, 2 mM EDTA, pH 7.4 was added. Meanwhile the Tris-based buffer containing 5 mM $CaCl_2$, 5 mM DTT, 0.132 mM BTC in 50 mM Tris-HCl, pH 7.4 was prepared. To confirm the Ca^{2+} dependent cross-linking activity, 5 mM $CaCl_2$ was substituted with 5 mM EDTA in the Tris-based. Following tTG immobilisation, the wells were washed once with 50 mM Tris-HCl, pH 7.4, and 100 µl of Tris-based was pipetted into the wells. The plate was incubated for one hour at 37°C and then the reaction was terminated by addition of 100 µl of 10 mM EDTA, pH 7.4. After two washes in TBS-Tween, pH 7.4 (100 mM Tris-HCl, 0.9% NaCl, 0.05% (v/v) Tween), the incorporated BTC was revealed by addition of 100 µl of extravidine peroxidase (EXAP) (dissolved 1/5000 in 3% (w/v) BSA in PBS, pH 7.4) for 1 hour at 37 °C. Following the removal of EXAP and three washes with TBS-Tween (pH 7.4), wells were pre-equilibrated with the developing buffer, and 100 µl of developing buffer containing TMB were added to each well. The reaction was stopped by 2.5 M H_2SO_4 and absorbance values measured at 450 nm as indicated before (Section 2.2.3.1).

2.2.4 Visualisation of FN-tTG matrix with double immuno-fluorescent staining

8-well glass chamber slides were coated with 125 µl per well of 5 µg/ml of human plasma FN dissolved in 50 mM Tris-HCl, pH 7.4 overnight at 4°C. After incubation, 20 µg/ml of tTG in PBS, 2 mM EDTA, pH 7.4 (250µl/well) was immobilised on FN coated and non-coated wells for 1 hour at 37°C. To investigate the potential induction of a rearrangement or change in FN and FN-tTG matrices, human osteoblast cells were seeded on assigned wells and allowed to attach and spread. The wells with and without cells were then fixed using 3.7% (w/v) paraformaldehyde in PBS, pH 7.4 for 15 minutes at room temperature. Fixed wells were washed 3 times with PBS, pH 7.4 and blocked with blocking buffer (3% (w/v) BSA in PBS, pH 7.4) for one hour at room temperature. After blocking, wells were incubated with 0.6 µg/ml of anti-mouse monoclonal antibody Cub7402 (Neomarkers, UK) and/or 0.6 µg/ml of anti-FN rabbit polyclonal antibody (Sigma-Aldrich, UK) overnight at 4°C. Non-specific anti-mouse monoclonal IgG1 and anti-rabbit IgG antibodies were also used to serve as negative controls. Following three-washes with PBS, pH 7.4, wells were incubated with anti-rabbit IgG-TRITC (raised in swine) (Dako, Denmark) and anti-mouse IgG-FITC (raised in sheep) (Dako, Denmark) diluted 1 in 500 in blocking buffer for 2 hours at room temperature. The slide was then washed three times with PBS, pH 7.4 and mounted with Vectashield mounting medium (Vector Laboratories, UK). The stained matrices were viewed by confocal microscopy using a Leica TCSNT system (Leica Lasertechnik, UK) equipped with an argon crypton laser.

2.2.5 Cell adhesion assay

2.2.5.1 Inhibition of RGD-mediated cell adhesion

Exponentially growing cells were trypsinised and collected into medium containing approximately 7% (v/v) fetal calf serum. After a five-minute centrifugation at 300 x *g* the cell pellet was washed twice in serum free medium to remove the traces of serum proteins. In the experiments performed with HOB and ECV304 cells, a suspension of $2x10^5$ cell/ml and in experiments done with fibroblast cells a cell

solution of $1.75x10^5$ cell/ml were prepared in serum free medium, and incubated with **GRGD**TP and **GRADS**P synthetic peptides (Calbiochem or Bachem, UK) at concentrations of 50 μg/ml (~75 μM), 100 μg/ml (~150 μM), 150 μg/ml (~225 μM), and 200 μg/ml (~300 μM) for 20 minutes at 37°C, in a 5% (v/v) CO_2, 95% (v/v) air atmosphere. Meanwhile coated wells were washed once with 50 mM Tris-HCl, pH 7.4 and serum free medium. Cells (100 μl/well) were seeded on wells coated with FN or FN fragments, with and without immobilised tTG and allowed to attach in the presence of the synthetic peptides. The FN coated wells were coated with gpl tTG (purified and dialysed by Dr.Li) in the third repeats of cell adhesion assays analysing the adhesion of Swiss 3T3, ECV304, HDF, and MDFTg2+/+ and -/- cells. The time was limited to 20-40 minutes to minimise the secretion of any endogenous proteins.

2.2.5.2 Cell fixation and permeablisation

Following cell adhesion and spreading, the medium was carefully removed and wells were gently washed once with PBS, pH 7.4. Cells were then fixed with 100 μl of 3.7% (w/v) paraformaldehyde dissolved in PBS, pH 7.4 for 15 minutes at room temperature and washed twice with PBS, pH 7.4. Following fixation, cells were permeabilised with 100 μl of 0.1% (v/v) Triton-X in PBS, pH 7.4 for 15 minutes at room temperature. The wells were then washed twice with PBS, pH 7.4.

2.2.5.3 May-Grunwald and Giemsa co-staining

To visualise the attached cells, a two-step staining process was employed to stain both cytoplasm and nucleus. Following fixation and permeablisation (Section 2.2.5.2), 100 μl of May-Grunwald stain (Sigma-Aldrich, UK) was added to the wells to stain the cell cytoplasm for 15 minutes at room temperature. The stain was then removed and wells were washed once with PBS, pH 7.4. The wells were then incubated with 100 μl of 5% (v/v) Giemsa stain (Sigma-Aldrich, UK) in dH_2O to co-stain the nucleus for 20 minutes at room temperature. The plate was finally washed twice with dH_2O and left to dry.

2.2.5.4 Quantification of cell adhesion

Digital images of three non-overlapping fields covering the centre of the well were acquired using a video digital camera (Olympus DP10) at 40 x magnification. The cell attachment and spreading were quantified using the Scion image analysis programme (http://www.scioncorp.com), which is developed at the National Institute of Health (Washington DC, USA). The number of cells per image was assessed through threshold and particle analysis settings with a minimum particle size of 50 pixels. Spread cells were discriminated from non-spread by their two-colour appearance (dark purple nucleus, pink cytoplasm). These were quantified by density slicing and particle analysis settings. The spread cell particles were selectively highlighted through the adjustment of the Lut intensity. The number of attached cells per well was calculated by summing up the number of cells from the three imagines of non-overlapping fields. Cell attachment on FN without RGD peptide was considered as the control value for the most of the experiments. The mean number of attached cells from three wells was calculated and that of control was considered as 100%. The mean number of attached cells (cell attachment) for each sample was then expressed as the percentage of cell attachment on FN. The mean percentage of attached cells that are spread (cell spreading) for each sample was determined separately, and the mean percentage of spread cells on FN control was expressed as 100%. The mean percentage of spread cells for each sample was then normalised against that of FN control. Cell spreading was defined as the process whereby a rounded cell is flattened as a consequence of ECM-mediated signal transduction leading to the rearrangement in the actin cytoskeleton.

2.2.6 Preparation of total cell lysates

A 6-well plate was coated with 1.5 ml of 5 μg/ml human plasma FN or heat-inactivated 3% (w/v) BSA in PBS, pH 7.4 by incubation at 4°C for overnight. The FN matrix was further coated with 3 ml of 20 μg/ml tTG as described previously (Section 2.2.2.2). Cells detached by trypsinisation were then plated onto wells at a density of $6x10^5$ cells/well (Section 2.2.5.1). Following cell adhesion and

spreading, the medium was removed, wells were washed once with ice-cold PBS, pH 7.4 and samples were centrifuged at 300 x *g* for 10 minutes in order to collect non-adherent cells. The adherent cells were lysed by addition of 50 µl of solubilisation buffer. The solubilisation buffer was composed of 1% (v/v) Nonidet, 0.5% (w/v) sodium deoxycholate, 0.1% (w/v) SDS, 1 mM benzamidine, 1 mM NaF, 1 mM Na_3VO_4, 0.1 mM PMSF and 1% (v/v) protein inhibitor cocktail (Sigma-Aldrich, UK). The plate was then placed on ice and lysates were collected with a scraper to be mixed with the corresponding cell pellet from non-adherent cells. Cell extracts were clarified by further centrifugation at 300x*g* for 5 minutes at 4°C. The supernatants were stored at -70°C until required for protein content estimation and electrophoresis.

2.2.7 Determination of protein concentration by the Lowry Method

The protein content of cellular extracts was determined using the commercial kit from Bio-Rad based on the Lowry method (Lowry *et.al.,* 1951). The determinations were made following the manufacturers instructions using BSA as the standard. Briefly, 5 µl of BSA solution ranging from 0.1-1.5 mg/ml, and 1µl of cell extract dissolved in 4µl of dH_2O, were added to wells of a microtitre plate in duplicate and triplicate, respectively. The wells were then incubated with 25µl of Reagent A (BioRad, UK), followed by 200 µl of Reagent B (BioRad, UK) for 15 minutes at room temperature. The absorbance values were recorded at 750nm using a SpectraFluor plate reader to produce the calibration graph.

2.2.8 Sodium Dodecyl-Sulphate Polyacrylamide Gel Electrophoresis

The protein extracts were resolved by the SDS-PAGE method, which was a modification of that described by Laemmli *et.al.* (1970), using the Atto-minigel system. The gels consisted of a 3% (w/v) polyacrylamide stacking gel and a 8 or 10% (w/v) resolving gel. The stacking gel was made using 0.25 M Tris, 0.2% (w/v) SDS stock solution, pH 6.8 and resolving gel contained 0.75 M Tris, 0.2% (w/v) SDS stock solution, pH 8.8. The polymerisation reaction was initiated by the

addition of the indicated volumes of freshly prepared 10% (w/v) ammonium persulphate and N,N,N',N'-tetramethylethylenediamine (TEMED). The stacking and resolving polyacrylamide gels were prepared according to table 2.1.

Resolving gels (80 x 60 x 0.75) were cast in Atto-mini gel plates stabilised with two gel clamps and a U-gasket. To provide an even upper surface water-saturated butan-2-ol was poured on the top of the gel to an approximate depth of 5 mm. The

Stock solution	**Final % (w/v) acrylamide**		
	3%	8%	10%
30% (w/v) acrylamide/0.8% (w/v) bis-acylamide	0.65 ml	4 ml	5 ml
Tris-SDS pH 6.8	1.25 ml	-	-
Tris-SDS pH 8.8	-	3.75 ml	3.75 ml
Distilled H_2O	3.05 ml	7.25 ml	6.25 ml
10% (w/v) ammonium persulphate	25 µl	50 µl	50 µl
TEMED	5 µl	10 µl	10 µl

Table 2.1 The recipe for the preparations of various percentages of polyacrylamide gels

gel was then left to polymerise for 45 minutes at room temperature. Following polymerisation water-saturated butan-2-ol was discarded, and the top surface of the gel was washed three times with distilled water. The excess water was gently removed from the edges of the plate using a filter paper. The stacking gel was then prepared and poured gently on the resolving gel by avoiding of the formation of air bubbles. A 10-well sample comb was gently placed and the gel was allowed to polymerise for 30 minutes at room temperature. After polymerisation the sample comb was gently removed from the stacking gel and wells were washed with Tris-glycine electrode running buffer, pH 8.5 (25 mM Tris-Base, 192 mM glycine and 0.1% (w/v) SDS). The clamps and the U-gasket were carefully removed and the gel plate was then placed into Atto-mini gel tank.

Equal amounts of protein from cell lysates were dissolved using a 1:1 ratio in 2x strength reducing-Laemmli buffer (125 mM Tris-HCl, pH 6.8, 20% (v/v) glycerol, 4% (v/v) SDS, 10% (v/v) 2-β-mercaptoethanol and 0.004% bromophenol blue) (Laemmli *et.al.*, 1970), denatured at 95°C for 5 minutes, and then cooled on ice. A maximum of 50 μg of protein was loaded into each well, along with full range rainbow molecular markers (Amersham, UK). Electrophoresis was performed at a constant voltage of 100V through the stacking gel, and then at 150 V until the Bromophenol Blue tracking dye reached the bottom of the resolving gel.

2.2.9 Western Blotting of proteins from polyacrylamide gels

Proteins separated by SDS-PAGE were electorphoretically blotted on a nitrocellulose membrane (Gelman Biosciences, UK) using a Bio-Rad wet blot system following the protocol of Towbin *et al.* (1979). The fibre pads, electroblotting papers and nitrocellulose sheets were soaked in ice-cold transfer buffer, pH 9.2 (48 mM Tris-HCl, 39 mM glycine, 0.0375% (w/v) SDS, and 20% (v/v) methanol). The protein gel was carefully removed from the cast and equilibrated in the transfer buffer for 10 minutes. The coloured gel holder cassette was opened and the pre-soaked filter pad was placed on the black side of the cassette. Next, four layers of wetted electrode paper were laid on the filter pad and bubbles were removed with a glass roller. The gel was then carefully flattened upon the paper and the soaked nitrocellulose was laid onto the gel. Another four layers of wetted electrode paper were placed on the top of the nitrocellulose membrane followed by the second pre-soaked filter pad, again removing any trapped air bubbles. The blotting cassette was then assembled and inserted into the blotting apparatus so that the membrane side of the assembly faced the anode electrode. The electroblotting apparatus was filled with 1 litre of ice cold transfer buffer and a frozen ice container was placed inside the tank to prevent the overheating of the system. The electrotransfer of the proteins was then performed at 150 mA for 90 minutes. The transfer of proteins was verified by the transfer of high weight molecular markers on the nitrocellulose membrane. The membrane was washed once with PBS, pH 7.4, and incubated in the blocking solution, 5% (w/v) Marvel in

TBS-Tween, pH 7.4, with gentle agitation for 45 minutes at room temperature to prevent the non-specific binding of antibodies.

2.2.10 Immuno-development of Western Blots

Following blocking, the membranes were incubated with the appropriate antibody diluted in a blocking buffer with gentle agitation at 4°C overnight. The blots were then washed three times for 15 minutes in the blocking buffer with agitation. Incubation with the suitable secondary antibody (conjugated to Horseradish Peroxidase), diluted 1: 1000 in the blocking buffer, was performed for 90 minutes at room temperature on a shaker. After incubation with the secondary antibody, another set of washes was performed in TBS-Tween, pH 7.4. Finally membranes were rinsed once with PBS-Tween, pH 7.4 (PBS, pH 7.4, 0.05% (v/v) Tween) followed by a wash in PBS, pH 7.4.

The immunodetection of blots was completed using the Amersham ECL Chemiluminescence system kit following the manufacturers instructions. Briefly, equal quantities of Reagent A and B (1 ml of each per blot) were mixed and put on the blots for one minute. The developing solution was then discarded and the blots were carefully wrapped in a cling film avoiding formation of air bubbles before placing in an autoradiography cassette. Immunodetection was carried out in the dark room with Kodak X-Omat films exposed to the immuno-probed blots for 5 to 30 minutes depending on the intensity of the signal. The film was developed in GBX developer (Sigma-Aldrich, UK), washed with water and then fixed with GBX fixer (Sigma-Aldrich, UK) followed by another extensive wash with water. The films were finally left to air dry.

To ensure equal protein loadings, primary and secondary antibodies were removed from membranes with stripping buffer (100 mM 2-mercaptoethanol, 2% (w/v) SDS, 50 mM Tris-HCl, pH 6.7). The membrane was submerged in stripping buffer and incubated at 50°C for 30 minutes with occasional agitation. After four sets of 15-minute washes in TBS-0.5%Tween(v/v), pH 7.4, the membrane was blocked in the blocking buffer for one hour at room temperature. The immunodetection was then performed as described above using a control mouse monoclonal anti-tubulin

antibody (Sigma-Aldrich, UK), diluted 1:1000 in the blocking buffer, followed by peroxidase conjugate monoclonal anti-mouse IgG (Dako, Denmark) (diluted 1:2000 in the blocking buffer).

2.2.11 Densitometric analysis of blots

The images of blots were captured by a Cosmicar camera through the annotating image capture system, Grab IT. The densitometry analysis of the bands was performed with QuantiScan software (Biosoft, UK). The net area values of bands obtained from the blot of the kinase of interest were normalised against values from corresponding tubulin bands using the negative control sample from the tubulin blot as a reference value. The differences between data sets were analysed by the paired-t test at 95% level of significance using the Mini-Tab statistical analysis programme (Mini-Tab Inc, USA).

2.2.12 Analysis of Protein Kinase Cα Translocation to Membrane

The 6-mm Petri dishes were sequentially coated with 22.5 μg of FN (in 50 mM Tris.HCl pH 7.4) and with 90 μg of tTG (in PBS, 2 mM EDTA) as stated before (Section 2.2.2). The HOB cells were grown to 70% confluency and serum starved for 18 hours before the experiment. Cells were trypsinised and resuspended in 1 mg/ml of trypsin soybean inhibitor (diluted in PBS, pH 7.4) for every millilitre of trypsin solution used for dissociation. Cells were then plated onto the FN and FN-tTG matrices at a density of $1.8x10^6$ cells/dish (Section 2.2.5.1). Following the treatment with RAD/RGD containing peptides, cells were allowed to attach for 30 min. In some cases, cells were treated with 50 nM PMA (dissolved in DMSO) for 10 minutes. The supernants of non-adherent cells were collected and pelleted at 300 x *g* for 10 minutes. Meanwhile, adherent cells were washed once with PBS (pH 7.4), collected by gentle scraping into 50 μl of ice-cold homogenisation buffer and mixed with the corresponding cell pellet from non-adherent cells. The homogenisation buffer consisted of 20 mM Tris-HCl, pH 7.4, 10 mM EGTA, 2 mM EDTA, 1 mM NaF, 1 mM Na_3VO_4, 50 nM okadaic acid, 0.1 mM PMSF and

1% (v/v) protein inhibitor cocktail (Sigma-Aldrich, UK). Cells were lysed by sonication three times for 15 seconds and centrifuged to pellet the nuclei and unbroken cells at 1300 x *g* for 10 minutes. The supernants were collected and further centrifuged at 100,000 x *g* for 60 minutes to separate cytosolic and membrane fractions. The resulting supernants were considered to be the cytosolic fraction. The pellet was resuspended in 30 μl of the homogenisation buffer and was considered to be the membrane (particulate) fraction. Protein concentrations of the fractions were determined using the Bio-Rad assay (Section 2.2.7). Equal amounts of protein from the cell fractions were diluted in Laemmli Buffer and separated on 8% polyacrylamide gel by SDS-PAGE as described (Section 2.2.8). Proteins were electrophoretically transferred to a nitrocellulose membrane, which is sequentially probed with mouse monoclonal anti-PKCα (Santa-Cruz, UK) and a peroxidase conjugate monoclonal anti-mouse IgG (Dako, Denmark) as mentioned before (Section 2.2.10).

2.2.13 Immuno-fluorescence visualisation of tyrosine phosphorylation levels

8-well glass chamber slides were coated with 5 μg/ml of human plasma FN overnight at 4°C and 20 μg/ml of tTG was immobilised on FN for 1 hour at 37°C as mentioned above (Section 2.2.4). The monolayer of sub-confluent HOB cells were serum-starved for 16 hours and then harvested as described before (Section 2.2.5.1). Following detachment of the cells, a cell suspension of $2x10^5$ cell/ml in DMEM was prepared and incubated with 100 μg/ml **GRGDTP** and **GRADSP** synthetic peptides for 20 minutes. Cells were seeded on FN or FN-tTG matrices ($5x10^4$ cells/well) and allowed to attach and spread for 40 to 60 minutes. The wells were then washed with PBS, pH 7.4 once and cells were fixed using 3.7% (w/v) paraformaldehyde in PBS, pH 7.4 for 15 minutes at room temperature. Fixed cells were washed 3 times with PBS, pH 7.4 with 5 minute intervals and permeabilised in 0.5% (w/v) TritonX-100 in PBS, pH 7.4 for 5 minutes at room temperature. Following another set of washes, wells were blocked with 5% (w/v) Marvel in PBS, pH 7.4 for 30 minutes at room temperature. The cells were then incubated with rabbit polyclonal anti-phosphotyrosine antibody diluted 1:100 in blocking

buffer, overnight at 4°C. The wells were washed three times with PBS, pH 7.4 and incubated with goat anti-mouse IgG-FITC (Dako, Denmark) diluted 1:200 in the blocking buffer for 2 hours at room temperature. The negative control wells were incubated with only with goat anti-mouse IgG-FITC. After three PBS (pH 7.4) washes, the slides were mounted with Vectashield mountant containing propidium iodide (Vector Laboratories, UK) and examined by a confocal fluorescent microscopy (Leica, UK). Five random images per sample were acquired using the Leica LCS software using constant PMT and section depth settings.

2.2.14 Measurement of cell viability

The viability of MDFTg2-/- cells was assessed by a non-radio active colorimetric assay system using tetrazolium salt XTT (sodium 3'-[1-(phenylamino-carbonyl)-3,4-tetrazolium}-bis (4-methoxy-6-nitor) benzene sulfonic acid hydrate). The XTT cell proliferation kit (Roche, UK) uses metabolically active cells to reduce the reaction mixture, composed of the tetrazolium salt XTT and the electron coupling reagent PMS (N-methyl dibenzopyrazine methyl sulfate), to orange coloured compounds of formazan. The assay is based on principle that intensity of the dye is proportional to the number of metabolic active cells and can be measured at a given wavelength with a spectrophotometer.

The MDFTg2-/- cells were pre-treated with RGD and RAD synthetic peptides and seeded on ($2x10^5$ cell/well) FN and FN/tTG coated 96-well plates. Following sixteen-hour incubation at 37°C in a 5%CO_2 atmosphere, the cells were further incubated with the reaction mixture for 4 hours. Absorbance was then measured at 492 nm wavelength to detect the formazan product, and 750 nm to detect the background absorbance. Cell viability is expressed as absorbance 492 nm after subtraction of values at 750 nm.

2.2.15 Detection of caspase-3 catalytic activity

The activity of caspase-3, a member of the cysteine aspartic acid-specific protease family, was studied using the CaspACE™ Assay, Colorimetric (Promega, UK)

system. The CaspACE™ Assay system is based on the colorimetric measurement of chromophore p-nitroaniline (pNA) after cleavage from the AC-labelled peptide substrate DEVD-pNA by caspase-3. The amount of yellow colour produced upon cleavage is proportional to the amount of caspase-3 activity in the sample.

6-well plates were coated with FN and FN-tTG as described previously (Section 2.2.2). MDFTg2-/- cells were seeded in duplicate onto FN and FN-tTG matrices in the presence and absence of RGD peptide, and incubated for 16 hours at 37°C in a 5% CO_2 atmosphere. In some cases, cells were treated with 1 μM of the protein kinase inhibitor staurosporine and/or with 50μM of cell-permeable pan-caspase inhibitor Z-VAD-FMK for 4 hours. As staurosporine is a known inducer of apoptosis and leads to the activation of caspace-3, the sample treated with staurosporine acted as a positive control. The sample treated with staurosporine and Z-VAD-FMK was considered as negative control, since Z-VAD-FMK blocks the activity of caspase-3 by irreversible binding to the cleavage site of the protease. Following incubation, the cells were harvested and washed in ice-cold PBS, pH 7.4 and resuspendend in cell lysis buffer provided in the assay kit. The protein content of the cell extracts was determined using the Bio-Rad assay (Section 2.2.7). Equal amounts of proteins from cell extracts were used (70 μg protein/sample) to prepare the reaction mixture containing 32% (v/v) caspase assay buffer, 2% (v/v) DMSO, 10 mM DTT, and 2% DEVD-pNA substrate. Following a 4-hour incubation at 37°C, the caspase-3 activity was measured by absorbance at 450 m.

2.2.16 Analysis of Anoikis by Flow Cytometry and Fluorescent Microscopy

The MDFTg2-/- cells were examined for the induction of anoikis through in situ labelling with the terminal deoxynucleotidyl transferase-uridine nucleotide nick-end labelling (TUNEL) method followed by flow cytometry or fluorescent microscopy. The TUNEL method is based on the ability of terminal deoxynucleotidyl transferase (TdT) to incorporate nucleotides coupled to a fluorescent molecule into 3'-strand breaks that occur in DNA during apoptosis.

The MDFTg2-/- cells ($6x10^5$ cells/well) were seeded on FN and FN-tTG coated plates in the presence and absence of RGD peptide and incubated 16 hours at 37°C

in a 5% CO_2 atmosphere. The attached cells along with cells in suspension were then collected and washed twice in PBS, pH 7.4 at the final concentration of $1.2x10^7$ cells/ml. Following the fixation of cells with 4% (w/v) paraformaldehyde in PBS, pH 7.4 for one hour at room temperature, the pellet was washed twice as before and cells were permeabilised in 0.1% (w/v) TritonX-100 in 0.1% sodium citrate for 2 minutes on ice. After another set of washes, samples were labelled with 50 µl of the reaction mixture containing TdT and FITC-dUTP at 37°C for 60 minutes by following the manufacturer protocol (Roche, UK). The cell samples were washed twice in PBS, pH 7.4 and diluted to a final volume of 500 µl and analysed by flow cytometry using a Beckman Counter EPICS XL. The percentage of apoptotic cells was evaluated using the WinMDI 2.8 software.

Cell death was also detected by *in situ* labelling of apoptosis induced DNA strand breaks using a confocal fluorescent microscopy (Leica, UK). In this experiment only non-adherent cells were labelled with propidium iodide and the reaction mixture, and fixed on 6.4 mm glass slide wells in triplicate (~5x 10^4 cells/well). The percentage of cells undergoing apoptosis was determined through three random images per well acquired with the Leica LCS software using constant PMT and section depth settings.

2.2.17 Statistical analysis

The differences between data sets in cell adhesion assays were analysed by the Mann-Whitney test at 95% level of significance, while paired-t test was used to determine the statistically significant absorbance and net area values at 95% level using the Mini-Tab statistical analysis programme (Mini-Tab Inc, USA). When $p<0.05$, the differences between sets of data was considered to be statistically significant and represented with the *, ⁑, and ∘ symbols on the graphs.

Chapter 3: Characterisation of fibronectin bound tissue transglutaminase complex

Chapter 3: Characterisation of fibronectin bound tissue transglutaminase complex

3.1 Introduction

Human plasma fibronectin is a dimeric protein with a molecular weight of 550kDa. It exists in a soluble form in plasma with a concentration of 300μg/ml and is a substrate for tTG and FXIIIa (Lorand and Conrad, 1984; Greenberg *et.al.,* 1992). Liver plasma membranes contain transglutaminase activity and a large molecular weight protein complex which serves as a substrate for the enzyme (Slife *et.al.,* 1986). Upon the solubilisation of liver plasma membranes in sodium dodecyl sulphate and disulphide reducing agents, this complex was recovered in the detergent-insoluble fraction (Tyrrell *et.al.,* 1988b). Further analysis of this detergent-insoluble complex identified fibronectin as the major component of the transglutaminase substrate complex (Tyrrell *et.al.,* 1988a). The cell surface expressed tTG on the intact rabbit hepatocytes has shown to act as a binding site for fibronectin and fibrinogen and form high molecular weight complexes by covalently incorporating itself into these glycoproteins (Fellin *et.al.,* 1981; Barsigian *et.al.,* 1991).

The binding of tTG to the extracellular matrix and specifically to FN was shown by Upchurch *et al.* (1987 and 1991). Following the permeabilisation of WI-38 human lung fibroblasts, tTG was found to co-localise with FN in the pericellular matrix. The binding of tTG to the cell matrix was disrupted when cells were previously treated with an anti-fibronectin antibody (Upchurch *et.al.,* 1987). In addition, endogenous tTG was shown to persist in the ECM several hours after puncture wounding of the lung fibroblasts (Upchurch *et.al.,* 1991). As the tTG was believed to be an intracellular enzyme, the authors suggested that the intracellular tTG interacts with extracellular fibronectin following cell rupture and release of the enzyme to the extracellular environment. Lorand *et al.* (1988) suggested that FN might act as a specific carrier for tTG and prevent the undesirable cross-linking of plasma proteins in pathological situations in which tTG becomes discharged into

the plasma. Using non-denaturating gel electrophoresis a change in mobility of the tTG found in the membrane depleted erythrocyte lysate was brought about by mixing with isolated plasma fibronectin, clearly indicating formation of a tight FN-tTG complex. In their follow-up study using non-denaturating electrophoresis, tTG was shown to bind to plasma FN in the absence of calcium, suggesting neither homologous nor heterologous cross-linking by ε-(γ-glutamyl)lysine or by disulphides occurred during the binding of tTG to FN (Turner and Lorand, 1989). A later study, using a microtiter plate-based immunochemical method to assay tTG-FN interactions, reported the inhibition of the binding with the reducing agents such as dithiothreitol and 2-mercaptoethanol and by treatment with chloride salts of sodium, barium, copper and zinc (Achyuthan *et.al.,* 1995).

Affinity binding studies identified a 42-kDa gelatin-binding domain of human plasma fibronectin as the tTG binding site (Turner and Lorand, 1989; Radek *et.al.,* 1993). The electron microscopy studies of erythrocyte tTG and liver tTG interaction with FN revealed that the enzyme binds within 5 to 10 nm of the N-terminus of the thin fibronectin strand, consistent with its proximity to the gelatin binding domain (LeMosy *et.al.,* 1992). In an attempt to investigate the FN-binding site of liver tTG, using peptide fragments of tTG, Jeong *et al.* (1995) demonstrated that the first 7 N-terminal amino acids residues of liver tTG are important for its association with FN. This was later confirmed by Gaudry *et al.* (1999) using the N-terminal deletion mutants of tTG.

These indications of the close relationship between tTG and FN, call for further investigations about the possible role of tTG in ECM stabilisation and in cell adhesion. It is now consolidated that tTG is important in cell-matrix interactions. Based on the findings that tTG can bind and form a tight complex with human plasma FN and can enhance cell adhesion, the following chapter describes the formation and characterisation of a tTG rich-FN matrix, which will be used in cell adhesion studies.

3.2 Methods

3.2.1 Detection of relative levels of tTG in cell assembled extracellular matrix

Induced and non-induced Swiss 3T3 TG3 cells were cultured for 16-18 days in 96-well plates and harvested as described previously (Section 2.2.2.3). Following the detachment of the cells, the matrix was blocked with 3% (w/v) Marvel in PBS, pH 7.4 for 30 minutes at room temperature. The wells were washed with PBS, pH 7.4, and ELISA and TG activity assays were performed on the matrices. In the ELISA assay, the wells were incubated with anti-tTG monoclonal antibody Cub7402 followed by peroxidase labelled anti-mouse IgG as indicated in Section 2.2.3.2. In the TG activity assay, wells were incubated with the Tris-based buffer (5 mM $CaCl_2$, 5 mM DTT, 0.132 mM BTC in 50 mM Tris-HCl, pH 7.4) for one hour at 37°C. The negative control wells were incubated with Tris-based buffer containing 5 mM EDTA instead of 5 mM $CaCl_2$. The cross-linking reaction was terminated by addition of 10 mM EDTA, pH 7.4, and the reaction was revealed as described in Section 2.2.3.1. The absorbance values were measured at 450 nm using a Spectrafluor plate reader. The differences between data sets were analysed by the paired-t test at 95% level of significance using the Mini-Tab statistical analysis programme (Mini-Tab Inc, USA).

3.2.2 Measurement of immobilised tTG activity

The activity of fibronectin (FN)-bound guinea pig liver tissue transglutaminase (tTG) was measured by incorporation of biotinylated cadaverine into fibronectin as described previously in Section 2.2.3.1. The activity of enzyme was analysed in serum free culture medium DMEM, DMEM with 5 mM Ca^{+2}, DMEM with 5mM DTT, and DMEM supplemented with 5 mM Ca^{+2} and 5 mM DTT. The detection of FN-bound enzyme activity in the Tris-based buffer (5 mM $CaCl_2$, and/or 5 mM DTT, 0.132 mM BTC in 50 mM Tris-HCl, pH 7.4), was undertaken as a positive control. The Ca^{2+} dependency of cross-linking activity was shown by substitution or addition of 5 mM EDTA to the incubating medium. The absorbance values were

measured at 450 nm. The paired-t test was used to determine the statistically significant absorbance values at 95% level using the Mini-Tab statistical analysis programme (Mini-Tab Inc, USA).

3.2.3 The inhibition of FN-bound tTG activity

To inhibit the enzyme activity of FN-immobilised tTG, the irreversible active-site directed inhibitor R283, a 2-[(2-oxopropyl)thio]imidazolium derivative (Freund *et.al.,* 1994), was used. The tTG was immobilised on FN coated wells for 1 hour at 37°C as described previously (Section 2.2.2.2). The wells were washed once with 50 mM Tris-HCl, pH 7.4 and then incubated with increasing concentrations of R283 (10 μM , 50 μM, 100 μM, 500 μM, and 1000 μM in dH_2O, pH 7.4) for 10 minutes at room temperature. After removal of the inhibitor, the TG activity assay was performed as described in Section 2.2.3.1. Results were obtained by measuring the absorbance at 450 nm. The paired-t test with 95% confidence interval was employed to determine the statistical difference between data sets.

3.2.4 The detection of relative levels of FN after blocking FN-tTG matrix with Cub7402 and the control antibody IgG1k

The wells of a 96-well plate were coated with FN (5 μg/ml in 50 mM Tris-HCl, pH 7.4) and incubated overnight at 4°C. The 20 μg/ml tTG solution was then placed on the coated FN matrices for 1 hour at 37°C as described in Sections 2.2.2.1 and 2.2.2.2. Following tTG immobilisation, the wells were washed once with 50 mM Tris-HCl, pH 7.4, and incubated with 40 μg/ml Cub 7402 and mouse IgG1 (in PBS, 2 mM EDTA, pH 7.4) for 1 hour at 37°C. The control wells were incubated only with PBS containing 2 mM EDTA, pH 7.4. After another wash, wells were blocked with 5% (w/v) Marvel in PBS, pH 7.4 (blocking buffer) for 30 minutes at room temperature. The wells were then incubated with 50 ng/ml of anti-FN rabbit polyclonal antibody (Sigma-Aldrich, UK), diluted in the blocking buffer, for two hours at room temperature. The wells were then washed three times with blocking buffer for 30 minutes. To detect the antigen-antibody complex, the wells were

incubated with 50 ng/ml of peroxidase labelled anti-rabbit IgG (Sigma-Aldrich, UK) diluted in the blocking buffer for 2 hours at room temperature. The wells were washed three times with the blocking buffer and once with PBS, pH 7.4. The wells were then pre-equilibrated with the developing buffer (phosphate-citrate buffer with urea and hydrogen peroxide) and 100 µl of developing buffer containing 7.5% (w/v) 3,3',5,5'-tetramethyl benzidine (TMB) were added to each well. The reaction was stopped by 2.5 M H_2SO_4 and absorbance values were measured at 450 nm as indicated previously (Section 2.2.3.1). The differences between data sets were analysed by the paired-t test at 95% level of significance using the Mini-Tab statistical analysis programme (Mini-Tab Inc, USA).

3.3 Results

3.3.1 Immobilisation and detection of FN-bound tTG

The optimum concentration of guinea pig liver tissue transglutaminase (gpl tTG) to be immobilised on fibronectin (FN) was determined and compared to that of tTG bound directly onto tissue culture plastic (TCP) using an ELISA type assay. The FN pre-coated wells of a microtitre plate were incubated with increasing concentrations of tTG, 10 μg/ml, 20 μg/ml, 30 μg/ml, 40 μg/ml and 50 μg/ml, dissolved in PBS containing 2 mM EDTA, pH 7.4. Similar concentrations of tTG were used to coat the TCP (figure 3.3.1). The relative levels of FN and TCP-bound tTG were detected with the monoclonal antibody Cub7402, which binds to a site close to the cysteine active site of the enzyme.

When 10 μg/ml of tTG was immobilised on matrices, a 2- and 4- fold increase in tTG antigen levels on FN and TCP, respectively, was detected. Immobilisation of 20 μg/ml tTG showed a further increase in the levels of matrix bound-tTG antigen with a 4- and 7-fold increase in FN and TCP matrices when compared to background values. The amount of tTG bound to both surfaces appeared to become saturated at the tTG concentration 20 μg/ml as no further statistically significant increase in the tTG antigen levels were detected when the matrices were incubated with 30 μg/ml, 40 μg/ml, and 50 μg/ml of the guinea pig liver enzyme. This result indicates that 20 μg/ml of tTG is the optimum concentration to be immobilised onto 5 μg/ml of TCP-coated FN, which was used in all further experiments.

3.3.2 Analysis of a native cell assembled extracellular matrix

As previously established (Verderio *et.al.,* 1998), the Swiss 3T3 TG3 cell line is capable of inducible expression of tTG using the tetracycline-regulated system. The physiological cell-assembled ECM was prepared by long-term culture of tTG induced and non-induced Swiss 3T3 TG3 cells with or without further addition of pre-activated tTG to cells 16 hours before their detachment. The level of tTG antigen and its activity in the deposited matrices were then determined.

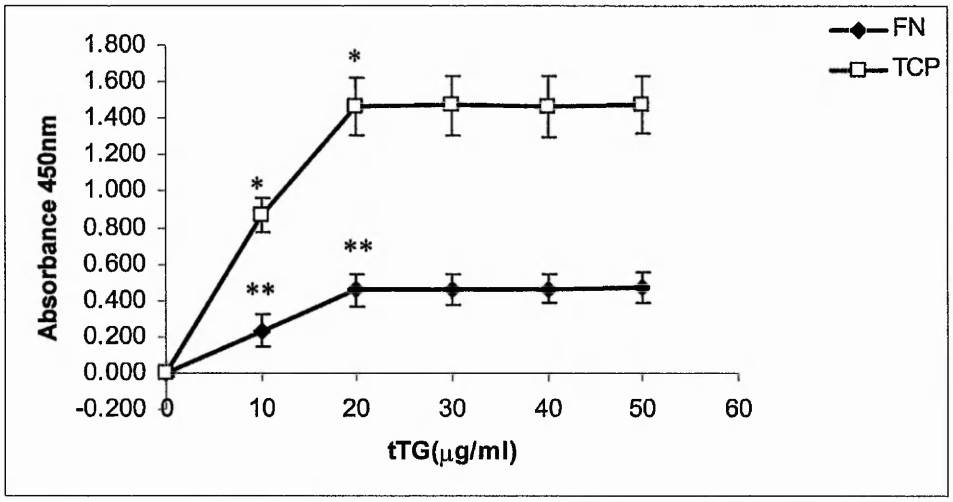


Figure 3.3.1 The ELISA detection of the relative levels of tTG bound to FN and plastic

The levels of tTG bound to FN and tissue culture plastic (TCP) at increasing concentrations were measured by incubation with monoclonal antibody Cub7402 using a modified ELISA assay as described in the Methods (Section 2.2.3.1). Data are expressed as mean ± S.D. absorbance values at 450 nm and are from three separate experiments, each performed in quadruplicate. The background readings were subtracted from the mean absorbance values to obtain the final values. The * and ** represent the statistical difference ($p<0.05$) in the increase of tTG levels for the bound tTG at 10 μg/ml and 20 μg/ml concentrations, compared to background levels.

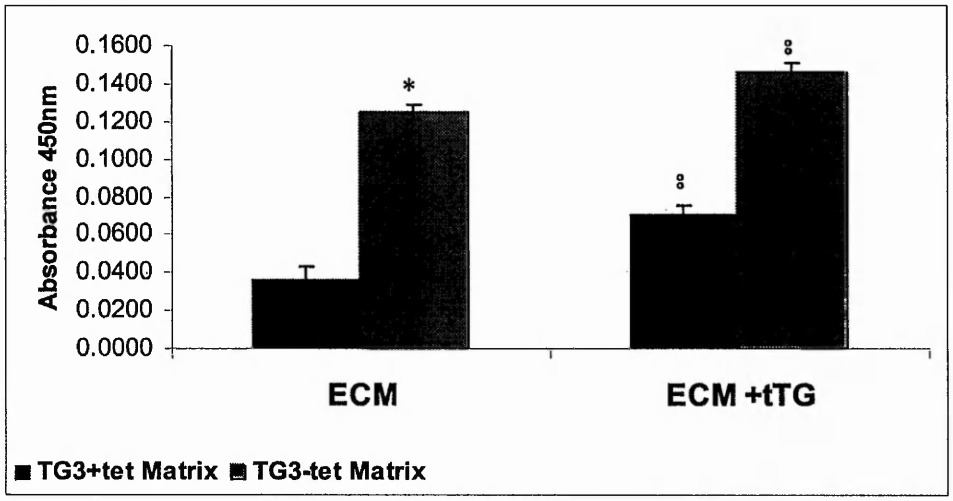


Figure 3.3.2a ELISA analysis of the relative levels of tTG in the physiological cell assembled matrix

The relative levels of tTG in the ECM assembled by non-induced cells (TG3+tet Matrix) and tTG-induced cells (TG3-tet Matrix) without (ECM) or with the further addition of free gpl tTG (ECM+tTG) to the ECM were detected by an ELISA-type assay described under Methods section 2.2.3.1. The data represents the mean ± S.D. absorbance values from three separate experiments, each performed in 8 replicates. The background readings, obtained from wells incubated only with the secondary antibody, were subtracted from the mean absorbance values to obtain the final values. The * indicates the statistically significant ($p<0.05$) absorbance value of TG3-tet Matrix when compared to TG3+tet Matrix. The statistically significant difference ($p<0.05$) between individual matrices upon addition of free gpl tTG was indicated with ∘ symbol.

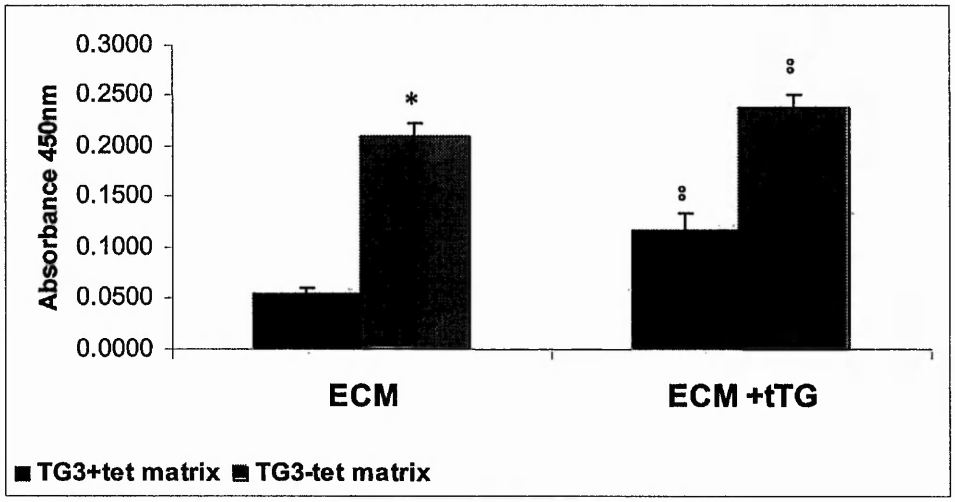


Figure 3.3.2b TG activity assay of the relative levels of tTG in the physiological cell assembled matrix

Biotin cadaverine incorporation by cell secreted tTG (ECM) and by free gpl tTG (ECM+tTG) added into non-induced cell assembled (TG3+tet) and induced cell assembled (TG3-tet) matrix was tested by a modified Elsa assay as described in Section 2.2.3.2. The results are expressed as mean ± S.D. absorbance values of three independent experiments done in 8 replicates. The background values were obtained from wells incubated with an inactive buffer, and subtracted from the mean absorbance values. The * indicates the statistically significant ($p<0.05$) absorbance value of TG3-tet Matrix when compared to TG3+tet Matrix. The statistically significant difference ($p<0.05$) between individual matrices upon addition of free gpl tTG was indicated with ¤ symbol.

The ELISA assay shown in figure 3.3.2a demonstrates a statistically significant difference in the tTG antigen levels between the ECM of cells over expressing tTG and those with background tTG, such that the induced cells deposited 3.5 fold more tTG into the matrix compared to the non-induced cells. This increase was confirmed with the detection of tTG activity in the two different matrices by incorporation of biotinylated cadaverine into FN (figure 3.3.2b). The tTG activity was found to be higher in the ECM assembled by the tTG-induced Swiss 3T3 TG3 cells.

The incubation of both cell populations with pre-activated gpl tTG overnight led to the incorporation of the enzyme into pre-existing matrices. The results from the ELISA and TG activity assays depicted a 2 fold increase in the relative levels of tTG antigen and activity in the non-induced, and a 1 fold increase in that of the induced cell assembled ECM after the addition of tTG.

3.3.3 Measurement of tTG bound to amino-terminal FN fragments

In order to determine the optimum concentration of tTG to be immobilised on the fibronectin amino terminal fragments containing the putative tTG binding site, the wells were coated with 70 kDa (42 μg/ml), 45 kDa (54 μg/ml), and 30 kDa (54 μg/ml) in stoichiometric excess (Verderio *et.al.,* 2000). The fragments were compared for their ability to associate with increasing concentrations of tTG (5 μg/ml, 10 μg/ml, 20 μg/ml and 30 μg/ml).

The 70 kDa fragment verified the highest affinity for tTG with an average absorbance value significantly higher than the other two shorter fragments. There is no statistically significant difference detected between the affinity of the 45 kDa and 30 kDa fragments for tTG (figure 3.3.3).

The detection of the relative levels of tTG by ELISA showed that the incubation of the amino-terminal FN fragments with 20 μg/ml tTG resulted in saturating levels of tTG immobilised on all fragments. That is, the amount of tTG bound to each fragment after incubation with 20 μg/ml tTG was not significantly different from the level bound using 30 μg/ml tTG.

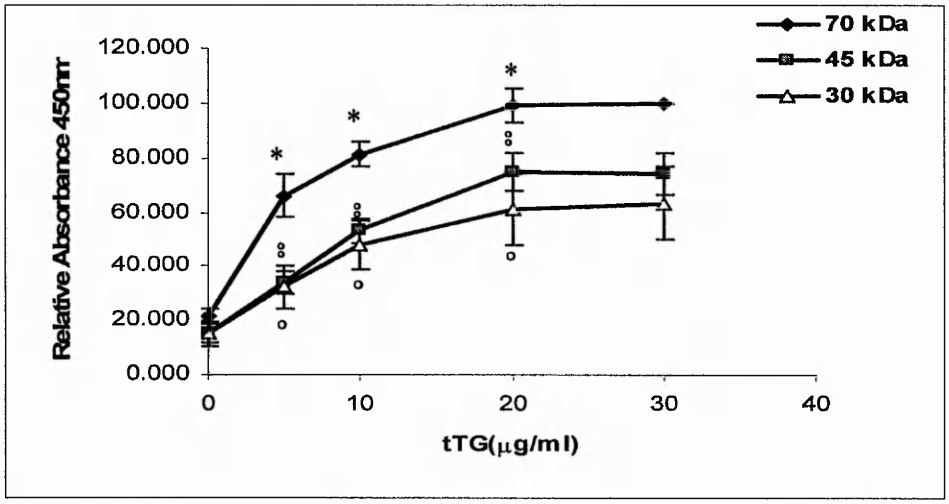


Figure 3.3.3 ELISA detection of the relative levels of tTG bound to the amino-terminal FN fragments

The relative levels of tTG bound to the amino-terminal FN fragments (70, 45, and 30 kDa) immobilised on TCP, at increasing concentrations of immobilised tTG was measured following the addition of monoclonal Cub 7402 antibody (Section 2.2.3.2). Each data point corresponds to the mean percentage of absorbance (Relative Absorbance 450nm) values ± S.D. of four separate experiments undertaken in quadruplicate. The ordinate represent the mean percentage absorbance value expressed as the mean percentage of absorbance value obtained for 30 µg/ml tTG bound to 70 kDa fragment (which represents 100%). The *, ⁘, and ∘ correspond to the statistically significant ($p<0.05$) difference in the increase of tTG levels bound to 70 kDa, 45 kDa, and 30 kDa respectively at 5 µg/ml, 10 µg/ml and 20 µg/ml concentrations.

3.3.4 The measurement of tTG cross-linking activity in culture medium

The measurement of the transamidating activity of FN-bound tTG in a Tris-based buffer containing calcium and 5 mM reducing reagent DTT (to reduce the active site Cys276) has been previously performed (Verderio *et.al.,* 2000). However, the activity status of FN-bound and cell secreted tTG in the cell culture medium DMEM was yet to be determined.

The activity of FN-bound tTG was demonstrated by measuring the enzyme activity in DMEM alone or DMEM supplemented with Ca^{+2} and DTT. The results were compared to the FN-bound enzyme activity measured in the presence of the Tris-based buffer containing Ca^{+2} and/or DTT. In Figure 3.3.4 it is shown that the activity of tTG once bound to FN was negligible when measured in DMEM, despite the medium containing an activating concentration of calcium of 1.9 mM. The transamidating activity does not alter upon an addition of further 5 mM calcium to the culture medium, instead it is substantially boosted about 4 fold by the addition of 5 mM DTT. When the culture medium was supplemented with both 5mM calcium and DTT, a further 2 fold increase in the tTG activity was observed confirming the calcium dependency of the transamidating reaction. Similar results were obtained when DMEM was substituted with the Tris-based buffer containing calcium and/or DTT.

The tTG activity in the induced and non-induced cell assembled matrix was measured in the presence of DMEM alone or DMEM with 5 mM DTT. As can be seen from the figure 3.3.5, there is no statistically significant difference between the activity of tTG in the non-induced and the induced matrix, when the TG activity assay was performed with DMEM alone. Upon addition of DTT to the culture medium, an approximately 2 fold increase in the tTG activity of induced matrix was observed. However, the incubation of the non-induced matrix with DMEM supplemented with DTT did not lead to a significant increase in the tTG activity.

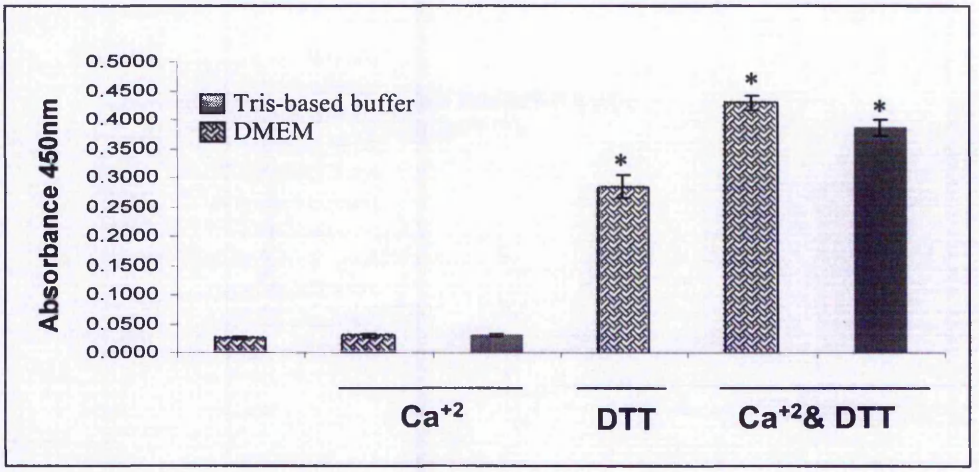


Figure 3.3.4 The measurement of FN-bound tTG activity

The activity of FN-bound tTG was measured by incorporation of biotinylated cadaverine into FN in either the culture medium DMEM, or DMEM with 5 mM Ca^{+2}, or DMEM with 5 mM of Ca^{+2} and DTT, or the activity buffer containing 5 mM Ca^{+2} or 5 mM Ca^{+2} and 5 mM DTT. Values represent the mean ± S.D. absorbance at 450 nm of three experiments each undertaken in quadruplicate. The final values were obtained by subtracting the background values (the absorbance values obtained from wells where 5 mM Ca^{+2} is substituted with 5 mM EDTA) from the mean absorbance values. The * presents the statistical difference ($p<0.05$) between absorbance value obtained from the wells incubated with DMEM only and wells incubated with DMEM or Tris-based buffer containing DTT and/or Ca^{+2}.

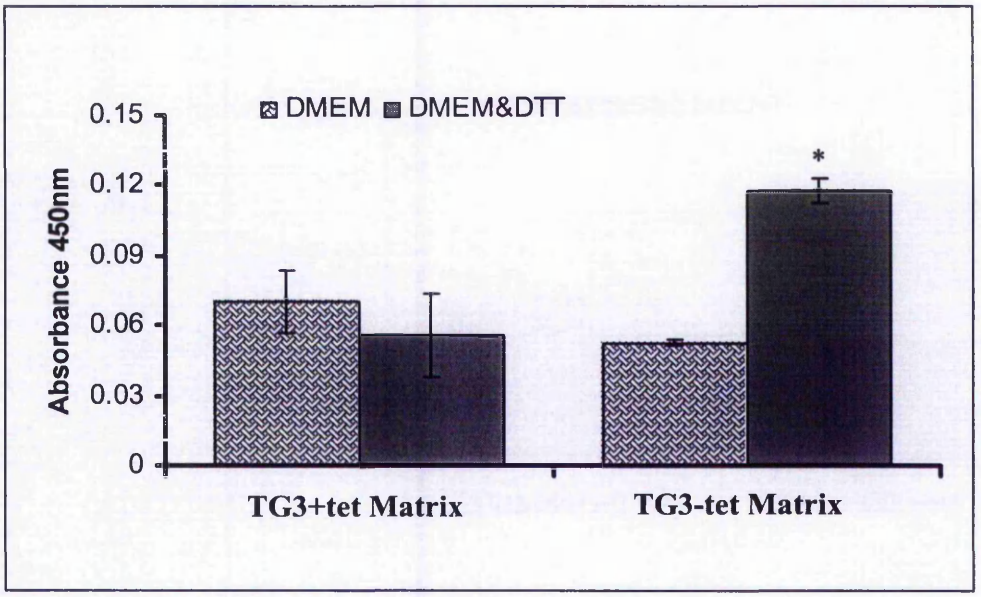


Figure 3.3.5 The measurement of tTG activity in physiological cell assembled matrix

The activity of cell secreted tTG in non-induced cell assembled (TG3+tet) and induced cell assembled (TG3-tet) matrix was analysed by incorporation of biotinylated cadaverine into FN in either the culture medium DMEM, or DMEM with 5 mM Ca^{+2} and 5 mM DTT. The results are expressed as mean ± S.D. absorbance at 450 nm of three independent experiments done in 8 replicates. The background values were obtained from wells incubated with an inactive buffer, and subtracted from the mean absorbance values. The * represent the statistical difference ($p<0.05$) when the absorbance values of non-induced and induced matrices were incubated with DMEM containing DTT, compared to the ones incubated with DMEM only.

3.3.5 Inhibition of the cross-linking activity of FN-bound tTG

The efficacy of the irreversible site directed tTG inhibitor R283 to silence the cross-linking ability of tTG immobilised on FN was established by measuring the bound tTG activity in the presence of increasing concentrations of the inhibitor.
As seen in Figure 3.3.6, the inhibitor reduced the transamidating activity of FN-bound tTG down to 50% at a concentration of 10 μM. When a concentration of 50 μM was used, a 70% decline was observed in enzyme activity. The maximum inhibition of the cross-linking activity, approximately 97%, was recorded at concentrations starting from 100 μM to 1000 μM.

3.3.6 The availability of FN after blocking the FN-tTG matrix

In order to determine whether tTG is important in the FN-tTG mediated cell adhesion, the matrix bound tTG was blocked by specific monoclonal Cub7402 in cell adhesion experiments. The accessibility of fibronectin bound to tTG after blocking with Cub7402 antibody was tested using an ELISA type assay. The matrix was also incubated with a non-specific control antibody sharing the same isotype IgG1 as the monoclonal Cub7402.
The absorbance 450 nm values obtained from each matrix shared similar values (figure 3.3.7). The change in the relative levels of tTG bound and unbound FN after blocking the FN-tTG matrix by Cub 7402 and IgG1, was found to be statistically insignificant. Thus, the obstruction of tTG by Cub7402 neither affects the accessibility of FN nor abolishes its availability in this complex.

3.3.7 The three dimensional detection of FN-tTG matrix

The immunohistochemical analysis of FN-tTG matrix was performed by visualising the FN, tTG and their association in the complex. The human osteoblast cells were used to detect any change in the FN-tTG complex when the cells were seeded on the matrix.

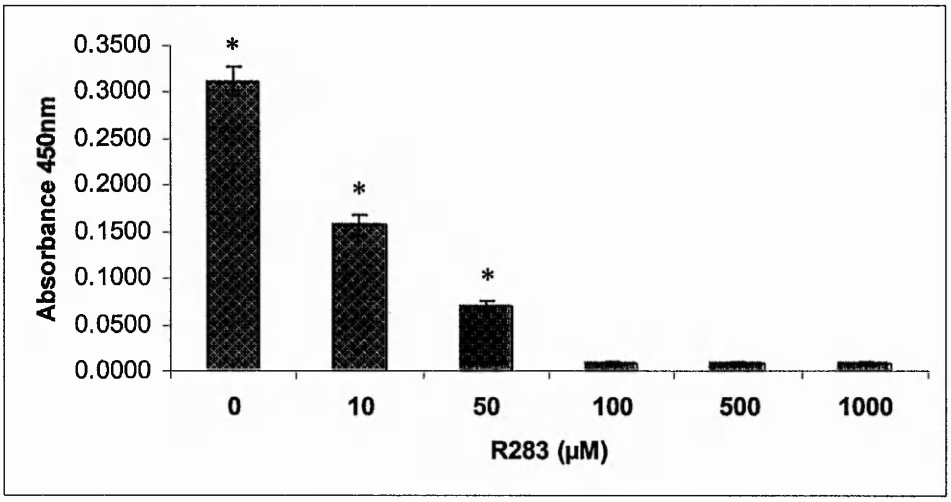


Figure 3.3.6 Inhibition of FN-bound tTG activity by R283

The inhibition of the crosslinking activity of FN-bound tTG in response to increasing concentrations of active site inhibitor R283 was performed as described previously in Section 3.2.3. Values represent the mean ± S.D. absorbance at 450 nm from three independent experiments, each of which was performed in 4 replicates. The final values were acquired by subtracting the background values obtained from the wells incubated with an inactive buffer from the mean absorbance values. The * represents the statistically significant difference ($p<0.05$) for the crosslinking activity of FN-bound tTG, when compared to FN-tTG coated wells incubated with 1000 μM R283 concentration.

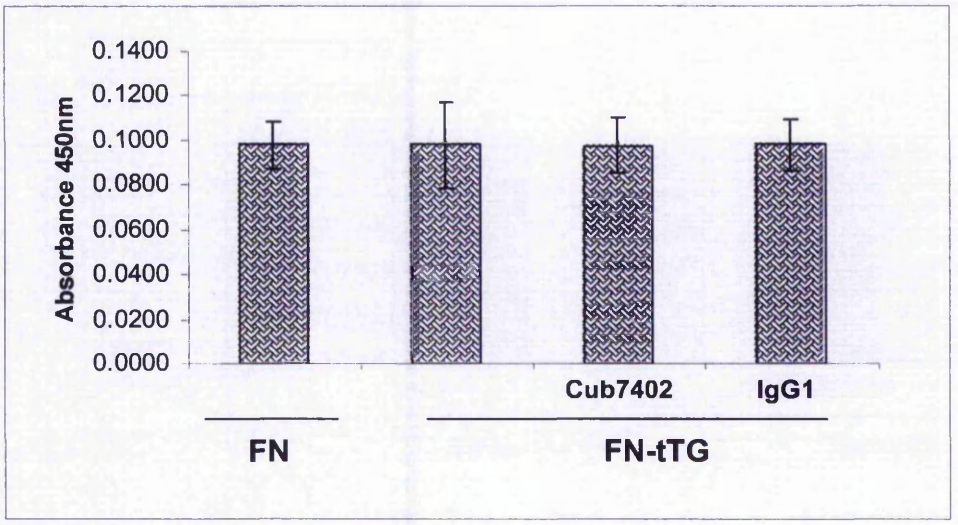
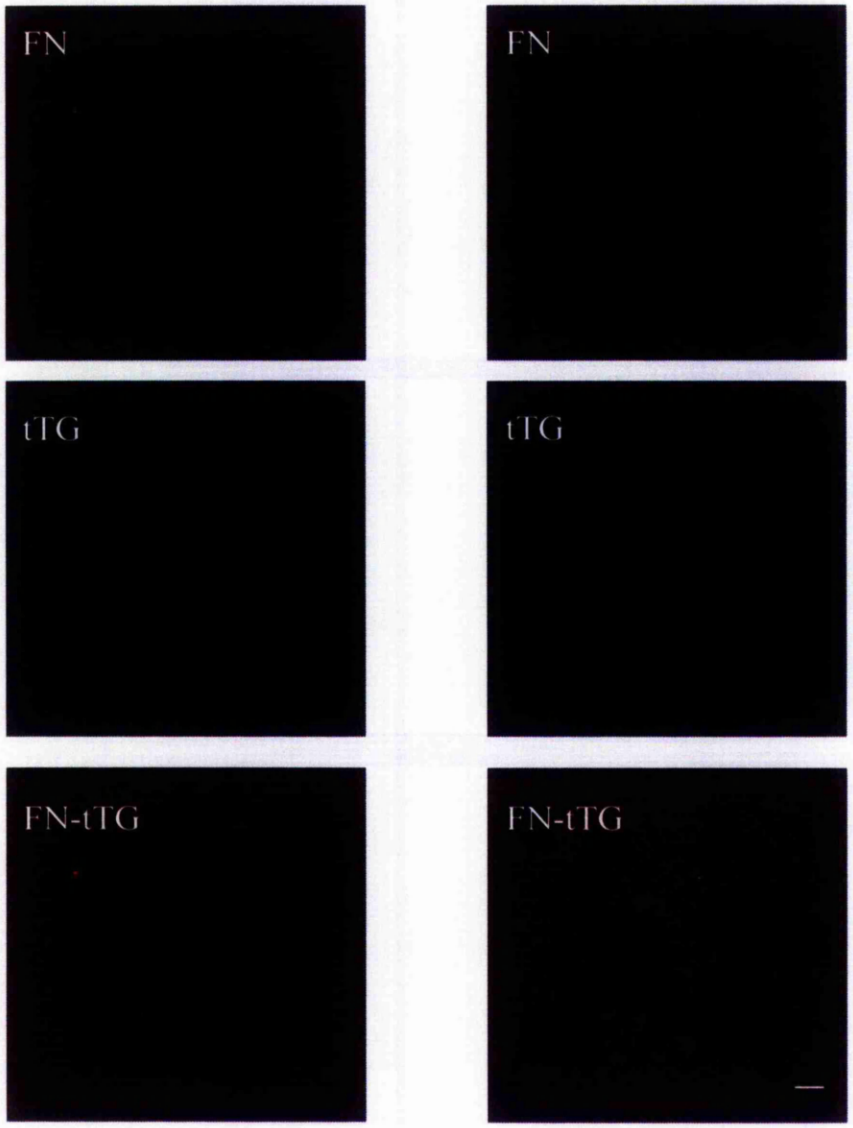


Figure 3.3.7 ELISA detection of FN levels after blocking the FN-tTG matrix with antibodies

The relative levels of FN were measured after blocking the tTG bound to the FN matrix, with Cub7402 and the control antibody IgG1 through an ELISA-type assay as explained in the Section 3.3.4. Data are expressed as mean ± S.D. absorbance values from three independent experiments, carried in quadruplicate. The background readings, obtained from wells incubated only with the secondary antibody, were subtracted from the mean absorbance values to obtain the final values.

Figure 3.3.8 The immuno-staining of FN and FN-bound tTG in the presence and absence of cell attachment

The FN-tTG matrix in the presence and absence of HOB cells was double-stained with anti-mouse monoclonal antibody Cub7402 and/or anti-FN rabbit polyclonal antibody. The double-staining was visualised using anti-rabbit IgG-TRITC (raised in swine) and anti-mouse IgG-FITC (raised in sheep) and viewed by confocal microscopy as described in Methods Section 2.2.4. The bar is equal to 10 μm.



FN-TG Matrix **FN-TG Matrix with HOB cells**

Detection of FN and tTG showed a uniform pattern of staining (figure 3.3.8). Upon addition of cells, no apparent change in association between FN and tTG was observed. This result showed first of all that FN-tTG association is detectable in the matrix and second, the addition of cells does not cause a change in the appearance of the matrix.

3.4 Discusssion

Evidence that tissue type transglutaminase is involved in the stabilisation of the extracellular matrix has been reported by several studies (Griffin *et.al.,* 2002). Fibronectin is a central component of the ECM and a high affinity binding partner for tTG (Mosher *et.al.,* 1991; Lorand *et.al.,* 1988; Achyuthan *et.al.,* 1995). Starting with the hypothesis that the non-enzymatic function of tTG in the extracellular environment is strictly dependent on its association with FN, a model matrix has been developed by immobilising tTG onto FN coated tissue culture plastic. The aim of this study was to assess the importance of this FN-tTG matrix in RGD-independent cell adhesion and in induction of intracellular signals that leads cell survival. For this purpose, it was essential to characterise the model fibronectin bound tissue transglutaminase matrix, before using it for the cell adhesion studies.

Previous studies have shown that tissue type transglutaminase can bind to human plasma fibronectin in the absence of calcium (Turner and Lorand, 1989; LeMosy *et.al.,* 1992). The complexing of the two proteins was non-covalent in nature and did not involve the cross-linking of the proteins either to themselves or to each other (Turner and Lorand, 1989). In the light of these findings, tTG was immobilised on FN coated tissue culture plastic in the presence of 2 mM EDTA. The efficient binding of gpl tTG to human plasma FN was demonstrated with an ELISA type assay and immunohistochemistry. The fibronectin, immobilised on tissue culture plastic at the concentration of 5 μg/ml, appeared to bind a saturating amount of tTG when it was incubated with 20 μg/ml free tTG. These represent the concentrations of FN and tTG solutions used to coat the wells, not the amount of immobilised FN and tTG actually bound. Analysis of the complex between purified tTG from human erythrocytes and human plasma fibronectin revealed a molecular ratio of 1.95 mol of tTG to 1 mol of FN (Turner and Lorand, 1989). The examination of complexes of erythrocyte tTG and plasma FN by rotary shadowing electron microscopy confirmed that erythrocyte tTG bound to FN with a stoichiometry of about 2:1. However, liver tTG appeared to bind FN with a lower affinity than erythrocyte tTG such that to achieve the binding of one FN molecule to two liver tTG, the molar ratio of liver tTG in the complex mixture was increased

up to 40:1. Similarly in this study, ELISA analysis of the model matrix showed that the fibronectin matrix was saturated with liver tTG at a molar ratio of 28:1. Given that, 100 μl of 20 μg/ml of tTG (77 kDa) that is added on the well previously incubated with 50 μl of 5 μg/ml FN (550 kDa), gives the molar ratio of 28:1.

To obtain another matrix system that is more closely related to the ECM *in vivo*, a transfected fibroblast cell line (Swiss 3T3 TG3), which is capable of inducible expression of tTG under the control of a tetracycline-regulated promoter, was used. Depending on the presence or absence of tetracycline in the medium, Verderio *et al.* (1998) showed that these cells can express high or low levels of tTG in association with FN at their cell surface. The ELISA and TG activity analysis of the ECM of long-term cultures of induced and non-induced Swiss 3T3 TG3 fibroblasts indicated that induced cells deposit FN-rich matrix with increased levels of tTG compared to the low background levels deposited by non-induced cells. This data signifies that this physiological matrix of cell assembled-FN and cell-secreted tTG can be used as an alternative matrix in the future cell adhesion studies.

In vitro binding studies have located the putative high affinity binding site(s) for human tTG to the N-terminal tail end of FN (LeMosy *et. al.,* 1992), in particular to the gelatin binding FN fragment (Turner and Lorand, 1989; Radek *et.al.,* 1993). Therefore, it was decided to determine whether the putative tTG high affinity binding site on the N-terminal of FN molecule could substitute for full length FN in the model FN-tTG matrix in future cell adhesion assays. tTG was immobilised on the tissue culture plates coated with the 70 kDa (matrix assembly, heparin and gelatin binding), 45 kDa (gelatin binding) and 30 kDa (first type I repeats, matrix assembly, heparin binding) N-terminal FN fragments. The concentrations of FN fragments utilised were the optimal found to saturate plastic and not necessarily equimolar as judged from measurements using an ELISA based assay with a polyclonal anti-FN antibody (Verderio *et.al.,* 2000). Detection of the relative levels of tTG by ELISA showed that incubation of the N-terminal FN fragments with 20 μg/ml tTG resulted in saturating levels of tTG immobilised on all fragments, suggesting this concentration of tTG to be used in the future cell adhesion assays.

tTG was immobilised on the FN matrix in the presence of EDTA, as it was important to establish its potential role as a novel transamidating-independent protein in cell adhesion assays. However, the calcium concentration (1.9 mM) in the culture medium might lead to the activation of the FN-bound enzyme. The activity of tTG immobilised on the FN matrix was therefore measured in cell culture medium, simulating the experimental conditions of a cell adhesion assay. The transamidating activity of the enzyme was found to be negligible in the cell culture medium, and did not alter upon addition of further calcium, but was significantly boosted by the addition of reducing agent dithiothreitol to the medium. Similarly, the ECM with increased level of cell-secreted tTG (TG3-tet Matrix) did not exhibit enzymatic activity above background levels (TG3+tet Matrix) when incubated with DMEM, unless in the presence of DTT. Hence under the conditions used, FN-bound and cell-secreted tTG are not active in the presence of the cell culture medium, unless its cysteine residues, which account for 2.6% of total amino acids, and in particular the active-site cysteine-277, are kept in a reduced state. This is in keeping with the data of Jones *et al.* (1997), which described that cell surface related tTG did not mediate the incorporation of biotin cadaverine into fibronectin unless the assay was performed in the presence of the reducing agent, dithiothreitol. The transamidating independent role of tTG was further investigated by utilising a 2-[(2-oxopropyl)thio]imidazolium derivative (R283), the inhibitor of tTG. It was necessary to determine the most effective R283 concentration needed to knock down the activity of FN-bound tTG without causing cell toxicity when used to provide an inactive FN-tTG matrix in the future cell adhesion studies. The activity of tTG immobilised on FN was shown to be blocked by the inhibitor R283 at the minimal concentration of 100μM, suggesting that concentration of the tTG inhibitor to be enough to completely inhibit the transamidation reactions mediated by tTG bound to FN.

With the model for the FN-tTG matrix established, it was important to assess the role of tTG in cell-surface interactions by blocking the FN-bound tTG with the monoclonal anti-tTG antibody Cub7402. In this chapter, it was demonstrated that the incubation of FN-tTG matrix with Cub7402 antibody fully preserved the

availability of FN in this complex, since no change in antibody recognition of FN was detected in the ELISA assay (figure 3.3.7).

In conclusion, characterisation of the *in vitro* FN-bound tTG matrix using both the full length FN and amino-terminal FN fragments, in addition to a physiological cell-secreted matrix sets the ground work on which the rest of the project can be accomplished. The effects of these matrices upon cell adhesion are subsequently investigated extensively in the following chapter.

Chapter 4: The role of fibronectin bound tissue transglutaminase in RGD-independent cell adhesion

Chapter 4: The role of fibronectin bound tissue transglutaminase in RGD-independent cell adhesion

4.1 Introduction

Matrix assembly results from orderly homophilic and heterophilic interactions of ECM molecules with themselves and with other molecules and the cell surface. This process results in a homopolymeric or a heteropolymeric complex of defined biochemical composition and architecture (Hynes and Zhao, 2000). A common theme in matrix assembly is that the initial non-covalent interactions are often followed by formation of disulfide bonds, such as the disulphide bonds formed between protomeric FN molecules during FN matrix assembly. Under the normal extracellular physiological conditions, FN matrices form only on the surface of certain cells *in vitro,* and specified sites during embryogenesis *in vivo* (Mosher, 1993). Only with wounding, or frequently during tumorigenesis and fibrosis, is fibronectin expressed locally and deposited into the ECM (Gailit and Clark, 1994). The interactions of cells with the pericellular fibronectin matrix play critical roles in cell adhesion, migration, growth, survival, differentiation, and gene expression. At least two components contribute "specificity" to this important recognition system; the FN matrix assembly and the cell surface receptors. The assembly of pericellular FN matrix must be properly controlled. In addition, responsive cells must express suitable receptors recognising the FN matrix. The main cell surface receptors that recognise the FN matrix are the integrins. FN binds integrins through a cell adhesive site comprising modules III8-III10. The most critical site in the interaction of FN with integrins is the Arg-Gly-Asp (RGD) sequence in the III10 module (Mosher, 1984). The amino acid sequence RGD was also identified in other adhesive proteins including, vitronectin, fibrinogen, laminin, entactin, denatured collagens, and osteopontin (Ruoslahti and Pierschbacher, 1987). Given that the RGD sequence is the key cell adhesion sequence recognised by nearly half of the over 20 known integrins, RGD containing synthetic peptides appeared to get a widespread use as the modulators of cell adhesion.

The first studies that used the RGD containing peptides coated a solid surface with the peptides, and thereby promoted cell adhesion (Koivunen *et.al.,* 1994). Recently, Kantlehner *et al.* (2000) confirmed that, the coating of bone implant surfaces with cyclic RGD pentapeptides stimulated the osteoblast adhesion and proliferation as well as the bone formation. The other line of work was focused on the role of soluble RGD peptides in cell adhesion and tumour biology. The presentation of RGD containing peptides to cells in solution mimicked the cell attachment signal of fibronectin and inhibited the attachment of cells to fibronectin (Pierschbacher and Ruoslahti, 1984), but not to collagen (Hayman *et.al.,* 1985). Screening of a number of RGD synthetic peptides revealed that the nature of the amino acid following the aspartic acid is important for the determination of the binding specificity of the peptide to adhesion receptors. For example, FN-derived GRGDSP peptide inhibited the binding of the fibronectin and vitronectin receptors to their ligands (Pytela *et.al.,* 1985a,b). The GRGDNP peptide showed a similar specificity but was about six-fold more active than the GRGDSP peptide at inhibiting the attachment of cells to fibronectin compared to vitronectin (Pierschbacher and Ruoslahti, 1987). The GRGDTP peptide, unlike the other peptides, inhibited the attachment of oesteosarcoma cells to type I collagen, as well as to fibronectin and vitronectin (Dedhar *et.al.,* 1987).

The RGD recognition of FN is believed to be active for bone cell and fibroblast attachment. These cells can bind to FN principally or entirely through the cell-binding region of FN (Puleo and Bizios, 1991; Verderio *et.al.,* 1998 and 2000). Previous work demonstrated a close association of FN with tTG at the cell surface/pericellular matrix, consistent with the *in vitro* specific binding of human plasma FN with the enzyme (Verderio *et.al.,* 1998; Gaudry *et.al.,* 1999; LeMosy *et.al.,* 1992). Recent findings suggested a new important role for FN-bound tTG in cell adhesion. In these studies the effect of the hexapeptide G**RGD**TP on HOB and Swiss 3T3-fibroblast cell adhesion to FN and FN/tTG complex was studied. The results showed that tTG once bound to fibronectin supports an RGD-independent cell adhesion (Verderio *et.al.,* 2000).

The work contained in this chapter has the main objective of gaining a deeper insight into the molecular mechanism(s) and physiological importance of the RGD-independent cell adhesion brought about by tTG when immobilised on FN. Human osteoblast cells were selected as the main cell model since they preferentially adhere on FN and biomaterials coated with FN-tTG *in vitro* (Heath *et.al.,* 2002), and comprise a well defined pattern of integrin cell-surface receptors, including mainly the RGD-binding β_1 subunit paired with α_1, α_2, α_3, α_5, and α_V subunits (Gronthos *et.al.,* 1997).

4.2 Methods

4.2.1 Inhibition of protein synthesis

To inhibit the protein synthesis, the antibiotic cycloheximide produced by *Streptomyces griseus,* was used in the cell adhesion assays. In cell adhesion experiments, HOB cells and Swiss 3T3 fibroblasts were pre-treated with 20 μg/ml of cycloheximide for 2 hours and resuspended in SFM containing 10 μg/ml of cycloheximide prior to the pre-incubation with increasing concentrations of RAD and RGD (0-200 μg/ml) synthetic peptide (Akimov *et.al.,* 2000). Cells were then seeded ($2x10^4$ HOB cells/well or $1.75x10^4$ Swiss 3T3 cells/well) on the microtiter plate coated with FN (5 μg/ml) or FN with immobilised tTG (20 μg/ml) and were allowed to attach between 20 to 40mins. Following the cell attachment and spreading, the cells were fixed and stained as described previously under Methods Sections 2.2.5. The quantitative assessment of cell attachment and spreading was performed as mentioned before (Section 2.2.5.4). The differences between data sets were analysed at 95% level of significance by the Mann-Whitney test using the Mini-Tab statistical analysis programme (Mini-Tap Inc, USA).

4.2.2 The inhibition of RGD-mediated cell adhesion of Swiss 3T3 fibroblasts to the cell assembled matrix

Transfected Swiss 3T3 fibroblasts, displaying inducible expression of tTG (clone TG3), were cultured in 96-well plates and induced as depicted by Verderio *et al.* (1998). After a 3-week growth, cells were detached using a non-enzymatic method as described earlier (Section 2.2.2.3). Following the detachment of the cells, wells were washed twice with PBS, pH 7.4 and the third wash was kept in the wells until Swiss 3T3 fibroblasts (wild type) were prepared for the cell adhesion assay. A cell suspension of $2x10^5$ cell/ml was prepared, and incubated with G**RGD**TP and G**RAD**SP synthetic peptides. Swiss 3T3 fibroblasts were then seeded on cell-deposited ECM and allowed to adhere for 16 hours in the presence of the synthetic peptides. The medium was then carefully removed and cells were fixed,

permeabilised, and stained as mentioned earlier (Section 2.2.5). The cell attachment and spreading of Swiss 3T3 fibroblasts on the cell assembled matrix in the presence of RAD synthetic peptides were assessed as described previously (Section 2.2.5.4). To assess the cell adhesion of Swiss 3T3 fibroblasts on the cell assembled matrix in the presence of RGD synthetic peptides, digital images of nine non-overlapping fields covering most of the well, acquired using a video digital camera Olympus DP10 at 10 x magnification. The number of cells per image was quantified using the Scion image analysis programme (National Institute of Health,Washington DC, USA). Mann-Whitney test with 95 % confidence interval was employed to determine the statistical difference between the data sets.

4.2.3 The inhibition of FN-bound tTG in cell adhesion assay

The cross-linking activity of FN-immobilised tTG was inhibited by incubation with the active-site specific inhibitor 2-[(2-oxopropyl)thio]imidazolium derivative, R283 (Freund *et.al.,* 1994) at the concentration of 100 μM, for 10 minutes in DMEM as mentioned earlier (Section 3.2.3). Meanwhile, for the cell adhesion assay on the inactivated FN-tTG matrix, the HOB cells at $2x10^5$ cell/ml concentration were also incubated with 100 μM R283 for 10 minutes. The medium containing R283 was then removed from the FN-tTG matrix and replaced with R283-supplemented DMEM containing the HOB cells in suspension. Cells were allowed to attach and spread for 20 minutes, the assay was then terminated and the cell adhesion of HOB cells were finally analysed as described previously (Section 2.2.5).

4.3 Results

4.3.1 The fibronectin bound-tTG supports cell adhesion

In the previous chapter a matrix model of immobilised FN with bound tTG was developed. In the following experiments, the role of FN-tTG matrix in supporting the RGD-independent cell adhesion was examined in the perspective of cell attachment and spreading. In the following chapters, the term cell adhesion was used to refer to both the attachment and spreading status of the cells. The term "cell attachment" is used to describe the total number of cells that are anchored to the relevant matrices. Cell spreading was defined as the process whereby a rounded cell is flattened through transmission of the signals generated by the extracellular adhesive associations. The pictures showing cell adhesion on FN-tTG matrix with and without RGD peptide, along with control cell adhesion on FN were printed for each cell line. However, the pictures of cell adhesion on FN-tTG were not shown due to limitation in space.

4.3.1.1 The FN-tTG matrix compensates for RGD inhibition of cell adhesion independently from endogenous ECM protein synthesis

Since tTG when immobilised on FN can restore cell attachment and spreading in HOB cells and Swiss 3T3 fibroblasts after inhibition by the RGD containing synthetic peptides, it was decided to rule out any effects of endogenous secreted adhesion molecules using the protein synthesis inhibitor, cycloheximide.

HOB cells were grown under sub-confluency and pre-treated with cycloheximide for 2 hours prior to harvesting, as described in the Methods (Section 4.2.1). The effect of the hexapeptide G**RGD**TP on the cycloheximide treated HOB cells was examined. HOB cells were treated with increasing concentrations of G**RGD**TP (or RGD) peptide and seeded on FN and FN-tTG matrices. To rule out a non-specific inhibition in cell attachment due to the presence of toxic levels of an exogenous hexapeptide, equivalent concentrations of the control G**RAD**SP peptide were used

Figure 4.3.1 Adhesion of cycloheximide-treated HOB cells to FN- and FN-tTG matrices in the presence of RAD and RGD peptides

a, Visualisation of cycloheximide treated HOB cells on FN and FN-tTG matrices in the presence of RGD peptide; **b,** effect of RAD peptide; **c,** effect of RGD peptide on the cell adhesion of cycloheximide treated HOB cells to FN and FN-tTG matrices. The cell adhesion assay was performed and the attachment and spreading of cyloheximide treated HOB cells were assessed as described in Sections 2.2.5 and 4.2.1. White arrows point to spread cells, whereas black arrows point to non-spread cells. Each data point corresponds to the mean percentage of attached cells (cell attachment) or the mean percentage of spread cells (cell spreading) ± S.D. of three separate experiments performed in triplicate. The ordinates in the top graphs represent the mean cell attachment expressed as mean percentage of control attachment to FN (which represents 100%) ± S.D. The mean number of cell attachment ± S.D. on FN in the 3 experiments was 174 ± 3, 200 ± 6, and 183 ± 5. The ordinates in the lower graphs indicate the mean percentage of spread cells where the mean percentage spreading value ± S.D. on FN was considered as 100%. The cell spreading was thereby expressed as the mean percentage of control spreading on FN ± S.D. The statistically significant difference ($p<0.05$) between FN control and cells seeded on the FN-tTG matrix in the presence or absence of RAD synthetic peptide was indicated with * symbol. The ♀ symbol indicates the statistically different cell adhesion values ($p<0.05$) of RGD treated cells on FN when compared to the FN control.

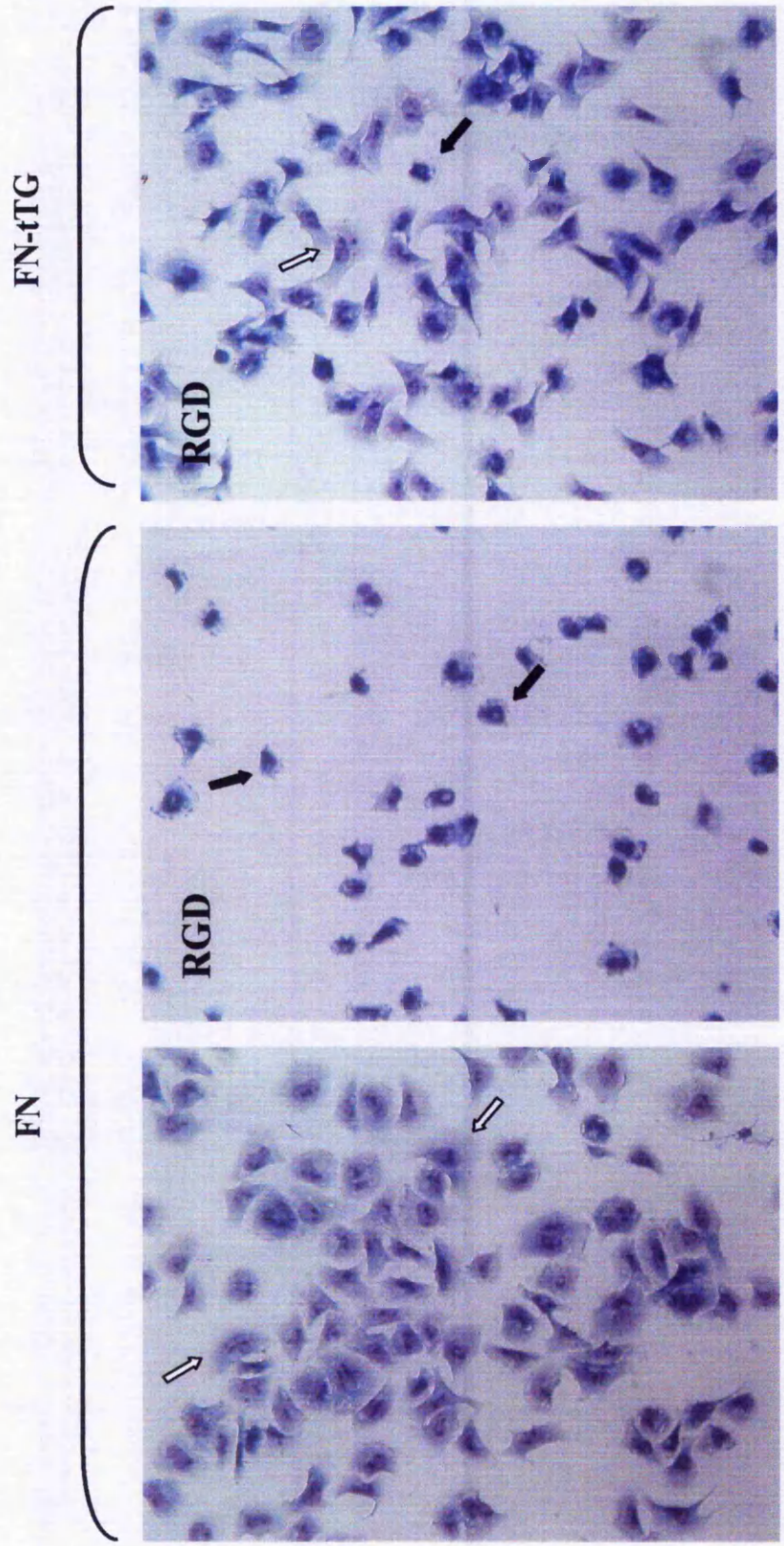


Figure 4.3.1a

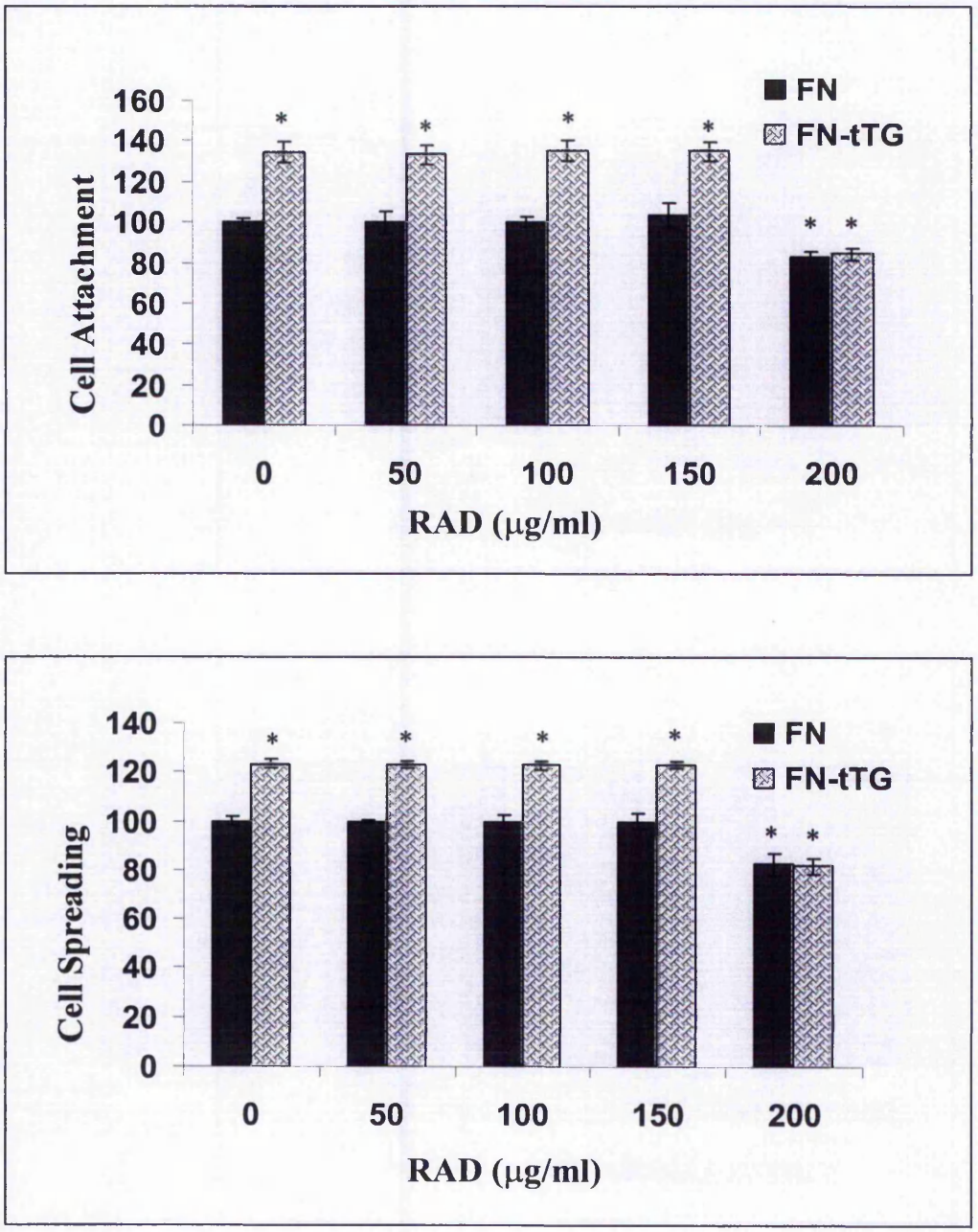
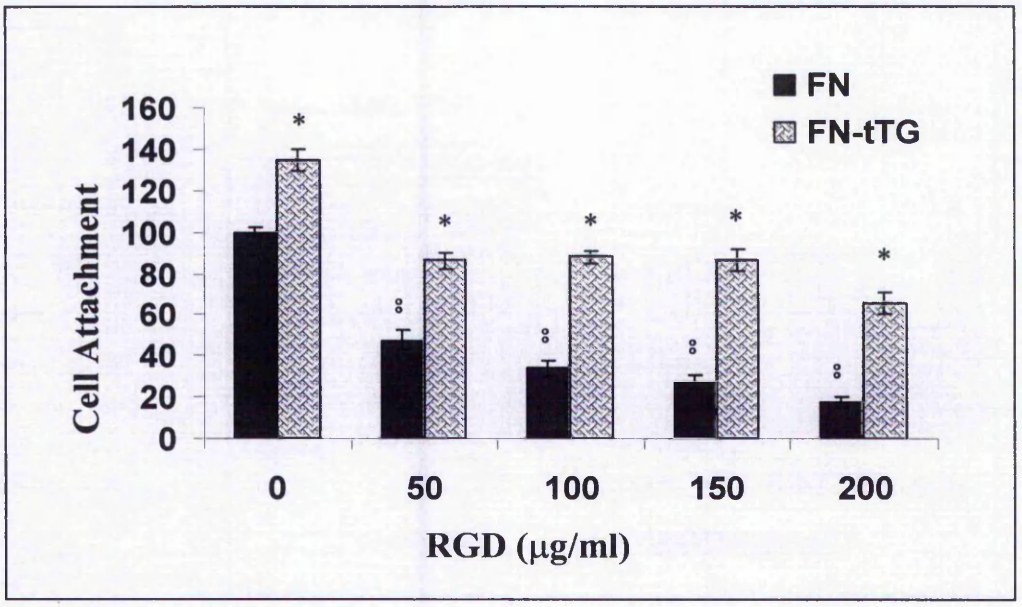

Cell Attachment
160
140
120
100
80
60
40
20
0
FN
FN-tTG
0
50
100
150
200
RAD (μg/ml)
Cell Spreading
140
120
100
80
60
40
20
0
FN
FN-tTG
0
50
100
150
200
RAD (μg/ml)

Figure 4.3.1b


FN
FN-tTG
Cell Attachment
160
140
120
100
80
60
40
20
0
0
50
100
150
200
RGD (μg/ml)

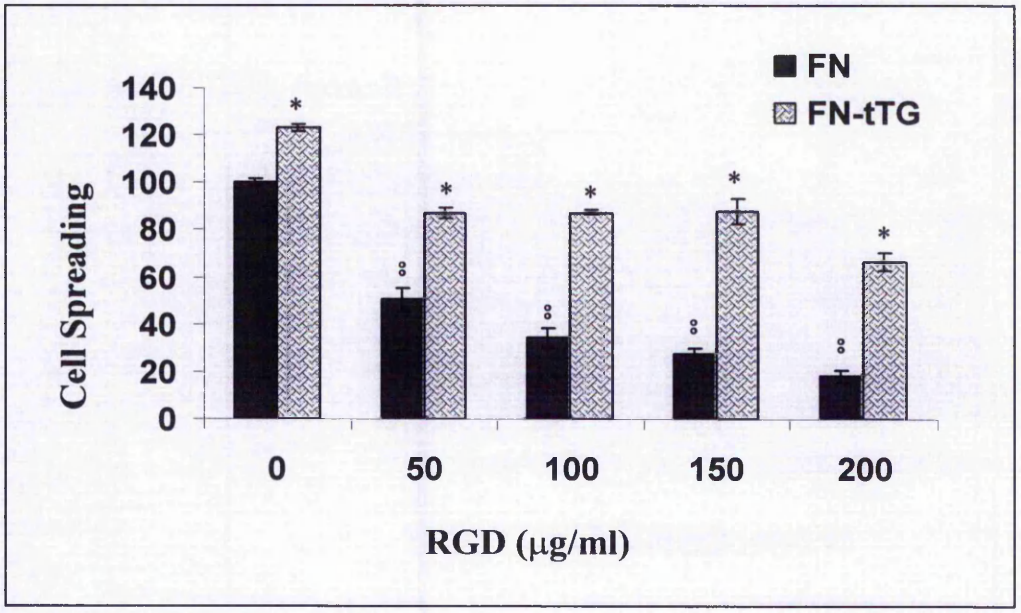

FN
FN-tTG
Cell Spreading
140
120
100
80
60
40
20
0
0
50
100
150
200
RGD (μg/ml)

Figure 4.3.1c

to treat the HOB cells. Once attached and spread, HOB cells had a cuboidal appearance. However, non-spread HOB cells displayed a round-like morphology (figure 4.3.1a). Results obtained from cell adhesion assays showed that the treatment of HOB cells with 50 to 150 μg/ml of RAD peptide resulted in a cell adhesion to FN, comparable to cell adhesion to FN without RAD peptide (FN control) (figure 4.3.1b). That is, no statistical difference was detected in cell attachment and cell spreading between the FN control and RAD treated cells at these low concentrations. Approximately a 34% increase in cell attachment and a 23% increase in cell spreading were observed when HOB cells were seeded on FN-tTG matrix in the absence of RGD peptide. The treatment of HOB cells with RGD peptide led a significant decrease in cell adhesion to FN (figure 4.3.1c). At 50 and 100 μg/ml RGD peptide, attachment on FN was significantly reduced (typically to 50-65% of control values on FN) (figure 4.3.1c, upper), but attachment to FN-tTG was not significantly inhibited at these same RGD peptide concentrations. Cell adhesion to FN-tTG, in the presence of 50 and 100 μg/ml RGD peptide, was 84-87% of control cell attachment to FN without RGD peptide. The treatment of cells with 150 μg/ml RGD peptide further decreased cell attachment and spreading to FN down to approximately 75% of control values on FN. In contrast, cell attachment and spreading on FN-bound tTG by inclusion of RGD peptide at 150 μg/ml concentration, was found to be 88% of the control. Only at 200 μg/ml, cell adhesion on FN-tTG was reduced to 65% in comparison to control FN without RGD peptide, indicating the non-specific effect of the hexapeptide at this concentration (figure 4.3.1b).

Swiss 3T3 fibroblasts displayed a comparable response to HOB cells. The attached and spread Swiss 3T3 cells demonstrated a flattened spindle-like morphology, while non-spread fibroblasts were either rounded in morphology or displayed a diamond-like appearance (figure 4.3.2a). The treatment of Swiss 3T3 fibroblasts with 50-150 μg/ml of RAD peptide did not affect their cell adhesion pattern, compared to that of FN control (figure 4.3.2b). However, when these cells were seeded on FN-tTG matrix in the presence or absence of RAD peptide, a typical 18% increase in cell attachment and spreading was detected in comparison to their

Figure 4.3.2 Adhesion of cycloheximide-treated Swiss 3T3 fibroblasts to FN-and FN-tTG matrices in the presence of RAD and RGD peptides

a, Visualisation of cycloheximide treated Swiss 3T3 fibroblasts on FN and FN-tTG matrices in the presence of RGD peptide; **b,** effect of RAD peptide; **c,** effect of RGD peptide on the cell adhesion of cycloheximide treated Swiss 3T3 fibroblasts to FN and FN-tTG matrices. The cell adhesion assay was undertaken and the attachment and spreading of cyloheximide treated Swiss 3T3 fibroblasts were analysed as described previously (Sections 2.2.5 and 4.2.1.). Spread cells were indicated with white arrows, while non-spread cells were shown with black arrows. Each data point represents the mean percentage of attached cells (cell attachment) or the mean percentage of spread cells (cell spreading) ± S.D. of three separate experiments performed in triplicate. Data are expressed as percentage of control values on FN, which represents 100%. Mean number of cell attachment and spreading values ± S.D. on FN control were 190 ± 14 and 154 ± 4. The mean percentage of control spreading on FN ± S.D. was assessed as 81 ± 2, which was taken as 100%. The * symbol represents significant difference ($p<0.05$) between FN control and cells seeded on the FN-tTG matrix in the presence or absence of RAD synthetic peptide. The ¤ symbol indicates the statistically different cell adhesion values ($p<0.05$) of RGD treated cells on FN when compared to FN control.

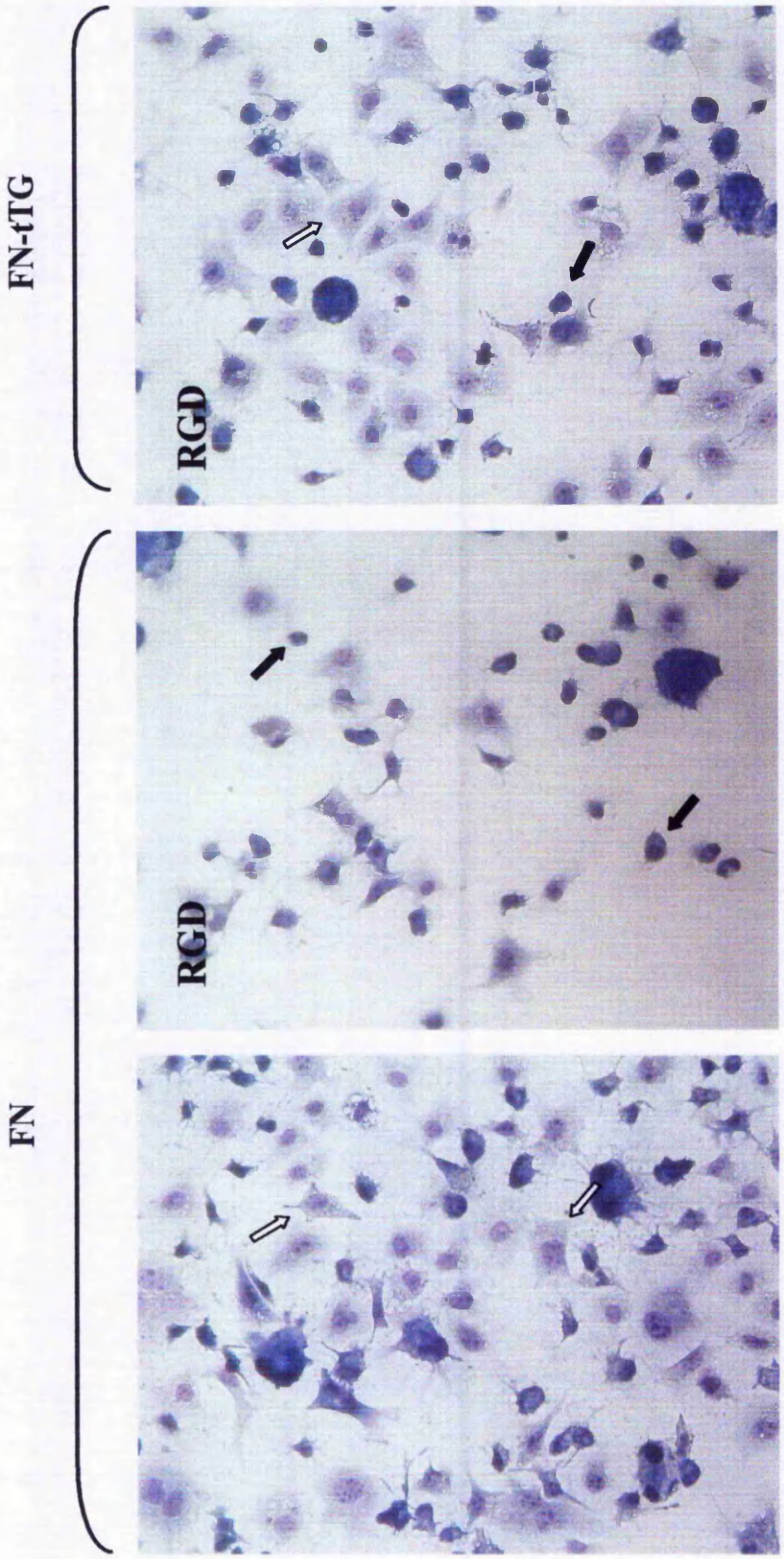
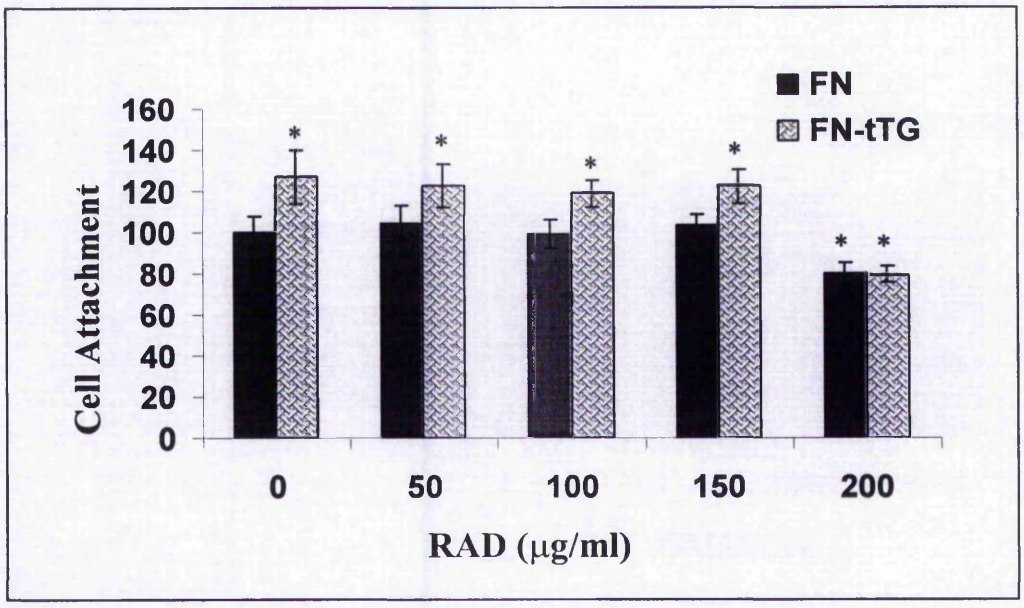


Figure 4.3.2a


FN
FN-tTG
Cell Attachment
160
140
120
100
80
60
40
20
0
0
50
100
150
200
RAD (μg/ml)

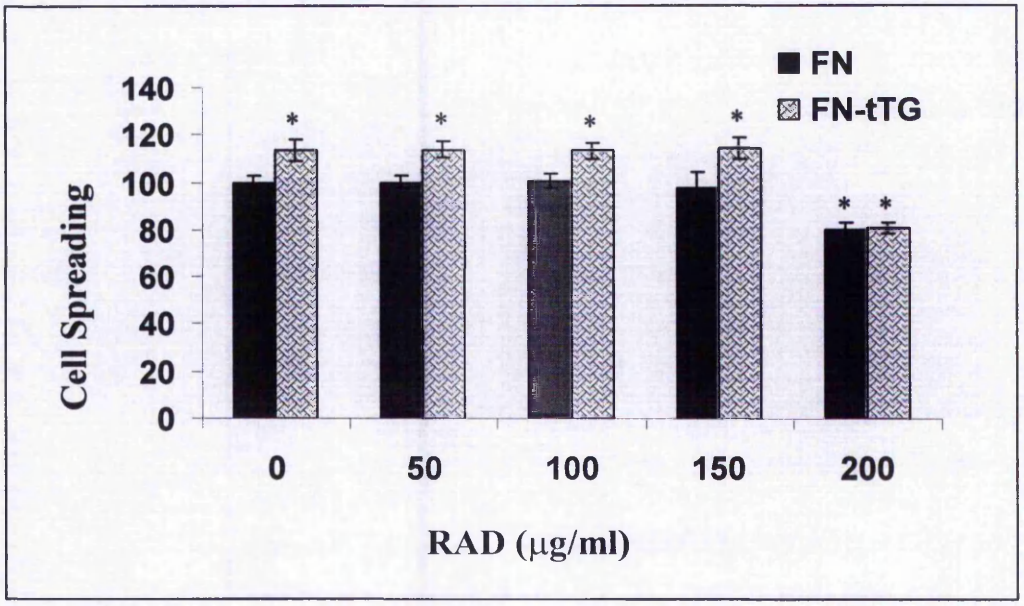
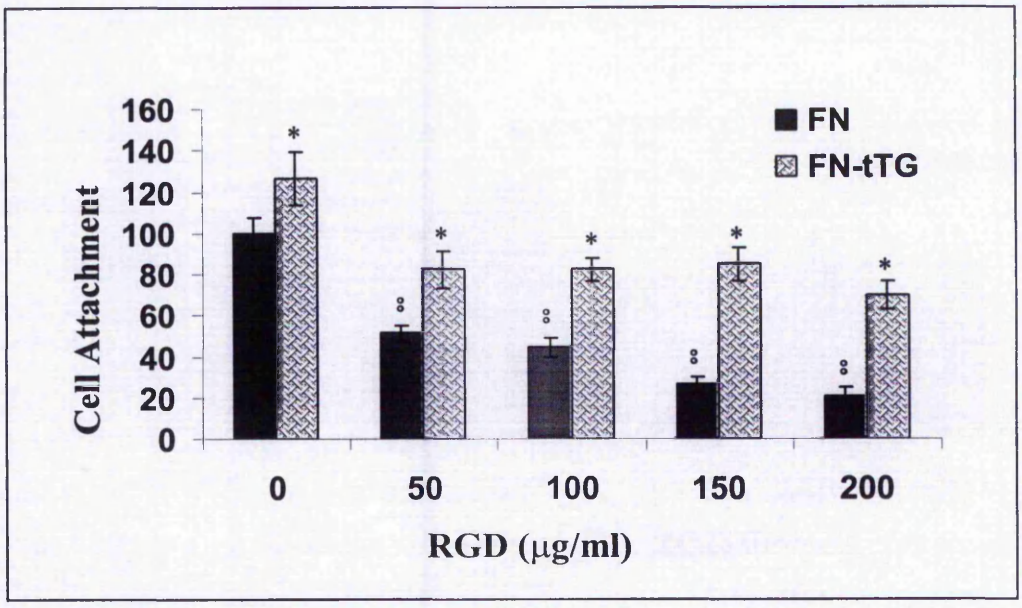

FN
FN-tTG
Cell Spreading
140
120
100
80
60
40
20
0
0
50
100
150
200
RAD (μg/ml)

Figure 4.3.2b


Cell Attachment
160
140
120
100
80
60
40
20
0
FN
FN-tTG
0
50
100
150
200
RGD (μg/ml)

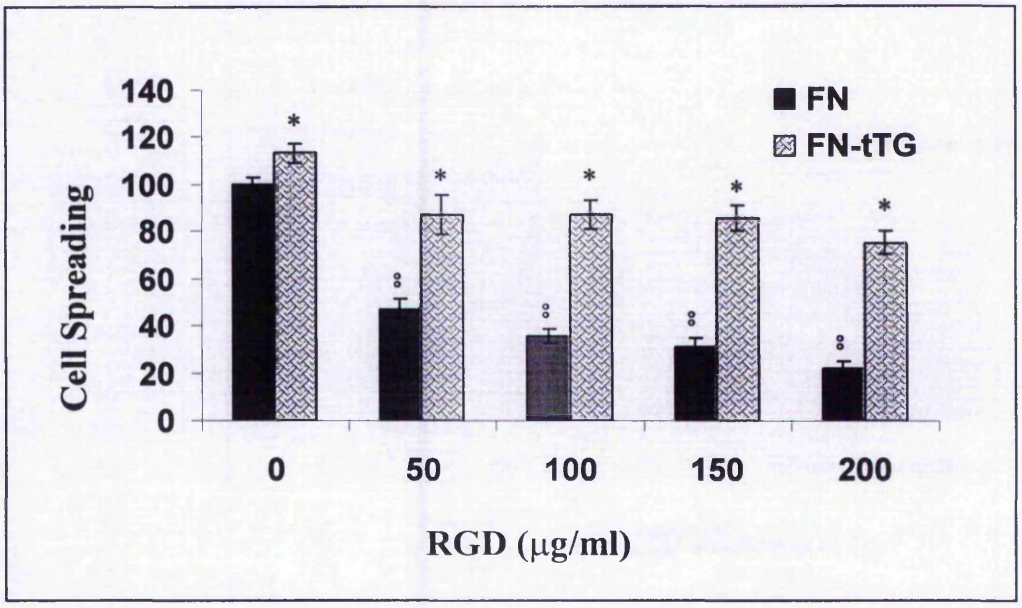

Cell Spreading
140
120
100
80
60
40
20
0
FN
FN-tTG
0
50
100
150
200
RGD (μg/ml)

Figure 4.3.2c

adhesion to FN. At 200 μg/ml of RAD peptide, cell attachment and spreading on FN and FN-tTG was found to be 79-84% of the control values on FN due to non-specific effect of the hexapeptide. The inhibition of attachment and spreading on FN by the RGD synthetic peptide was estimated as 50% at a concentration of 50 μg/ml (figure 4.3.2c). The cell attachment was further decreased to 44-26% of control FN levels at concentrations of 100 μg/ml and 150 μg/ml RGD peptide. Incubation of cells with 100 μg/ml and 150 μg/ml RGD peptide, also significantly reduced cell spreading on FN, typically to 31-35% of the control value. At 200 μg/ml concentration, the RGD peptide inhibited the cell attachment and spreading up to 80% of that of control FN levels. The attachment and spreading of Swiss 3T3 cells was restored to between 85-90%, once seeded on the FN-tTG matrix at 50, 100, and 150 μg/ml RGD peptide. These results indicate that HOB and Swiss 3T3 cells, pre-treated with cycloheximide, were capable of RGD-independent cell attachment and spreading on the FN-tTG matrix comparable to that of their non-treated cell counterparts.

4.3.1.2 The fibronectin bound tTG supports RGD independent cell adhesion in different cell types.

To assess whether the RGD-independent cell-adhesion pathway mediated by FN-tTG can be used with different cell types, experiments were also carried on an epithelial-like human urinary bladder carcinoma cell line (ECV304), primary human dermal fibroblast, and mouse dermal fibroblasts isolated from Tg2 wild type and knock out transgenic mice.

Exponentially growing ECV304 cells were trypsinised, washed once in DMEM medium with serum and twice with medium without serum as described previously (Section 2.2.5). The ECV304 cells were then treated with increasing concentrations of control inactive RAD (0-200 μg/ml) and active RGD peptide (0-200 μg/ml), and plated on FN and FN-tTG matrices for 4 hours. Cell adhesion of ECV304 cells to FN and FN-tTG matrices in the presence or absence of the synthetic peptides was compared.

Figure 4.3.3 The RGD-independent cell-adhesion of ECV304 cells cells in response to FN-tTG matrix

a, Visualisation of ECV304 cells on FN and FN-tTG matrices in the presence of RGD peptide; **b,** effect of RAD peptide; **c,** effect of RGD peptide on the cell adhesion of ECV304 cells to FN and FN-tTG matrices. The cell adhesion assay was performed and the attachment and spreading of ECV304 cells were assessed as described in Sections 2.2.5 and 4.2.1. White arrows point to spread cells, whereas black arrows point to non-spread cells. Data was represented as the mean percentage of attached cells (cell attachment) or the mean percentage of spread cells (cell spreading) ± S.D. of three separate experiments carried out in triplicate. Each data point was expressed as a percentage of control values on FN, which represents 100%. Mean number of cell attachment ± S.D. on FN in the 3 experiments was calculated as 324 ± 10, 308 ± 3, and 441 ± 18. The mean percentage of spreading ±S.D. on FN in the 3 experiments was 94 ± 2, 88 ± 2, and 90 ± 1, which was considered as 100%. The statistically significant difference ($p<0.05$) between FN control and cells seeded on the FN-tTG matrix in the presence or absence of RAD synthetic peptide was indicated with * symbol. While, the ¤ symbol was used to indicate the statistically different cell adhesion values ($p<0.05$) of RGD treated cells on FN when compared to the FN control.

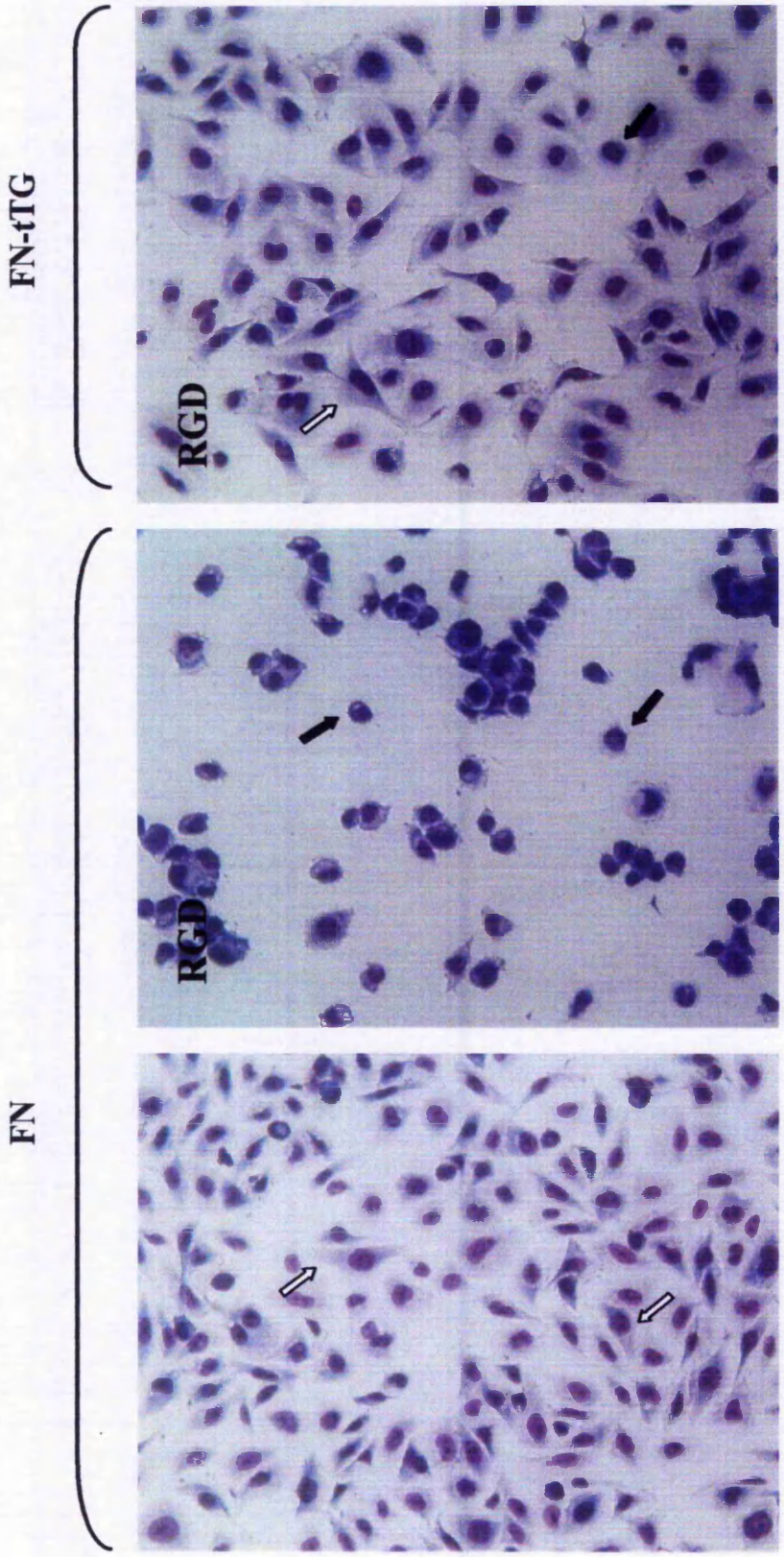
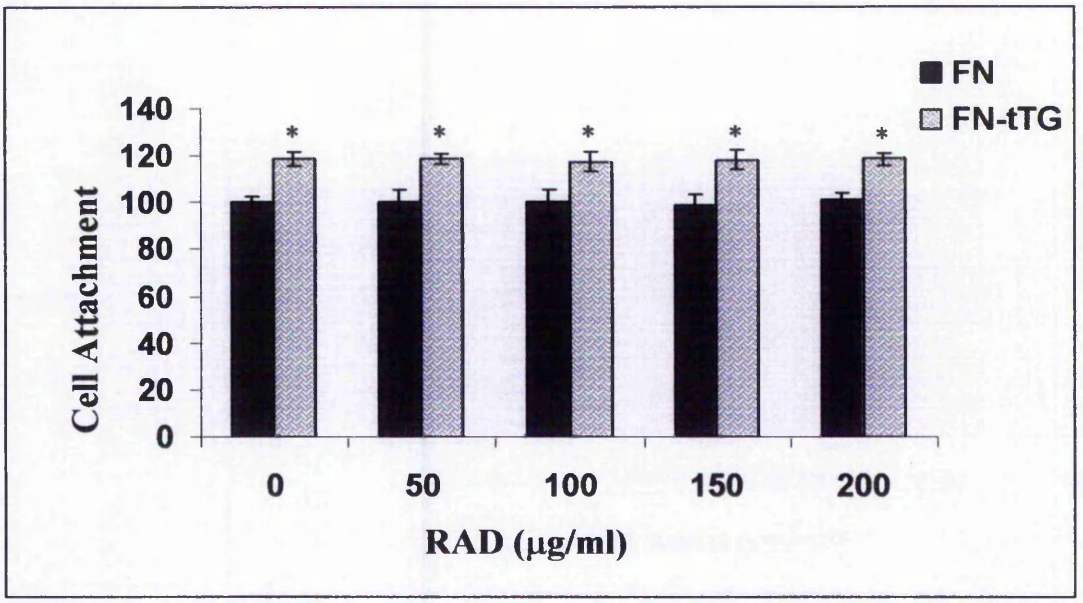


Figure 4.3.3a


FN
FN-tTG
Cell Attachment
140
120
100
80
60
40
20
0
*
0
50
100
150
200
RAD (μg/ml)

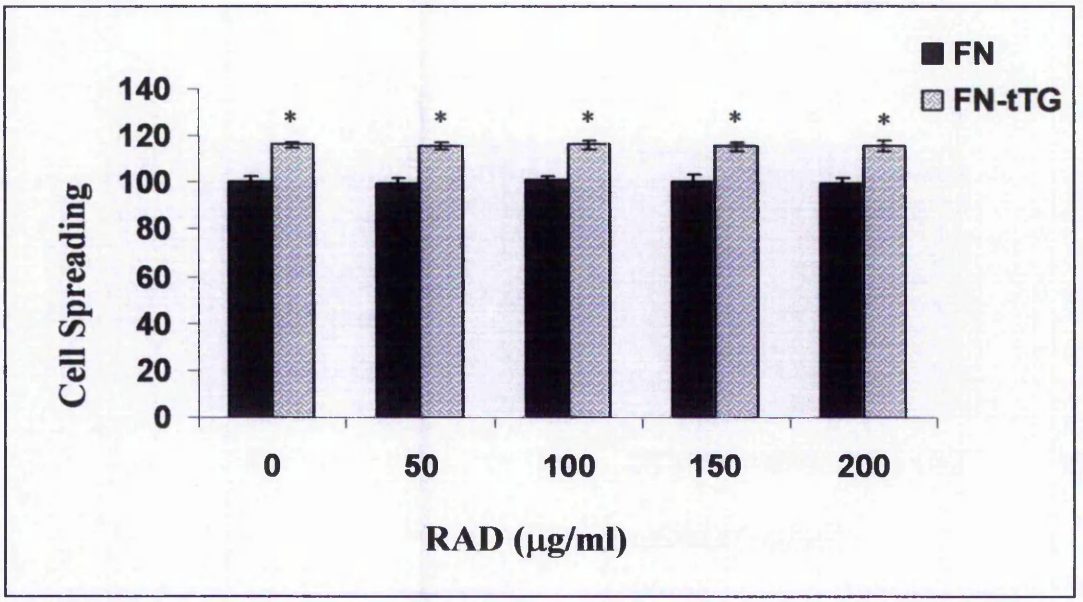
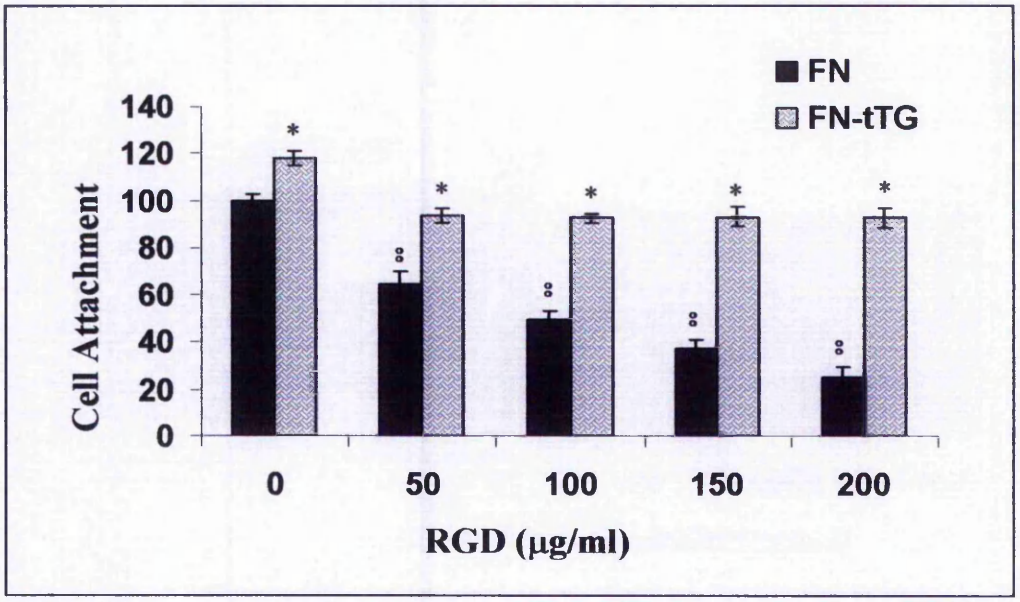

FN
FN-tTG
Cell Spreading
140
120
100
80
60
40
20
0
*
0
50
100
150
200
RAD (μg/ml)

Figure 4.3.3b


FN
FN-tTG
Cell Attachment
140
120
100
80
60
40
20
0
0
50
100
150
200
RGD (μg/ml)

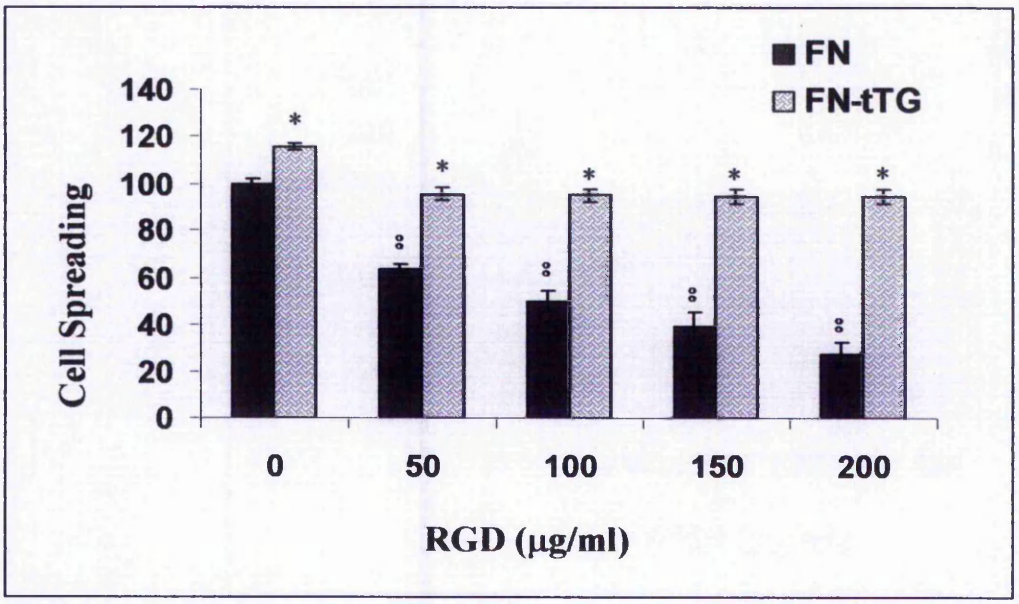

FN
FN-tTG
Cell Spreading
140
120
100
80
60
40
20
0
0
50
100
150
200
RGD (μg/ml)

Figure 4.3.3c

When plated on FN coated wells, ECV 304 cells showed a flattened appearance with a dark purple nucleus and a pink surrounding cytoplasm. The RGD treatment demonstrated its effect on cells seeded on the FN matrix by changing the cell morphology to a more rounded, crenated shape (figure 4.3.3a). Upon seeding RGD-inhibited ECV304 cells onto the FN-tTG matrix, the cell morphology was restored to that of the FN control. ECV304 cells treated with 50-200 μg/ml of RAD peptide demonstrated no significant difference in cell adhesion compared to that of FN alone (figure 4.3.3b). On the FN-bound tTG matrix, ECV304 cells showed a significant 18% increase in cell attachment and a 15% increase in cell spreading, regardless of the RAD treatment. The treatment of ECV304 cells with 50 μg/ml of RGD peptide resulted in an approximately 40% decrease in cell adhesion to FN in comparison to control FN without RGD peptide. Increase in RGD peptide concentration to 100 μg/ml led to a further significant 10% decrease in cell attachment and spreading (figure 4.3.3c). At concentrations of 150 and 200 μg/ml, cell adhesion was approximately 35% and 25% of that of control cell adhesion to FN in the absence of RGD peptide. The levels of cell attachment and spreading was restored to nearly control levels (95% of control values on FN), when cells were seeded onto FN-tTG at all RGD peptide concentrations used. This experiment indicated that ECV304 cells can mediate an RGD-independent cell adhesion in response to tTG in complex with FN.

So far the presence of an RGD-independent pathway mediated by fibronectin bound tTG was shown to exist in the immortalised cell lines. To investigate whether this pathway is also a common mechanism in primary cell lines, dermal fibroblasts from human and mouse origin were used in the inhibition experiments.

Primary human dermal fibroblasts were incubated with competitive concentrations of the RGD peptide, in parallel with equal concentration of the inactive control RAD peptide, and then seeded on FN with or without immobilised tTG. On the FN matrix, in the absence of RGD peptide, human dermal fibroblasts displayed a very flat, almost rectangular appearance. By the treatment of RGD peptide, cells exhibited an impaired cell attachment with a decreased ability to spread (figure 4.3.4a). Cell attachment to FN in the presence of 50-150 μg/ml of RAD peptide was not affected negatively, however at the highest concentration of 200 μg/ml,

Figure 4.3.4 The RGD-independent cell-adhesion of human dermal fibroblasts to FN with immobilised tTG

a, Visualisation of human dermal fibroblasts on FN and FN-tTG matrices in the presence of RGD peptide; **b,** effect of RAD peptide; **c,** effect of RGD peptide on the cell adhesion of human dermal fibroblasts to FN and FN-tTG matrices. The cell adhesion assay was carried out and the attachment and spreading of human dermal fibroblasts were analysed as described previously (Sections 2.2.5 and 4.2.1). Spread cells were indicated with white arrows, while non-spread cells were shown with black arrows. The percentage of cell attachment (cell attachment) or the percentage of cell spreading (cell spreading) ± S.D. shown are the mean values from three separate experiments performed in triplicate. The mean cell attachment and spreading values were expressed as percentage of control values on FN (which represents 100%). Mean attachment and spreading values ± S.D. on FN control were 320 ± 17 and 244 ± 6. The mean percentage of control spreading on FN ± S.D. was assessed as 75 ± 2, which was taken as 100%. Mean number of attached cells ± S.D. on FN in the 3 experiments was calculated as 267 ± 18, 349 ± 10, and 345 ± 22. The * symbol represents significant difference ($p<0.05$) between FN control and cells seeded on the FN-tTG matrix in the presence or absence of RAD synthetic peptide. The ¤ symbol indicates the statistically different cell adhesion values ($p<0.05$) of RGD treated cells on FN when compared to FN control.

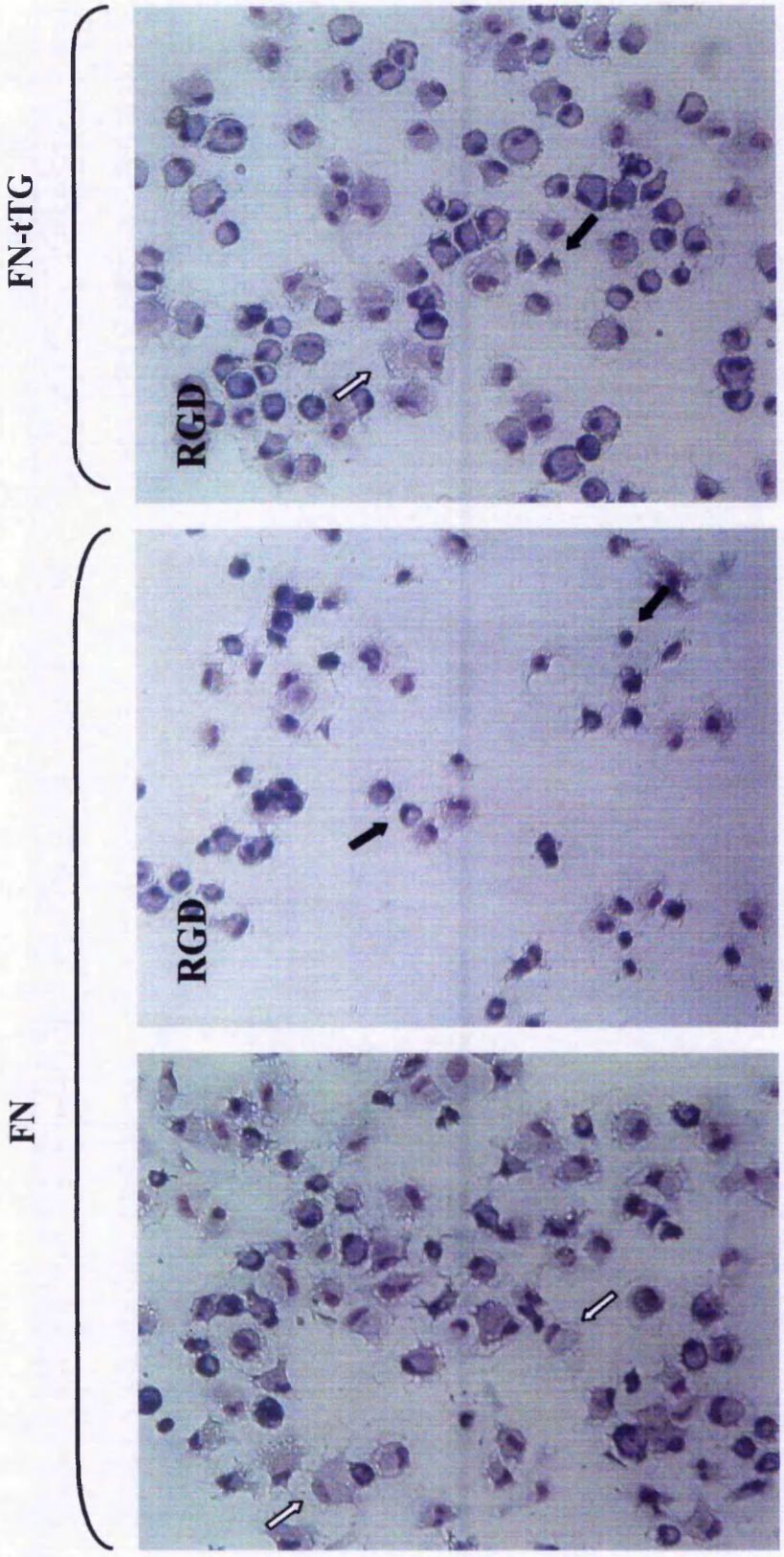
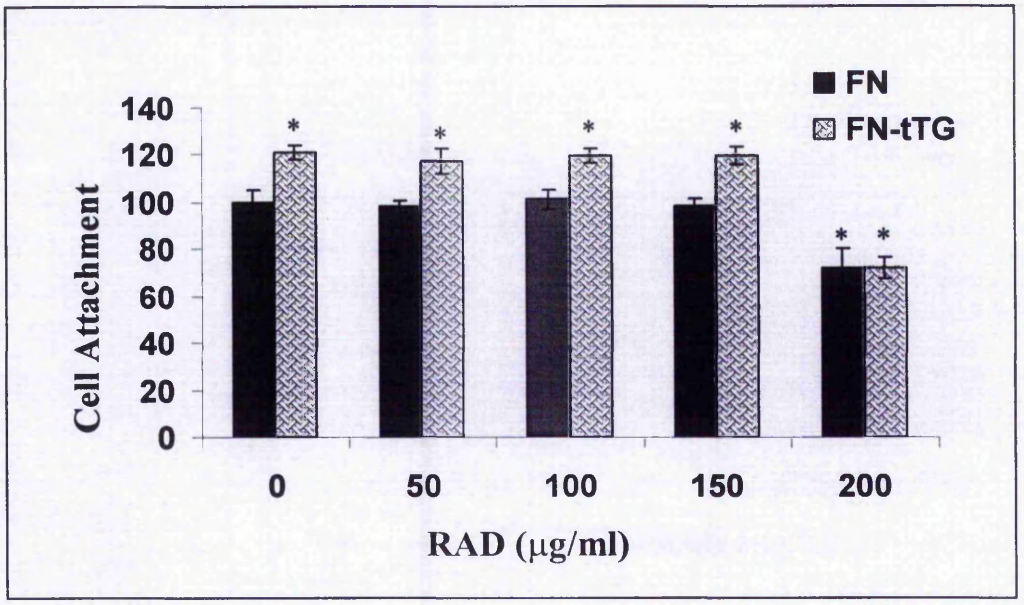


Figure 4.3.4a


FN
FN-tTG
Cell Attachment
140
120
100
80
60
40
20
0
0
50
100
150
200
RAD (μg/ml)

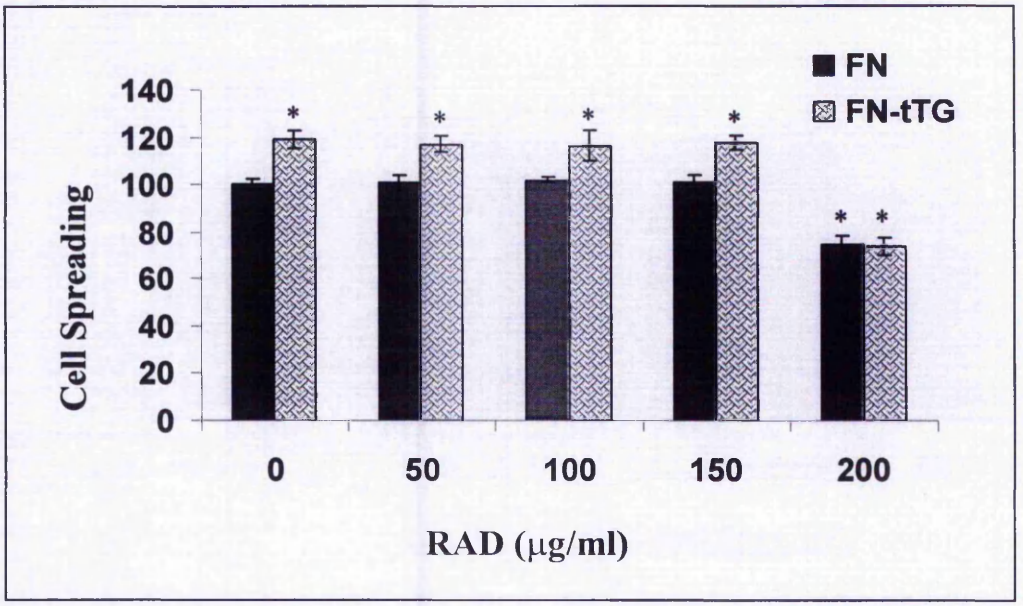
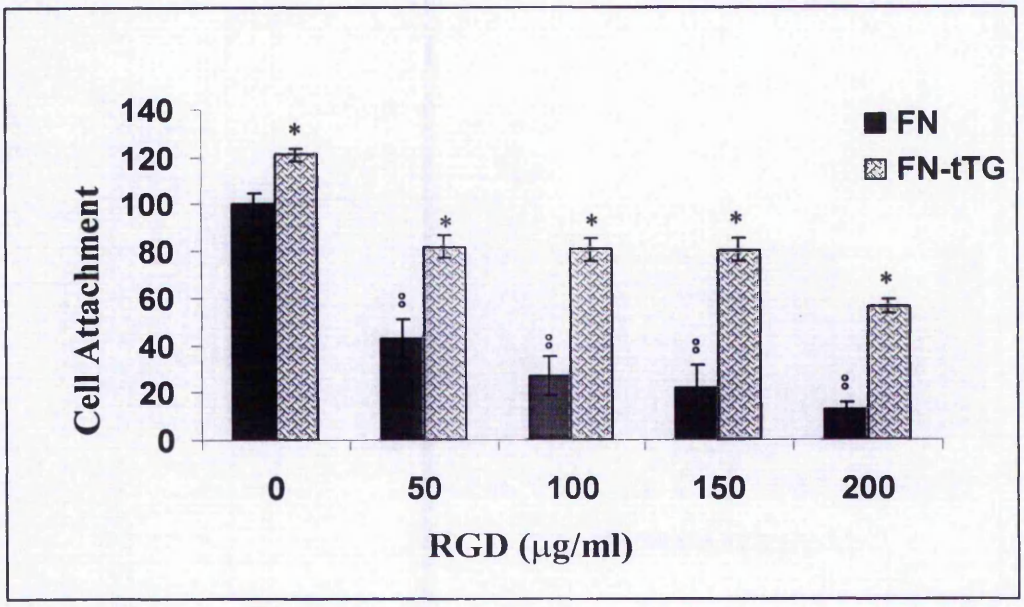

FN
FN-tTG
Cell Spreading
140
120
100
80
60
40
20
0
0
50
100
150
200
RAD (μg/ml)

Figure 4.3.4b


Cell Attachment
140
120
100
80
60
40
20
0
FN
FN-tTG
0
50
100
150
200
RGD (μg/ml)

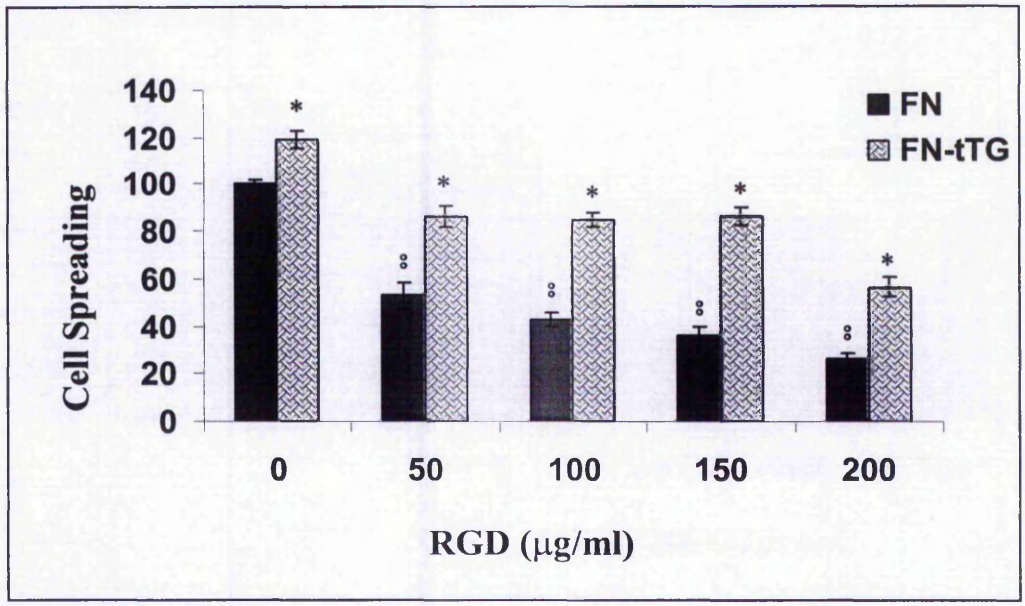

Cell Spreading
140
120
100
80
60
40
20
0
FN
FN-tTG
0
50
100
150
200
RGD (μg/ml)

Figure 4.3.4c

cell attachment and spreading on FN showed a 30% decrease (figure 4.3.4b). When cells were plated on FN-tTG, human dermal fibroblasts demonstrated an enhanced cell adhesion with a 20% increase in the cell attachment and spreading. Comparison of the cell adhesion to FN in the absence of RGD peptide and cell adhesion to FN at 50 and 100 μg/ml RGD peptide showed that RGD treatment of cells at these concentrations brought about a 60-75% decrease in cell attachment, and a 50-60% decrease in cell spreading (figure 4.3.4c). Further increase in the RGD concentration to 150 μg/ml did RGD concentration to 150 μg/ml did not lead to a further significant decrease in cell attachment, but decreased the levels of cell spreading by another 10%. The cell attachment and spreading values on FN was dropped to their lowest levels, 12% and 26% of control FN levels, by the treatment of primary fibroblasts with 200 μg/ml of RGD peptide. The defective cell attachment and spreading due to the RGD inhibition was restored when cells were seeded on the FN-tTG matrix. At 50-150 μg/ml RGD peptide, attachment on FN-tTG was determined as 80% of the control values found on FN. The cell spreading on FN-tTG appeared to be enhanced more than attachment by around 5% at these same RGD peptide concentrations. Only at 200 μg/ml was the cell attachment to FN-tTG significantly lower in comparison to control FN levels without RGD peptide, due to toxic effect of the hexapeptide at high concentrations.

Using the same approach the effect of the RGD peptide on primary mouse dermal fibroblasts (MDFs) was examined. Primary mouse dermal fibroblasts (MDFs) were isolated from the skin of tTG-deficient (Tg2-/-) and wild type (Tg2+/+) 9-months old mice and maintained as described before (Section 2.2.1.2). Non-confluent cultures of mouse dermal fibroblasts wild type for tTG (MDFTg2+/+) were plated on FN or FN-tTG, and incubated with RAD and RGD peptides under serum-free conditions. Once attached and spread MDFTg2+/+ were very flattened giving the appearance of an irregularly shaped circle, however, non-spread MDFTg2+/+ cells displayed a smaller round-like morphology (figure 4.3.5a). The treatment of these cells with RAD peptides at concentrations of 50 to 150 μg/ml resulted in no changes in cell adhesion when compared to non-treated cells seeded on FN (figure 4.3.5b). However, at 200 μg/ml RAD peptide cells demonstrated a 25% decrease of

Figure 4.3.5 Adhesion of MDFTg2+/+ cells to FN-and FN-tTG matrices in the presence of RAD and RGD peptides

a, Visualisation of MDFTg2+/+ cells on FN and FN-tTG matrices in the presence of RGD peptide; **b,** effect of RAD peptide; **c,** effect of RGD peptide on the cell adhesion of MDFTg2+/+ cells to FN and FN-tTG matrices. The cell adhesion assay was performed and the attachment and spreading of cyloheximide treated HOB cells were assessed as described in Sections 2.2.5 and 4.2.1. White arrows point to spread cells, whereas black arrows point to non-spread cells. Each datum point represents the mean percentage of attached cells (cell attachment) or the mean percentage of spread cells (cell spreading) ± S.D. of three separate experiments performed in triplicate. The ordinates in the top graphs represent the mean cell attachment expressed as mean percentage of control attachment to FN ± S.D., which represents 100%. The mean number of cell attachment ± S.D. on FN in the 3 experiments was 202 ± 7, 303 ± 8, and 281 ± 12. The ordinates in the bottom graphs indicate the mean percentage of spread cells, expressed as the mean percentage of control spreading on FN±S.D. The mean percentage spreading value ± S.D. on FN in the 3 experiments was 77 ± 1, 76 ± 6, 80 ± 3, which was normalised to 100%. The statistically significant difference ($p<0.05$) between FN control and cells seeded on the FN-tTG matrix in the presence or absence of RAD synthetic peptide was indicated with * symbol. While, the ¤ symbol was used to indicate the statistically different cell adhesion values ($p<0.05$) of RGD treated cells on FN when compared to FN control.

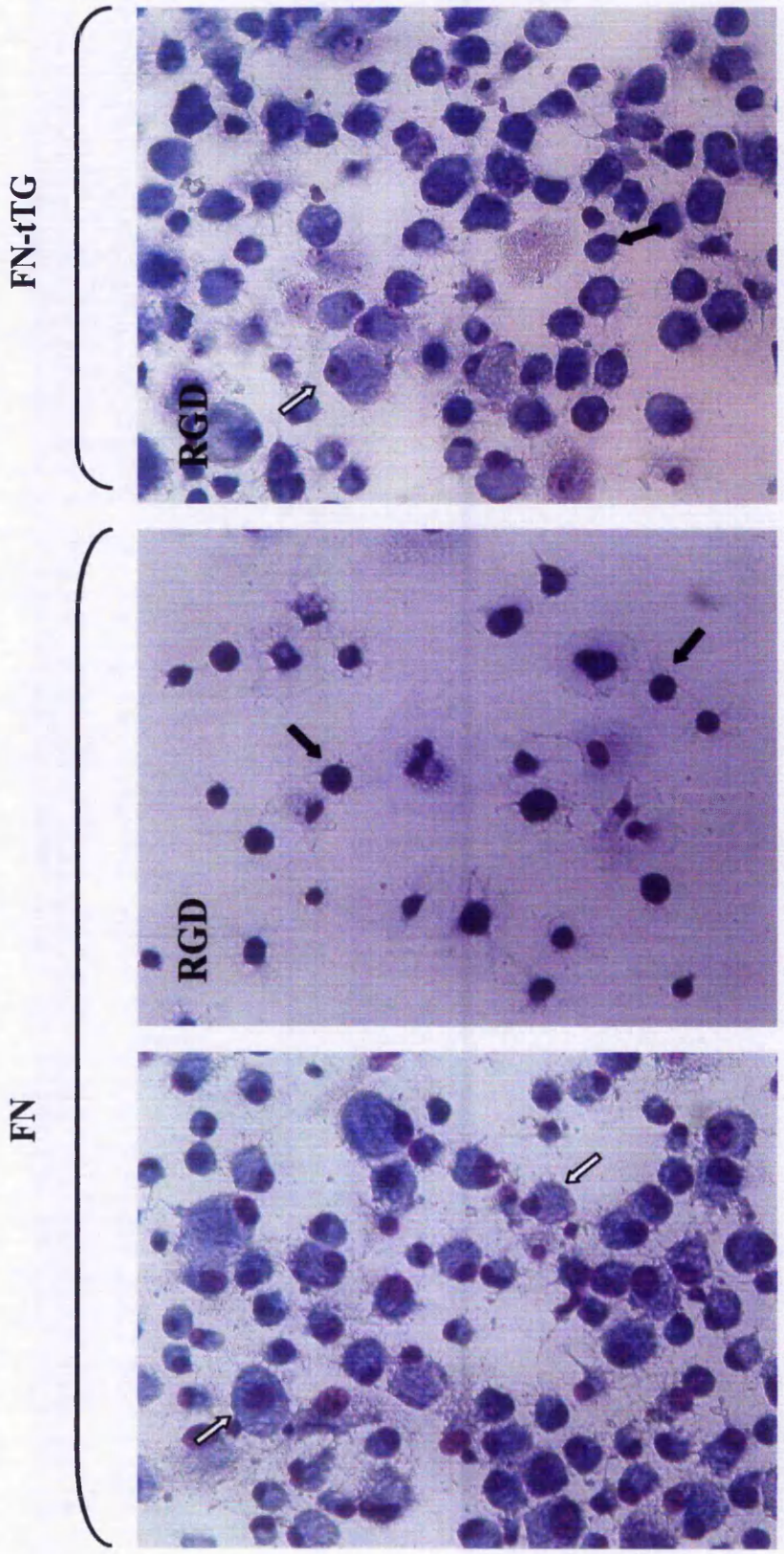
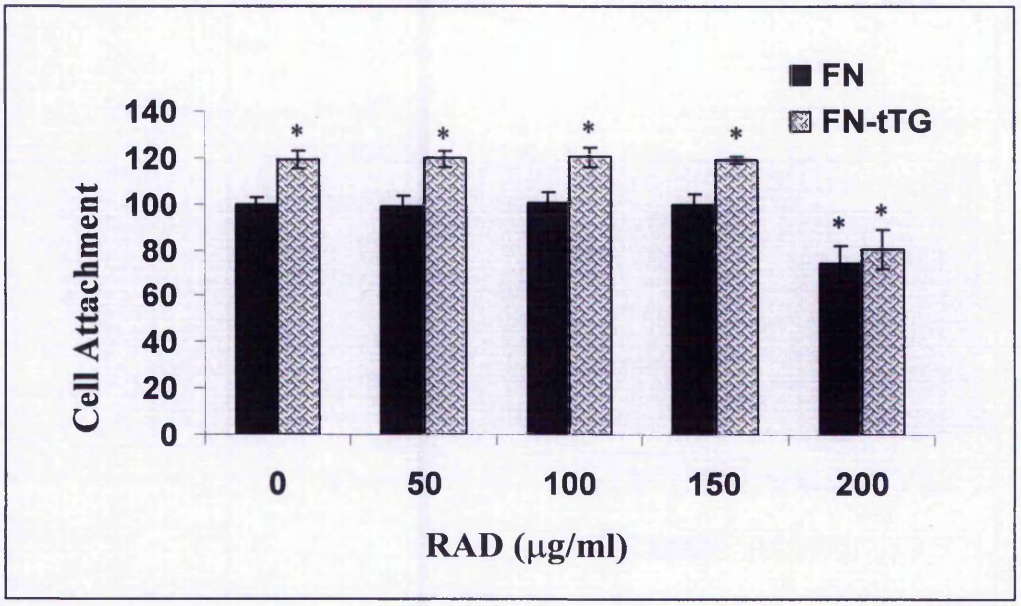


Figure 4.3.5a


FN
FN-tTG
Cell Attachment
140
120
100
80
60
40
20
0
0
50
100
150
200
RAD (μg/ml)

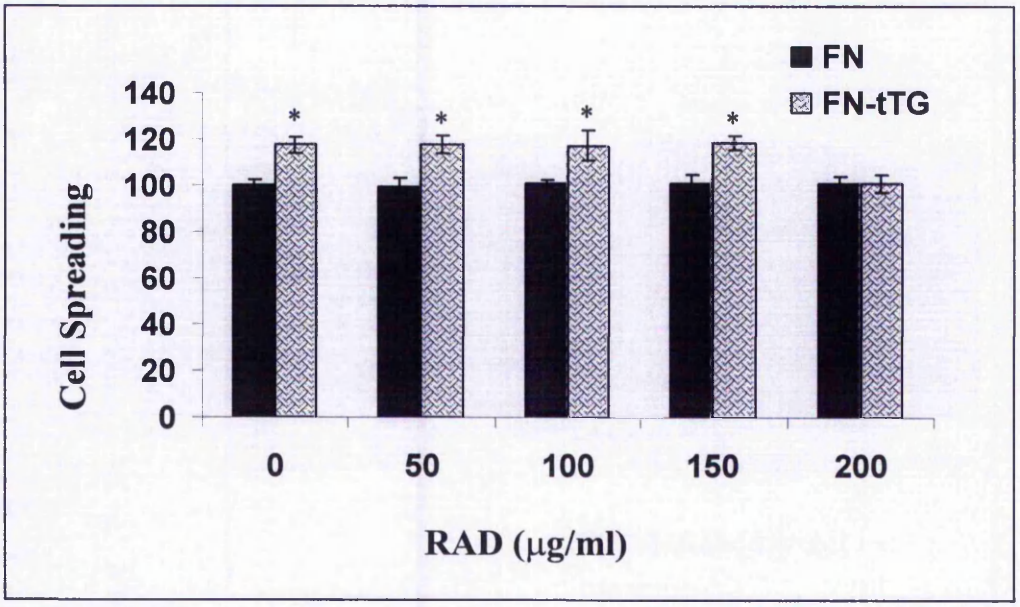
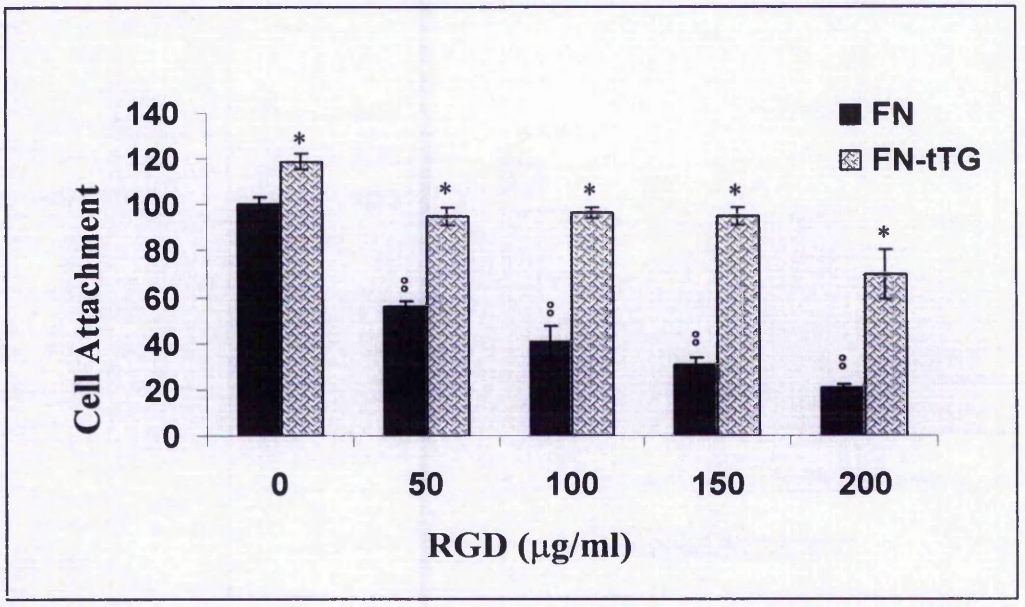

FN
FN-tTG
Cell Spreading
140
120
100
80
60
40
20
0
0
50
100
150
200
RAD (μg/ml)

Figure 4.3.5b


Cell Attachment
140
120
100
80
60
40
20
0
FN
FN-tTG
0
50
100
150
200
RGD (μg/ml)

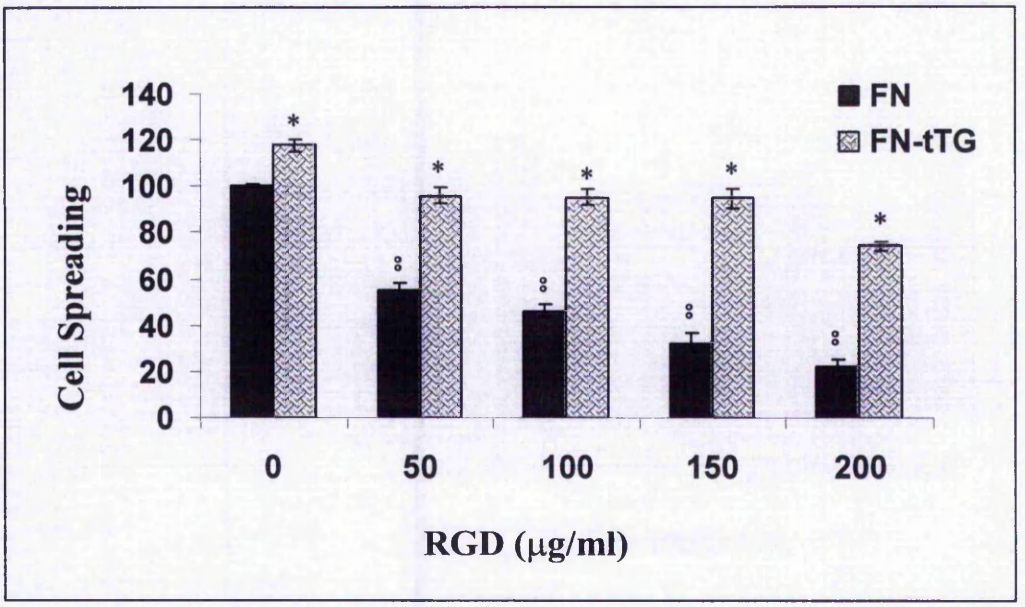

Cell Spreading
140
120
100
80
60
40
20
0
FN
FN-tTG
0
50
100
150
200
RGD (μg/ml)

Figure 4.3.5c

cell attachment on FN and FN-tTG. Interestingly, RAD peptide at this concentration did not affect the MDFTg2+/+ cell spreading, as the level of cell spreading was not found to be statistically different from the level observed on control FN. Approximately a 20% increase in cell adhesion, was observed when MDFTg2+/+ cells were seeded on the FN-tTG matrix, in the absence of RDG peptide. The treatment of MDFTg2+/+ cells with 50 and 100 μg/ml of RGD peptide caused a significant 45% and 60% decrease in cell adhesion when compared to the FN matrix, but the cell attachment and spreading values on FN-tTG were not considerably inhibited at these same RGD peptide concentrations (figure 4.3.5c).

When MDFTg2+/+ cells were seeded on the FN-tTG matrix in the presence of RGD peptide at 50 and 100 μg/ml concentrations, they displayed a comparable cell attachment and spreading to the FN control without RGD peptide. Further increasing the concentrations of RGD peptide (150 and 200 μg/ml), led to a 20-30% decrease in the number of attached and spread cells on the FN matrix. Even at these high concentrations of RGD peptide, cell adhesion was rescued when the MDFTg2+/+ cells were seeded on the tTG bound FN matrix. Cell adhesion on FN-tTG in the presence of 150 and 200 μg/ml RGD peptide was, respectively, 95% and 70% of control cell adhesion value recorded on FN alone.

To further explore the role of FN-bound tTG in mediating the RGD-independent cell adhesion of MDFs, mouse dermal fibroblasts devoid of tTG (MDFTg2-/-) were used as a cell model in the adhesion assay. MDFTg2-/- cells were grown to sub-confluency and pre-treated with the hexapeptide G**RGD**TP in serum free conditions. MDFTg2-/- cells treated with increasing concentrations of G**RGD**TP (or RGD) peptide, were seeded on FN and FN-tTG matrices. As before, MDFTg2-/- cells were also treated with equivalent concentrations of the control G**RAD**SP peptide to exclude any non-specific inhibition of cell adhesion due to the presence of toxic levels of an exogenous hexapeptide peptide. Figure 4.3.6a shows the typical morphology of MDFTg2-/- cells on FN and FN-tTG matrices in the presence and absence of RGD peptide. Once attached and spread MDFTg2-/- cells appeared as very large and flattened cells, while non-attached fibroblasts were of untidy appearance, displayed either a rounded morphology or a crenated-like

Figure 4.3.6 Adhesion of MDFTg2-/- cells to FN-and FN-tTG matrices in the presence of RAD and RGD peptides

a, Visualisation of MDFTg2-/- cells on FN and FN-tTG matrices in the presence of RGD peptide; **b,** effect of RAD peptide; **c,** effect of RGD peptide on the cell adhesion of MDFTg2-/- cells to FN and FN-tTG matrices. The cell adhesion assay was carried out and the attachment and spreading of MDFTg2-/- cells were analysed as described previously (Sections 2.2.5 and 4.2.1.). Spread cells were shown with white arrows, while non-spread cells were indicated with black arrows. Data was represented as the mean percentage of attached cells (cell attachment) or the mean percentage of spread cells (cell spreading) ± S.D. of three separate experiments carried out in triplicate. Each data point was expressed as percentage of control values on FN, which represents 100%. Mean number of attached cells ± S.D. on FN in the 3 experiments was calculated as 140 ± 17, 178 ± 8, and 158 ± 14. The mean percentage of spreading ±S.D. on FN in the 3 experiments was 73 ± 2, 76 ± 1, and 75 ± 1, which was considered as 100%. The * symbol represents significant difference ($p<0.05$) between FN control and cells seeded on the FN-tTG matrix in the presence or absence of RAD synthetic peptide. The ♀ symbol indicates the statistically different cell adhesion values ($p<0.05$) of RGD treated cells on FN when compared to FN control.

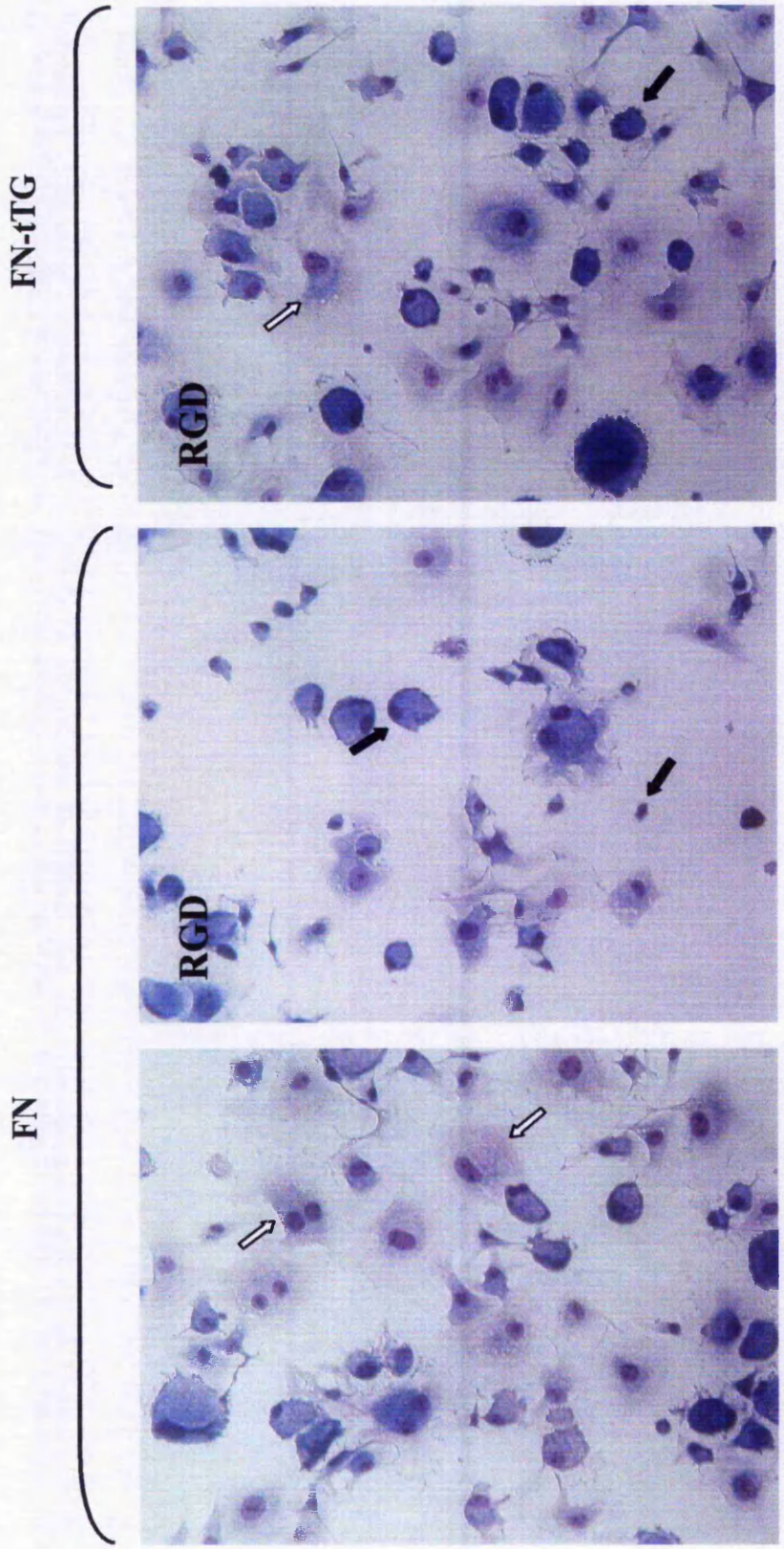
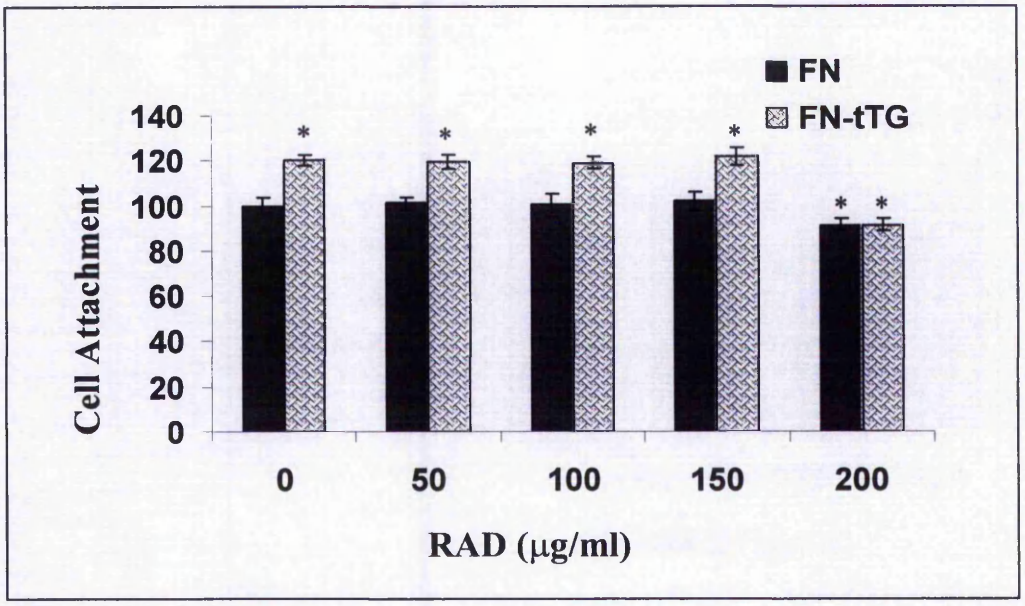


Figure 4.3.6a


FN
FN-tTG
Cell Attachment
140
120
100
80
60
40
20
0
0
50
100
150
200
RAD (μg/ml)

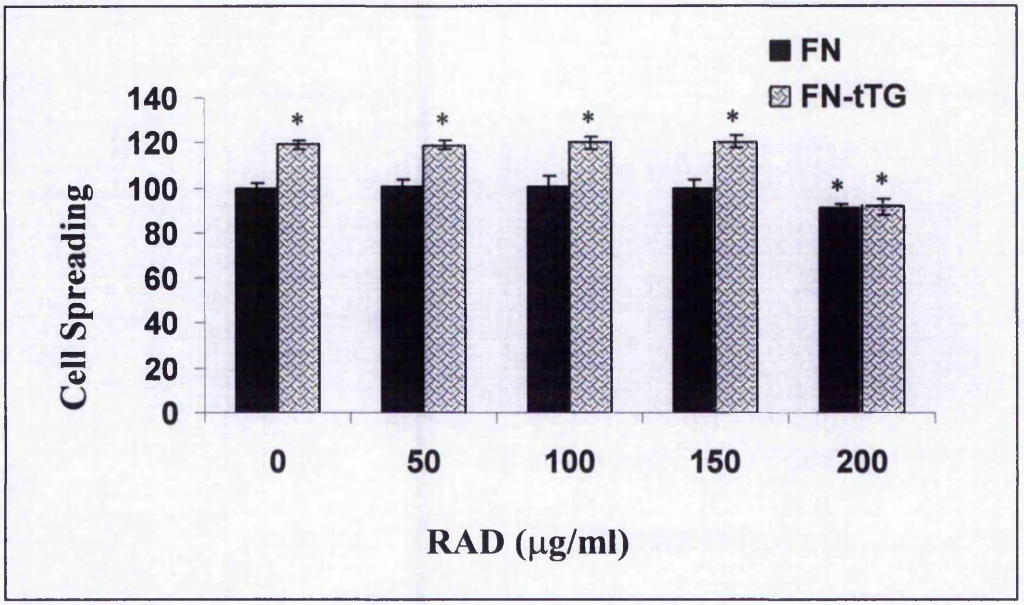
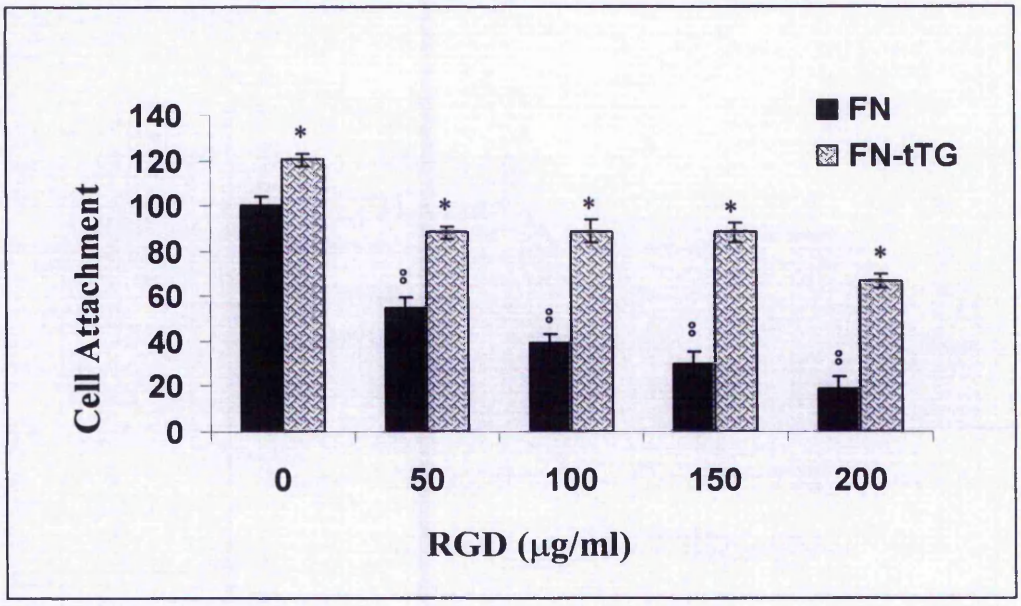

FN
FN-tTG
Cell Spreading
140
120
100
80
60
40
20
0
0
50
100
150
200
RAD (μg/ml)

Figure 4.3.6b


Cell Attachment
140
120
100
80
60
40
20
0
FN
FN-tTG
0
50
100
150
200
RGD (μg/ml)

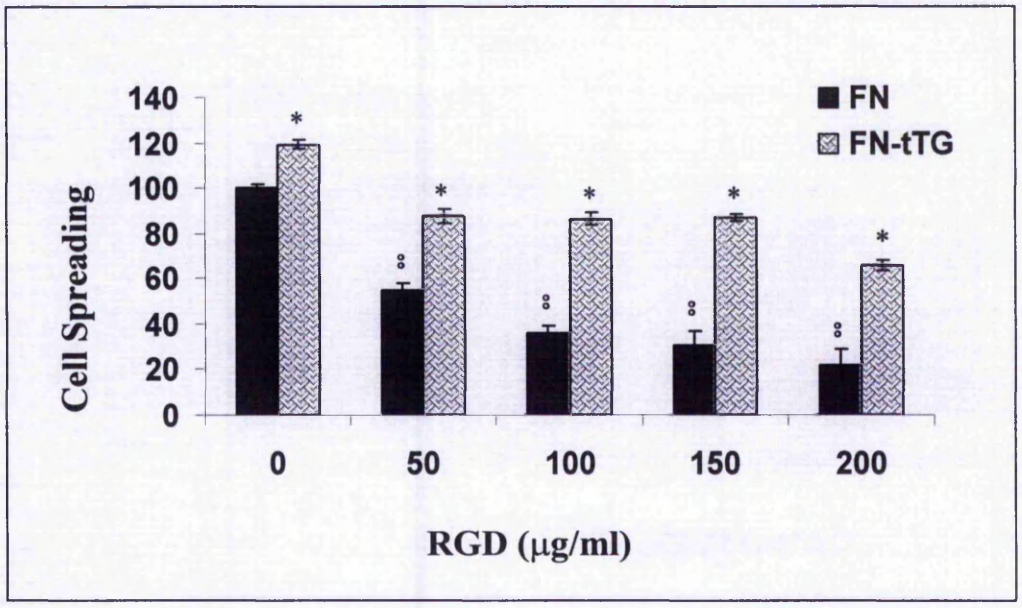

Cell Spreading
140
120
100
80
60
40
20
0
FN
FN-tTG
0
50
100
150
200
RGD (μg/ml)

Figure 4.3.6c

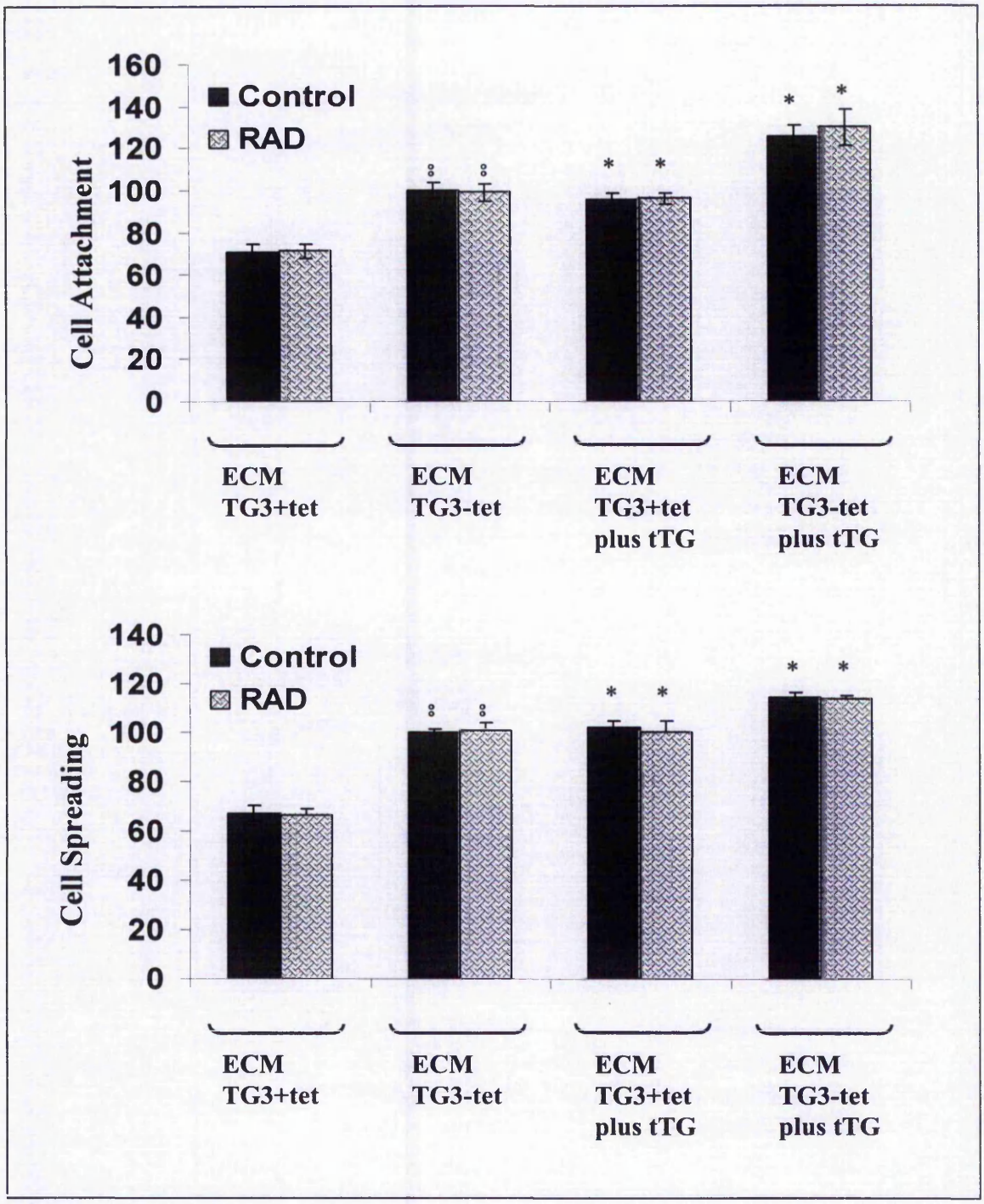
appearance. As can be seen in figure 4.3.6b, the treatment of MDFTg2-/- cells with 50 to 150 μg/ml of RAD peptide resulted in a cell adhesion to FN comparable to that of FN alone, since no statistical difference was detected in attachment and cell spreading between FN control and RAD treated cells at these low concentrations. The use of the RAD peptide at concentrations higher than 150 μg/ml, however, gave rise to an unspecific inhibition of cell adhesion with a 10% decrease below the control values found on FN. In the absence of RDG peptide, on the FN-bound tTG matrix MDFTg2-/- cells showed a significant 20% increase in cell attachment and cell spreading in comparison to their adhesion to FN alone. The treatment of MDFTg2-/- cells with RGD peptide brought about a significant decrease in cell adhesion to FN (figure 4.3.6c). The inhibition of attachment and spreading on FN by the RGD synthetic peptide was only 40% of control values recorded on FN at the concentration of 50μg/ml, but a steeper decrease in cell adhesion was observed at the peptide concentrations of 100-200 μg/ml (typically to 60-85% of control FN levels without RGD). In the presence of RGD peptides, cell adhesion on the FN-tTG matrix was significantly different to the cell adhesion on FN, as the values for cell attachment and spreading were restored to that of control levels. At the non-toxic concentrations of RGD peptide, cell adhesion on FN-tTG was around 88% of the non-treated control cells on FN. Only at 200 μg/ml was the cell adhesion on FN-tTG reduced to 66% of that of the control FN levels without RGD peptide (figure 4.3.1b). These experiments indicated that tTG, once immobilised on FN, can rescue RGD-impaired cell adhesion of primary dermal fibroblasts of human and mouse origin.

4.3.1.3 A cell assembled matrix of FN and tTG restores RGD inhibition of cell attachment.

Having established that exogenously provided gpl tTG bound to FN supports an RGD-independent mechanism, a tTG rich FN matrix assembled by the transfected fibroblasts cell line, Swiss 3T3 TG3, was used as an alternative matrix system in cell adhesion assays. Such an ECM was prepared by long-term

Figure 4.3.7 Adhesion of Swiss 3T3 fibroblasts to the cell assembled matrix

The physiological cell assembled matrix was prepared and the cell adhesion assay was performed as described in Sections 2.2.2.3 and 4.2. 2. The attachment and spreading of Swiss 3T3 cells were assessed as mentioned previously (Methods 2.2.5). Data represent the mean percentage of attached cells (cell attachment) or the mean percentage of spread cells (cell spreading) ± S.D. of three separate experiments performed in triplicate. The cell attachment was expressed as the mean percentage of attachment to the induced-matrix (ECM TG3-tet) ± S.D, which represents 100%. The mean number of cells attached ± S.D. on the induced-matrix was 239 ± 10. The mean number of spread cell ± S.D. on the induced-matrix was found to be 217 ± 7, indicating a 90 ± 3 mean percentage of control spreading on induced-matrix ± S.D, which was taken as 100%. The * symbol represents significant difference in cell adhesion ($p<0.05$) following further addition of gpl tTG to the induced and non-induced matrix. The ¤ symbol indicates the statistically different values ($p<0.05$) of cell adhesion on induced matrix compared to non-induced (ECM TG3+tet) matrix.


Cell Attachment
160
140
120
100
80
60
40
20
0
Control
RAD
ECM TG3+tet
ECM TG3-tet
ECM TG3+tet plus tTG
ECM TG3-tet plus tTG
Cell Spreading
140
120
100
80
60
40
20
0
Control
RAD
ECM TG3+tet
ECM TG3-tet
ECM TG3+tet plus tTG
ECM TG3-tet plus tTG

culture of tTG induced (ECM TG3-tet) and non-induced Swiss 3T3 TG3 cells (ECM TG3+tet) without or with further addition of pre-activated tTG (ECM TG3-tet and ECM TG3+tet, plus tTG) to cells 16 hours before their detachment. Cells were then removed from both matrices, and in their place wild-type Swiss 3T3 fibroblasts were seeded in the presence of increasing concentrations of RGD peptide. Cells were then allowed to adhere for 16 hours in the presence of the RGD synthetic peptide. RAD peptide (100 μg/ml) was used to treat cell as a positive control, to rule out any non-specific inhibition of cell adhesion due to toxicity.

Comparison of cell attachment and spreading on the induced ECM and non-induced ECM demonstrated a significant difference in cell adhesion values (figure 4.3.7). When Swiss 3T3 fibroblasts were seeded on the ECM TG3-tet matrix, the cell attachment and spreading was 30% more than the values observed on the ECM TG3+tet matrix. The treatment of cells with the RAD peptide did not exhibit any inhibitory effect on cell adhesion to both conditioned matrices. The cell attachment and spreading to non-induced matrix with additional tTG (ECM TG3+tet plus tTG) was found to be comparable to the cell adhesion on the induced matrix. On the ECM TG3-tet plus tTG matrix, cells displayed a 25% increase in their attachment and spreading, when compared to their attachment to the induced matrix alone. Similar results were obtained when cells were seeded on these matrices comprising additional tTG in the presence of the RAD peptide.

The treatment of Swiss 3T3 fibroblasts with increasing concentrations of RGD synthetic peptide resulted in the impairment of cell attachment of these cells to the non-induced cell assembled matrix. This impairment was not observed on the induced cell assembled matrix (figure 4.3.8). Cell attachment on the ECM TG3+tet matrix in the presence of 30 μg/ml of RGD peptide, was 65% less than the one observed on the ECM TG3-tet matrix. However, cell attachment was significantly increased, when cells were seeded on the very same matrix containing additional tTG. At 50 μg/ml RGD peptide, attachment on the ECM TG3+tet matrix was further reduced by another 10%, when compared to cell attachment on the ECM TG3-tet matrix at the same RGD concentration. Nevertheless, on the ECM TG3+tet matrix containing increased amounts of tTG, the cell attachment levels were found

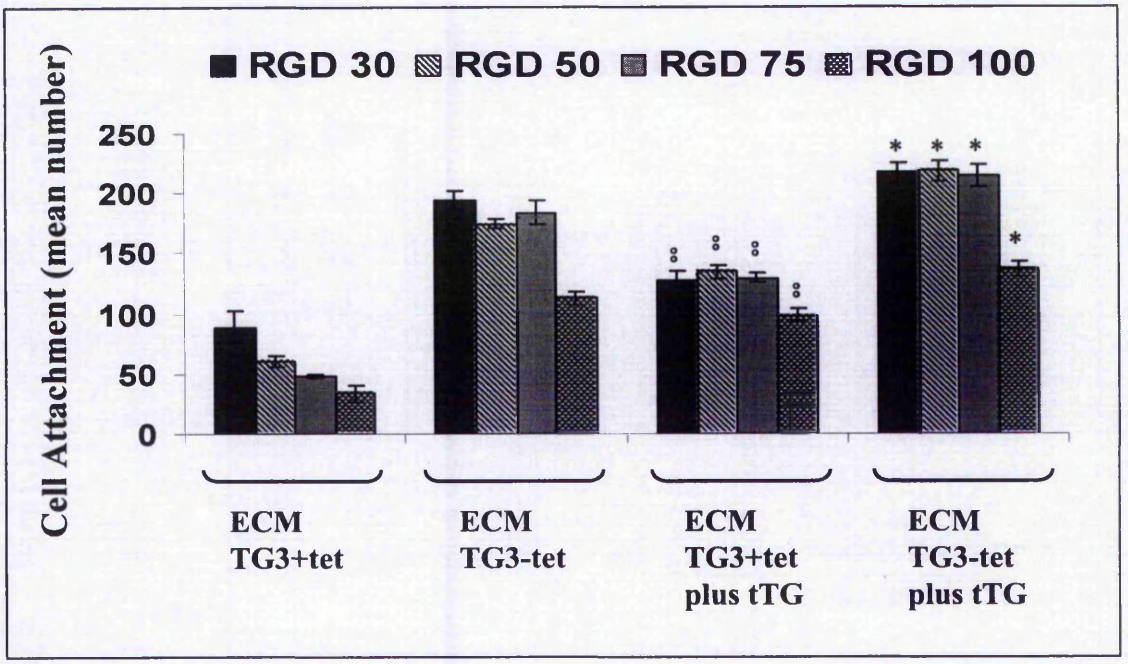


Figure 4.3.8 RGD-independent cell adhesion of Swiss 3T3 fibroblasts to the cell assembled matrix

The physiological cell assembled matrix was prepared and the cell adhesion assay was performed as described previously (Sections 2.2.2.3 and 4.2.2). The RDG-dependent cell attachment of Swiss 3T3 cells to physiological cell assembled matrix, was challenged with increasing concentrations of RGD synthetic peptide (30-100μg/ml) (RGD 30-100). The result was assessed as described under the Section 4.2.2. Each data point represents the mean number of attached cells (cell attachment) ± S.D. of three separate experiments performed in triplicate. The statistically significant difference ($p<0.05$) in cell attachment of RGD-treated Swiss 3T3 fibroblasts to induced and induced+tTG matrices is indicated with the * symbol. The ∘ symbol indicates the same for RGD-treated Swiss 3T3 fibroblasts when compared to non-induced and non-induced+tTG matrices.

be similar to the levels on the induced matrix. The treatment of Swiss 3T3 fibroblast with 75 μg/ml of RGD peptide resulted in a 75% inhibition in attachment of cells to the non-induced matrix, but cell attachment to the tTG rich non-induced matrix was inhibited only by 30% when compared to cell attachment levels on the induced matrix at this same RGD peptide concentration. At 100 μg/ml RGD peptide, no further significant decrease in cell attachment levels on the non-induced matrix was detected. The cell attachment was rescued once cells were seeded on the tTG rich ECM TG3+tet matrix.

The RGD-independent cell adhesion on the ECM TG3-tet matrix could be significantly increased when gpl tTG was incorporated on this matrix. At all RGD peptide concentrations (30-100 μg/ml), the cell attachment was increased 10-20% on the ECM TG3-tet matrix with the additional tTG, when compared to the cell attachment on the induced matrix alone.

4.3.2 tTG can support the RGD-independent cell adhesion only in complex with full length FN

4.3.2.1 The importance of tTG bound to FN to mediate RGD-independent cell adhesion

To eliminate the possible interaction of tTG bound to tissue culture plastic with cell surface receptors during RGD-independent cell adhesion, FN coated plates were blocked with 3%(w/v) nonfat milk protein Marvel, before the immobilisation of gpl tTG. HOB cells were seeded onto the unblocked and marvel-blocked matrices, in the presence of 150 μg/ml of RAD and RGD synthetic peptides.

The treatment of HOBs with RAD peptide at the concentration of 150 μg/ml did not lead to any non-specific inhibition in cell adhesion. The cell attachment and spreading was shown to be enhanced by 21% by the FN-tTG matrix regardless of marvel blockage in the presence or absence of the RAD peptide. As shown in figure 4.3.9, HOB cell adhesion to FN was decreased to 48% of control values on FN in the presence of the RGD peptide. The cell adhesion of RGD-treated cells was restored to 90% of control values on the unblocked FN-tTG matrix as well as

Figure 4.3.9 Comparison of the RGD-independent cell adhesion of HOB cells to unblocked and marvel-blocked FN-tTG matrices

The unblocked and blocked FN-tTG matrix was prepared and the cell adhesion assay was performed as described in Sections 2.2.2.2 and 2.2.2.3. The attachment and spreading of HOB cells were assessed as mentioned previously (Methods 2.2.5). Each data point corresponds to the mean percentage of attached cells (cell attachment) or the mean percentage of spread cells (cell spreading) ± S.D. from three separate experiments each performed in triplicate. The ordinate in the upper graph represents the mean cell attachment, expressed as the mean percentage of control attachment to un-blocked FN (which represents 100%) ± S.D. The mean number of attached cells ± S.D. on control FN matrix in the 3 experiments was 353 ± 6, 289 ± 3, and 332 ± 6. The ordinate in the lower graph indicates the mean percentage of spread cells, expressed as mean percentage of control spreading on FN ± S.D. The mean percentage spreading value ± S.D. on FN in the 3 experiments was 82 ± 1, 77 ± 1, 75 ± 1, which was considered as 100%. The * symbol represents significant difference ($p<0.05$) in cell adhesion on marvel blocked matrix when compared to cells seeded on the FN matrix in the presence or absence of RGD synthetic peptide. The ¤ symbol indicates the statistically different values ($p<0.05$) for cell adhesion found between the cells seeded on FN and the cells seeded on the FN-tTG matrix in the presence or absence of RGD synthetic peptide.

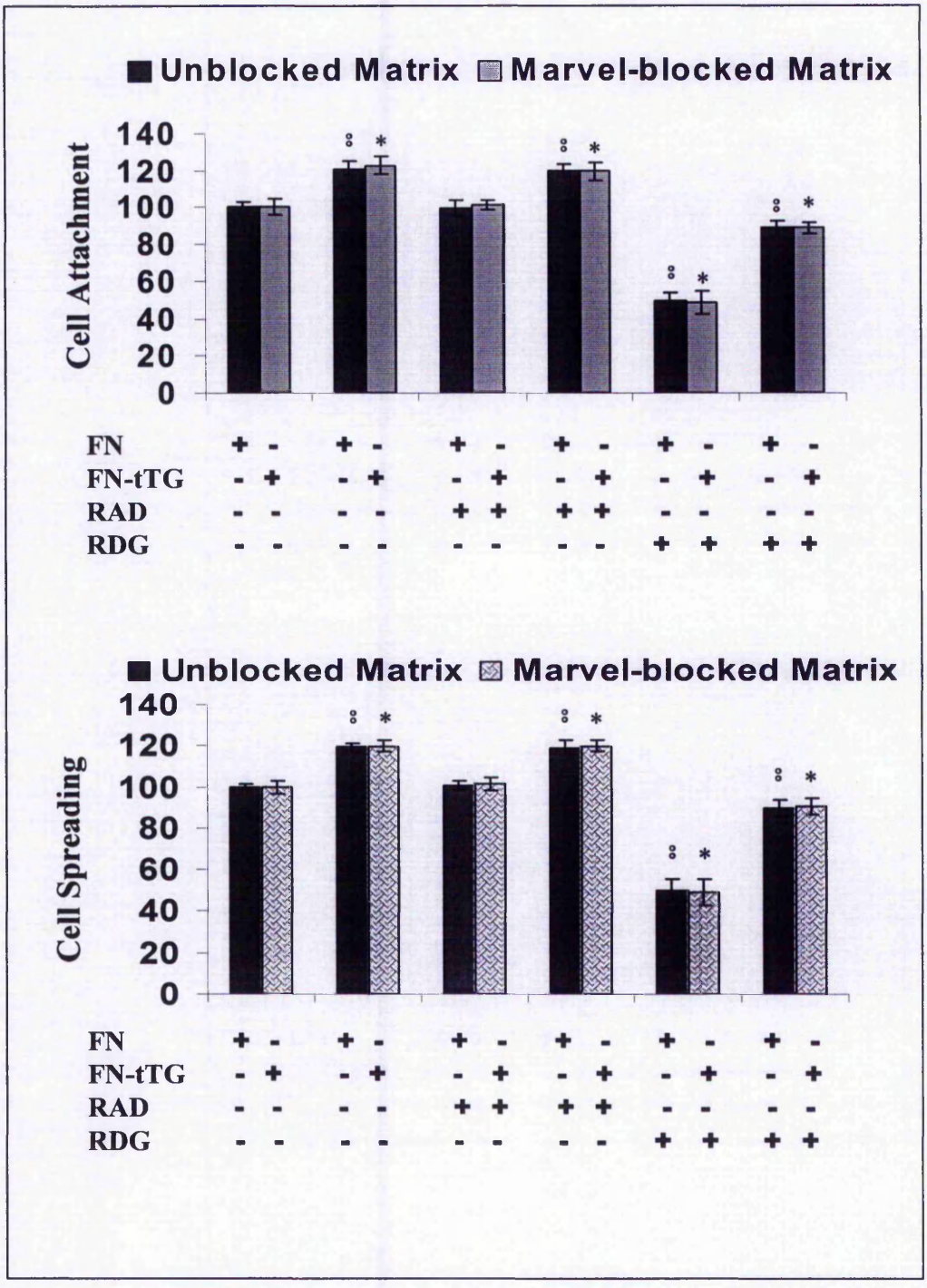
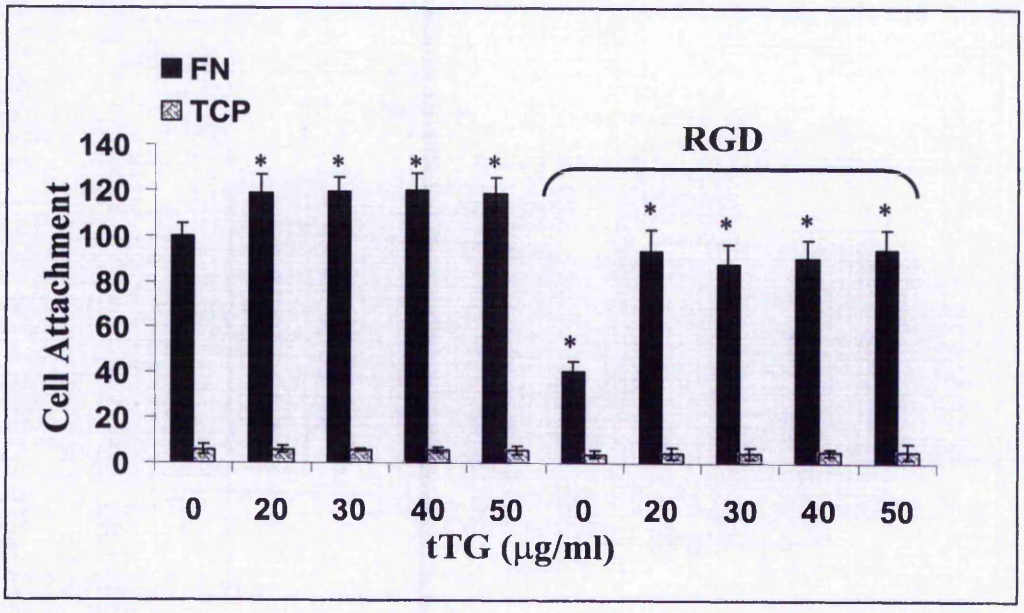
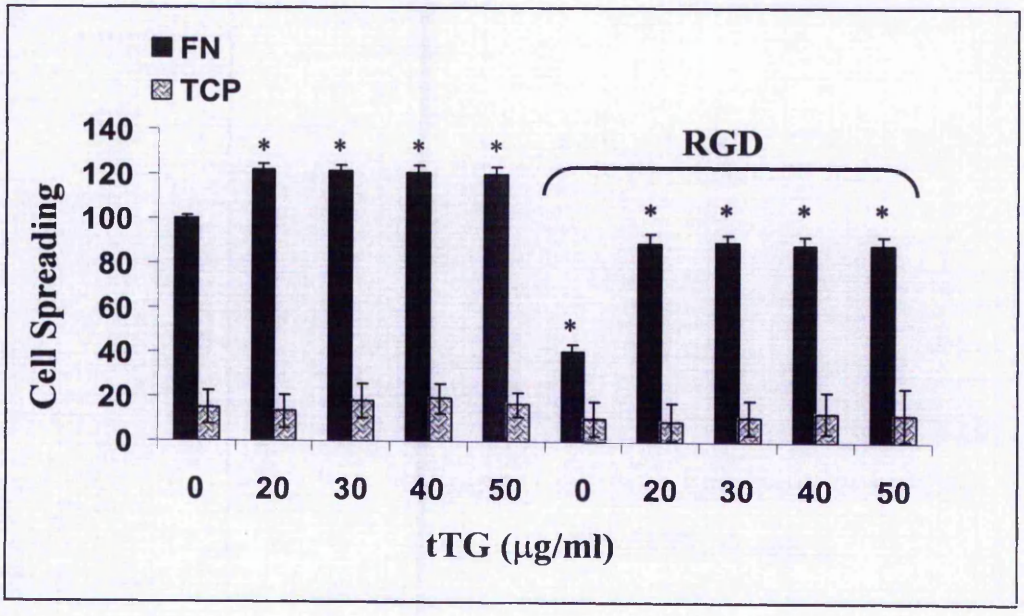

Unblocked Matrix
Marvel-blocked Matrix
Cell Attachment
140
120
100
80
60
40
20
0
FN
FN-tTG
RAD
RDG
Unblocked Matrix
Marvel-blocked Matrix
Cell Spreading
140
120
100
80
60
40
20
0
FN
FN-tTG
RAD
RDG

Figure 4.3.10 Comparison of RGD-independent cell adhesion of HOB cells to FN-tTG and TCP-tTG matrices

The tTG rich FN and tissue culture plastic (TCP) matrix was prepared as described in Section 2.2.2.2. Cell adhesion assay was performed and the attachment and spreading of HOB cells were analysed as described previously (Sections 2.2.5 and 4.2.1.). Data are presented as the mean percentage of attached cells (cell attachment) or the mean percentage of spread cells (cell spreading) ± S.D. from three separate experiments performed in triplicate. Data are expressed as a percentage of control values on FN, which represents 100%. Mean number of attachment and spreading values ± S.D. on FN control were 281 ± 15 and 211 ± 12. The mean percentage of control spreading on FN ± S.D. was assessed as 81 ± 4, and normalised to 100%. The statistically significant difference ($p<0.05$) between FN control and cells seeded on tTG rich FN matrices in the presence or absence of RGD synthetic peptide, is indicated with * symbol.


FN
TCP
RGD
Cell Attachment
140
120
100
80
60
40
20
0
0
20
30
40
50
0
20
30
40
50
tTG (μg/ml)


FN
TCP
RGD
Cell Spreading
140
120
100
80
60
40
20
0
0
20
30
40
50
0
20
30
40
50
tTG (μg/ml)

on the marvel-blocked FN-tTG matrix, indicating that tTG bound to FN mediates the RGD-independent cell adhesion of HOBs.

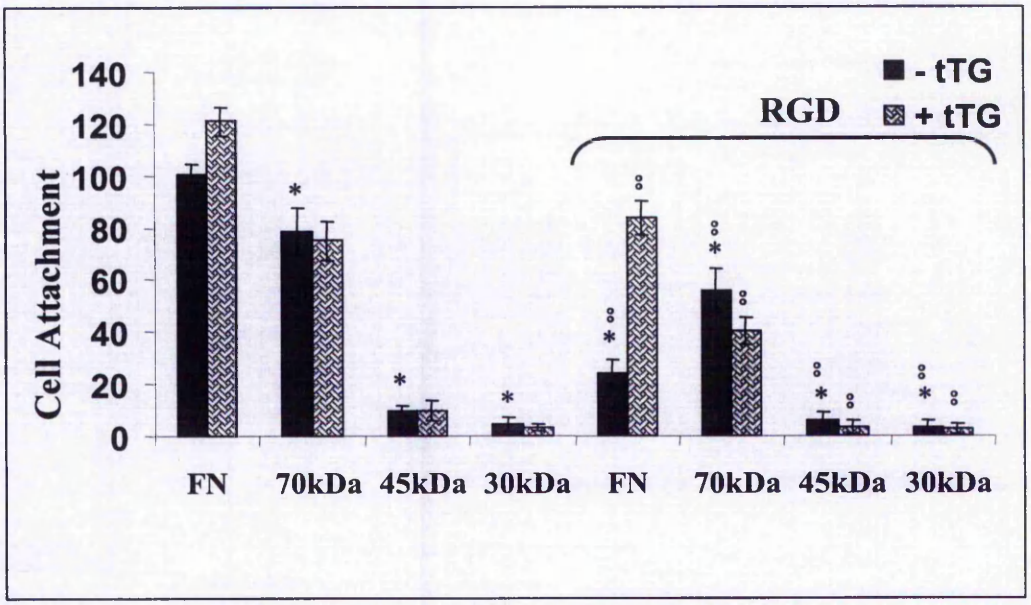
To confirm the above finding, increasing concentrations of gpl tTG (0-50 μg/ml) were immobilised on tissue culture plastic (TCP) with or without prior coating of FN. The effect of the RGD peptide on HOB cell adhesion in tTG rich FN and TCP matrices was investigated using the cell adhesion assay (figure 4.3.10). The immobilisation of 20 μg/ml of tTG on FN resulted in a 20% increase in cell attachment and spreading in comparison to cell adhesion on FN without RGD peptide. The further increase in tTG concentration bound to FN did not increase the cell attachment and spreading values more than the 20%. The tTG coated TCP (0-50 μg/ml of tTG) failed to support cell adhesion of HOB cells during the 30-minutes time period of the cell adhesion assay. As expected, the RGD treatment of HOB cells impaired the cell adhesion on FN by about 60%. In agreement with the previous data, cell attachment and spreading on FN-bound tTG matrices was not significantly inhibited by the treatment of the RGD peptide. Regardless of the amount of tTG present in the FN-tTG matrix, the cell adhesion to FN-tTG in the presence of RGD peptide was shown to be no more than 90% of the values obtained on FN control. When cells were seeded on the tTG rich TCP in the presence of RGD peptide, cell attachment and spreading were found to be negligible, suggesting that tTG supports RGD-independent cell adhesion only when it is in complex with FN.

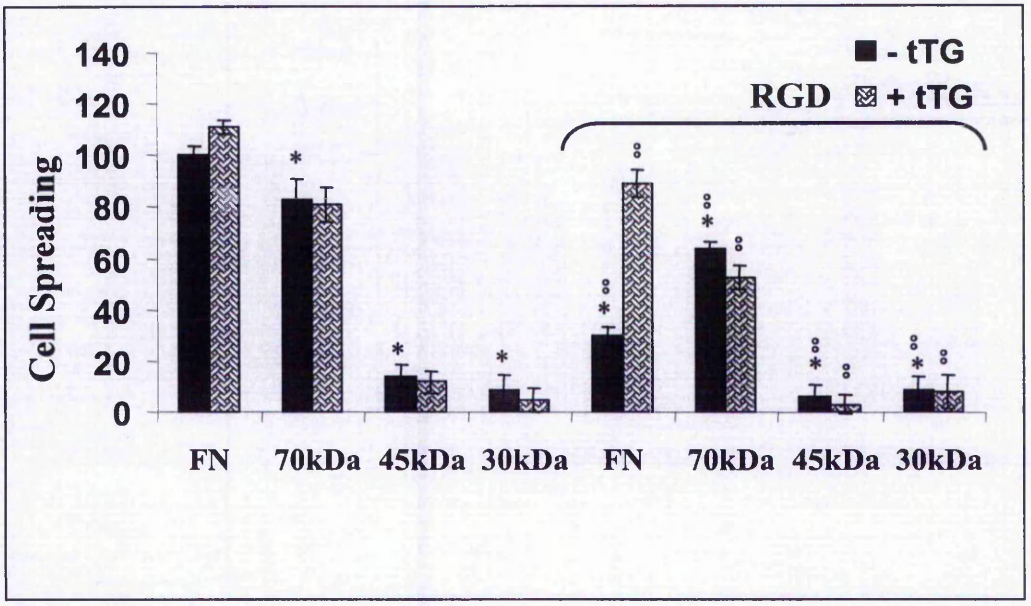
4.3.2.2 tTG immobilisation on amino-terminal FN fragments is not sufficient to support RGD-independent adhesion

Since tissue transglutaminase when immobilised on FN can restore cell attachment and spreading after inhibition by RGD peptides, it was decided to determine whether peptides containing the putative tTG high affinity binding site on the N-terminal of FN molecule could substitute for FN in supporting the tTG mediated RGD-independent cell adhesion. tTG was therefore immobilised on the N-terminal FN fragments and the adhesion of HOB cells were then examined in the presence and absence of RGD peptides.

Figure 4.3.11 The RGD-inhibition of HOB cell adhesion on amino terminal FN fragments with and without immobilised tTG

The matrix of FN amino-terminal fragments were prepared as described previously (Section 2.2.2.1) with (+tTG) or without (-tTG) further immobilisation of tTG. The assessment of HOB cell adhesion in response to amino-terminal FN fragments and tTG was done as described under Sections 2.2.5. Each data point corresponds to the mean percentage of attached cells (cell attachment) or the mean percentage of spread cells (cell spreading) ± S.D. of three separate experiments performed in triplicate. The mean number of cells attached and spreading values were expressed as a percentage of control values on FN (which represents 100%). Mean number of cells attached ± S.D. on control FN in the 3 experiments was 365 ± 20, 464 ± 17, and 407 ± 10. The mean percentage of spreading ± S.D. on control FN was assessed as 91 ± 2, 88 ± 6, and 86 ± 2, which was taken as 100%. The * symbol represents significant difference ($p<0.05$) between the FN control and cells seeded on the FN amino-terminal fragments in the presence or absence of RGD synthetic peptide. The ⁑ symbol indicates the statistically different values ($p<0.05$) for the RGD treated cells, when compared to the FN control.


Cell Attachment
140
120
100
80
60
40
20
0
- tTG
+ tTG
RGD
FN
70kDa
45kDa
30kDa
FN
70kDa
45kDa
30kDa


Cell Spreading
140
120
100
80
60
40
20
0
- tTG
+ tTG
RGD
FN
70kDa
45kDa
30kDa
FN
70kDa
45kDa
30kDa

As can be seen on figure 4.3.11, cells adhered efficiently on the 70 kDa fragment alone, as both cell attachment and spreading were approximately 80% of the values obtained on FN. Cells adhered very poorly on the 45 kDa and 30 kDa fragments with cell attachment and cell spreading around 10% and 3% of that of FN control, therefore these fragments were undesirable to show the effect of RGD inhibition on cell adhesion. In the presence of the RGD peptide, cell attachment and spreading values on the 70 kDa fragment were significantly inhibited by 40% of that of FN control. The RGD inhibition of cells seeded on 45 kDa and 30 kDa fragments did not show a significant decrease when compared with the cell adhesion values on these fragments without the RGD treatment. The immobilisation of tTG on the fragments failed to restore cell adhesion but bestowed a further inhibition on both cell attachment and spreading. In the presence of the RGD peptide, a further decrease (approximately 15%) in cell adhesion was observed for the cells seeded on the 70 kDa+tTG matrix. Similarly, tTG immobilisation on 45 kDa and 30 kDa fibronectin fragments did not appear to enhance cell adhesion to these matrices. This result indicates that immobilisation of tTG on amino-terminal FN fragments is not sufficient to support RGD-independent adhesion.

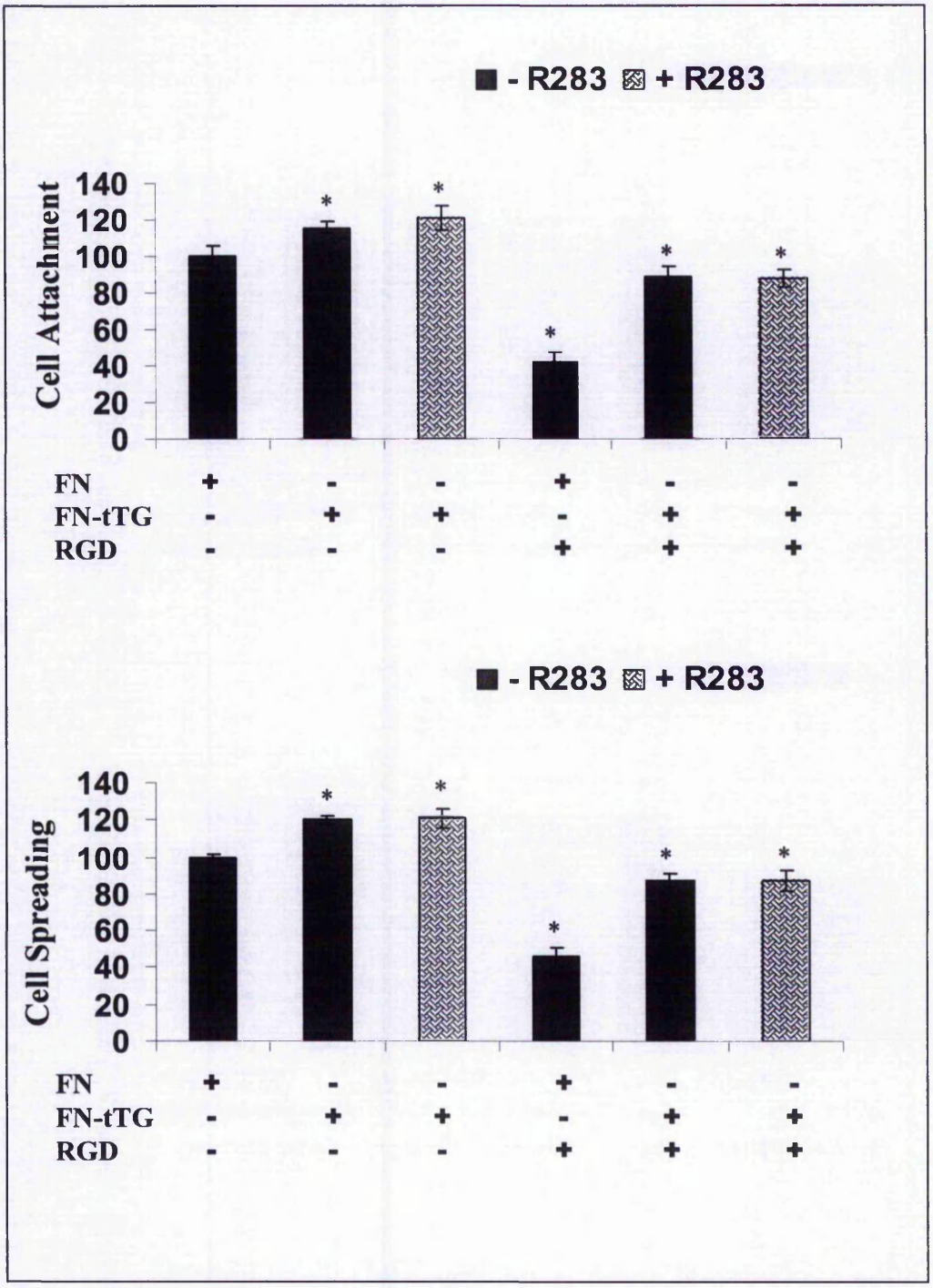
4.3.3 tTG cross-linking activity is not required to restore impaired cell adhesion

The importance of the Ca^{2+}-dependent ε-(γ-glutamyl) lysine cross-linking activity of tTG in stimulating RGD-independent cell adhesion was examined by the inhibition of the enzymatic activity of tTG immobilised on FN with the active site directed inhibitor R283. RGD-treated HOB cells were incubated with 100 μM of R283 and plated on the FN matrix coated with either catalytically active or inactive gpl tTG.

The level of cell attachment and spreading observed on the R283-treated FN-tTG matrix did not significantly differ from that observed on FN-tTG alone. That is, the FN-tTG matrix bestowed a 15% enhancement in HOB cell adhesion irrelevant of its active status (figure 4.3.12). The incubation of HOB cells with 100 μM of R283

Figure 4.3.12 The RGD-independent cell adhesion of HOB cells to FN-tTG following inactivation of tTG

The control (-R283) and inactive (+R283) FN-tTG matrix was prepared and the cell adhesion assay was performed as described in Sections 3.2.3 and 4.2.3. The attachment and spreading of HOB cells was assessed as mentioned previously (Methods 2.2.5). Data are represented as the mean percentage of attached cells (cell attachment) or the mean percentage of spread cells (cell spreading) ± S.D. from three separate experiments performed in triplicate. The mean cell attachment and spreading values were calculated as percentage of control values on FN, which represents 100%. Mean attachment and spreading values ± S.D. on FN control were assessed as 285 ± 16 and 226 ± 3. The mean percentage of control spreading on FN ± S.D. was calculated as 79 ± 1, and normalised to 100%. The statistically significant difference ($p<0.05$) between FN control and cells seeded on control and inactive FN/tTG matrix in the presence or absence of RGD synthetic peptide, is indicated with the * symbol.


- R283
+ R283
Cell Attachment
140
120
100
80
60
40
20
0
FN + - - + - -
FN-tTG - + + - + +
RGD - - - + + +
- R283
+ R283
Cell Spreading
140
120
100
80
60
40
20
0
FN + - - + - -
FN-tTG - + + - + +
RGD - - - + + +

did not confer any toxic effects to the cells since their level of cell adhesion was comparable to that of non-treated cells. The number of cells that attached in the presence of RGD peptide on FN-bound control and inactive tTG was found to be 87% of the control cells adhered on the FN matrix alone. Similarly, after the RGD inhibition, the spreading of cells was restored by either control FN-tTG or inactive tTG immobilised on FN.

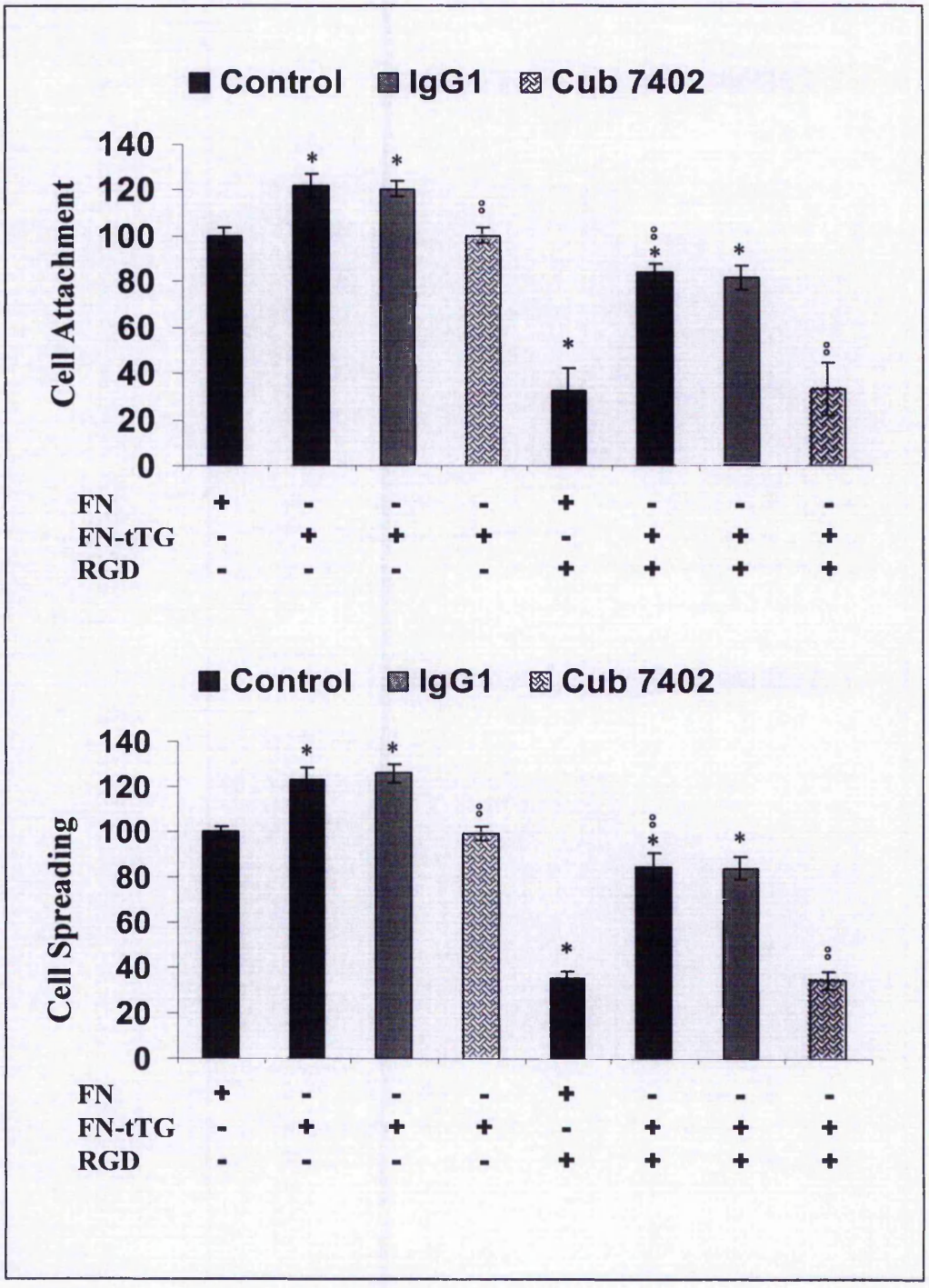
4.3.4 Evidence for a direct role of FN-associated tTG in RGD-independent binding to cells

To elucidate whether the availability of tTG in the FN-tTG complex could affect the RGD-independent cell adhesion process, FN-bound tTG was blocked by using the monoclonal Cub7402 antibody. The obstruction of tTG by Cub7402 would block any interaction of the enzyme with the cell surface. Any possible non-specific toxic effect of antibody incubation was excluded by use of a control antibody sharing the same isotype, IgG1, as Cub7402. Using this approach, the FN-tTG matrix was incubated with Cub7402 and IgG1 and the contribution of tTG to RGD-independent cell adhesion was examined.

An increase of approximately a 25% in cell attachment and cell spreading was observed when HOB cells were seeded on the FN-tTG matrix, but cell adhesion was not significantly increased above the control FN levels when cells were seeded on the FN-tTG matrix blocked by Cub7402. The compensation of RGD inhibition by the FN-tTG matrix, was completely abolished when cells were seeded on the Cub7402 hindered FN-tTG matrix. The incubation of the FN-tTG matrix with the control IgG1 antibody did not lead to any significant change in cell attachment and spreading of HOB cells on this control matrix in the presence or absence of the RGD peptide.

Figure 4.3.13 The importance of tTG in the support of the RGD-independent cell adhesion when immobilised on FN

The FN-bound tTG was incubated with Cub7402 and the control antibody IgG1 as described in Section 3.2.4. The cell adhesion assay was performed and adhered HOB cells then examined for cell attachment and spreading as described under Methods 2.2.5. Data represent the mean percentage of attached cells (cell attachment) or the mean percentage of spread cells (cell spreading) ± S.D. from three separate experiments performed in triplicate. The ordinate in the top graph represents the mean cell attachment expressed as mean percentage of control attachment to FN (which represents 100%) ± S.D. The mean number of cell attachment ± S.D. on FN in the 3 experiments was 231 ± 10, 193 ± 2, and 229 ± 13. The ordinate in the bottom graph indicates the mean percentage of spread cells, expressed as the mean percentage of control spreading on FN ± S.D. The mean percentage spreading value ± S.D. on FN in the 3 experiments was 81 ± 1, 71 ± 2, 72 ± 2, which was taken as 100%. The * symbol indicates the statistically different values of cells ($p<0.05$) seeded on different matrices other than FN control in the presence or absence of RGD synthetic peptide. The ¤ symbol represents the statistically significant difference ($p<0.05$) between cells seeded on control FN-tTG matrix and cells seeded on IgG1 and Cub 7402-incubated FN-tTG matrices, in the presence or absence of RGD synthetic peptide.


Control
IgG1
Cub 7402
Cell Attachment
140
120
100
80
60
40
20
0
FN + - - - + - - -
FN-tTG - + + + - + + +
RGD - - - - + + + +
Control
IgG1
Cub 7402
Cell Spreading
140
120
100
80
60
40
20
0
FN + - - - + - - -
FN-tTG - + + + - + + +
RGD - - - - + + + +

4.4 Discusssion

The preparation of an *in vitro* tTG rich FN matrix presents the opportunity to study tTG function in the ECM and in cell adhesion. Although the initial findings revealed the involvement of FN-bound tTG enzyme in the RGD-independent cell adhesion of HOB and Swiss 3T3 cells (Verderio *et.al.*, 2000), the molecular mechanism and the physiological significance of this finding still remained to be answered. In this chapter the molecular mechanisms underlying this novel RGD-independent cell adhesion process were further investigated.

In the cell adhesion assays the contribution of immobilised tTG on FN to cell adhesion was examined by inhibiting integrin-mediated RGD-dependent cell adhesion with competitive concentrations of soluble RGD peptides. Assaying for inhibition of cell attachment by RGD synthetic peptides suffers from the drawback that impurities in peptides may make them non-specifically active in inhibition assays. Hence, to avoid the non-specific inhibition, the cell adhesion assays should include a control peptide. In this project, since the hexapeptide G**RGD**TP was employed in inhibition studies, an inactive hexapeptide G**RAD**SP was chosen to be used as a control against toxicity and non-specific effects in all cell adhesion assays.

Initial experiments investigated the effect of RGD peptide on HOB and Swiss fibroblast by seeding the cells onto the FN-tTG matrix for 20 to 30 minutes. Although keeping the assay period short would help to minimise the secretion of endogenous ECM proteins, the risk of contaminating the supplied *in vitro* FN and FN-tTG matrices still exists. To rule out the possibility that the previously observed RGD-independent cell adhesion was due to binding of cells to cell-secreted proteins rather than the supplied FN-tTG matrix, the adhesion assay was performed in the presence of the protein synthesis inhibitor, cycloheximide. Cycloheximide inhibits protein translation in eukaryotes resulting in the inhibition of protein synthesis leading to cell growth arrest. Therefore, pre-treatment of cell monolayer prior to cell adhesion assay would lead to an inhibition in endogenous ECM protein synthesis by cells and prevent the contamination of the provided FN and FN-tTG matrices. Under these conditions, the HOB and Swiss 3T3 cells demonstrated an

enhanced cell attachment and spreading on the FN-tTG matrix without RGD peptide, confirming the role of FN-bound tTG as an adhesion-promoting complex (Heath *et.al.,* 2002). The examination of the RGD-independent cell adhesion of cycloheximide pre-treated HOB and Swiss 3T3 cells on FN-bound tTG showed that the inhibition of protein synthesis/secretion does not alter the response of cells to the FN-tTG matrix.

In an attempt to confirm these observations and to examine whether this RGD-independent novel cell adhesion pathway was common to other cell types, the effect of various concentrations of RGD peptide on the inhibition of cell attachment and spreading was examined using ECV304 cells, human dermal fibroblasts, and mouse dermal fibroblast wild type and knockout for tTG. The levels of attachment and spreading appeared to be enhanced in each cell line when they were seeded on the FN-tTG matrix in the absence of the inhibitory peptide. Although RGD peptide bestowed different levels of inhibition in each cell line, the inhibitory effect was largely attenuated when cells were seeded on the FN-tTG matrix in the presence of RGD peptide. For example, the attachment and spreading of MDFTg2+/+ and human dermal fibroblasts on FN was significantly decreased with excess peptide, in a more sensitive way than other cell types. On the other hand, the FN-tTG supported cell adhesion with comparable values to that of the FN control for ECV304 and MDFTg2+/+ cells. These results suggest that tTG immobilised on plasma FN supports cell adhesion of different cell types via an RGD-independent cell adhesion mechanism.

At this stage, the role of tTG in this novel adhesion pathway was further investigated using a matrix system more closely related to the ECM *in vivo*. Recently, it was shown that over-expression of tTG in Swiss 3T3 cells increased the deposition of enzyme into the ECM (Verderio *et.al.,* 1999; Balklava *et.al.,* 2002). Preliminary experiments showed that a matrix of cell-assembled FN with bound cell-secreted tTG can be obtained through long term culturing of induced and non-induced Swiss TG3 fibroblasts (Section 3.3.2). The data reported here shows that the FN-rich ECM with increased amounts of cell-secreted tTG could support a better cell adhesion in comparison to the ECM with background levels of tTG. The treatment of fibroblasts with increasing concentrations of RGD peptide

resulted in a significant decrease in cell attachment to the non-induced cell assembled ECM matrix, but not to the induced ECM matrix. The further incorporation of gpl tTG in both conditioned cell deposited ECM further increased the cell attachment levels in the presence and absence of the RGD peptide. Therefore, these data have confirmed the existence of a tTG-mediated RGD-independent cell adhesion pathway in a more physiological matrix system, which is closer to the *in vivo* model.

Given that FN and tTG is sequentially immobilised to the tissue culture plastic surface, it remains possible that the two proteins are immobilised directly and independently onto the plastic. It was therefore desirable to block the FN matrix prior to tTG immobilisation and detect how the blocked matrix can affect the RGD-independent cell adhesion. The RGD-independent cell adhesion on blocked matrix was found not to be different to that on the un-blocked FN-tTG matrix. In the follow-up experiment, the FN matrix and TCP was coated with increasing concentrations of tTG and the cell adhesion assay was performed with RGD-treated HOB cells. Negligible cell adhesion was observed when cells were seeded on tTG coated TCP, indicating that only tTG bound to FN, not tTG bound to plastic, supports the RGD-independent cell adhesion. In addition, further increase in tTG concentrations immobilised on FN did not bring about an increase in the level of compensation of cell adhesion, confirming that 20 μg/ml of tTG was enough to saturate 5 μg/ml of FN matrix.

In vitro binding studies have located the putative high affinity binding site(s) for human tTG on the N-terminal end of FN, either on type I_{3-5} repeats included in the 30 kDa fragment (LeMosy *et. al.,* 1992) or within the 45 kDa gelatin binding fragment (Jeong *et. al.,* 1995). In this report, the ability of tTG immobilised on FN amino terminal fragments, to mediate RGD-independent cell adhesion was examined using HOB cells. In the absence of the RGD peptide cells adhered efficiently on the 70 kDa fragments, however cells adhered very poorly on the 45 kDa and 30 kDa N-terminal FN fragments. This result is in disagreement with the finding showing that tTG-over-expressing transfected fibroblasts adhered and spread on surfaces coated with 42 kDa FN fragment (Akimov *et.al.,* 2000). However, at this work the authors used BSA as the blocking reagent, which might

contain FN due to impurity and if so could contaminate the 42 kDa matrix resulting in the observed cell adhesion. Interestingly, in the presence of the RGD peptide, a decrease in cell adhesion levels was detected on the 70 kDa fragment, although this fragment does not constitute the RGD sequence. This data is consistent with the previous finding that the amino-terminal FN fragments and RGD peptides cross-compete for binding to the integrin $\alpha_5\beta_1$ (Hocking *et.al.,* 2000). The quantitative assessment of RGD inhibition on the fibronectin fragments indicated that the immobilisation of tTG not only failed to compensate RGD-dependent cell adhesion; but it further inhibited cell attachment and spreading. As a consequence, tTG when bound to the amino-terminal proteolytic fragments of FN is not sufficient to support the RGD-independent cell adhesion, suggesting the requirement for the entire FN molecule.

Whilst the tTG has been implicated in cell adhesion of multiple cell types, the significance of transamidation activity of the enzyme in this process still remains controversial. Previous studies have established the importance of the Ca^{+2}-dependent ε-(γ-glutamyl)lysine cross-linking activity of tTG in ECM deposition/stabilisation (Gentile *et.al.,* 1992; Martinez *et.al.,* 1994; Aeschlimann and Thomazy 2000) However, recent findings indicate a novel transamidating-independent role for tTG in cell adhesion (Akimov *et.al.,* 2000; Takahashi *et.al.,* 2000; Balklava *et.al.,* 2002). In this study, under the conditions used to immobilise tTG onto the FN matrix, the aim was to reduce the transamidating activity of the enzyme to a minimum. The transamidation-free role played by FN-bound tTG in RGD-independent cell adhesion was confirmed by utilising the active-site directed tTG inhibitor in the cell adhesion studies. Data showed that the level of cell adhesion to FN with immobilised inactivated tTG was comparable to the FN-bound tTG not treated with the inhibitor, with or without pre-treatment of cells with the RGD synthetic peptide. This finding clearly indicates that the FN-bound tTG does not have to be catalytically active to support the RGD-independent cell adhesion.

In the light of these results it is temping to speculate that tTG when complexed with FN exposes a cryptic site in fibronectin initiating an RGD-independent cell adhesion process. However, it is equally possible that once tTG is bound on FN, it undergoes a conformational change, which leads to its recognition by a cell surface

receptor as a "bona fide" cell adhesion protein, and potentiates a cell adhesion process independently from the RGD-mediated direct binding to fibronectin. The importance of tTG in complex with FN in its interaction with the cell surface was investigated by using an enzyme specific monoclonal antibody Cub 7402. It was recently demonstrated that the blocking of cell-surface related tTG in stably transfected Swiss 3T3 fibroblasts with monoclonal antibody Cub 7402 was found to decrease cell adhesion in both induced and non-induced cells (Verderio *et. al.*, 1998). Using a similar approach FN-bound tTG was blocked in conditions that fully preserved the availability of FN in this complex (Section 3.3.6). The obstruction of tTG bound to FN not only cancelled the role of the FN-bound tTG as an adhesion-promoting complex but also completely abolished the compensation of RGD-impaired cell adhesion. This result suggests a direct role for tTG in complex with FN in the RGD-independent binding to cells.

Chapter 5: The characterisation of intracellular signalling in the RGD-independent cell adhesion pathway

Chapter 5: The characterisation of intracellular signalling in the RGD-independent cell adhesion pathway

5.1 Introduction

Within recent years it has been realised that in the absence of appropriate ECM contact, anchorage-dependent cells may undergo a detachment-induced programmed cell death. This form of apoptosis was first documented by Meredith *et al.* (1993), and was termed as anoikis, an ancient Greek word meaning 'homelessness', by Frisch and Francis (1994). In these initial studies, anoikis was studied in cells from endothelial and epithelial origin. Following reports described anoikis occurring in numerous adherent cell types such as fibroblasts (McGill *et.al,* 1997; Hadden and Henke, 2000) neuronal cells (Bonfoco *et.al,* 2000), pancreatic islet cells (Wang and Rosenberg, 1999), as well as in mammary epithelial cells (Boudreau *et.al,* 1995), bronchial epithelial cells (Aoshiba *et.al,* 1997), kidney epithelial cells (van de Water *et.al,*, 1999), intestinal epithelial cells (Strater *et.al,* 1996), and keratinocytes (Haake and Polakowska, 1993). Anoikis seems to play an important physiological role in tissue and cell homeostasis during development, renewal, and regression (Michel, 2003).

The intracellular signalling leading to apoptosis attributable to the loss of matrix contact, as well as signals propagated from cell-ECM adhesion complexes have been explored over the last two decades. The intracellular mechanisms of anoikis involve the repression of anti-apoptotic bcl-2 proteins, the activation of caspases and the impediment of anchorage-induced survival kinases, such as focal adhesion kinase (FAK), Ras-Raf kinase complex, extracellular signal-regulated kinase (ERK), phosphoinositide-3 kinase (PI3K)/Akt, and c-Jun-NH_2-terminal kinase (JNK) (Frisch and Screaton, 2001). In addition, the substantial differences in cytoskeletal structures between attached and non-attached cells suggest a possible role for the cytoskeletal filaments and Rho GTPases in the regulation of anoikis signalling.

Focal adhesion kinase, a 125 kDa non-receptor tyrosine kinase, is a component of focal contacts and is phosphorylated following integrin-mediated adhesion or integrin clustering (Lyman *et.al.,* 1997). The activation of FAK is not well understood, but evidence suggests that FAK may be recruited to nascent focal adhesions via its interaction with the cytoskeletal proteins talin and paxillin, and the cytoplasmic tail of integrin β subunits (Schlaepfer *et.al.,* 1999). Once activated, FAK is auto-phosphorylated at tyrosine 397 (Y-397), which creates a binding site for the Src homology 2 (SH2) domain of Src or Fyn kinase (Schaller *et. al.,* 1994; Shi and Boettiger, 2003). The Src kinase then activates a number of proteins, including the docking protein $p130^{CAS}$, adapter proteins Crk and Nck, which leads to the activation of JNK (Schlaepfer *et.al.,* 1999; Miyamoto *et.al.,* 1995; Oktay *et.al.,* 1999). FAK is also implicated in direct or Src-kinase mediated activation of PI3K (Chen *et.al.,* 1996). Integrin-FAK signalling complexes have been shown to play a role in the regulation of anchorage-dependent cell survival. A high level of apoptosis results if FAK expression is attenuated by anti-sense technology or anti-FAK antibodies (Xu *et.al.,* 1996; Hungerford *et.al.,* 1996; Duxbury *et. al.,* 2003). Conversely, constitutive expression of FAK by tethering it to the plasma membrane confers resistance against anoikis in epithelial cells (Frisch *et.al.,* 1996).

Among the signals generated by integrin-mediated cell adhesion is the activation of Ras/Raf/MEK/ERK cascade. There is evidence that Src kinase phosphorylates FAK at tyrosine 925. When phosphorylated, FAK is capable of activating ERK through recruitment of an adaptor protein-guanine nucleotide exchange factor complex, Grb2-mSOS, and GTP loading and activation of small GTPase Ras (Schlaepfer *et.al.,* 1994). The integrin mediated Ras activation may also occur through a FAK-independent pathway, which includes integrin coupling with caveolin and activation of Fyn/Shc kinase, resulting in the recruitment of Grb-mSOS complex (Wary *et.al.,* 1996, and 1998). The Ras-GTP complex, in turn, binds to the serine/threonine kinase Raf-1 and recruits it to membrane where it becomes active. The Raf protein kinases are shown to link Ras to mitogen and extracellular regulated kinase 1 (MEK) and mitogen-activated protein kinase ERK1 and ERK2 (Kolch, 2000). Recent reports have pointed a role for the ERK pathway in anoikis. The enhanced expression of ERK by the activation of the EGF receptor

is associated with protection against anoikis in suspended keratinocytes (Jost *et.al.*, 2001). Anoikis rescue by ERK has also been demonstrated by the expression of active Raf in fibroblast and epithelial cells (Le Gall *et.al.*, 2000).

To study the function of FN in the anchorage mediated cell survival, RGD-containing synthetic peptides have been used extensively as inhibitors of integrin-ligand interaction. The observation that RGD-like peptides induce inhibition of adhesion and trigger apoptosis has been reported for many cell lines, including fibroblasts (Hadden and Henke, 2000), endothelial (McGill *et.al.*, 1997), mesangial (Chen *et.al.*, 1997), thyroid (Vitale *et.al.*, 1998), and epithelial cells (Firsch and Francis, 1994). However, it has been recently shown that the RGD-binding domain alone has a limited ability to rescue cells from anoikis, indicating that activation of integrins might not itself be sufficient to regulate cell survival (Jeong *et.al.*, 2001). Emerging evidence suggests that the heparin-binding domain of fibronectin, which is known to synergistically interact with heparan sulphate proteoglycans and integrin $\alpha_4\beta_1$ integrin, also plays an important role in cell survival (Kapila *et.al.*, 1999; Jeong *et.al.*, 2001).

The major group of heparan sulphate proteoglycans are the syndecans, which are composed of a single transmembrane domain, a short cytoplasmic domain, and a larger extracellular domain that bears 3-5 glycosaminoglycan chains, mostly heparan sulphate (Zimmermann and David, 1999). The four mammalian syndecans have a distinctive pattern of expression characterised with the individual cell types, tissues and developmental stages (Woods, 2001). Briefly, syndecan-1,-2, and -3 are the major syndecans of epithelial, fibroblastic, and neuronal cells, respectively, whereas syndecan-4 is distinctively present in a wide range of cells that form stable adhesions (Woods and Couchman, 2000). Of the four members of the family, syndecan-4 is the one that is consistently present in focal adhesions (Woods and Couchman, 1994). There is much evidence to implicate syndecan-4 in partnership with integrins in the formation of focal adhesions. Initial studies have shown that primary fibroblasts seeded on substrates coated with the cell binding domain of fibronectin did not form focal adhesions or stress fibres unless they were incubated with clustering antibodies against syndecan-4 ectodomain (Woods *et.al.*, 1986; Bloom, *et.al.*, 1999; Saoncella *et.al.*, 1999). On activation, phosphatidylinositol

4,5-biphosphate binds to the cytoplasmic domain of syndecan-4 and induces the translocation and activation of PKC-α (Bass and Humphries, 2000). There is a possible role for syndecan-4 in stimulating the rearrangement of the actin cytoskeleton into ordered stress fibers by Rho-family GTPases. Syndecan-4 interacts with the cytoplasmic protein syndesmos via its cytoplasmic domain. When over-expressed in fibroblasts, syndesmos enhances cell spreading and actin stress fiber formation. The connection of syndecan-4 with syndesmos may implicate a role for syndecan-4 in the activation of Rho GTPases and in the assembly of actin stress fibers (Baciu *et.al.*, 2000). Collectively, these reports implicate syndecan-4 as a key receptor for focal adhesion formation on FN.

The results from the previous chapter (Chapter 4) have shown that RGD-dependent cell adhesion on FN could be interrupted with small concentrations of RGD peptide (50-150 μg/ml), and FN-tTG complex alone is sufficient to sustain an RGD-independent cell adhesion. In view of these findings it was therefore important to demonstrate whether this novel cell adhesion complex might potentiate intracellular signals that might rescue cells from a possible RGD-dependent anoikis.

5.2 Methods

5.2.1 Inhibition of $\alpha_4\beta_1$ integrin mediated cell adhesion

To inhibit the $\alpha_4\beta_1$ integrin mediated cell adhesion in Swiss 3T3 fibroblast, the function blocking anti-α_4 integrin mouse monoclonal antibody, and the CS-1 FN fragment (H-Glu-Ile-Leu-Asp-Val-Pro-Ser-Thr-OH) were used. In the first line of experiments, Swiss 3T3 fibroblasts resuspended in DMEM ($1.75x10^5$ cells/ml) were pre-treated with 30 μg/ml of anti-α4 integrin antibody for 15 minutes in the presence of 100 μg/ml of **GRADSP** or **GRGDTP** peptides. The control cells were incubated with mouse IgG1 antibody (30 μg/ml) in the presence of **GRADSP** or **GRGDTP** peptides at the same concentrations. In the second line of experiments, Swiss 3T3 fibroblasts were treated with 75 μg/ml CS-1 FN fragment with or without addition of 75 μg/ml **GRGDTP** peptide. The cells incubated with 150 μg/ml **GRADSP** were used as a positive control to check the toxicity levels of the exogenous peptide-treatment. Cells were then seeded on the 96-well plate coated with FN (5 μg/ml) or FN with immobilised tTG (20 μg/ml) and were allowed to attach for 40min. Following the cell attachment and spreading, the cells were fixed, permeabilised and stained as described previously (Section 2.2.5). The quantitative assessment of cell attachment and spreading was performed as mentioned earlier under Methods Section 2.2.5.4. The differences between data sets were analysed by the Mann-Whitney test at 95% level of significance using the Mini-Tab statistical analysis programme (Mini-Tab Inc, USA).

5.2.2 The digestion of cell-surface heparan sulphate chains of HOB cells

The HOB cells were cultured to sub-confluency and detached from their substratum as described previously (Section 2.2.5). Following the detachment of the cells, a cell suspension of $2x10^5$ cell/ml in DMEM was prepared and incubated with 15 mU/ml of heparitinase (dissolved in 100mM Tris-HCl, pH 7.0) or protease-free chondroitinase ABC (dissolved in 100mM Tris-HCl, pH 8) for 40 minutes at

37°C. The cells were then further treated with **GRGDTP** and **GRADSP** synthetic peptides for another 20 minutes. HOB cells were then seeded on FN and FN-tTG matrices and allowed to adhere for 20 to 30 minutes. The medium was then carefully removed and cells were fixed, permeabilised, and stained as depicted earlier (Section 2.2.5). Digital images of three non-overlapping fields were acquired and the number of cells per image was quantified using the Scion image analysis programme (National Institute of Health, Washington DC, USA) as described before (Section 2.2.5.4). The Mann-Whitney test was employed to determine the statistical difference between the data sets at 95% confidence interval.

5.2.3 The inhibition of PKC-α activity in HOB cells

The monolayer of sub-confluent HOB cells were serum-starved for 16 hours and then incubated in DMEM containing 5 μM of PKC-α inhibitor Go6976 (dissolved in DMSO) or with an equal volume of DMSO for 30 minutes. HOB cells were then harvested as described before (Section 2.2.5.1) and incubated with 100μg/ml **GRGDTP** and **GRADSP** synthetic peptides for 20 minutes. Cells were seeded on FN or FN-tTG matrices and allowed to attach and spread for 30 to 40 minutes. The assay was then terminated and the cell adhesion of HOB cells were finally analysed as described previously (Section 2.2.5.4). The statistical differences between the data sets at 95% level of significance were analysed using the Mann-Whitney test.

5.3 Results

5.3.1 RGD-independent cell adhesion does not require the activation of $\alpha_4\beta_1$ integrin

To investigate the possibility that RGD-independent cell adhesion to FN-tTG might be mediated by $\alpha_4\beta_1$ integrin, Swiss 3T3 fibroblasts were treated with the function blocking anti-α_4 integrin mouse monoclonal antibody P1H4. To eliminate any non-specific inhibition in cell adhesion due to the presence of toxic levels of an exogenous antibody, equivalent concentrations of the control IgG1 antibody, sharing the same isotype as anti-α_4 antibody, were used to treat the Swiss 3T3 fibroblasts. Blocking of α_4 subunit of $\alpha_4\beta_1$ integrin did not lead to a significant reduction in cell attachment and spreading of Swiss 3T3 fibroblasts on either FN or FN-tTG matrices (figure 5.3.1). The cell adhesion of P1H4 treated fibroblasts to FN and FN-tTG was, respectively, 100% and 116% of control cell adhesion to FN in the presence of RAD (100 μg/ml) peptide. A similar result was obtained when cells were treated with control IgG1 antibody and seeded on these matrices. The treatment of Swiss 3T3 cells with 100 μg/ml of RGD peptide resulted in a 60% decrease in attachment (figure 5.3.1a) and a 50% decrease in spreading on FN matrices (figure 5.3.1b). No further decrease in cell adhesion was detected in adhesion of IgG1 or P1H4 pre-treated cells on FN in the presence of RGD peptide. When seeded on FN-tTG matrix, the inhibition in cell adhesion was restored to nearly normal levels with a 85% of control cell attachment to FN. Cells treated with IgG1 or P1H4 antibodies in the presence of RGD peptide displayed a comparable response to the FN-tTG matrix, in that a 85-90% compensation in cell adhesion was observed when antibody-treated cells were seeded on the FN-tTG matrix with RGD peptide.

To confirm any potential role of $\alpha_4\beta_1$ integrin in RGD-independent pathway cell adhesion assays were performed in the presence of soluble CS-1 peptide. Swiss 3T3 fibroblasts were treated with equal amounts (75 μg/ml) of RGD and/or CS-1

Figure 5.3.1 Importance of $\alpha_4\beta_1$ integrin function in the support of the RGD-independent cell adhesion of Swiss 3T3 fibroblasts.

The treatment of Swiss 3T3 cells with the control IgG1 and the anti-α4 integrin antibody, and the analysis of cell adhesion were performed as described in Sections 2.2.5 and 5.2.1. Each data point corresponds to the mean percentage of attached cells (cell attachment) or the mean percentage of spread cells (cell spreading) ± S.D. of three separate experiments performed in triplicate. The ordinates in the top graphs represent the mean cell attachment expressed as the mean percentage of control attachment to FN in the presence of RAD peptide (which represents 100%) ± S.D. The mean number of attached cells ± S.D. of control in the 3 experiments was 172 ± 16, 129 ± 6, and 177 ± 8. The ordinates in the lower graphs indicate the mean percentage of spread cells, expressed as mean percentage of spreading on FN in the presence of RAD ± S.D. The mean percentage spreading values ± S.D on FN in the presence of RAD were 81 ± 3, 72 ± 2, 75 ± 2 in the 3 experiments, which was taken as 100%. The * symbol represents the statistically significant values of cell attachment and spreading ($p<0.05$) compared to that recorded for the RAD control.

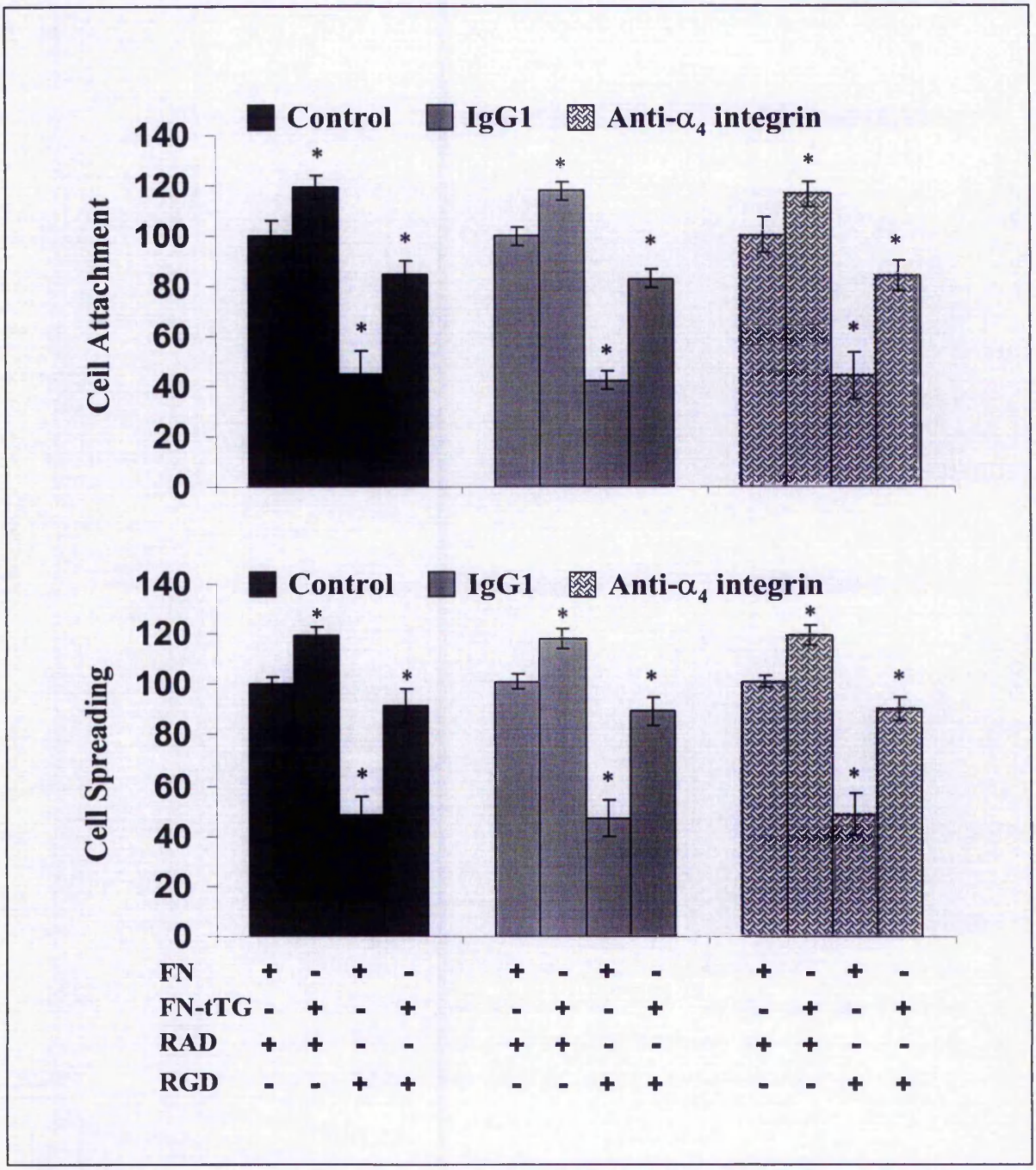
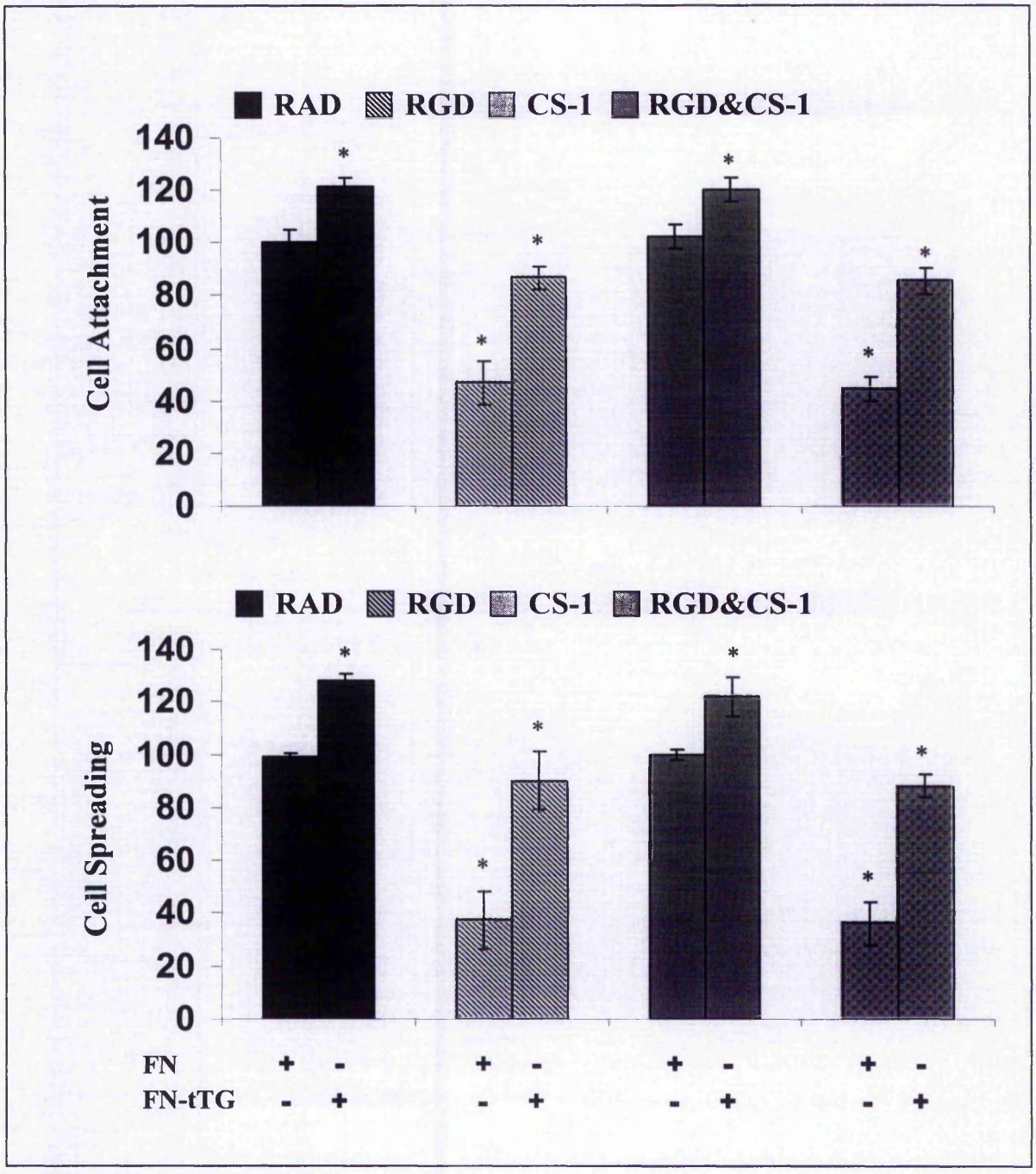

Control
IgG1
Anti-α4 integrin
Cell Attachment
Cell Spreading
140
120
100
80
60
40
20
0
FN + - + - + - + - + - + -
FN-tTG - + - + - + - + - + - +
RAD + + - - + + - - + + - -
RGD - - + + - - + + - - + +

Figure 5.3.2 Effect of FN CS-1 fragment on the cell adhesion of Swiss 3T3 fibroblasts to FN and FN-tTG matrices

The Swiss 3T3 fibroblasts were treated with RAD/RGD peptides and FN CS-1 fragment as described before (Section 5.2.1). The attachment and spreading of Swiss 3T3 fibroblasts were evaluated as mentioned in Section 2.2.5.4. Data are presented as the mean percentage of attached cells (cell attachment) or the mean percentage of spread cells (cell spreading) ± S.D. of three separate experiments carried out in triplicate. The cell attachment was expressed as the mean percentage of attachment of RAD treated cells to the FN matrix (RAD control) ± S.D., which represents 100%. The mean number of attached cells ± S.D. on RAD control was 583 ± 13. The mean percentage of RAD control spreading on FN ± S.D. was found to be 73 ± 5, which was then normalised to 100%. The statistically significant different ($p<0.05$) cell adhesion values other than the RAD control (100%) is represented with * symbol.


RAD
RGD
CS-1
RGD&CS-1
Cell Attachment
140
120
100
80
60
40
20
0
RAD
RGD
CS-1
RGD&CS-1
Cell Spreading
140
120
100
80
60
40
20
0
FN
FN-tTG

peptide and seeded on FN or FN-tTG matrices. Any possible non-specific toxic effect of exogenous peptide incubation was excluded by use of 150 μg/ml of RAD peptide.

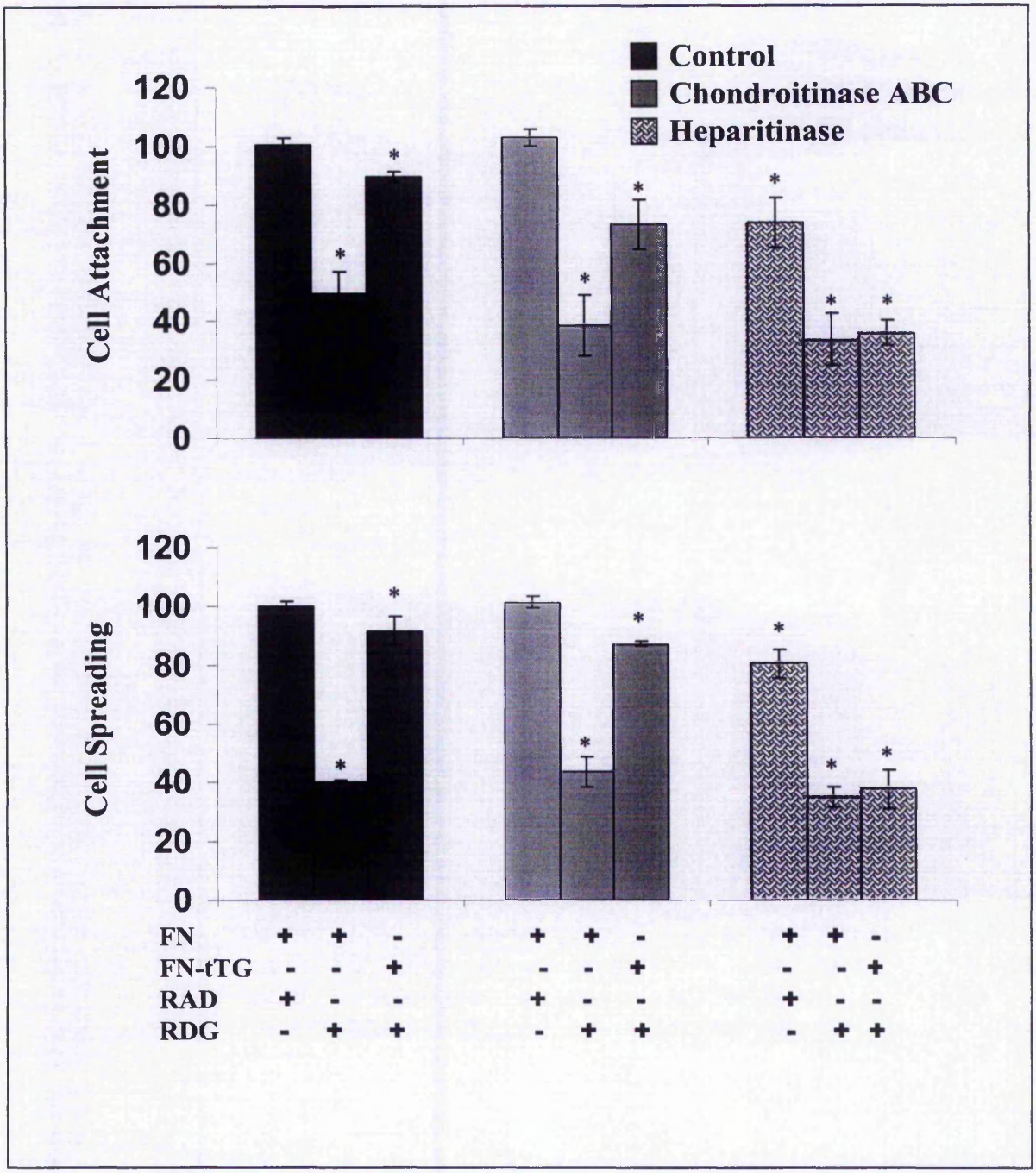
The treatment of Swiss 3T3 fibroblasts with 75 μg/ml of CS-1 peptide did not affect their cell adhesion pattern compared to that of FN with RAD peptide (figure 5.3.2). The effect of FN-tTG matrix as an enhancer of cell attachment and spreading was also observed when these cells were seeded on FN-tTG matrix in the presence CS-1 peptide. A typical 20% increase in cell attachment and spreading on the FN-tTG matrix was detected in cells treated with RAD or CS-1 peptides, in comparison to their adhesion on FN. The inhibition of attachment and spreading (figure 5.3.2) of Swiss 3T3 fibroblasts on FN by the RGD peptide was analysed as 60%. The double treatment of fibroblasts with 75 μg/ml of RGD and CS-1 peptides did not cause a further reduction in the inhibition of cell adhesion on FN. The attachment and spreading of Swiss 3T3 cells was restored to between 85-90%, once seeded on the FN-tTG matrix in the presence of RGD or RGD/CS-1 peptides. These results indicate that Swiss 3T3 cells, treated with the function blocking anti-integrin α_4 antibody or the CS-1 soluble peptide, were capable of RGD-independent cell attachment and spreading on FN-tTG.

5.3.2 The digestion of cell-surface heparan sulphate chains abolish RGD-independent cell adhesion

The importance of cell-surface proteoglycans in FN-tTG mediated RGD-independent cell adhesion pathway was investigated by cell adhesion assays using glysosaminoglycan-degrading enzymes. HOB cells were grown under sub-confluency and pre-treated with protease-free chondroitinase ABC lyase and heparitinase for 1 hour, as described in the Methods (Section 5.2.2). The effect of chondroitinase ABC lyase and heparitinase on the cell adhesion of RAD and RGD treated-HOB cells to FN and FN-tTG matrices was assessed. Results obtained from cell adhesion assays showed that the treatment of HOB cells with 15 mU/ml of chondroitinase ABC lyase resulted in a cell adhesion to FN comparable to the

Figure 5.3.3 Role of cell-surface heparan sulphate chains in the RGD-independent cell adhesion of HOB cells

The treatment of cells with chondroitinase ABC lyase and heparitinase was performed as described under Methods (Section 5.2.2). The cell adhesion assay was carried out and the attachment and spreading of HOB cells were analysed as explained in Section 2.2.5. The percentage of attached cells (cell attachment) or the percentage of spread cells (cell spreading) ± S.D. shown are the mean values from three separate experiments performed in triplicate. The mean cell attachment and spreading values were expressed as the percentage of control values of RAD-treated cells seed on FN (which represents 100%) ± S.D. The mean number of cell attachment ± S.D. of control taken from 3 experiments was 269 ± 6, 143 ± 8, and 131 ± 7. The mean percentage spreading value ± S.D on FN in the presence of RAD was 98 ± 5, 91 ± 2, 89 ± 1 in the 3 experiments, and normalised to 100%. The statistically significant difference ($p<0.05$) between the RAD control and cells treated with chondroitinase ABC lyase and heparitinase in the presence or absence of RGD synthetic peptide, is shown with * symbol.


Control
Chondroitinase ABC
Heparitinase
Cell Attachment
120
100
80
60
40
20
0
Cell Spreading
120
100
80
60
40
20
0
FN + + - + + - + + -
FN-tTG - - + - - + - - +
RAD + - - + - - + - -
RDG - + + - + + - + +

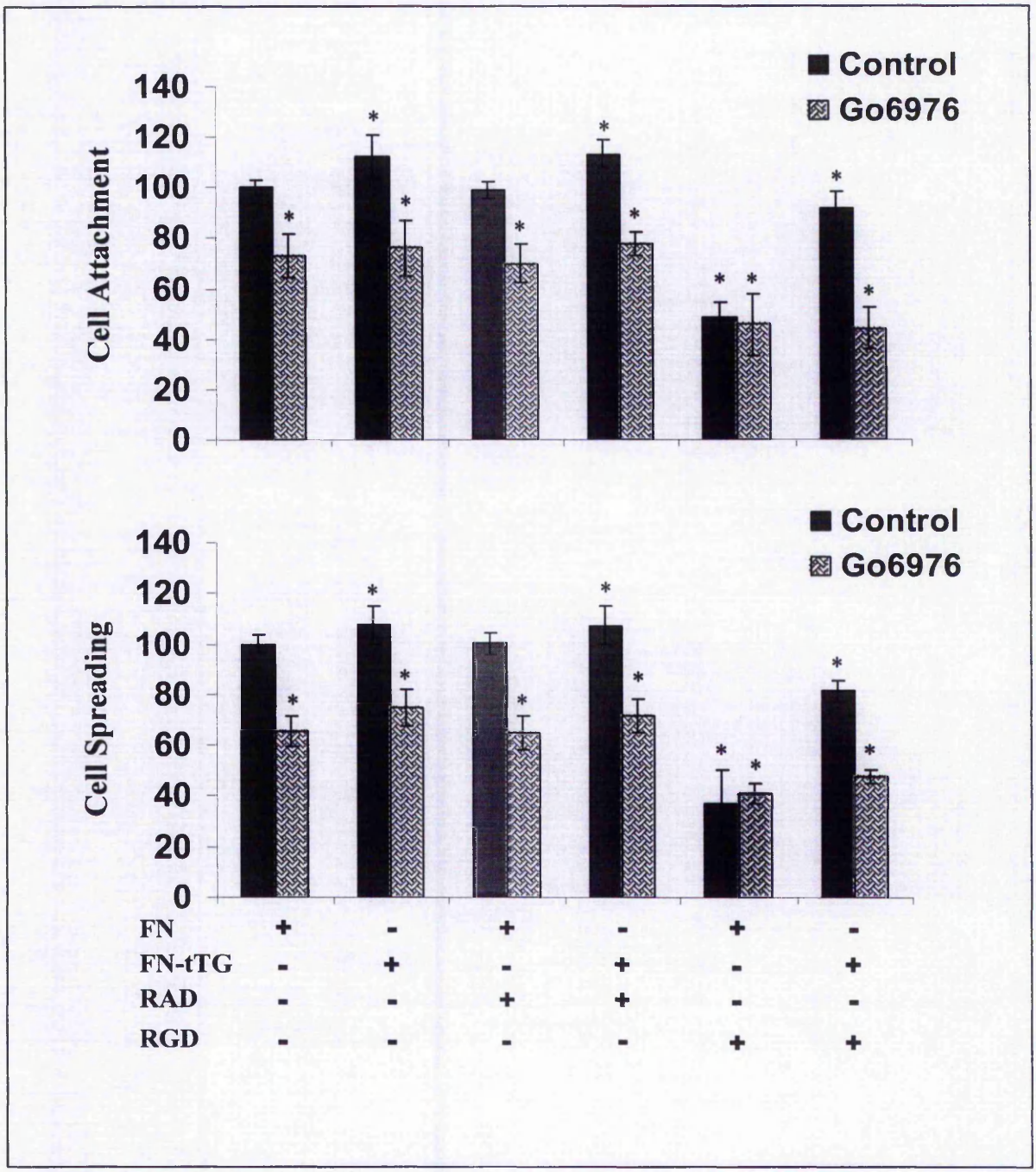
control cells on FN with RAD peptide (RAD control), as no significant difference was detected in cell attachment and cell spreading between the control RAD and chondroitinase ABC lyase treated cells (figure 5.3.3). However, when compared to the RAD control, approximately a 30% decrease in cell attachment and a 15% decrease in cell spreading was observed when HOB cells were seeded on FN, after heparitinase treatment. The cell attachment on FN-tTG matrix was increased to 15% of cell adhesion on FN in the presence of RAD (data is left out of the figure for clarity). The inhibition of attachment and spreading on FN by the RGD synthetic peptide was analysed as 50% at the concentration of 100 μg/ml. No significant difference in RGD inhibition of cell adhesion was observed in chondroitinase ABC lyase pre-treated HOB cells. However, the heparitinase-treated HOB cells displayed a further reduction (70%) in cell adhesion to FN at the same concentration of RGD peptide. The level of cell attachment and spreading was restored to almost control levels (95% of control values on FN), when control cells were seeded onto FN-tTG. The compensation in cell adhesion was found to be 70-80% of control levels, when chondroitinase ABC lyase pre-treated HOB cells were seeded on FN-tTG in the presence of RGD peptide. In the presence of RGD peptides, cell adhesion of heparitinase-treated cells on the FN-tTG matrix was not significantly different to the cell adhesion on FN, indicating that the digestion of cell-surface heparan sulphate chains abolish the RGD-independent cell adhesion.

5.3.3 The activation of PKC-α is necessary for RGD-independent cell adhesion

5.3.3.1 The RGD-independent cell adhesion in response to FN-tTG is blocked by the PKC-α inhibitor

To investigate whether the activity of PKC-α is essential in the RGD-independent cell adhesion pathway, sub-confluent monolayers of HOB cells were pre-treated with PKC-α inhibitor Go6976 as described previously (Section 5.2.3). The effect of Go6976 treatment on RGD inhibition of cell adhesion to FN and FN-tTG matrices was assessed. The treatment of HOB cells with Go6976 led to a significant 30% decrease in cell attachment and spreading on FN, compared to that

Figure 5.3.4 The involvement of PKC-α in adhesion of HOB cells to FN and FN-tTG matrices in the presence of RGD and RAD peptide. The HOB cells were treated with PKC-α inhibitor Go6976 and cell adhesion assay was performed as described previously (Section 5.2.3). The attachment and spreading of HOB cells were analysed as mentioned under Methods (Section 2.2.5). Each data point represent the mean percentage of attached cells (cell attachment) or the mean percentage of spread cells (cell spreading) ± S.D. of three separate experiments performed in triplicate. The ordinates in the top graphs represent the mean cell attachment expressed as mean percentage of non-treated HOB cell (control) attachment to FN ± S.D, which represents 100%. The mean attachment value ± S.D. of FN control was 184 ± 12. The ordinates in the lower graphs designate the mean percentage of spread cells, expressed as mean percentage of spreading on FN ± S.D. The mean percentage of control spreading on FN ± S.D was assessed as 80 ± 3, and normalised to 100%. The * symbol represents significant difference ($p<0.05$) between the FN control and cells treated with Go6976 inhibitor and seeded on FN and FN-tTG matrices in the presence and or absence of RAD and RGD peptide.


Control
Go6976
Cell Attachment
140
120
100
80
60
40
20
0
Control
Go6976
Cell Spreading
140
120
100
80
60
40
20
0
FN + - + - + -
FN-tTG - + - + - +
RAD - - + + - -
RGD - - - - + +

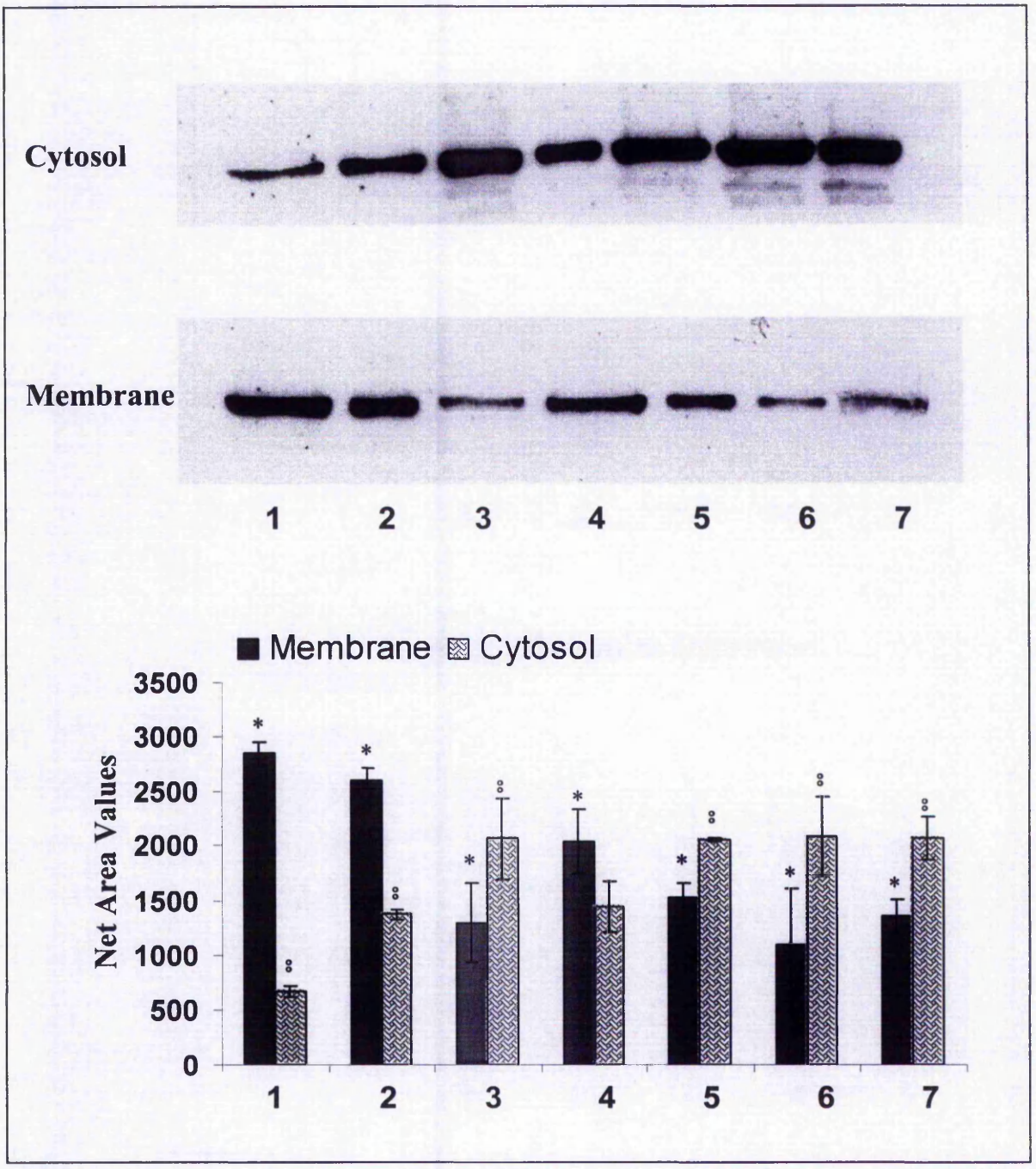
of FN control (figure 5.3.4). Cell adhesion to FN-tTG was 107-115% of control cell adhesion to FN in non-treated cells. In contrast, cell adhesion on FN-tTG displayed by Go7689-treated cells was only 70% cell attachment and spreading of control values on FN. Similar results were obtained when cells treated with PKC-α inhibitor were seeded on FN and FN-tTG matrix in the presence of RAD peptide. Once treated with RGD peptide, cell adhesion of Go6976- and non-treated cells to FN was inhibited up to 55-60% of cell attachment and spreading values evaluated for control FN. The defective cell attachment and spreading due to RGD inhibition was restored when non-treated cells were seeded on the FN-tTG matrix. However, the impairment in cell attachment and spreading was not restored when Go6976 treated-cells were seeded on the very same FN-tTG matrix, suggesting the importance of PKC-α activity in the RGD-independent cell adhesion process.

5.3.3.2 Evidence for the translocation of PKC-α to membranes during RGD-independent cell adhesion

The translocation of PKCα to the cell membrane was studied using non-treated HOB cells and HOB cells treated with Go6976. Both cell populations were allowed to attach on FN and FN-tTG matrices in the presence of RAD and RGD peptides. As a positive control of PKCα translocation, cells seeded on FN in the presence of RAD peptide were treated with 50 nM PMA. Cells were fractionated by ultra centrifugation into membrane and cytosolic rich fractions, which were then analysed for the amount of PKCα antigen by SDS-PAGE (3% (w/v) polyacrylamide stacking gel and a 8% (w/v) resolving gel) and Western Blotting.
The PKCα antigen could be found in both the cytosolic and membrane fractions of cells (figure 5.3.5). The amount of PKCα antigen was approximately 10% higher in the membrane fraction of cells treated with PMA than that of control cells seeded on FN in the presence of RAD peptide. The treatment of cells with RGD peptide resulted in less translocation of PKCα to the membrane from the cytosol, as the

Figure 5.3.5 Characterisation of PKC-α translocation during the RGD-independent cell-adhesion of HOB cells to FN –tTG matrix.

The HOB cells were treated with PMA and PKC-α inhibitor Go6976 and allowed to attach to FN and FN-tTG matrices as depicted in Sections 2.2.12 and 5.2.3. The cytosol and membrane fractions of 7 samples, -PMA treated cells (lane 1), non-treated cells (lane 2) seeded on FN in the presence of RAD, RGD-treated cells seeded on FN (lane 3) or FN-tTG (lane 4), Go-6976 treated cells seeded on FN in the presence of RAD (lane 5), Go-6976 treated cells seeded on FN (lane 6) or FN-tTG (lane 7) in the presence of RGD-, from 5 independent experiments were prepared, Western blotted and immunoprobed with mouse monoclonal PKC-α antibody (2 μg/blot). The upper blot represents the levels of PKC-α (80 kDa) in the cytosolic fraction (50 μg protein/sample) while, the lower blot indicates the levels of PKC-α translocated to membrane (30 μg protein/sample). The densitometry of PKC-α bands was expressed as the mean net area values ± S.D from five separate experiments. The * symbol represents significant difference ($p<0.05$) in the membrane fractions between net area values of the control RAD (sample 2) and PMA and Go6976 treated cells seeded on FN and FN-tTG matrices in the presence and absence of RGD and RAD peptide. The ¤ symbol indicates the statistically different values in cytosolic fraction of treated cells when compared to the RAD control.


Cytosol
Membrane
1
2
3
4
5
6
7
Membrane
Cytosol
Net Area Values
3500
3000
2500
2000
1500
1000
500
0
1
2
3
4
5
6
7

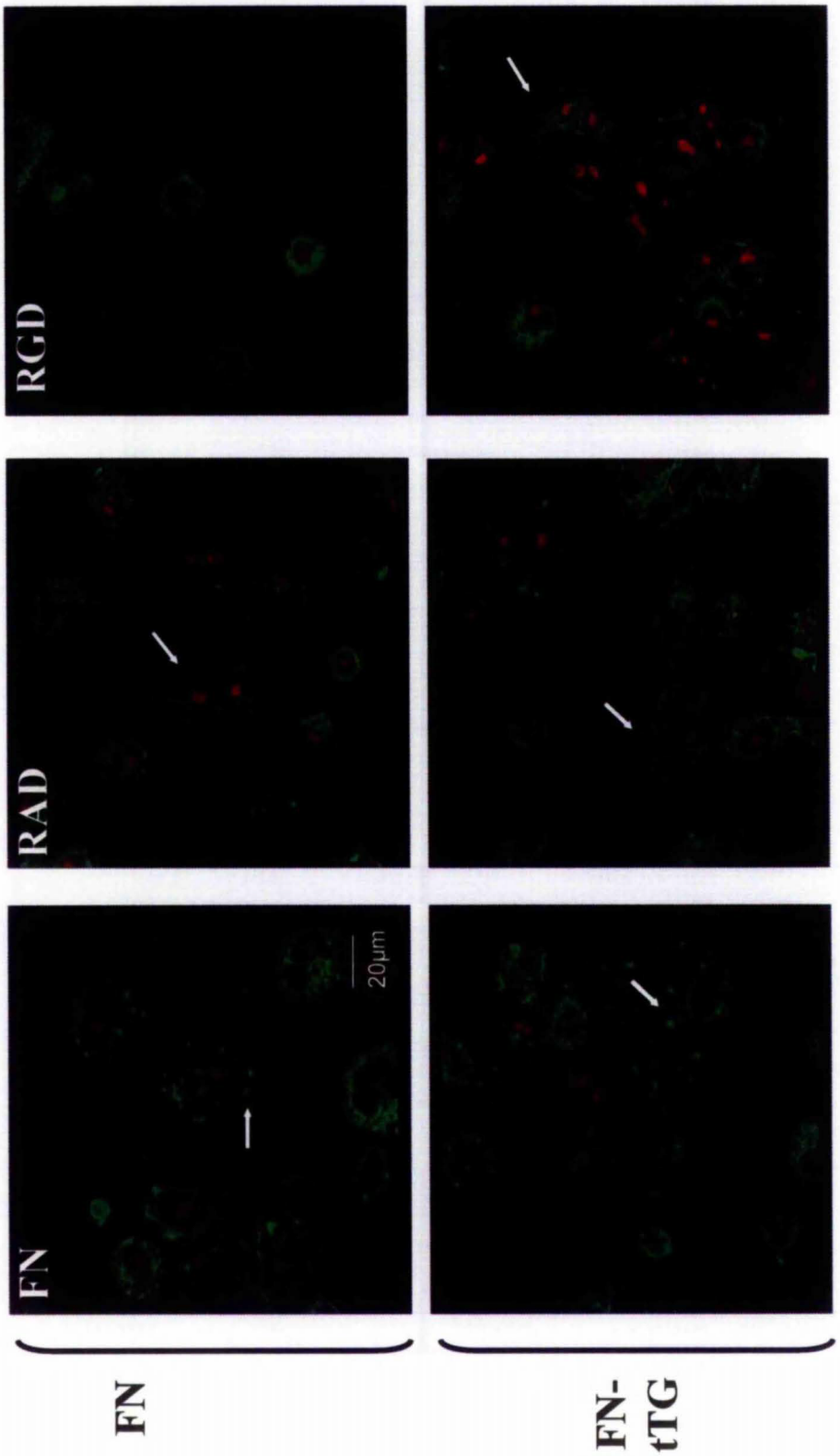
amount of PKCα antigen in the membrane fraction of RGD treated cells was shown to be 50% of that found in the RAD control. The levels of PKCα translocation in cells seeded on FN-tTG in the presence of RGD, was found to be 77% of control RAD levels. Following Go6976-treatment of HOB cells, a considerable decrease in the translocation of PKCα to the membrane was observed. When Go6976-treated cells were seeded on FN or FN-tTG matrices in the presence of RGD or RAD peptide, a two-fold reduction in PKCα antigen levels in the membrane fraction was identified. The incubation of Go6976-treated cells with RGD did not lead to any further significant decrease in the levels of membrane associated-PKCα. As expected, the levels of cytosolic PKCα were high for samples when a low translocation to membrane was measured.

5.3.4 The intracellular level of tyrosine phosphorylation is increased by FN-tTG matrix.

The differences in intracellular levels of tyrosine phosphorylation were investigated in RAD- or RGD–treated HOB cells seeded on FN and FN-tTG matrices. Following the cell adhesion (1 hour), cells were labelled with anti-phospho-tyrosine primary antibody, and subsequently with a FITC-conjugated secondary antibody. Cells stained with only the secondary antibody were used to adjust the background level of fluorescence. The confocal laser microscopic analysis of attached HOB cells showed that RGD peptide negatively affected the formation of focal adhesions and the tyrosine phosphorylation levels (figure 5.3.6). In the control cells that were attached and spread on FN in the presence or absence of RAD peptide, tyrosine phosphorylated proteins showed a clear distribution from cytosol to membrane. These cells exhibited a flat morphology and initial formation of focal adhesion contacts. Cells seeded on FN-tTG matrix were spread with fully formed focal adhesion points, which were positively stained for phospho-tyrosine proteins. The images of cells adhered to FN in the presence of RGD showed that these cells did not possess the characteristic focal contacts seen in the FN control cells, and displayed a very rounded-appearance. In RGD-treated cells staining of

Figure 5.3.6 Visualisation of tyrosine phosphorylation levels by immuno-fluorescence during the adhesion of HOB cells to FN and FN-tTG matrices in the presence of RAD and RGD peptides.

The cell adhesion assay was performed and the attached cells were fixed, permeablised and probed with rabbit polyclonal anti-phosphotyrosine (0.75 µl/sample). The staining was visualised using anti-rabbit IgG-FITC (raised in goat) and viewed by confocal microscopy as explained under the Methods Section 2.2.13. White arrows point to cells positive for tyrosine phosphorylation. The bar is equal to 20µm.


FN
RAD
RGD
20μm
FN
FN-
tTG

phospho-tyrosine proteins became very weak and condensed in the cytoplasm of these non-spread cells. In contrast, on FN-tTG, cells incubated with RGD peptide appeared to maintain control levels of phosphorylated tyrosine proteins, although they appeared less spread and more rounded than control cells seeded on FN without RGD. This experiment gave the first indication that there is a change in the levels of intracellular phophospho-tyrosine proteins during RGD-independent cell adhesion of HOB cells to FN-tTG.

5.3.5 FN-tTG signalling activates focal adhesion kinase

To explore the status of focal adhesion kinase activity, the phosphorylation level of FAK at tyrosine 397 residue was measured during RGD-independent cell adhesion of HOB cells to FN-tTG. Before signalling assays, HOB cells were cultured in DMEM medium containing 0.2% FCS for 24 hours for synchronisation purposes. HOB cells were harvested, pre-treated with RGD or RAD peptide, and then seeded on FN and FN-tTG coated TCP along with BSA coated plastic, which acted as a negative control as it provides a non-stick substratum for the cells. Cells were allowed to attach to the provided matrices for 60 minutes. The content of phospho- and total FAK of different samples was monitored by observing changes in the FAK-Y397 and total FAK antigen levels as detected by Western Blotting. The Western Blots displayed in figure 5.3.7 shows an SDS-PAGE (3% (w/v) polyacrylamide stacking gel and a 8% (w/v) resolving gel) separation of protein extracts from HOB cells seeded on BSA, FN and FN-tTG matrices in the presence of RAD and RGD peptides. A reduction in tyrosine phosphorylation levels of FAK can clearly be seen in negative control cells seeded on BSA coated wells (figure 5.3.7a) with the amount of FAK-Y397 antigen being 27% of that of the FN control. The treatment of cells with RAD peptide did not lead to a significant change in the levels of phospho-FAK antigen when compared to the levels of the FN control. When cells were seeded on FN-tTG in the presence or absence of RAD peptide, a slight increase in antigen levels was assessed, but this increase was not found to be statistically significant. The levels of FAK-Y397 antigen dropped to around 45% of control FN levels in cells seeded on FN in the presence of RGD peptide. However,

Figure 5.3.7 Western Blot Analysis of tyrosine phosphorylated and total FAK levels during RGD-independent cell adhesion of HOB cells.

a, Effect of RGD inhibition on tyrosine phosphorylation; **b,** the total levels of FAK during the adhesion of HOB cells to FN and FN-tTG matrix. The HOB cell lysates of 7 samples (50 μg protein/sample), non-treated cells seeded on BSA (lane 1), FN (lane 2), and FN-tTG (lane 3), RAD-treated cells seeded on FN (lane 4), and FN-tTG (lane 5) and RGD-treated cells FN (lane 6), and FN-tTG (lane 7), from 3 independent experiments were prepared, Western blotted and probed with rabbit polyclonal anti-FAK-Y-397 antibody (1:1000 dilution) (a) or mouse monoclonal anti-FAK (0.6 μg/blot) (b) as described before (Section 2.2.7-2.2.10). The upper blot represents the levels of phosphorylated FAK at tyrosine 397 (a), or levels of total FAK (b). Equal loading was ensured by probing the blots with anti-α-tubulin antibody (0.3 μg/blot) as can be seen in the lower blots. The densitometric values obtained for the bands was normalised against the values for the tubulin bands and represented as the mean net area value (relative FAK-Y397 or relative FAK) ± S.D. from three separate experiments. Each data point was expressed as a percentage of control FN level, which represents 100%. The * symbol indicates the statistically different values ($p<0.05$) when compared to the FN control.

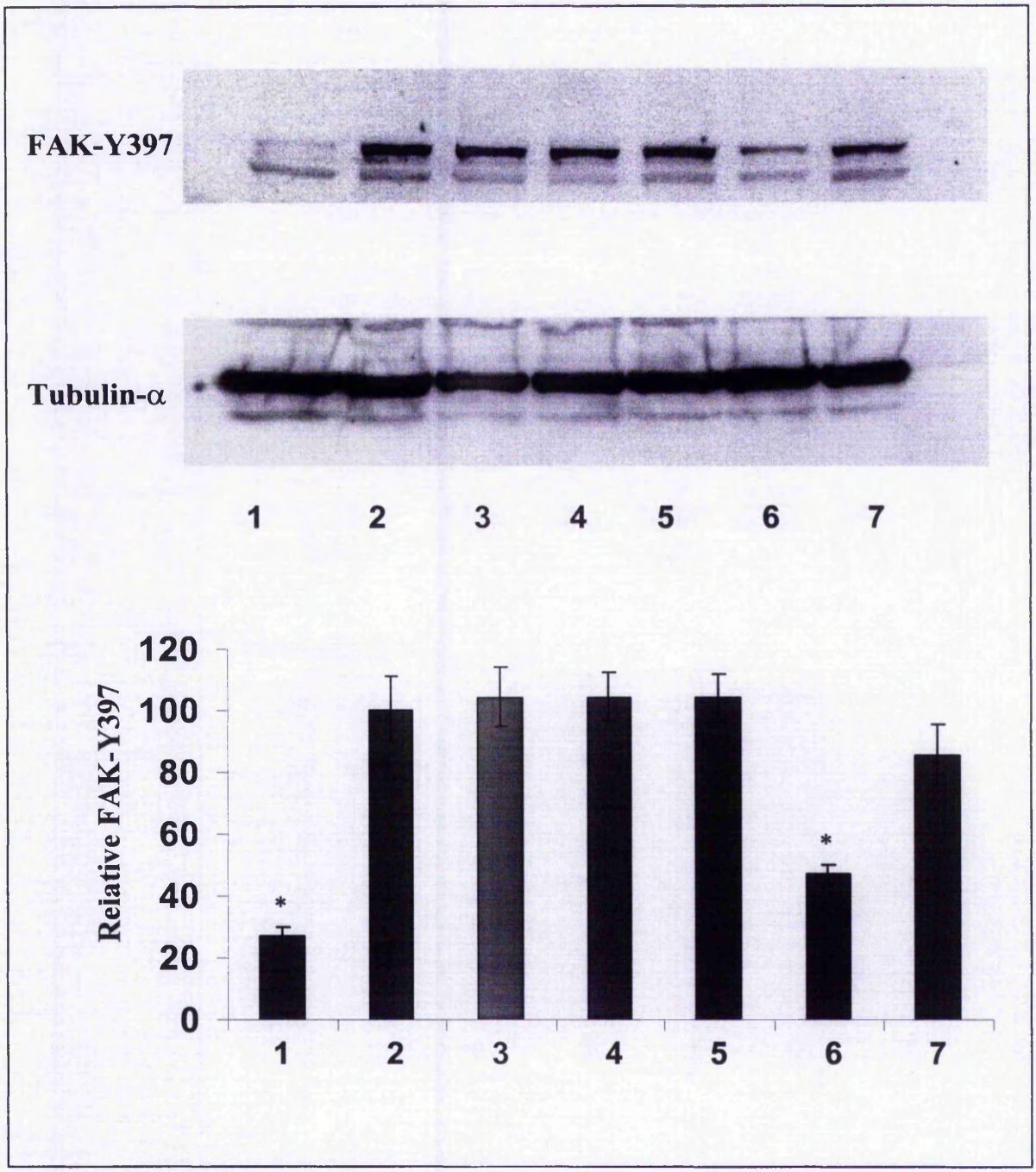

FAK-Y397
Tubulin-α
1
2
3
4
5
6
7
Relative FAK-Y397
120
100
80
60
40
20
0
*
*

Figure 5.3.7a

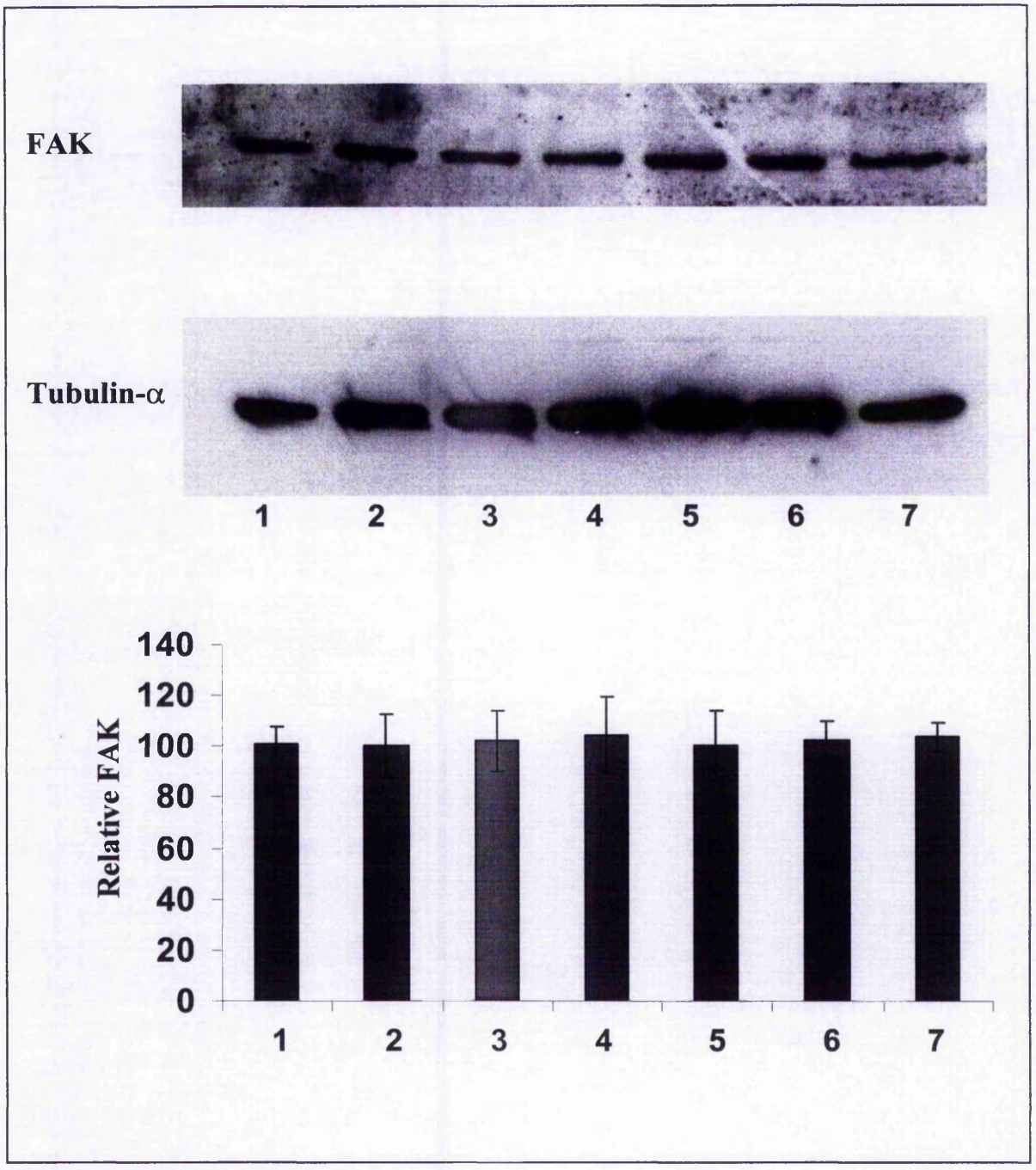

FAK
Tubulin-α
1
2
3
4
5
6
7
Relative FAK
140
120
100
80
60
40
20
0
1
2
3
4
5
6
7

Figure 5.3.7b

in response to FN-tTG the amount of FAK phosphorylation was found to be approximately 85% of that of control cells on FN.

Western Blots were performed in parallel to explore the total FAK levels in the same protein extracts. The blot (figure 5.3.7b) shows that all cell samples displayed a similar banding pattern with no significant changes in the levels of total FAK. These results imply that FAK is one of the major intracellular signalling mediators in the RGD-independent cell adhesion.

5.3.6 The role of PKC-α in the tyrosine phosphorylation of FAK

Having established that tyrosine phosphorylation of FAK is important in the RGD-independent pathway, the importance of PKC-α activity in phosphorylation of FAK was studied using HOB cells. Prior to the experiment, cells were incubated in serum free medium DMEM for 16 hours. Cells were then treated with PKC-α inhibitor Go6976 before and during the experiment. HOB cells were seeded on FN and FN-tTG matrices in the presence of RGD or RAD peptides. To further induce the PKC-α activity, cells adhered on FN with RAD were treated with PMA. The levels of total and tyrosine phosphorylated form of FAK in the samples were examined by immunoprobing of Western Blots from cell extracts as described above. Figure 5.3.8a presents the content of FAK phosphorylated at Tyrosine 397 (FAK-Y397), while figure 5.3.8b shows the total FAK levels, in control and Go6976 treated cells plated on FN and FN-tTG with or without RGD peptide. As expected, tyrosine phosphorylation of FAK in cells seeded on FN matrix with RGD peptide was decreased to 45% of that found in control cells plated on FN in the presence of RAD peptide (control levels). The treatment of cells with PMA did not result in a statistically significant increase in FAK-Y397 antigen levels when compared to control levels. The amount of phospho-FAK antigen returned back to nearly control levels (83% of control values on FN), when cells were seeded onto FN-tTG in the presence of RGD peptide. In Go6976-treated cells, the decrease in FAK-Y397 antigen levels was evident, considering the 30% decrease in the levels of FAK phosphorylation in cells seeded on FN with RAD peptide. For the Go6976-

Figure 5.3.8 Role of PKC-α in the activation of FAK during RGD-independent cell adhesion of HOB cells to FN-tTG matrix.

a, Effect of PKC-α inhibitor Go6976 on the tyrosine phosphorylation; **b,** the total FAK levels during the RGD-independent adhesion of HOB cells to FN-tTG matrix. The HOB cells were treated with PMA and PKC-α inhibitor Go6976 and assay was performed as described under Method Section 5.2.3. The samples, PMA treated cells (lane 1), non-treated cells (lane 2) seeded on FN in the presence of RAD, RGD-treated cells seeded on FN (lane 3) or FN-tTG (lane 4), Go-6976 treated cells seeded on FN in the presence of RAD (lane 5), Go-6976 treated cells seeded on FN (lane 6) or FN-tTG (lane 7) in the presence of RGD, were prepared, lysed (50 μg protein/sample) and Western Blotted. The blots from 6 independent experiments were immunoprobed with rabbit polyclonal anti-FAK-Y-397 antibody (1:1000 dilution) (a), while blots from 3 independent experiments probed for mouse monoclonal anti-FAK (0.6 μg/blot) (b). The top images are representative blots showing the levels of phospho-FAK (a) or total FAK levels (b) for the seven samples. The bottom imagines presents the blots probed with α-tubulin control antibody (0.3 μg/blot). The densitometric values of the bands for phospho- and total FAK were normalised against the values for the tubulin bands. Data in histogram are the mean percentage of net area values ± S.D., and expressed as the percentage of the control RAD values (which represents 100%). The * symbol indicates statistically significant ($p<0.05$) net area values for phospho-FAK and total FAK, when compared to the control RAD.

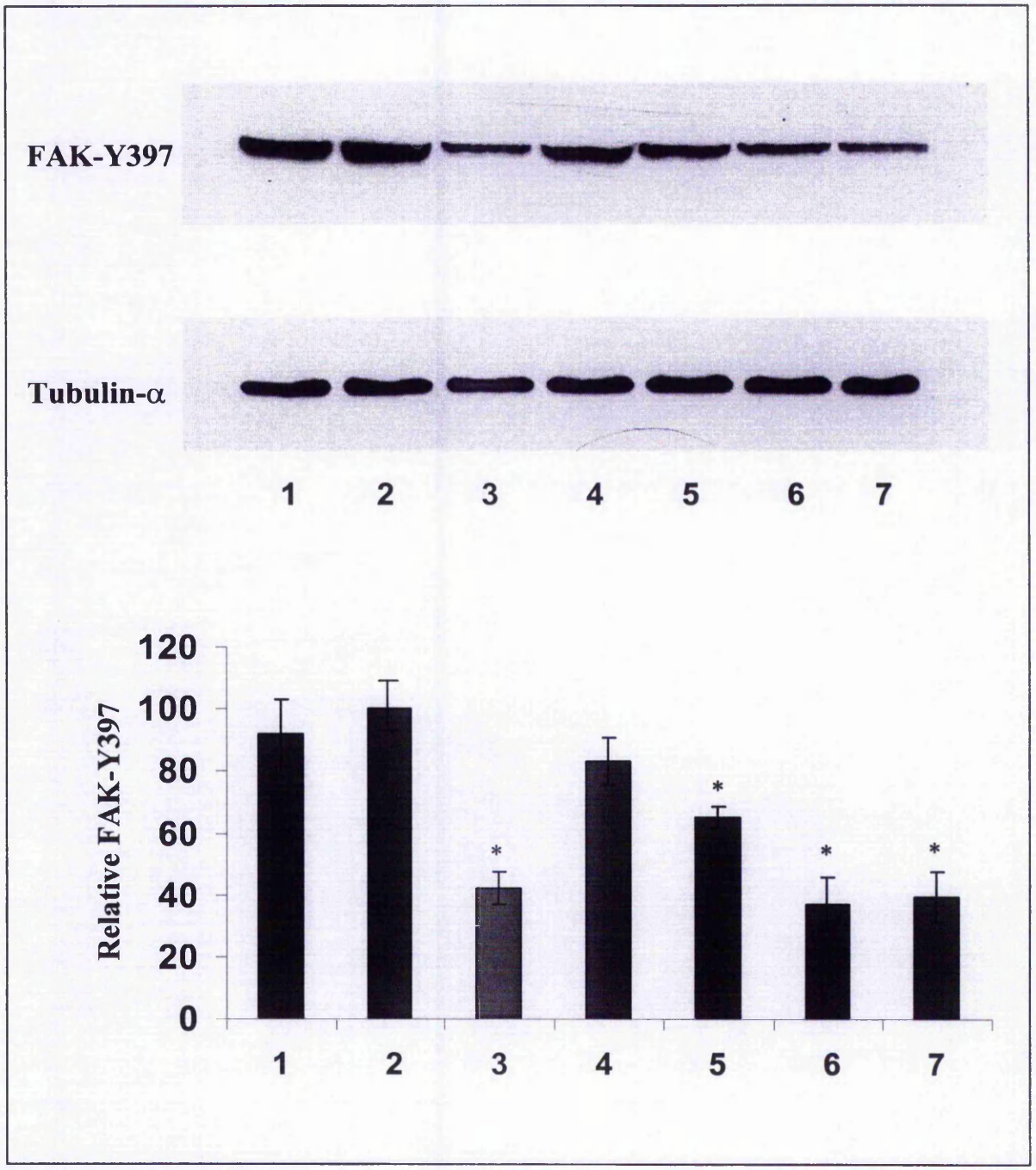

FAK-Y397
Tubulin-α
1 2 3 4 5 6 7
Relative FAK-Y397
120
100
80
60
40
20
0
*
*
*
*
1 2 3 4 5 6 7

Figure 5.3.8a

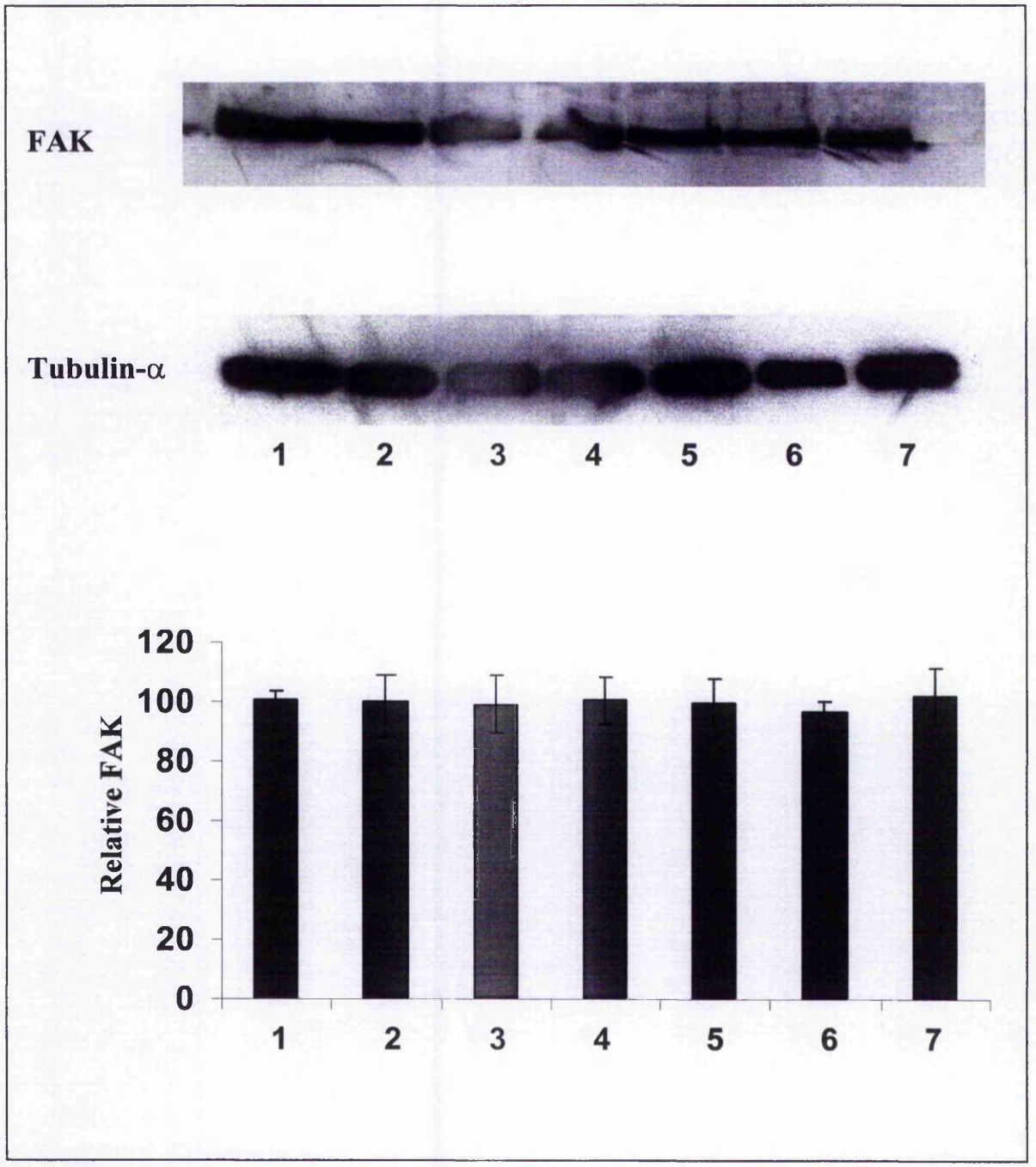

FAK
Tubulin-α
1
2
3
4
5
6
7
Relative FAK
120
100
80
60
40
20
0
1
2
3
4
5
6
7

Figure 5.3.8b

treated cells seeded on FN and FN-tTG, the reduction in the content of phospho-FAK antigen was approximately 60% in comparison to control levels.
When the total FAK levels was monitored in HOB cell samples prepared under the same conditions, a similar amount of FAK antigen was detected for all samples. Once again, the treatment of HOB cells with RGD peptide resulted in a decrease in FAK phosphorylation levels and the PKC-α inhibitor abolished the compensation of RGD inhibition by FN-tTG.

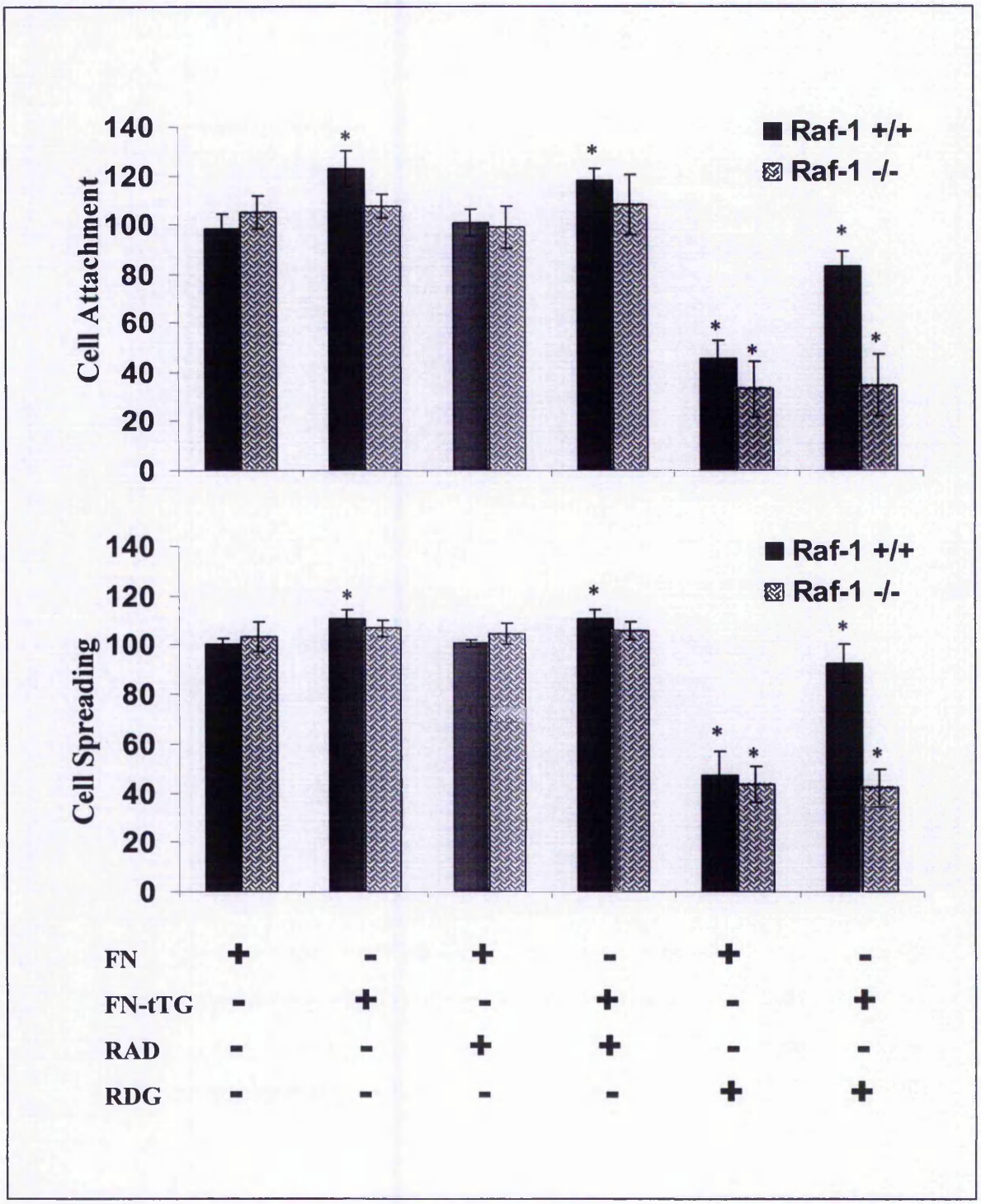
5.3.7 The characterisation of cell survival signalling pathway induced during RGD-independent cell adhesion

5.3.7.1 The loss of Raf-1 impairs the restoration of cell adhesion by FN-tTG complex

In order to investigate whether the rescue of cell adhesion by FN-tTG following RGD inhibition requires Raf-1 kinase, the Raf-1 wild type and knock out 3T3-like immortalised fibroblast cell lines were used in the cell adhesion assay. The Raf-1 wild type (Raf-1 +/+) and knock out (Raf-1 -/-) cells were harvested, and a cell solution of $1.75x10^5$ cell/ml was pre-treated with 100 μg/ml of RAD and RGD peptide. Cells were then seeded on FN and FN-tTG matrices and allowed to attach for 40 minutes. The effect of the hexapeptide **GRGDTP** on these cells was examined, as described previously (Section 2.2.5). Once attached and spread Raf-1 +/+ cells displayed Swiss 3T3 fibroblast like appearance, however, Raf-1 -/- cells demonstrated a non-homogenous morphology with flattened spindle-like cells and cuboidal cells. Results obtained from cell adhesion assays showed that Raf-1 -/- cells attached and spread on FN matrix comparable to Raf-1 +/+ cells (figure 5.3.9). When Raf -1 +/+ cells were seeded on the FN-tTG matrix with or without RAD peptide, a significant 20% increase in cell attachment and 10% increase in cell spreading were observed. However, no statistically significant change in cell adhesion of Raf-1 -/- cells to FN-tTG matrix was detected, when compared to Raf-1 +/+ control cell adhesion on FN. The treatment of Raf-1 +/+ and -/- cells with RGD peptide resulted in approximately 60% decrease in attachment and spreading

Figure 5.3.9 Adhesion of Raf +/+ and Raf -/- fibroblasts to FN and FN-tTG matrices in the presence of RAD and RGD peptides.

The cell adhesion assay was performed and the attachment and spreading of mouse Raf-1 wild type (Raf +/+) and knock out (Raf -/-) 3T3-like immortalised fibroblast cell lines were assessed as described in Sections 2.2.5. Each data point represents the mean percentage of attached cells (cell attachment) or the mean percentage of spread cells (cell spreading) ± S.D. from three separate experiments performed in triplicate. The ordinates in the top graphs represent the mean cell attachment expressed as mean percentage of control attachment of Raf +/+ fibroblasts on FN ± S.D., which represents 100%. The mean attachment and spreading values of Raf +/+ fibroblasts on FN ± S.D. were calculated as 157 ± 17 and 114 ± 13, respectively. The ordinates in the bottom graphs indicate the mean percentage of spread cells, expressed as a percentage of control Raf +/+ fibroblasts spread on FN±S.D. The mean percentage of control spreading on FN ± S.D. was shown to be 73 ± 8, which was considered as 100%. The * symbol indicates the statistically significant difference between data sets when compared to values presented by Raf +/+ fibroblasts on FN .


Cell Attachment
140
120
100
80
60
40
20
0
Raf-1 +/+
Raf-1 -/-
Cell Spreading
140
120
100
80
60
40
20
0
Raf-1 +/+
Raf-1 -/-
FN + - + - + -
FN-tTG - + - + - +
RAD - - + + - -
RDG - - - - + +

on FN matrices. When seeded on the FN-tTG matrix, the inhibition of cell adhesion in Raf-1 +/+ cells was restored to nearly normal levels with 83-90% of control cell adhesion recorded on FN. Intriguingly, Raf-1 -/- cells treated with RGD peptide displayed no increase in cell adhesion in response to the FN-tTG matrix, in that cell attachment and spreading of Raf-1 -/- cells on the FN-tTG matrix was found to be 35-40% of that of control FN levels. This suggests that the loss of Raf-1 impairs the restoration of RGD-independent cell adhesion by the FN-tTG complex in fibroblast cells.

5.3.7.2 Role of the MEK-ERK pathway in FN-tTG mediated signalling

The involvement of the MEK-ERK pathway in FN-tTG induced RGD-independent cell adhesion was explored by measuring phosphorylation levels of ERK1 and ERK2 at the tyrosine 204 residue in HOB cells. For this purpose, synchronised HOB cells were seeded on BSA, FN, and FN-tTG coated 6-well plates at a density of $6x10^5$ cells/well and allowed to attach for 1 hour with or without RGD or RAD peptides (150μg/ml). To monitor the levels of phospho-and total ERK1/2, equal amounts of protein from each cell sample was separated by SDS-PAGE (3% (w/v) polyacrylamide stacking gel and a 10% (w/v) resolving gel) and then Western Blotted. When the blots were immunoprobed with the anti-phospho ERK1/2 antibody, a significant reduction in phospho-ERK1/2 levels was evident in samples where cells were not adhered. As can be seen in figure 5.3.10a, in HOB cells seeded on BSA matrix, tyrosine phosphorylation levels of ERK1 and ERK2 (p-ERK1/2) were reduced to 40% and 60% respectively of that of the FN control. In comparison to control levels, the content of p-ERK1/2 antigen was not significantly different in the cells seeded on FN and FN-tTG with or without RAD peptide. The effect of RGD peptide on the amount of p-ERK1/2 antigen was apparent, considering the 50% reduction in p-ERK1 and 30% reduction in p-ERK2 antigen levels observed in cells seeded on FN with RGD. In response to FN-tTG, the cell content of ERK1 and ERK2 phosphorylation was found to be approximately 85% and 95% of that of control cells seeded on FN.

Figure 5.3.10 Western Blot Analysis of phospho-tyrosine and total ERK1/2 levels during RGD-independent cell adhesion of HOB cells. **a,** Effect of RGD inhibition on tyrosine-phosphorylated ERK1/2 ; **b,** the total ERK1/2 levels during the adhesion of HOB cells to FN and FN-tTG matrix. The HOB cell lysates (40 μg protein/sample) were prepared and proteins was separated as described in Sections 2.2.7 and 2.2.10. The samples, non-treated cells seeded on BSA (lane 1), FN (lane 2), and FN-tTG (lane 3), RAD-treated cells seeded on FN (lane 4), and FN-tTG (lane 5) and RGD-treated cells FN (lane 6), and FN-tTG (lane 7), were then immuno-blotted and probed with mouse monoclonal anti-phospho ERK1 (44 kDa) and ERK2 (42 kDa) antibody (a, top image) (2 μg/blot) or rabbit polyclonal anti-ERK1/2 (b, top image) (1:1000 dilution). The blots were stripped and reprobed with mouse monoclonal anti-α-tubulin (0.3 μg/blot) to ensure the equal loading (bottom images). The density of bands for each sample was normalised against the corresponding values for tubulin bands. Data presented are the normalised mean net area values ± S.D. from five separate experiments for phospho-ERK1/2 (p-ERK1/2) and three separate experiments for total ERK1/2 (ERK1/2) levels, expressed as the mean percentage of the control FN value ± S.D., which represents 100%. The * symbol represents significant difference in net area values ($p<0.05$) in comparison to the FN control.

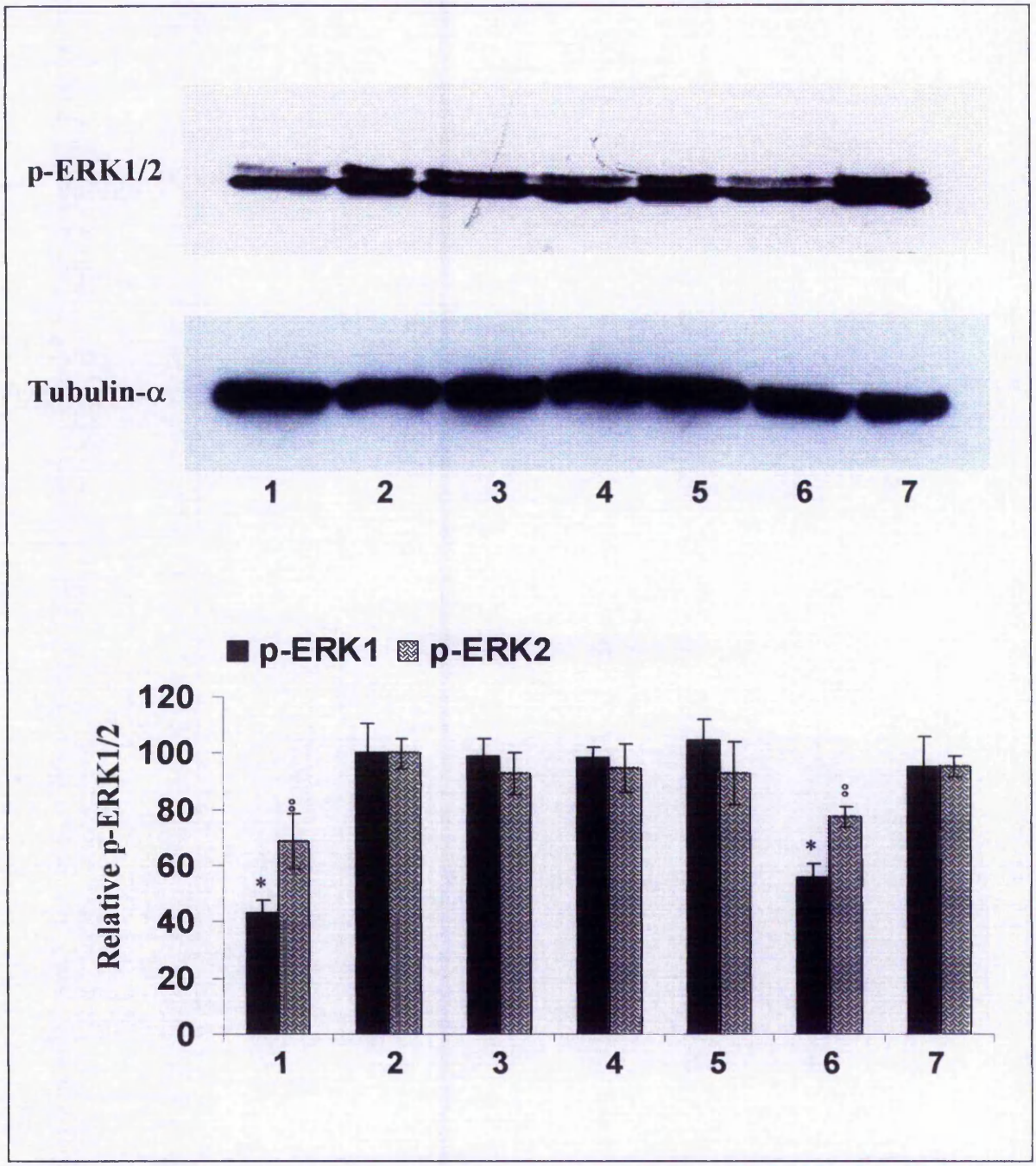


Figure 5.3.10a

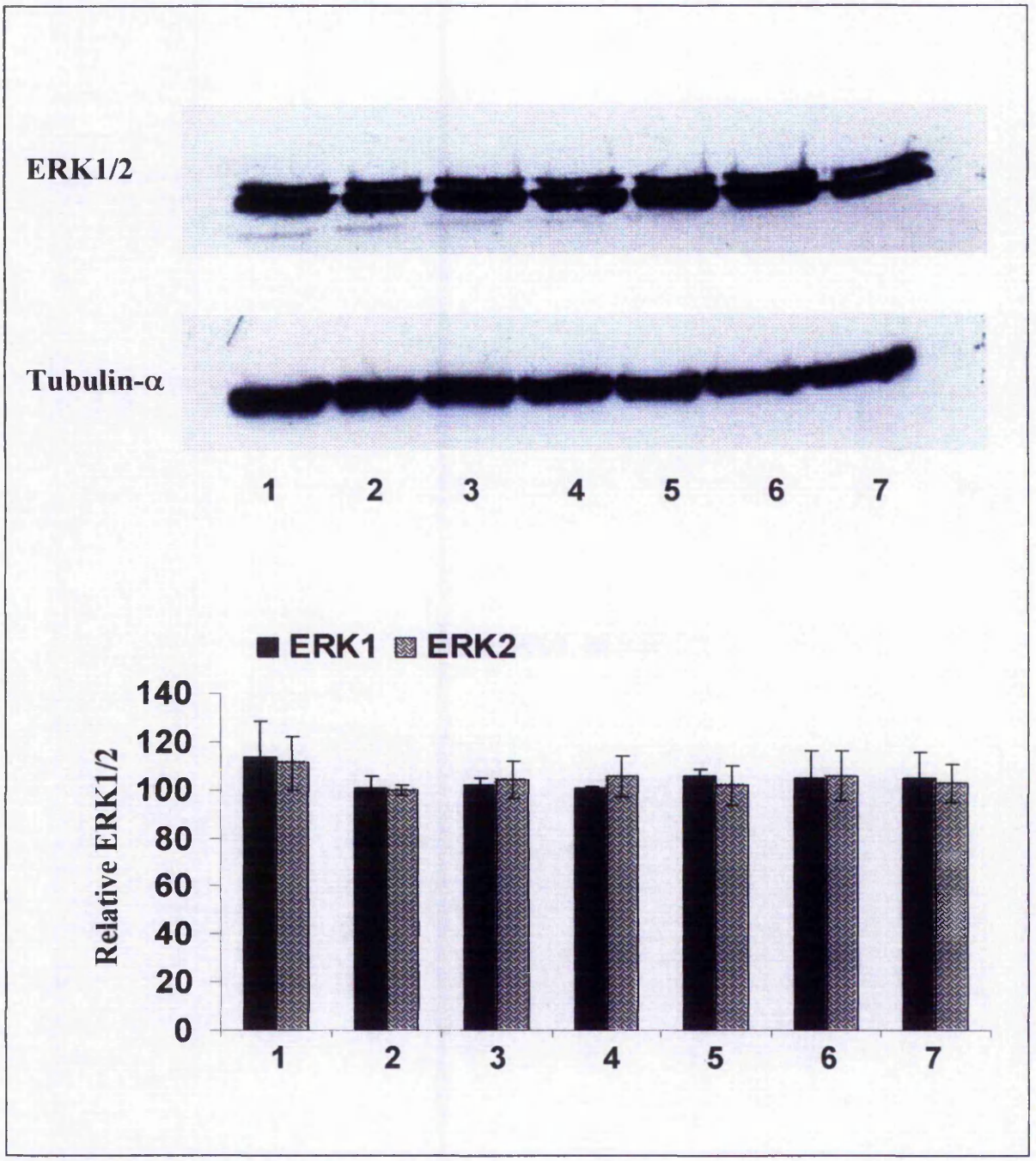


Figure 5.3.10b

Western Blots were preformed using protein extracts prepared under the same experimental conditions to explore the total ERK1/2 levels. The blot displayed in figure 5.3.10b shows that all cell samples displayed a similar banding pattern without a statistically significant difference in the levels of total ERK1/2. These results suggest that the MEK-ERK pathway is involved in FN-tTG mediated signalling during the RGD-independent cell adhesion.

5.3.7.3 The RGD-independent cell signalling is linked to JNK1/2 kinase

The effect of RGD inhibition on the activation of JNK1/2 was tested using HOB cells. The phosphorylation levels of JNK1 at threonine 183 and JNK2 at tyrosine 185 residues and the total JNK1/2 levels in HOB cell lysates were measured by Western Blotting using the procedure described above (Section 5.3.7.2). Figure 5.3.11a represents the content of phospho-JNK1/2 (pJNK1/2), while figure 5.3.11b shows the total JNK1/2 levels, in HOB cells plated on BSA, FN and FN-tTG with or without RGD peptide. The tyrosine phosphorylation of JNK1 and JNK2 in cells seeded on the FN matrix with RGD peptide was decreased to 75% and 58% respectively of that found in control cells plated on FN. The plating of cells on the FN-tTG matrix did not result in a statistically significant increase in p-JNK1/2 antigen levels when compared to control levels. The amount of phospho-JNK1/2 antigen was restored to almost 90% of the control values on FN, when cells were seeded onto FN-tTG in the presence of the RGD peptide.

Western Blots were performed in parallel to investigate the effect of RGD inhibition on the total JNK1/2 levels in the same protein extracts. As with the data presented in figure 5.3.11b, the treatment of HOB cells with RGD peptide did not result in any significant decrease in total JNK levels, when compared to control FN levels. These results suggest that FN-tTG mediated RGD-independent cell signalling is linked to JNK1/2.

Figure 5.3.11 Western Blot Analysis of levels of activated phospho JNK1/2 and levels of total JNK1/2 proteins during the RGD-independent cell adhesion of HOB cells.

a, Effect of RGD inhibition on the levels of phospho-tyrosine JNK1/2; **b,** total JNK1/2 during the adhesion of HOB cells to FN and FN-tTG matrix. The HOB cell lysates (50 μg protein/sample) of 7 samples, non-treated cells seeded on BSA (lane 1), FN (lane 2), and FN-tTG (lane 3), RAD-treated cells seeded on FN (lane 4), and FN-tTG (lane 5) and RGD-treated cells FN (lane 6), and FN-tTG (lane 7), from 3 independent experiments were prepared, Western blotted and probed with mouse monoclonal anti-phospho JNK1 (46 kDa) and JNK2 (54 kDa) (a, top blot) (6 μg/blot), or rabbit polyclonal anti-JNK1/2 antibody (b, top blot) (1:500 dilution) as described before (Sections 2.2.7-2.2.10). Equal loading was ensured by stripping and reprobing the blots with anti-α-tubulin antibody (3 μg/blot) as can be seen in the lower blots. The density of the bands was normalised against values for tubulin bands and represented as the mean net area value (relative p-JNK1/2 or relative JNK1/2) ± S.D. of three experiments. Each data point was expressed as a percentage of the control FN level, which represents 100%. The * symbol indicates the statistically different values ($p<0.05$) when compared to the FN control.

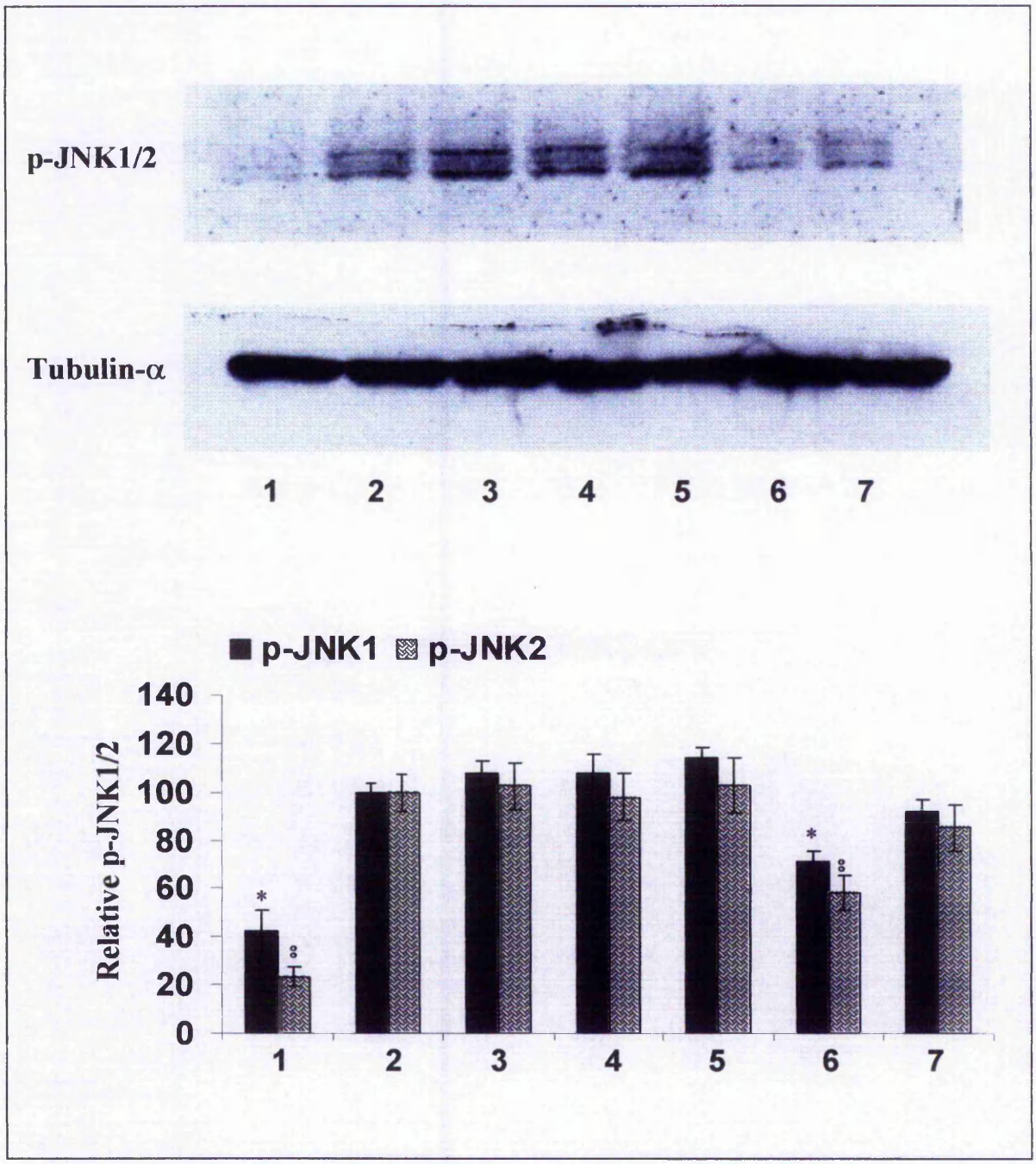


Figure 5.3.11a

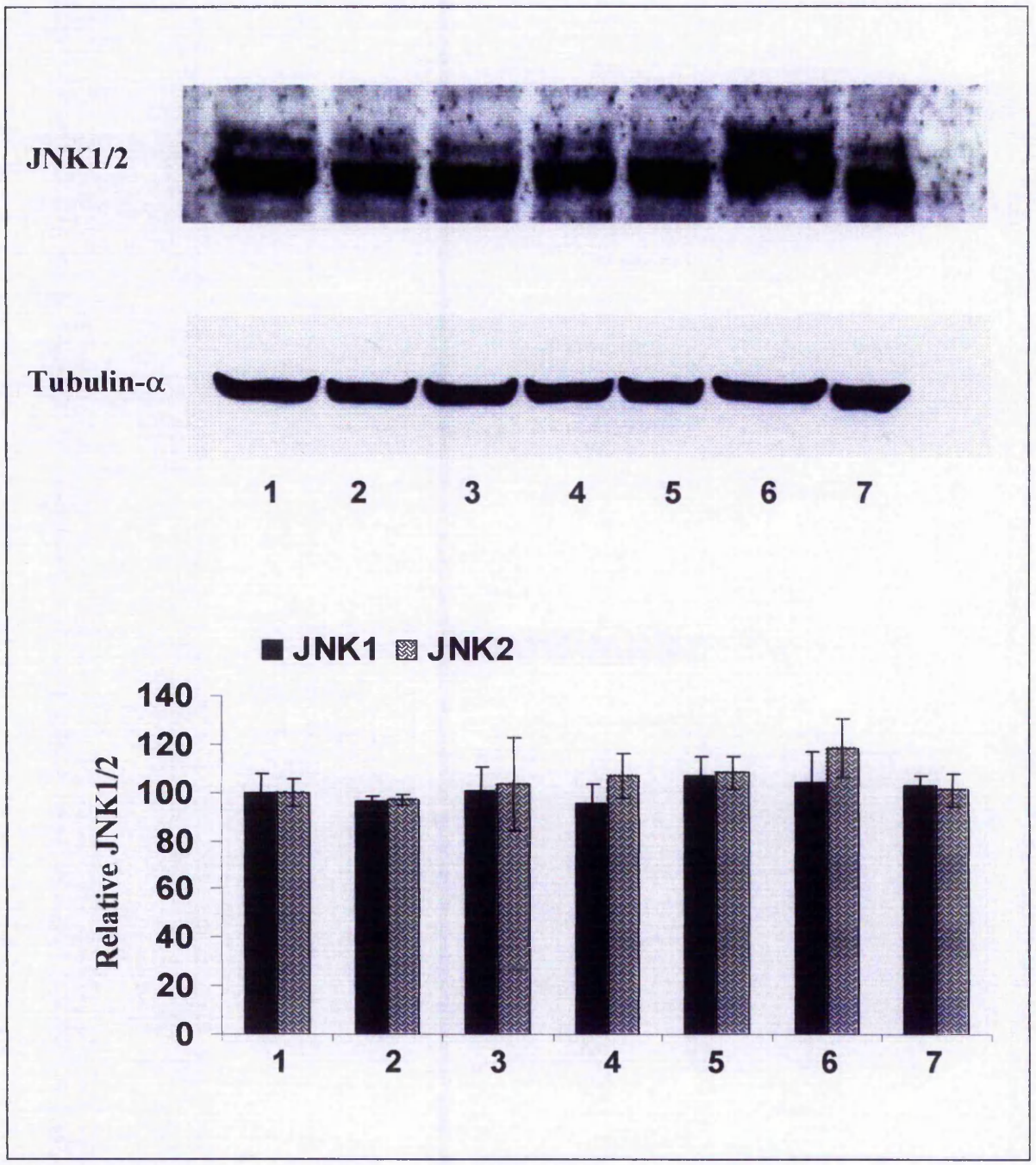


Figure 5.3.11b

5.3.8 FN-bound tTG rescues primary dermal fibroblast from anoikis

To elucidate whether the inhibition of the RGD-dependent adhesion can result in apoptosis and whether the FN-tTG complex can prevent cell death following RGD inhibition, primary MDFTg2+/+ and -/- fibroblasts were used in the cell-survival assays. Using a cell line deprived of tTG would also elucidate the importance of intracellular tTG in the FN-tTG mediated RGD-independent cell adhesion signalling. Cells were treated with the RGD peptide (150 μg/ml) and seeded on FN and FN-tTG matrices under the serum free conditions. To rule out any non-specific toxic effect of long-term incubation of cells with an exogenous hexapeptide peptide, cells were also treated with the equivalent concentration of the control RAD peptide. Following a 16 hour-incubation at 37°C in a 5%CO_2 atmosphere, the cell viability was assayed using the XTT cell proliferation assay kit as depicted previously in Section 2.2.14. Figure 5.3.12 shows a graph of cell viability as measured by the absorbance of the cleaved tetrazolium salt XTT produced by metabolically active cells. The cell viabilities of MDFTg2+/+ and -/- fibroblasts on the FN matrix were found to be comparable to each other. The treatment of cells with RAD peptide did not lead to a significant reduction in the cell survival levels. However, the treatment of MDFTg2+/+ and -/- cells on FN with RGD peptide resulted in approximately 40% decrease in cell viability, when compared to that of control cells on FN. In the presence of RGD peptide, survival of the MDFTg2+/+ and -/- cells on the FN-tTG matrix was significantly different to the cell survival on FN, as the absorbance values were almost restored to those of control levels. At the same concentrations of RGD peptide, cell survival of both cells on FN-tTG was around 90% of the non-treated control cells on FN, suggesting that tTG bound to FN confers resistance to RGD-dependent anoikis in primary dermal fibroblasts independently from its intracellular activity.

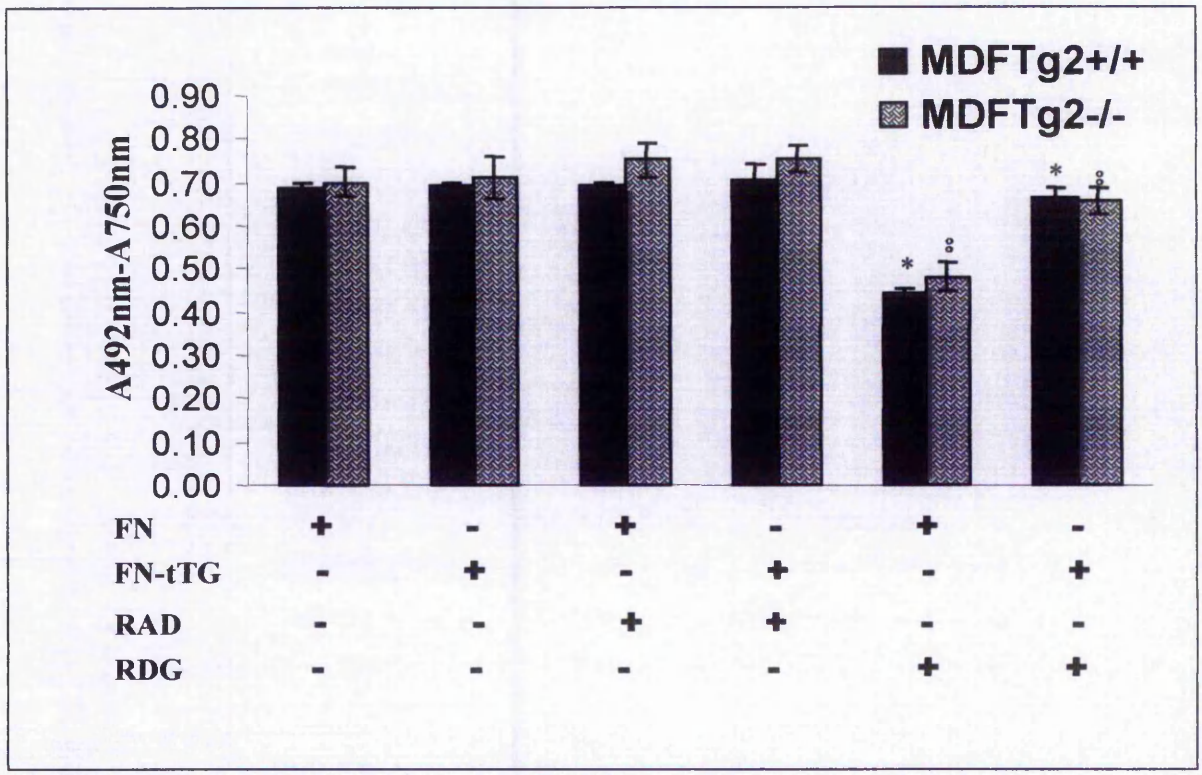


Figure 5.3.12 Effect of RGD peptide on survival of MDFTg2-/- fibroblasts

The viability of MDF Tg2 +/+ and -/- fibroblast following RGD treatment was assessed by the XTT cell proliferation assay as described in Section 2.2.14. Data represent the mean absorbance (A492nm-A750nm) ± S.D. of 8 replicates from a typical experiment repeated on 3 separate occasions. The * indicates the statistically significant differences ($p<0.05$) in absorbance values in comparison to the FN control.

5.3.8.1 Caspase-3 is activated in MDFTg2-/- cells undergoing anoikis by inhibition of RGD-independent integrin function

The activity of caspase-3 protease was investigated in MDFTg2-/- cells undergoing anoikis. Cells were cultured on FN and FN-tTG matrices with or without RGD for 16 to 18 hours and equal amounts of proteins from cell extracts were analysed for the activity of caspase-3 (70 μg protein/sample) using CaspACE^{TM} assay system as described under Methods Section 2.2.16.

In the positive control, caspase-3 activity was induced by the treatment of cells with the protein kinase inhibitor staurosporine. In the negative control, the caspase-3 activity was blocked by the incubation of staurosporine treated cells with the pan-caspase inhibitor Z-VAD-FMK. The results show that the caspase-3 activity in the negative control cell sample was 13% in comparison to values observed in positive control cell sample (figure 5.3.13). The levels of caspase-3 activation in cells grown on FN in the presence of RGD peptide was approximately 60% of that of positive control. When cells were cultured on FN-tTG with RGD peptide, however, the amount of active caspase-3 was not significantly different from cells grown on FN without RGD peptide. The level of caspase-3 activation in these cells was found to be only 28% of that of positive control, indicating that there is caspase-3 activation in cells undergoing apoptosis due to loss of RGD-dependent cell adhesion.

5.3.8.2 The inhibition of RGD-independent integrin function results in nuclear fragmentation

The effect of RGD-dependent inhibition on cell survival was further studied by examining the morphological signs of apoptosis in MDF Tg2-/- cells undergoing anoikis. Cells were cultured in the presence or absence of RGD peptide (150 μg/ml) on FN and FN-tTG matrices for 16 hour at 37°C in a 5%CO_2 atmosphere as described above. The MDFTg2-/- cells were fluorescently labelled for endonucleolysis using the TUNEL method, which utilises TdT enzyme to

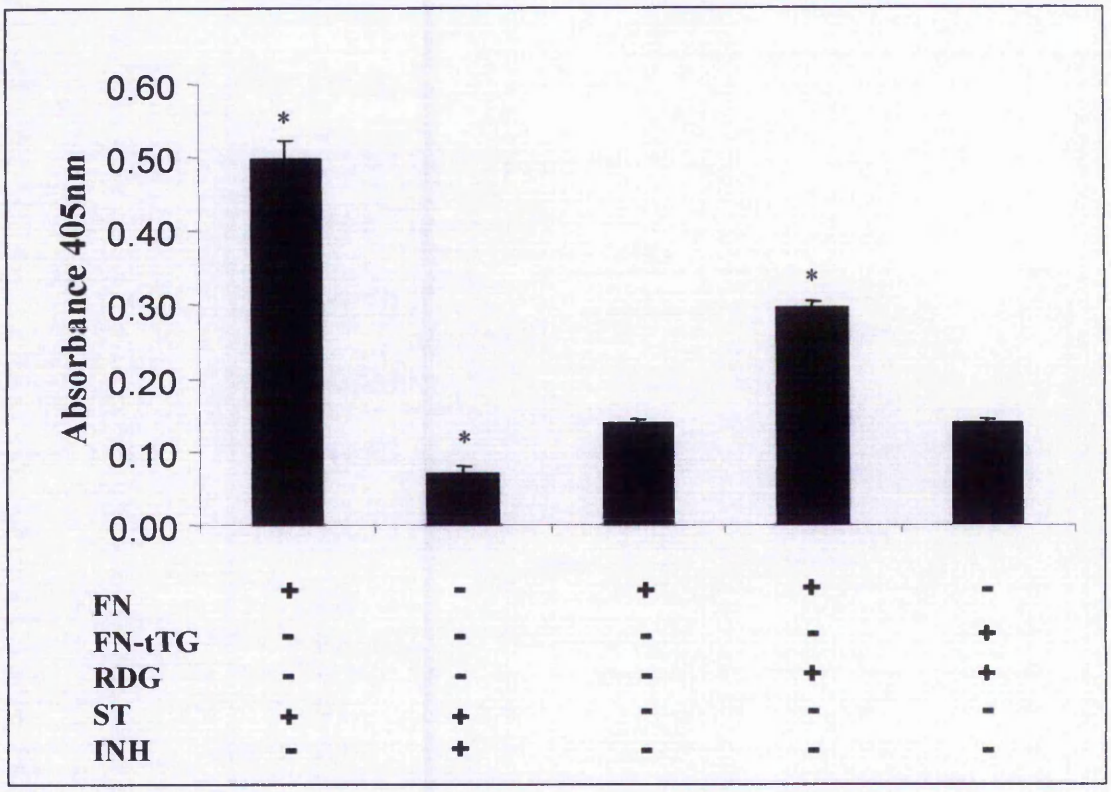


Figure 5.3.13 Analysis of Caspase-3 activity levels during RGD peptide-stimulated anoikis of MDFTg2-/- fibroblasts.

The activity of caspase-3 in MDFTg2 -/- fibroblast following RGD treatment was studied using the CaspACE™ assay, as described before (2.2.16). Data are expressed as mean ± S.D. absorbance values at 405nm and are from three separate experiments, each performed in triplicate. The background readings were subtracted from the mean values to obtain the final values. The * symbol indicates the statistically different values for caspase-3 activity ($p<0.05$) when compared to the activity obtained for the FN control.

Figure 5.3.14 Analysis of RGD peptide-induced apoptosis in MDFTg2-/- fibroblasts.

a, The flow cytometric analysis of apoptotic nuclei in MDFTg2-/- fibroblasts due to the RGD inhibition; **b,** quantification of mean number of apoptotic cells; **c,** immuno-fluorescence staining of fragmented nuclei of MDFTg2-/- fibroblasts undergoing anoikis. **a,** The nuclear fragmentation of MDFTg2-/- fibroblasts seeded on FN or FN-tTG matrices in the presence and absence of RGD peptide was determined by flow cytometry as explained under Method Section 2.2.15. The bar corresponds to positive region of fragmented nuclei (% apoptotic nuclei), set by the negative standart (n.s) of cells. Md, stands for median fluorescent channel. **b,** The MDFTg2-/- fibroblasts in suspension were processed for in-situ detection of DNA fragmentation as described before (Section 2.2.15). **c,** Data are expressed as the mean number of apoptotic cells ± S.D. from a typical experiment undertaken in triplicate. Total cells analysed for 15-hour incubation was around 450, while approximately 400 cells were quantified for the 30-hour incubation.

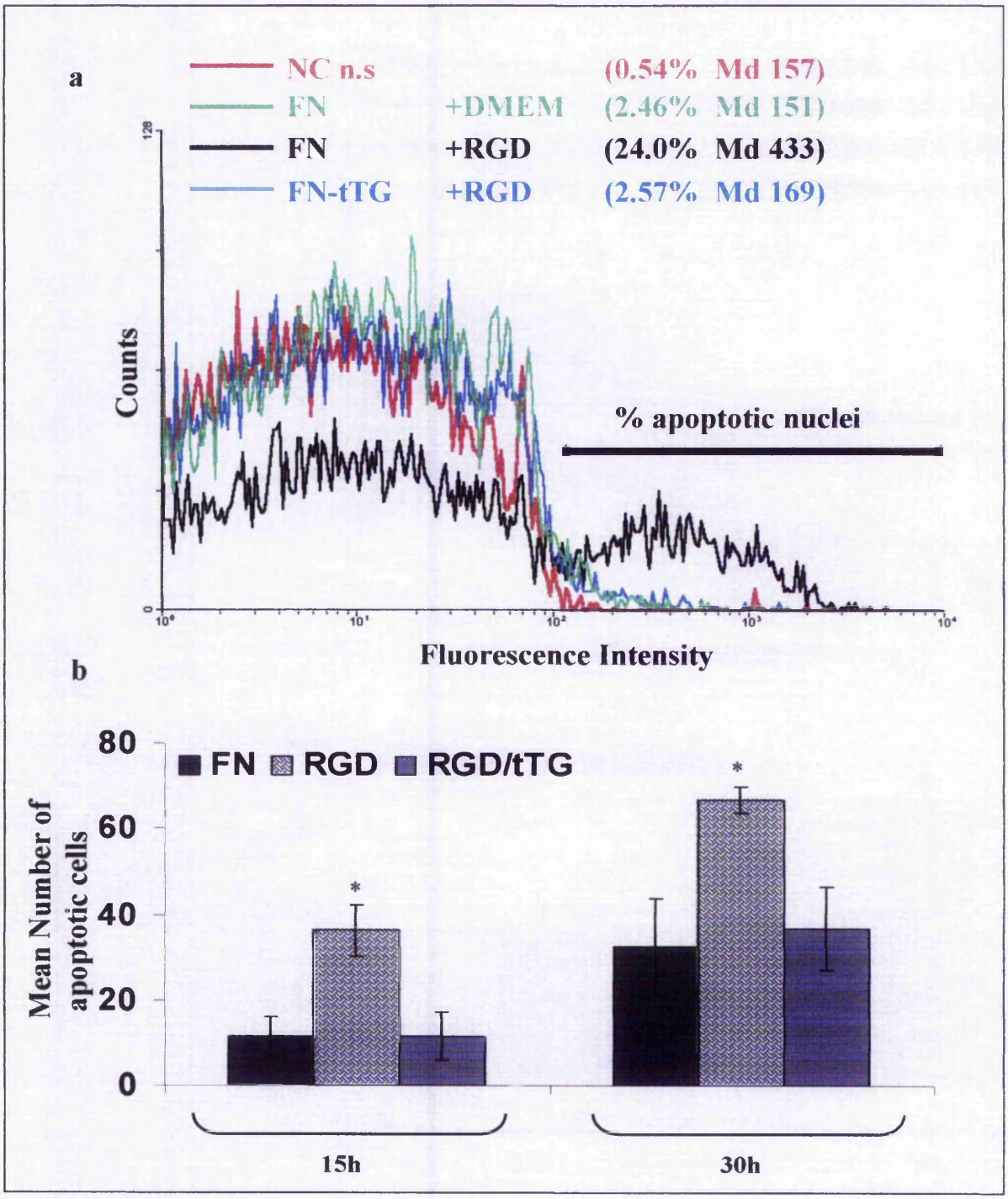


Figure 5.3.14 a and b

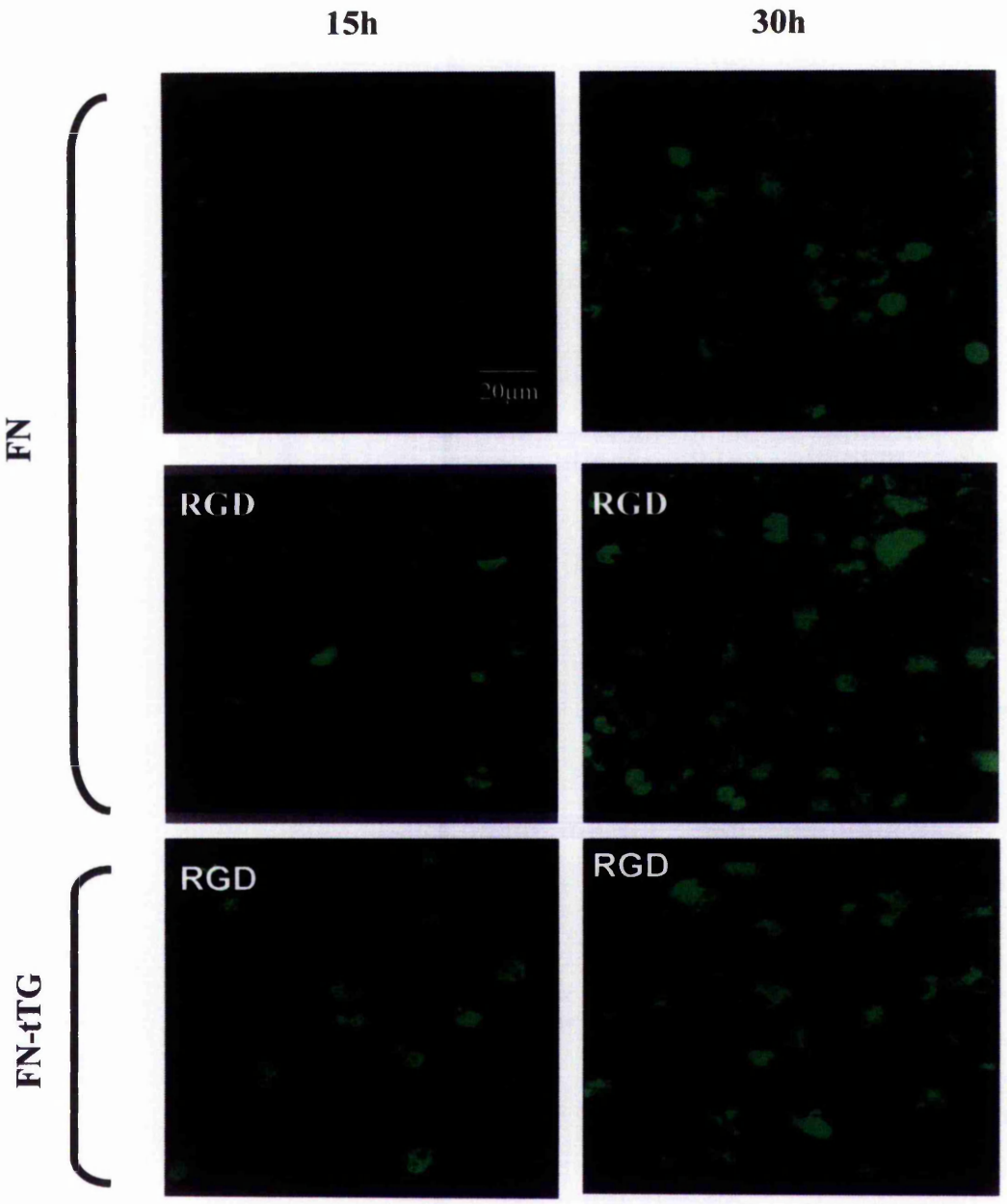


Figure 5.3.14c

incorporate FITC-dUTP into DNA strand breaks. The extend of labelling of apoptotic nuclei was quantified with flow cytometry as described before (Section 2.2.15) (figure 5.3.14a). The background fluorescence intensity was determined using cells undergoing anoikis and incubated with FITC-dUTP in the absence of enzyme TdT (red histogram). The cells grown overnight on FN under serum free conditions (blue histogram) demonstrated only 2.6% apoptotic nuclei, however, 24% of the fibroblasts cultured on FN in the presence of RGD peptide were found to be positive for endonucleolysis. This effect of RGD peptide was not detected in fibroblasts grown on FN-tTG with RGD peptide, as the levels of apoptotic nuclei in these cells were shown to be approximately 2.6%.

To further confirm this finding, the level of apoptosis was examined in the non-attached MDFTg2-/- fibroblasts cultured on FN and FN-tTG matrices with or without RGD peptide. The DNA strand breaks were labelled using the TUNEL staining and was visualised and quantified by confocal microscopy as mentioned before under Methods Section 2.2.15. Figure 5.3.14b shows a graph of mean number of apoptotic cells constructed by the quantification of the immunostained apoptotic cells seen in the figure images (figure 5.3.14c). After 15 hours, 36% of the RGD treated fibroblasts seeded on FN were found to be apoptotic. In contrast, the percentage of apoptotic cells grown on the FN-TG matrix in the presence of RGD peptide was less than 10%. After 30-hour incubation of cells, nuclear fragmentation was not only evident in fibroblast cells grown on FN in the presence RGD peptide but also in the control fibroblasts grown on FN without RGD peptide due to serum starvation. However, the difference in the level of apoptosis was still statistically significant, as RGD-treated cells cultured on FN-tTG displayed 30% less apoptotic cells than their counterparts seeded on FN. These results suggest that tTG when bound to FN acts as a cell survival molecule in RGD-treated cells undergoing anoikis.

5.4 Discusssion

Specific association of integrins with FN implicated the RGD/synergy domain as the main cell binding domain, which is recognised mostly by the $\alpha_5\beta_1$ integrins. The $\alpha_5\beta_1$ integrins take part in many cellular processes involving FN, such as cell adhesion, spreading, and migration on FN substrata, and the assembly of the FN matrix (Miyamoto *et.al.*, 1998). However, embryonic mouse fibroblasts null for α_5 were shown to be able to assemble the FN matrix, form focal contacts, and migrate in response to FN, suggesting another integrin or a disintegrin receptor may also be involved in these cellular responses to FN (Yang *et.al.*, 1993). The findings in the previous chapter favoured a similar hypothesis in that some other cell surface receptor was able to restore the inhibition of $\alpha_5\beta_1$ integrin function with RGD peptide when cells were seeded on the FN-tTG matrix. One candidate for mediating cell-FN-tTG matrix interaction in the presence of RGD peptide is $\alpha_4\beta_1$ integrin, a versatile cell adhesion receptor involved in both cell-cell and cell-ECM interactions. The two most effective ligands for $\alpha_4\beta_1$ integrin are the vascular cell adhesion molecule-1 (VCAM-1), and FN (Sharma *et.al.*, 1999), although recently the matrix glycoprotein thrombospondin-1 has also been identified as a ligand for this integrin (Decker *et.al.*, 2002). The $\alpha_4\beta_1$ integrin is mainly expressed on leukocytes, and lymphocytes, but also found in smooth muscle, neuronal crest-derived cells and fibroblasts, where it supports cell adhesion, spreading and migration on FN substrata (Chan *et.al.*, 1992; Petruzzelli *et.al*, 1999). It appears that the CS-I site located in the alternatively spliced IIICS or V region of FN is the main binding sequence recognised by $\alpha_4\beta_1$ integrins (Wayner *et.al.*, 1989; Garcia-Pardo *et.al.*, 1990), while the RGD sequence in the cell binding domain (Mould *et.al.*, 1991; Sanchez-Aparicio *et.al.*, 1994) and a cryptic site in repeat III_5 (Moyano *et.al.*, 1997) can also support cell adhesion less effectively, upon activation $\alpha_4\beta_1$.

In order to investigate the possibility that cell adhesion to FN-tTG may be mediated by $\alpha_4\beta_1$ integrin, cell adhesion assays were conducted using Swiss 3T3 cells since these cells, unlike HOB cells, are known to express $\alpha_4\beta_1$ integrin on their cell surface (Stephens *et.al.*, 2000; Gronthos *et.al.*, 1997). Previous studies have shown

that cell adhesion and spreading on FN was inhibited by anti-α_4 antibodies and the soluble CS-1 fragment (Garcia-Pardo *et.al.*, 1990; Guan and Hynes 1990). However, results in this chapter have shown that the treatment of Swiss 3T3 fibroblasts with the function blocking anti-α_4 antibody and the CS-1 peptide fail to inhibit cell adhesion to FN, implying the $\alpha_5\beta_1$ integrins as the main FN-receptor in this cell line. The inhibition of $\alpha_4\beta_1$ activity did not have any effect on the RGD-independent cell adhesion mediated by FN-tTG complex, indicating that the activation of $\alpha_4\beta_1$ is not needed for this process.

Given that cell attachment and spreading on FN depends on adhesion mediated signals involving both integrins and cell-surface heparan sulphate receptors (Tumova *et.al.*, 2000), it is possible that cell adhesion to the FN-tTG matrix might be mediated by a heparan sulphate proteoglycan (HSPG). To test this hypothesis, sulphated heparin and chondroitin chains on the cell surface of HOB cells were digested using heparitinase and protease-free chondroitinase ABC, respectively. Treatment of HOB cells with heparitinase led to a reduction in cell attachment to FN, confirming the importance of cell-membrane HSPGs in the adhesion of osteoblast-like cells (Dalton *et.al.*, 1995). This treatment also resulted in a complete abolishment of the RGD-independent cell attachment and spreading on FN-tTG. In contrast, the degradation of chondroitin sulphate chains neither had an effect on cell attachment and spreading on FN nor altered the RGD-independent cell adhesion on FN-tTG. This result suggests the involvement of a cell-surface HSPG, but not a chondroitin sulphate proteoglycan (CSPG), in the RGD-independent cell adhesion mediated by FN-tTG complex.

If FN-tTG complex supports the RGD-independent cell adhesion via a HSPG receptor, then it was desirable to identify this receptor. Both syndecan and glypican proteoglycans carry heparin sulphate chains, and can be considered as the candidate receptors. However, glypicans are widely expressed in the central nervous system and well-documented for their function in embryonic development. Although glypicans can bind to interstitial collagens and fibronectin, their role in cell-matrix interactions are yet to be clarified (Tumova *et.al.*, 2000). Syndecans, on the contrary, are shown to take part in cell-matrix interactions, in modification of cytoskeletal organisation and the adhesive phenotype, thus might act as a strong

candidate HSPG receptor. One syndecan receptor expressed ubiquitinously and associated with focal adhesions, is the syndecan-4 receptor. Previous studies have shown that the syndecan-4 downstream signalling specifically involves the activation and translocation of PKCα to the plasma membrane (Baciu and Goetinck, 1995; Oh *et.al.*, 1997a, b). Therefore, it was of interest to assess the importance of PKCα activity in the RGD-independent cell adhesion using a selective PKCα inhibitor, Go6976. Results from cell adhesion assays showed that the treatment of HOB cells with Go6976 led to a decrease in cell attachment and spreading on FN matrix, which was comparable with the inhibition of adhesion following heparitinase treatment. The PKCα inhibitor reduced the RGD-independent cell attachment and spreading in response to FN-tTG, indicating that the PKCα is necessary for FN-tTG to restore cell adhesion in the presence of RGD peptide. The RGD-independent cell adhesion was affected in a similar way by the heparitinase and the PKCα inhibitor; this might suggest syndecan-4 as the likely HSPG recognised by the FN-tTG complex.

Further experiments were undertaken to determine the effect of FN and FN-tTG matrix on the translocation of PKCα to the cell membrane. In agreement with previous findings, the PKCα activator PMA induced an increase in PKCα translocation to membrane, while Go6986 inhibitor led to a substantial decrease in the membrane PKCα levels (Oh *et.al.*, 1997b; Haller *et.al.*, 1998; Cheng *et.al.*, 2001). The comparison between the two cellular compartments of cells seeded on FN and FN-tTG in the presence of RGD suggests a FN-tTG induced translocation of PKCα from cytosol to membrane. These data are consistent with the previous report showing that the translocation of PKCα to membranes was abolished when vascular smooth muscle cells was incubated with RGD peptides (Haller *et.al.*, 1998). The treatment with Go6976 inhibitor, down-regulated the PKCα translocation to membranes in cells seeded on FN-tTG following RGD incubation. This result suggests that PKCα inhibition abolished the FN-tTG mediated RGD-independent cell adhesion by inhibiting the translocation of PKCα from the cytosolic compartment to the membrane.

Having established that FN-tTG does not exert a merely cell adhesive function, bypassing the RGD inhibition, but potentiates signals leading to activation and translocation of PKCα, it was decided to examine the tyrosine phosphorylation levels of kinases that are involved in the anchorage-dependent signalling cascades. Initial experiments investigated the levels of tyrosine phosphorylated proteins in HOB cells seeded on FN and FN-tTG matrices with or without RGD peptide. Data clearly showed that the decrease in phospho-tyrosine levels observed in RGD-treated cells seeded on FN was nearly restored to normal levels when the very same cells were seeded on FN-tTG, suggesting that the RGD-independent cell adhesion induces the tyrosine phosphorylation of proteins.

Among the events that occur during either "outside-in" signalling through FN receptors is the phosphorylation of FAK at tyrosine 397 residue (Giancotti and Ruoslahti, 1999). Recently, Shi and Boettiger (2003) have shown that the level of phosphorylation of FAK Y397 is a direct consequence of the number of $\alpha_5\beta_1$-FN bonds. The data reported here shows that the attachment of HOB cells to FN and FN-tTG matrices induced tyrosine phosphorylation of FAK in comparison to cells in suspension. As expected, the disengagement of integrins from the FN matrix with RGD peptide resulted in a decrease in the phosphorylation of FAK, but not in total FAK levels, suggesting that the observed decrease in the phospho-FAK levels is not due to a cleavage of FAK by phosphatases. However, in response to FN-tTG the level of FAK phosphorylation in the presence of RGD was found to be comparable to that of the FN control. This data suggests that the rescue of cell adhesion by FN-bound tTG following the blocking of integrins via the RGD peptide enhances tyrosine phosphorylation of FAK and therefore implies FAK as being one of the intracellular signalling mediators of FN-tTG. Consistent with this result, Lyman *et al.* (1997) found that the activation of FAK can occur despite the inhibition of integrin association, suggesting another possible receptor responsible for FAK activation.

FAK is activated when integrins are ligated, but syndecan-4 receptor also appears to play some role (Jeong *et.al.*, 2001). Several reports have suggested a role for PKCα in FAK activation (Tang *et.al.*, 1995; Lewis *et.al.*, 1996; Tsuchida *et.al.*, 2000). To test the hypothesis that FAK is activated through PKCα, FAK

phosphorylation levels were measured in Go6976 treated cells seeded on FN and FN-tTG matrices in the presence and absence of RGD. When compared to that of control cells seeded on FN, the levels of FAK activation appeared to stay the same in cells treated with PKCα activator PMA. Furthermore the Go6976 inhibitor led to only a minor decrease in the phosphorylation of FAK compared to that of control FN. Taken together, these results suggest that FAK is not a downstream effector of PKCα, and the decrease in the phospho-FAK levels seen in Go6976 treated cells is possibly due to the inhibition of cell adhesion by the inhibitor.

Recent evidence supports a link between cell survival and FAK activation/tyrosine auto-phosphorylation at Y397 (Chen *et.al.* 1996), which implies that signalling might be conveyed from FAK to downstream effector kinases. One candidate is the Raf-1 kinase, since accumulating evidence indicates a potential cell survival role for Raf-1, which appears to be separate from its kinase activity (Huser *et.al.*, 2001). Using fibroblasts null and wild-type for Raf-1 kinase, cell adhesion assays were performed to determine the role of Raf-1 in RGD-independent cell adhesion in response to FN-tTG. Unlike Raf-1 +/+ cells, Raf-1 -/- cells did not exhibit an RGD-independent cell adhesion to the FN-tTG matrix in the presence of RGD peptide, suggesting that the rescue of cell adhesion by FN-tTG following the RGD inhibition depends on the Raf-1 function.

The Raf protein kinases are well-known for their role as the upstream regulators of the ERK kinase signalling cascade (Kolch, 2000). Previous studies have reported that Raf-1 kinase can directly phosphorylate and activate the protein kinase MEK, which in turn phosphorylates and activates ERK1 and ERK2 at tyrosine 204 site (Payne *et.al.*, 1991; Howe and Juliano, 1998). In this study, the Western Blot analysis of phospho-ERK1/2 levels demonstrated that the inhibition of cell adhesion in HOB cells by RGD peptides leads to a reduction in the tyrosine phosphorylation levels of ERK1/2. This reduction is not due to the proteolytic cleavage of non-phosphorylated ERK1/2 as no change in the basal levels of ERK1/2 was detected. The cells seeded on FN-tTG with RGD, however, showed comparable tyrosine phosphorylation of ERK1/2 to control cells. This gives support to the statement that RGD-independent cell adhesion mediated by FN-tTG signals through ERK1 and 2.

Initial reports suggested pro-apoptotic roles for JNK in stress-related induction of apoptosis (Hibi *et.al.*, 1993; Xia *et.al.*, 1995; Tournier *et.al.*, 2000). Frisch *et al.* (1997) showed that the detachment of epithelial cells from matrix induces the activation of JNK kinase, which is critical for execution of anoikis. In contrast to previous reports, new evidence suggested an anti-apoptotic role for JNK in some cell types (Smith *et.al.*, 1997; Potapova *et.al.*, 1997; Almeida *et.al*, 2000). Hence, the difference between the current findings and the previous studies might be due to the different regulation of JNK in the different cell types. In order to elucidate the role of JNK kinase in RGD-independent cell adhesion of HOB cells to FN-tTG, the levels of phosphorylation of JNK1 at threonine 183 and JNK-2 at tyrosine 185 residues was investigated. In agreement with Almeida *et al.* (2000), the level of JNK activity in attached HOB cells was considerably higher than that of detached cells. No detectable change in the total JNK1/2 levels points out that the decrease in phospho-JNK1/2 was not due to the activity of proteases. The RGD-inhibition of JNK1/2 activity was reversed in cells seeded on FN-tTG. The obtained results suggested that JNK1/2 might be involved in the downstream signalling that is transmitted by FN-tTG during RGD-independent cell signalling.

The activation of key kinases of the cell survival pathway during the RGD-independent cell adhesion hints at a potential role for the FN-tTG complex as a cell survival matrix protein. Using primary mouse dermal fibroblasts null and wild type for tTG, the effect of long term RGD-inhibition of integrins on FN and FN-tTG matrix was examined. Previously work from Hadden and Henke (2000) showed that the incubation of lung fibroblasts with soluble fibronectin peptides makes these cells susceptible to anoikis. In the same way, by blocking cell adhesion with RGD peptide, cell survival was decreased below control levels both in MFDTg2 +/+ and -/- seeded on the FN matrix, but not on FN-tTG (figure 5.3.11). This result suggested that intracellular tTG might not be essential in the FN-tTG mediated RGD-independent cell adhesion signalling, although previous studies proposed a survival role for intracellular tTG under conditions of retinoic acid induced cell differentiation and apoptosis (Antonyak *et.al.*, 2001 and 2002). To determine the activation of apoptotic machinery, it was decided to investigate the activity of caspase-3 during the inhibition of integrin function in MDFTg2-/- cells seeded on

FN and FN-tTG matrices. Caspase-3 is one of the last caspases to be activated in the caspase cascade and leads to irreversible phase of apoptosis where chromatin condensation and DNA fragmentation occurs (Frisch and Screaton, 2001). Comparison of caspase-3 activation levels among control cells seeded on FN and RGD-treated cells seeded on FN and FN-tTG indicated that caspase-3 was activated in cells on FN with RGD; however, cells on FN-tTG with RGD peptide did not show a significant increase in caspase-3 activity. It is therefore possible that FN-tTG inhibits RGD-mediated apoptosis via caspases. Nuclear fragmentation, another diagnostic feature of apoptosis, was also investigated in cells seeded on FN and FN-tTG with or without RGD. Results from the TUNEL analysis showed that the blocking of integrins by RGD peptide led to an increase in apoptotic nuclei levels when compared to the FN control. In contrast, the level of total apoptotic cell death in cells on FN-tTG was not substantially altered by the incubation of RGD peptide. These results once again indicate that adhesion of cells to the FN-tTG complex plays a major role in RGD-independent cell survival.

Chapter 6: Discussion

Chapter 6: Discussion

The extracellular matrix to which cells adhere is a complex mixture of structural and functional proteins secreted by the cells themselves, which is insolubilised in the extracellular space by unique macromolecular interactions and/or cross-linking. The ECM provides a mechanical framework that supports attachment sites for cell surface receptors and a reservoir for signalling factors that regulate diverse physiological processes including angiogenesis, cell migration, cell proliferation, inflammation, immune responsiveness and wound healing. Adhesive proteins such as fibronectin, laminin, vitronectin, and collagen are associated with this solid matrix phase and recognised as an important regulator of anchorage-dependent apoptosis. It appears that the subtle changes in ECM composition and tissue architecture are critical for the suppression of the apoptotic machinery (Grossmann, 2002; Badylak, 2002). Fibronectin is one of the main components of the ECM, and known to greatly affect both cell signalling and proliferation (Sechler *et.al.,* 1998; Hocking *et.al.,* 2000). It is therefore possible that the modulation of FN may provide important signals in the regulation of adhesion-related apoptosis. In this respect, the aim of this thesis was to elucidate the importance of tTG, a high affinity binding protein to FN and modulator of FN matrix activity, on FN-mediated cell survival. The results presented here show for the first time that matrix FN when bound to tTG can mediate a novel RGD-independent cell adhesion process, which promotes the survival of anchorage-dependent cells when the RGD-dependent integrin function is lost.

A number of reports have analysed the function of tTG using cells stably transfected with tTG cDNA in sense or anti-sense orientation (Gentile *et.al.,* 1992; Melino *et.al.,* 1994; Mian *et.al.,* 1995; Jones *et.al.,* 1997; Verderio *et.al.,* 1998; Stephens *et.al.,* 2004). Other studies have used agents that increase the expression of tTG in cells, such as retinoic acid (Moore *et.al.,* 1984; Davies *et.al.,* 1985; Chen *et.al.,* 2001) that may cause increases in the expression of other genes leading to unspecific biological responses. Unlike other investigations, this study utilises a tTG-rich FN matrix model mimicking the *in vivo* physiological and pathological conditions, to characterise the role played by tTG in the ECM. In support of this model, previous data have shown that when tTG is externalised to the cell surface it

accumulates and associates with FN in the pericellular matrix (Gaudry *et.al.*, 1999a). The enzyme is deposited to ECM both under normal physiological conditions (Verderio *et.al.*, 1998) and in response to cellular damage, inflammation or cell stress (Haroon *et.al.*, 1999; Johnson *et.al.*, 1999; Upchurch *et.al.*, 1991). The secretion of tTG from cells has shown to be accompanied by enhanced cell attachment to FN (Upchurch *et.al.*, 1991; Gentile *et.al.*, 1991) either through cross-linking of FN (Jones *et.al.*, 1997; Verderio *et.al.*, 1998) or via cross-linking independent specific association of tTG with the FN matrix. In the latter case, tTG was proposed to act as a novel cell adhesion protein or cell-surface co-receptor for FN (Isobe *et.al.*, 1999; Akimov *et.al.*, 2000; Balklava *et.al.*, 2002). Given the high affinity association of tTG with FN (Turner and Lorand, 1989; LeMosy *et.al.*, 1992), and its involvement in cell adhesion, it is likely that upon binding, tTG and FN may alter each others function and form a matrix complex with distinctive adhesive roles, which may be essential to provide adhesion-mediated cell survival in response to the loss of cell adhesion in situations of cell wounding or cell stress.

Initial studies examined the role of the FN-tTG matrix in cell-matrix interactions by inhibiting the "classical RGD-dependent adhesion pathway" using a human osteoblast-like cell line (HOB) and Swiss 3T3 fibroblasts (Verderio *et.al.*, 2000). By using RGD containing synthetic peptides or integrin function blocking antibodies directed towards the synergy site on the α_5 subunit and RGD-interacting site on the β_1 subunit on HOB and Swiss 3T3 fibroblasts, it was shown that loss of cell-matrix interaction, due to inhibition of interaction of the $FNIII_{10}$ RGD-cell binding site with $\alpha_5\beta_1$ integrins, can be restored if these cells were seeded on a FN-tTG matrix. Further examinations have shown that the RGD-independent cell adhesion of HOB and Swiss 3T3 fibroblasts to the FN-tTG matrix does not necessarily rely on the endogenously secreted ECM proteins. Cells from different origin were used to study whether the FN-tTG matrix can re-establish cell adhesion lost due to the inhibition of RGD-dependent integrin function by using the RGD synthetic peptide. Restoration of cell adhesion on the FN-tTG matrix following blocking of the RGD-dependent pathway was shown to occur in ECV304 cells, human dermal fibroblasts, and mouse dermal fibroblast wild type (MDFTg2+/+)

and knockout for tTG (MDFTg2-/-), suggesting that tTG when bound to FN supports an RGD-independent cell adhesion process in multiple cell types.

The establishment of a Swiss 3T3 cell line overexpressing tTG under the control of a tetracycline-controlled regulatory plasmid provided the possibility of creating a physiological matrix consisting of cell-assembled FN and cell-secreted tTG (Verderio *et.al.*, 1998). tTG-transfected Swiss 3T3 fibroblasts were shown to lay down fibrillar FN, which was associated with tTG at their cell surface (Verderio *et.al.*, 1998; Gaudry *et.al.*, 1999a; Balklava *et.al.*, 2002). In keeping with these findings, it was demonstrated that fibroblasts overexpressing tTG deposited an ECM more abundant in tTG than their non-transfected counterparts. Non-transfected Swiss 3T3 fibroblasts attached better on the physiological matrix assembled by cells overexpressing tTG than the physiological matrix assembled by cells expressing basal levels of tTG, regardless of RGD treatment.

Once released from cells, tTG forms a tight complex with FN as shown by immunofluorescence and immunogold microscopy (Gaudry *et.al.*, 1999a; Verderio *et.al.*, 1998 and 1999). There is evidence indicating a role for tTG in extracellular stabilisation of FN either through its cross-linking function (Jones *et.al.*, 1997; Verderio *et.al.*, 1998) or its cross-linking independent specific association with FN (Akimov *et.al.*, 2000; Balklava *et.al.*, 2002; Verderio *et.al.*, 2003). The results presented here provide convincing data to indicate that cell adhesion to FN-tTG is independent from the intrinsic tTG ability to covalently modify the FN matrix by calcium-dependent transamidation. Experiments have shown that neither purified guinea pig liver tTG immobilised on FN nor the cell-secreted tTG deposited in fibroblast-ECM is catalytically active unless pre-activated with a reducing agent (Jones *et.al.*, 1997; Weiss *et.al.*, 1998). In fact, LeMosy *et al.* (1992) reported that tTG sequestration by FN results in the down regulation of cross-linking activity on large-size protein substrates. In contrast, incubation of cells with fluorescently labelled tTG substrates indicated that tTG is catalytically active when present at the cell surface (Verderio *et.al.*, 1998; Nicholas *et.al.*, 2003). However, this cross-linking activity does not seem to be essential for either cell attachment and/or migration (Akimov *et.al.*, 2000 and 2001; Isobe *et.al.*, 1999; Balklava *et.al.*, 2002; Stephens *et.al.*, 2004). It is therefore plausible that tTG is catalytically active at the

cell surface when first secreted due to the high Ca^{+2}/GTP ratio, but once it is released and sequestered by FN it loses its transamidating activity in the oxidising extracellular environment and then functions as a novel cell adhesion protein bound to FN.

In confirmation of this is the finding that inhibition of the cross-linking activity of FN-bound tTG in cell adhesion assays does not affect the RGD-independent cell adhesion process. On the other hand, the recent work showing that the incubation of the FN-tTG complex with GTP-γS abolishes the RGD-independent cell adhesion suggests that the Ca^{+2}-mediated tertiary structure of tTG is essential for this process. The exposure of cryptic cell adhesion sites within the tTG molecule might occur when enzyme takes on the Ca^{+2}-induced open conformation (Verderio *et.al.*, 2000).

If the restoration of cell attachment and spreading presented on the FN-tTG matrix is due to the interaction of TCP-bound tTG with the cell surface, then the coating of TCP with tTG alone should in theory produce the same effect. A previous study has suggested that a tTG-coated plastic surface enhanced adhesion of human lymphocyte-like leukaemia cells in a tTG concentration-dependent manner (Isobe *et.al.*, 1999). However, the simple binding of tTG to the plastic did not support RGD-dependent or independent cell adhesion of HOB cells even at high tTG concentrations. Similarly, the blocking of FN matrix with non-fat milk protein prior to tTG immobilisation did not lead to any inhibition of the RGD-independent compensation of cell adhesion on the FN-tTG matrix. Another intriguing result found in the cell adhesion studies was the effect of tTG when bound to N-terminal FN fragments, containing the putative tTG binding site, on the adhesion of HOB cells. Past studies assigned the putative tTG binding site on FN to the N-terminal FN peptide containing either the gelatin binding domain or type I_{3-5} repeats (Turner and Lorand, 1989; LeMosy *et.al.*, 1992; Radek *et.al.*, 1993). No cell adhesion was seen on plastic coated with 45kDa and 30kDa N-terminal FN fragments regardless of the presence of tTG, in contrast to that previously reported (Akimov *et.al.*, 2000). It was also demonstrated that the immobilisation of tTG to the 70kDa FN N-terminal, which can support cell adhesion and which contains the putative tTG binding site, was not sufficient to re-establish the RGD-dependent loss of cell-

matrix interaction, suggesting the requirement for the full-length FN molecule. As the blocking of tTG bound to FN by the tTG specific antibody Cub7402 greatly reduces the RGD-independent cell adhesion, this suggests the requirement of a direct interaction of tTG with the cell surface. The mechanism of cell adhesion therefore appears to be both tTG and FN dependent and likely to result from reciprocal modulation of the two proteins. Upon binding, tTG might modify FN by virtue of an intrinsic protein disulphide isomerise activity (PDI), which has been recently ascribed to it (Hasegawa *et.al.,* 2003). However, it should be noted that the PDI activity of tTG is not inhibited by nucleotides including GTP, while the function of FN-tTG is (Verderio *et.al.,* 2000), thus PDI-mediated FN modification seems unlikely to occur in the FN-tTG matrix complex.

The readily apparent differences between the cytoskeletal structures of attached versus suspended cells suggest that the ECM can modulate the organisation of the cytoskeleton and cell function (Katz *et.al.,* 2000). It has been shown that the FN-tTG matrix can stimulate the formation of some focal adhesion complexes in the presence of either RGD synthetic peptides or function blocking antibodies raised against the cell binding sequences on the α_5 and β_1 integrin subunits (Verderio *et.al.,* 2000). Although the formed actin stress fibers appeared to be less complex than normal, they were sufficient to support the formation of distinct RGD-independent focal contacts. It is possible that the formation of these unique focal contacts might be due to either enhanced presentation of the ECM to integrin receptors involving domains other than the synergy and the RGD-cell binding domain, or the interaction of the FN-tTG complex with other cell-surface receptor proteins. The first hypothesis appears to be less likely as the FN-tTG mediated focal adhesions were still established in the presence of function blocking antibodies which are known to cause conformational inactivation of the target integrins, hence disabling the receptor from inducing "outside-in" signalling (Humphries, 2000). In this case, the restoration of cell adhesion and focal contacts in the RGD-independent pathway should be a consequence of direct interaction of FN-tTG complex with a cell surface receptor.

Recent findings have shown that the adhesion of lymphocyte-like cells to tTG is mediated by $\alpha_4\beta_1$ integrins (Isobe *et.al.,* 1999), raising the likelihood that the FN-

tTG might also interact with this cell surface receptor. However, it was lately reported that matrix binding to the $\alpha_4\beta_1$ integrin does not mediate the reorganisation of the actin cytoskeleton, (Sechler *et.al.*, 2000), therefore if the $\alpha_4\beta_1$ integrin was the receptor concerned in the interaction with the FN-tTG complex during RGD-independent cell adhesion, there should not be any formation of actin stress fibers during this process. In support of the notion that FN-tTG does not mediate cell adhesion through the $\alpha_4\beta_1$-induced RGD-independent pathway, the data here showed that the adhesion of Swiss 3T3 fibroblasts on the FN-tTG matrix was not inhibited by the function blocking anti-α_4 antibody or the CS-I peptide in the presence or absence of RGD competitive peptide. In addition, the HOB cell line in which the existence of a FN-tTG mediated RGD-independent cell adhesion was first identified, is reported to express low or negligible levels of $\alpha_4\beta_1$ integrin (Gronthos *et.al.*, 1997).

An early study looking at the redistribution of the enzyme to the particulate fraction indicated there was a tight association between tTG and the insoluble rat lung matrix which was found to be rich in heparan sulphate (Cocuzzi and Chung, 1986). Later work presented evidence to indicate that tTG is involved in the formation of high molecular weight dermatan sulphate proteoglycans in bovine aortic endothelial cell cultures, which was reduced in the presence of the tTG inhibitor mono-dansylcadaverine and chondroitinase ABC (Kinsella and Wight, 1990). Taken together these findings suggest the possibility that FN-tTG may mediate RGD-independent cell adhesion through a heparan-sulphate or a chondroitin-sulphate proteoglycan. A clear significant decrease in RGD-independent cell adhesion on FN-tTG was observed when HOB cells were treated with heparitinase but not chondroitinase ABC, suggesting that cell surface HSPGs rather than CSPGs are essential for the RGD-independent cell adhesion process. Within the C-terminal of FN, the HepII/IIICS region contributes to the interactions of FN with cell-surface HSPG and integrins, which is essential for the formation of adhesion contacts and critical for sustained cell survival (Mostafavi-Pour *et.al.*, 2001; Woods 2001; Jeong *et.al.*, 2001). Once in complex with FN, tTG could induce RGD-independent cell adhesion by enhancing HSPG-mediated adhesion, through a mechanism in which tTG would bind to the cell-surface HSPGs leading to

increased exposure of the C-terminal heparin-binding domain of FN. The fact that FN-tTG can increase cell adhesion up to 30% in the absence of RGD inhibition suggests that HSPGs are not fully engaged when cells are seeded on the FN matrix. Of the known members of HSPG, only syndecan-4 has been found in focal contacts and suggested as the key receptor for focal adhesion formation on FN (Woods and Couchman, 1994; Ishiguro *et.al.*, 2000). The activation of syndecan-4 leads to hyperactivation of PKCα and stimulates Rho GTPase activities as well as FAK auto-phosphorylation (Oh *et.al.*, 1997a and b; Saoncella *et.al.*, 1999; Wilcox-Adelman *et.al.*, 2002). The finding that cell adhesion mediated by FN-tTG requires PKCα activity since the treatment of HOB cells with PKCα inhibitor Go6976 blocks this process, fits well with the observations of Baciu and Goentick (1995) that the localisation of syndecan-4 to focal adhesions did not occur unless PKCα was activated by TPA or serum. In this sense, recruitment of syndecan-4 to focal contacts is dependent on PKCα, and syndecan-4, in turn, modulates the PKCα translocation to the cell membrane where PKCα is activated through association with phosphatidylinositol 4,5-biphosphate (Baciu and Goentick 1995; Oh *et.al.*, 1997a). Indeed, the inhibition of cell adhesion by the RGD peptide and the Go6976 treatment of HOB cells led to a substantial decrease in the membrane levels of PKCα, indicating that the disassociation of syndecan-4 with focal contacts due to inhibition of cell adhesion and the Go6976 treatment leads to decreased activation of PKCα.

The work presented in this thesis shows that the RGD-independent cell adhesion mediated by FN-tTG leads to tyrosine phosphorylation of proteins, suggesting the activation of intracellular signalling pathways during this process. In addition, Verderio *et al.* (2002) suggested the involvement of RhoA GTPase, which regulates the assembly of focal adhesions and actin stress fibers, in the RGD-independent cell adhesion process. It was reported that the retained spread morphology of cells in response to FN-tTG following RGD inhibition, was abolished when cells were pre-treated with RhoA GTPase inhibitor C3 exotransferase. The Rho-mediated regulation of focal adhesions and stress fibers in cells plated on FN coincides with the activation of FAK (Schlaepfer *et.al.*, 1999). In many cases, the events leading to FAK tyrosine phosphorylation have been

shown to be dependent on integrin activation. However, the maximal phosphorylation of FAK requires both the integrin-binding and heparin-binding domains of FN (Jeong *et.al.*, 2001). As the FN-tTG mediated RGD-independent cell adhesion is dependent on HSPGs, it was of interest to determine what effect FN-tTG mediated signalling might have on the auto-phosphorylation of FAK. In this context, it was shown that the function of FN-tTG is linked to the activity of cell survival FAK, as FAK tyrosine phosphorylation levels were restored in response to FN-tTG following the RGD inhibition. To date no intrinsic catalytic activity of syndecan-4 was established, yet syndecan-4 was shown to modulate focal adhesion kinase phosphorylation, suggesting the activation of PKCα to initiate syndecan-4 directed signalling events. The PKCα activation precedes cell spreading on FN (Woods and Couchman, 1994), and its direct activation by phorbol esters has been shown to stimulate focal adhesion formation and FAK tyrosine phosphorylation (Bruce-Staskal and Bouton, 2001). However, in the later study the authors treated the cells with phorbol esters in the presence of serum, which might be responsible for the activation of FAK. Recent work on FN-null fibroblasts using serum free conditions demonstrated that FAK phosphorylation in cells attached to the cell-binding domain fragment of FN can be restored by activation of Rho by LPA, but not by activation of PKCα with PMA. In addition, the levels of FAK Y397 in syndecan-4 null fibroblast was only rescued by the addition of LPA or re-expression of syndecan-4, indicating that clustering of syndecan-4 is necessary for FAK activation and that the signal is mediated by Rho, but not PKCα (Wilcox-Adelman *et.al.*, 2002). In agreement with this finding, the results here demonstrated that the activation of PKCα activity by PMA did not lead to a significant increase in phosphorylation levels of FAK. Although the treatment of cells with Go6976 resulted in a substantial decrease in activation of PKCα, it only led to a slight decrease in phosphorylation of FAK Y397, which was comparable to the levels of inhibition of cell adhesion following the heparitinase treatment. This suggests that the observed decrease in FAK phosphorylation levels in the cells pre-treated with Go6976 might be due to inhibition in clustering and recruitment of syndecan-4 to focal contacts, which in turn would reduce FAK phosphorylation in a Rho-dependent manner.

There have been numerous reports linking Raf-1 kinase to integrin-mediated and mitogen-stimulated activation of MAPK cascade (Kolch, 2000). However, recent studies on c-Raf-1 deficient mice indicated that MEK kinase activity of Raf-1 is not essential for mouse development and that Raf-1 plays a key role as an anti-apoptotic protein (Mikula *et.al.*, 2001; Huser *et.al.*, 2001). The fibroblast derived from c-Raf-1 deficient mice showed an indistinguishable morphology and similar MEK/ERK activation levels when compared with the wild type fibroblasts. Nevertheless, Raf-1 -/- fibroblasts displayed an increased sensitivity to apoptosis induced by a number of stimuli, suggesting an essential function for Raf-1 to counteract apoptosis (Mikula *et.al.*, 2001). Consistent with this finding, Raf-1 was shown to promote cell survival, independently from its MEK kinase function, by inhibiting the pro-apoptotic, stress-activated protein kinase (ASK1) through protein-protein interactions (Chen *et.al.*, 2001). Interestingly, the use of Raf-1 +/+ and -/- fibroblasts in cell adhesion assays suggested that Raf-1 kinase is necessary for the RGD-independent cell adhesion mediated by FN-tTG complex, since this pathway was impeded in Raf-1 -/- fibroblasts. In contrast, it was found that cell adhesion to FN was not affected by the loss of Raf-1, suggesting that Raf-1 function is not essential for the classical-RGD-dependent cell adhesion to FN. It is possible that Raf-1 is required in the RGD-independent cell adhesion process to prevent detachment-induced apoptosis; however, as the loss of Raf-1 had an immediate effect on cell adhesion, the function of Raf-1 in this process appears to be more upstream. Although the activation of Raf-1 downstream effectors is well established, the events in upstream of Raf-1 are currently somewhat controversial. Previous studies have led to a model that the interaction of Raf-1 with Ras recruits the Raf-1 to the plasma membrane where it can be activated by phosphorylation on tyrosine residues (Kolch, 2000). In contrast, mutant Raf-1 proteins lacking the tyrosine sites were shown to be activated in growth-factor stimulated cells, suggesting existence of alternative mechanism(s) in the activation of Raf-1 (Marais *et.al.*, 1995). Kolch *et al.* (1993) reported that PKCα activates Raf-1 by direct phosphorylation of serine 499 residue. Following studies confirmed the PKCα activity as a Raf-1 activator, and demonstrated the association of PKCα with Raf-1 (Cai *et.al.*, 1997; Cheng *et.al.*, 2001). Based on these findings, one can speculate

about the function of Raf-1 in the RGD-independent cell adhesion pathway. Perhaps the simplest explanation is that, the interaction of Raf-1 with PKCα somehow induces the formation of the PKCα-syndecan-4 complex, which in turn mediates the RGD-independent cell adhesion.

The cell adhesion to ECM has been also shown to activate the well-known ERK/MAPK cascade. The activation of ERK (p42/p44) pathway reported to prevent apoptosis induced by anchorage and serum removal (Le Gall, *et.al.*, 2000). Since the inhibition of RGD-dependent cell adhesion on FN led to a decrease in the phosphorylation of ERK1/2 kinase, this initially suggested that ERK was activated by integrin-mediated cell adhesion in HOB cells. In addition, the ERK1/2 phosphorylation levels were induced almost back to normal levels in response to FN-tTG, suggesting that ERK1/2 might also get activated through a RGD-independent cell adhesion pathway. Given that the FN-tTG complex activates FAK, an upstream effector of Raf/MEK/ERK cascade, it is not surprising that it also induces the activation of ERK1/2 kinase. However, a recent study has demonstrated that endothelial cells treated with Go6976 showed an inhibition in early activation of ERK1/2, signifying a mediatory role for PKCα activation in ERK1/2 activation (Cheng *et.al.*, 2001). It is therefore equally possible that ERK1/2 kinase might be activated by FAK or PKCα in response to FN-tTG during RGD-independent cell adhesion.

Recent evidence showed that stimulation of both integrin aggregation and G protein-coupled receptors enhance JNK activity, implicating JNK in adhesion dependent cell survival (Igishi *et.al.*, 1999; Almeida *et.al.*, 2000). In keeping with these reports, the attachment of HOB cells to FN led to an enhanced JNK activity when compared to cells in suspension or to RGD-treated cells on FN. The JNK was also activated in cells seeded on FN-tTG through the RGD-independent cell adhesion pathway. Previous studies connected the JNK pathway to FAK activity since the activation of Src kinase by FAK was shown to activate the docking protein $p130^{CAS}$, adapter proteins Crk and Nck, which leads the activation of JNK (Miyamoto *et.al.*, 1995; Schlaepfer *et.al.*, 1999). Later, Almeida *et al.* (2000) proposed that the FAK-p130Cas complex is responsible for the activation of JNK through a Ras/Rac1/Pak1/MKK4 pathway in fibroblasts. Unfortunately, with the

current knowledge in hand, it is not possible to determine which one of these pathways is activated to induce JNK activation during the RGD-independent cell adhesion pathway.

Consistent with the finding that the RGD-independent cell adhesion to FN-tTG is linked to the cell survival factors FAK, Raf-1 kinase, ERK, and JNK, is the observation that the FN-tTG complex can rescue mouse primary dermal fibroblasts null for tTG from the detachment-induced apoptosis (anoikis) with the maintenance of cell viability. The use of MDFTg2-/- cells in the survival assays suggested that the pro-survival function of tTG is essentially extracellular and not intracellular as proposed by recent studies (Antonyak *et.al.*, 2001 and 2002). Apoptosis induced by the RGD inhibition of integrin-mediated adhesion has been previously reported, however the blocking of integrin-mediated survival signals is not sufficient to induce maximal apoptosis of anchorage-dependent cells (Kapila *et.al.*, 1999; Hadden and Henke *et.al.*, 2000; Jeong *et.al.*, 2001). In this regard, the incubation of mouse primary fibroblast null and wild type for tTG with the RGD peptide resulted only in a partial decrease in cell survival. Recent studies showed that the high affinity heparin binding domain of FN is also important in protecting cells from undergoing apoptosis, presumably by the HSPG-mediated survival signals (Kapila *et.al.*, 1999; Jeong *et.al.*, 2001). These findings may be reconciled with the data in this report as the FN-tTG complex was shown to induce cell survival through an RGD-independent, HSPG-dependent cell adhesion pathway.

The mechanism(s) by which RGD-inhibition triggers an apoptotic signalling pathway in MDFTg2 -/- fibroblasts was not fully addressed in this study. However, initial studies showed that caspase-3 was activated in the absence of the integrin-mediated survival signals. Caspase-3 is involved in the proteolytic processing of key kinases necessary for survival, and the caspase inhibitors block this processing, hence rescuing cells from apoptosis (Widmann *et.al.*, 1998). For example, the inhibition of caspase-3 activity with the pan-caspase inhibitor Z-VAD-FMK rescued MDFTg2 -/- cells from staurosporine-induced cell death. It is possible that caspase-3 activation by the RGD peptide incubation leads to the cleavage of FAK in MDFTg2-/- cells seeded on FN, while the FN-tTG matrix blocks the activation of caspase-3, thus enabling the FAK activity/stability under the same conditions. In

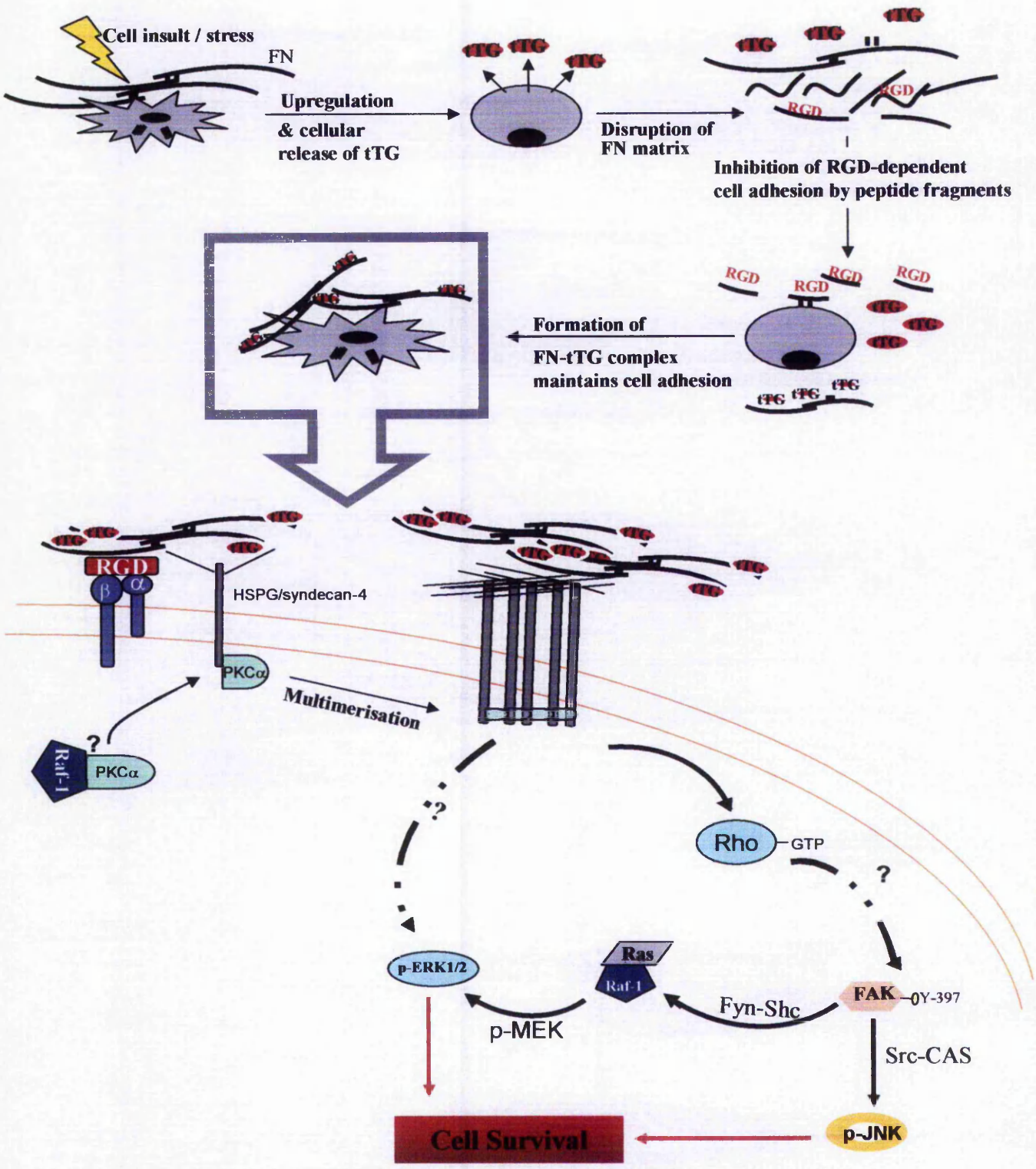


Figure 6.1 Importance of FN-tTG in the maintenance of RGD-independent cell adhesion following cell stress/injury.

support of this hypothesis, Jeong *et al.* (2001) showed that the heparin-binding domain of FN is necessary to block caspase-3 mediated cleavage of FAK in fibroblast undergoing anchorage-dependent apoptosis. Upon apoptotic stimuli, active caspase-3 enters the nucleus, where it cleaves several nuclear proteins resulting in nuclear condensation and DNA fragmentation (Green and Reed, 1998). In keeping with this notion, the nuclear disintegration and DNA fragmentation was evident in RGD-treated MDFTg2 -/- cells seeded on FN matrix, but not in cells seeded on FN-tTG matrix.

In summary, work presented in this thesis documents the importance of the FN-tTG cell adhesion complex in the RGD-independent rescue of cells from anoikis. The physiological relevance of this RGD-independent cell adhesion could be during tissue injury due to the disruption of the FN matrix by numerous proteases and subsequent generation of soluble FN peptides (figure 6.1). These peptides, containing the RGD cell binding domain, could interfere with RGD-dependent cell adhesion to the intact FN matrix and induce anoikis. Numerous studies reported tTG externalisation and deposition to the ECM in response to tissue damage. Once associated with FN, tTG becomes less susceptible to proteolysis by metalloproteinases (Belkin *et.al.*, 2001). Hence, it is possible that during wound repair a complex of tTG and FN conferring resistance to proteolytic degradation by metalloproteinases could be formed in the oxidising extracellular environment of the wound area and mediate the RGD-independent cell adhesion. The extracellular effect of this potential FN-tTG adhesion complex is to ensure the adhesion-mediated cell survival via interaction with the HSPG receptors, and consequent activation of the cell survival kinases.

The apparent association of syndecan-4 with focal adhesions, and the increased expression of this HSPG at sites of tissue injury, suggests that the FN-tTG might be recognised by syndecan-4. It is therefore important that future work should define the role of syndecan-4 in the FN-tTG mediated RGD-independent cell adhesion. Studies to further define the function of Raf-1 and mechanism(s) of ERK1/2 and JNK1/2 activation, as well as the molecular events that give rise to the induction of RGD-dependent anoikis, will significantly enhance our understanding of the RGD-independent cell survival pathway.

References

References

Abe, S., Yamashita, K., Kohno, H., and Ohkubo, Y. (2000). Involvement of transglutaminase in the receptor-mediated endocytosis of mouse peritoneal macrophages. *Biol. Pharm. Bull.*, **23,** 1511-1513

Achyuthan, K.E., and Greenberg CS. (1987). Identification of a guanosine triphosphate-binding site on guinea pig liver transglutaminase. Role of GTP and calcium ions in modulating activity. *J. Biol. Chem.*, **262,** 1901-1906

Achyuthan, K.E., Goodell, R.J., Kennedye, J.R., Lee, K.N., Henley, A., Stiefer, J.R. and Birckbichler PJ. (1995). Immunochemical analyses of human plasma fibronectin-cytosolic transglutaminase interactions. *J. Immunol Methods*, **180,** 69-79

Adany, R. (1996). Intracellular factor XIII: cellular distribution of factor XIII subunit a in humans. *Semin. Thromb. Hemost.*,. **22,** 399-408

Aeschlimann, D., and Paulsson, M. (1991). Cross-linking of laminin-nidogen complexes by tissue transglutaminase. *J. Biol. Chem.*, **266**, 15308-15317

Aeschlimann, D., and Paulsson, M. (1994). Transglutaminases: protein cross-linking enzymes in tissues and body fluids. *Thromb. Haemost.*, **71,** 402-415

Aeschlimann, D., and Thomazy, V. B. (2000). Protein crosslinking in assembly and remodelling of extracellular matrices: the role of transglutaminases. *Connect. Tissue Res.*, **41**, 1-27

Aeschlimann, D., Kaupp, O., and Paulsson, M. (1995). Transglutaminase-catalyzed matrix cross-linking in differentiating cartilage: identification of osteonectin as a major glutaminyl substrate. *J. Cell Biol.*, **129,** 881-892

Aeschlimann, D., Mosher, D., and Paulsson, M. (1996). Tissue transglutaminase and factor XIII in cartilage and bone remodeling. *Semin. Thromb. Hemost.*, **22,** 437-443.

Aeschlimann, D., Wetterwald, A., Fleisch, H., and Paulsson, M. (1993). Expression of tissue transglutaminase in skeletal tissues correlates with events of terminal differentiation of chondrocytes. *J. Cell Biol.*, **120,** 1461-1470

Akimov, S.S., and Belkin, A.M. (2001). Cell surface tissue transglutaminase is involved in adhesion and migration of monocytic cells on fibronectin. *Blood,* **98,** 1567-1576

Akimov, S.S., Krylov, D., Fleischman, L.F., and Belkin, A.M. (2000). Tissue transglutaminase is an integrin-binding adhesion coreceptor for fibronectin. *J. Cell Biol.*, **148**, 825-838

Aleanzi, M., Demonte, A.M., Esper, C., Garcilazo, S., and Waggener, M. (2001). Celiac disease: antibody recognition against native and selectively deamidated gliadin peptides. *Clin. Chem.*, **47,** 2023-2028

Almeida, E.A., Ilic, D., Han, Q., Hauck, C.R., Jin, F., Kawakatsu, H., Schlaepfer, D.D., and Damsky, C.H. (2000). Matrix survival signaling: from fibronectin via focal adhesion kinase to c-Jun NH(2)-terminal kinase. *J. Cell. Biol.*, **149,** 741-754

An, G., Meka, C.S., Bright, S.P., and Veltri, R.W. (1999). Human prostate-specific transglutaminase gene: promoter cloning, tissue-specific expression, and down-regulation in metastatic prostate cancer. *Urology,* **54,** 1105-1111

Antonyak, M.A., Boehm, J.E., and Cerione, R.A. (2002). Phosphoinositide 3-kinase activity is required for retinoic acid-induced expression and activation of the tissue transglutaminase. *J. Biol. Chem.*, **277,** 14712-14716

Antonyak, M.A., McNeill, C.J., Wakshlag, J.J., Boehm, J.E., and Cerione, R.A. (2003). Activation of the Ras-ERK pathway inhibits retinoic acid-induced stimulation of tissue transglutaminase expression in NIH3T3 cells. *J. Biol. Chem.*, **278,** 15859-15866

Antonyak, M.A., Singh, U.S., Lee, D.A., Boehm, J.E., Combs, C., Zgola, M.M., Page, R.L., and Cerione, R.A. (2001). Effects of tissue transglutaminase on retinoic acid-induced cellular differentiation and protection against apoptosis. *J. Biol. Chem.*, **276,** 33582-33587

Aoshiba, K., Rennard, S.I., and Spurzem, J.R. (1997). Cell-matrix and cell-cell interactions modulate apoptosis of bronchial epithelial cells. *Am. J. Physiol.*, **272,** L28-37.

Aota, S., Nagai, T., and Yamada, K.M. (1991). Characterization of regions of fibronectin besides the arginine-glycine-aspartic acid sequence required for adhesive function of the cell-binding domain using site-directed mutagenesis. *J. Biol. Chem.*, **266,** 15938-15943

Azim, A. C., Marfatia, S. M., Korsgren, C., Dotimas, E., Cohen, C. M., and Chishti, A. H. (1996). Human erythrocyte dematin and protein 4.2 (pallidin) are ATP binding proteins. *Biochemistry,* **35,** 3001–3006

Baciu, P.C., and Goetinck, P.F. (1995). Protein kinase C regulates the recruitment of syndecan-4 into focal contacts. *Mol. Biol. Cell.*, **6,** 1503-1513

Baciu, P.C., Saoncella, S., Lee, S.H., Denhez, F., Leuthardt, D., Goetinck, P.F. (2000). Syndesmos, a protein that interacts with the cytoplasmic domain of syndecan-4, mediates cell spreading and actin cytoskeletal organization. *J. Cell Sci.*, **113,** 315-324

Badylak, S.F. (2002). The extracellular matrix as a scaffold for tissue reconstruction. *Semin. Cell Dev. Biol.*, **13,** 377-383

Baek, K.J., Das, T., Gray, C.D., Desai, S., Hwang, K.C., Gacchui, R., Ludwig, M., and Im, M.J. (1996). A 50 kDa protein modulates guanine nucleotide binding of transglutaminase II. *Biochemistry,* **35,** 2651-2657

Baldwin, D. Jr., Prince, M., Marshall, S., Davies, P., and Olefsky, J.M. (1980). Regulation of insulin receptors: evidence for involvement of an endocytotic internalization pathway. *Proc. Natl. Acad. Sci. U S A,* **77,** 5975-5978

Bale, M.D., and Mosher, D.F. (1986). Thrombospondin is a substrate for blood coagulation factor XIIIa. *Biochemistry,* **25,** 5667-5673

Balklava, Z., Verderio, E., Collighan, R., Gross, S., Adams, J., and Griffin, M. (2002). Analysis of tissue transglutaminase function in the migration of Swiss 3T3 fibroblasts: the active-state conformation of the enzyme does not affect cell motility but is important for its secretion. *J. Biol. Chem.*, **277,** 16567-16575

Ballestar, E., Abad, C., and Franco L. (1996). Core histones are glutaminyl substrates for tissue transglutaminase. *J. Biol. Chem.*, **271,** 18817-18824

Barnes, R.X., Bungay, P.1., Elliott, B.M., Walton, P.L., and Griffin, M. (1985). Alterations in the distribution and activity of transglutaminase during tumour growth and metastasis. *Carcinogenesis,* **6**, 459-463

Barry, E.L., and Mosher, D.F. (1990). Binding and degradation of blood coagulation factor XIII by cultured fibroblasts. *J. Biol. Chem.*, **265**, 9302-9307

Barry, E.L.R., and Mosher, D.F. (1988). Factor XIII cross-linking of fibronectin at cellular matrix assembly sites. *J. Biol. Chem.*, **263,** 10464-10469

Barsigian, C., Stern, A.M., and Martinez, J. (1991). Tissue (type II) transglutaminase covalently incorporates itself, fibrinogen, or fibronectin into high molecular weight complexes on the extracellular surface of isolated hepatocytes. *J. Biol. Chem.,*, **266**, 22501-22509

Bass, M,D, and Humphries, M.J. (2002). Cytoplasmic interactions of syndecan-4 orchestrate adhesion receptor and growth factor receptor signalling. *Biochem. J.*, **15,** 1-15

Battaglia, D.X., and Shapiro, B.M. (1988). Hierarchies of protein cross-linking in the extracellular matrix: involvement of an egg surface transglutaminase in early stages of fertilization envelope assembly. *J. Cell Biol.*, **107**, 2447-2454

Becher, M.W., Kotzuk, J.A., Sharp, A.H., Davies, S.W., Bates, G.P., Price, D.L., Ross, C.A. (1998). Intranuclear neuronal inclusions in Huntington's disease and dentatorubral and pallidoluysian atrophy: correlation between the density of inclusions and IT15 CAG triplet repeat length. *Neurobiol. Dis.*, **4,** 387-397

Belkin, A.M., Akimov, S.S., Zaritskaya, L.S., Ratnikov, B.I., and Deryugina, E.I., and Strongin, A.Y. (2001). Matrix-dependent proteolysis of surface transglutaminase by membrane-type metalloproteinase regulates cancer cell adhesion and locomotion. *J. Biol. Chem.*, **276,** 18415-18422

Bendixen, E., Borth, W., and Harpel, P.C. (1993). Transglutaminases catalyze cross-linking of plasminogen to fibronectin and human endothelial cells. *J. Biol. Chem.*, **268,** 21962-21967

Beninati, S., Abbruzzese, A., and Cardinali, M. (1993). Differences in the post-translational modification of proteins by polyamines between weakly and highly metastatic B16 melanoma cells. *Int. J. Cancer,* **53,** 792-797

Bernassola, F., Federici, M., Corazzari, M., Terrinoni, A., Hribal, M.L., De Laurenzi, V., Ranalli, M., Massa, O., Sesti, G., McLean, W.H., Citro, G., Barbetti, F., and Melino, G. (2002). Role of transglutaminase 2 in glucose tolerance: knockout mice studies and a putative mutation in a MODY patient. *FASEB J.*, **16,** 1371-1378

Birckbichler, P.J., and Patterson, M.K. Jr. (1978). Cellular transglutaminase, growth, and transformation. *Ann. N Y Acad. Sci.*, **312,** 354-365

Birckbichler, P.J., and Patterson, M.K. Jr. (1980). Transglutaminase and epsilon-(gamma-glutamyl) lysine isopeptide bonds in eukaryotic cells. *Prog. Clin. Biol. Res.*, **41,** 845-855

Birckbichler, P.J., Bonner, R.B., Hurst, R.E., Bane, B.L., Pitha, J.V., and Hemstreet, G.P. 3rd. (2000). Loss of tissue transglutaminase as a biomarker for prostate adenocarcinoma. *Cancer,* **89,** 412-423

Birckbichler, P.J., Orr, G.R., Carter, H.A., and Patterson, M.K. Jr. (1977). Catalytic formation of epsilon-(gamma-glutamyl)lysine in guinea pig liver transglutaminase. *Biochem. Biophys. Res. Commun.*, **78,** 1-7

Birckbichler, P.J., Orr, G.R., Conway, E., Patterson, M.K. Jr. (1977). Transglutaminase activity in normal and transformed cells. *Cancer. Res.*, **37,** 1340-1344

Bonfoco, E., Chen, W., Paul, R., Cheresh, D.A., and Cooper, N.R. (2000). beta1 integrin antagonism on adherent, differentiated human neuroblastoma cells triggers an apoptotic signaling pathway. *Neuroscience,* **101,** 1145-1152

Bono, P., Rubin, K., Higgins, J.M., and Hynes, R.O. (2001). Layilin, a novel integral membrane protein, is a hyaluronan receptor. *Mol. Biol. Cell,* **12,** 891-900

Booth, N.A. (1999). Fibrinolysis and thrombosis. *Baillieres Best Pract. Res. Clin. Haematol.,* **12,** 423-433

Bottenus, R.E., Ichinose, A., and Davie, E.W. (1990). Nucleotide sequence of the gene for the β-subunit of human factor XIII. *Biochemistry,* **29,** 11195-11209

Boudreau, N., Sympson, C.J., Werb, Z., and Bissell, M.J. (1995). Suppression of ICE and apoptosis in mammary epithelial cells by extracellular matrix. *Science,* 1995 **267,** 891-893

Boulton, T.G., Nye, S.H., Robbins, D.J., Ip, N.Y., Radziejewska, E., Morgenbesser, S.D., DePinho, R.A., Panayotatos, N., Cobb, M.H., and Yancopoulos, G.D. (1991). ERKs: a family of protein-serine/threonine kinases that are activated and tyrosine phosphorylated in response to insulin and NGF. *Cell,* **65,** 663-675

Bowness, J.M., Folk, J.E., and Timpl, R. (1987a). Identification of a substrate site for liver transglutaminase on the aminopropeptide of type III collagen. *J. Biol. Chem.,* **262,** 1022-1024

Bowness, J.M., Henteleff, H., and Dolynchuk, K.N. (1987b). Components of increased labelling with putrescine and fucose during healing of skin wounds. *Connect. Tissue Res.,* **16,** 57-70

Bowness, J.M., Tarr, A.H., and Wong, T. (1988). Increased transglutaminase activity during skin wound healing in rats. *Biochem. Biophys. Acta.,* **967,** 234-240

Brenner, B., Koppenhoefer, U., Weinstock, C., Linderkamp, O., Lang, F., and Gulbins, E. (1997). Fas- or ceramide-induced apoptosis is mediated by a Rac1-regulated activation of Jun N-terminal kinase/p38 kinases and GADD153. *J. Biol. Chem.,* **272,** 22173-22181

Brown-Augsburger, P., Broekelmann, T., Mecham, L., Mercer, R., Gibson, M.A., Cleary, E.G., Abrams, W.R., Rosenbloom, J., and Mecham, R.P. (1994). Microfibril-associated glycoprotein binds to the carboxyl-terminal domain of tropoelastin and is a substrate for transglutaminase. *J. Biol. Chem.,* **269,** 28443-28449

Bruce, S.E., Bjarnason, I., and Peters, T.J. (1985). Human jejunal transglutaminase: demonstration of activity, enzyme kinetics and substrate

specificity with special relation to gliadin and coeliac disease. *Clin. Sci. (Lond).* **68,** 573-579

Bruce-Staskal, P.J., and Bouton, A.H. (2001).PKC-dependent activation of FAK and src induces tyrosine phosphorylation of Cas and formation of Cas-Crk complexes. *Exp. Cell Res.*, **264,** 296-306

Bultmann, H., Santas, A.J., and Peters, D.M. (1998). Fibronectin fibrillogenesis involves the heparin II binding domain of fibronectin. *J. Biol. Chem.*, **273,** 2601-2609

Bungay, P.J., Owen, R.A., Coutts, .IC., and Griffin, M. (1986). A role for transglutaminase in glucose-stimulated insulin release from the pancreatic beta-cell. *Biochem. J.*, **235**, 269-278

Bungay, P.J., Potter, J.M., and Griffin, M. (1984). A role for polyamines in stimulus-secretion coupling in the pancreatic beta-cell. *Biosci. Rep.*, **4**, 869-877

Burgeson, R.E. (1993). Type VII collagen, anchoring fibrils, and epidermolysis bullosa. *J. Invest. Dermatol.*, **101,**:252-5

Buxman, M.M., and Wuepper, K.D. (1975). Keratin cross-linking and epidermal transglutaminase. A review with observations on the histochemical and immunochemical localization of the enzyme. *J. Invest. Dermatol.*, **65,** 107-112

Buxman, M.M., and Wuepper, K.D. (1976). Isolation, purification and characterization of bovine epidermal transglutaminase. *Biochim. Biophys. Acta,* **452,** 356-369

Cai, D., Ben, T., and De Luca, L.M. (1991). Retinoids induce tissue transglutaminase in NIH-3T3 cells. Biochem. *Biophys. Res. Commun.*, **175,** 1119-1124

Cai, H., Smola, U., Wixler, V., Eisenmann-Tappe, I., Diaz-Meco, M.T., Moscat, J., Rapp, U., and Cooper, G.M. (1997). Role of diacylglycerol-regulated protein kinase C isotypes in growth factor activation of the Raf-1 protein kinase. *Mol. Cell. Biol.*, **17,** 732-741

Calderwood, D.A., Shattil, S.J., and Ginsberg, M.H. (2000). Integrins and actin filaments: reciprocal regulation of cell adhesion and signaling. *J. Biol. Chem.*, **275,** 22607-22610

Carrell, N.A., Erickson, H.P., and McDonagh, J. (1989). Electron microscopy and hydrodynamic properties of factor XIII subunits. *J. Biol. Chem.*, **264**, 551-556

Chakravarty, R., and Rice, R.E. (1989). Acylation of keratinocyte transglutaminase by palmitic and myristic acids in the membrane anchorage region. *J. Biol. Chem.*, **264,** 625-629

Chan, B.M.C., Kassner, P.D., Schiro, J.A., Byers, H.R., Kupper, T.S., and Hemler, M.E. (1992). Distinct cellular functions mediated by different VLA integrin αsubunit cytoplasmic domains. *Cell,* **68,** 1051-1060

Chen, H., and Mosher, D.F. (1996) Formation of sodium dodecyl sulfate-stable fibronectin multimers. Failure to detect products of thiol-disulfide exchange in cyanogen bromide or limited acid digests of stabilized matrix fibronectin. *J. Biol. Chem.,* **271,** 9084-9089

Chen, H.C., Appeddu, P.A., Isoda, H., Guan, J.L. (1996). Phosphorylation of tyrosine 397 in focal adhesion kinase is required for binding phosphatidylinositol 3-kinase. *J. Biol. Chem.,* **271,** 26329-26334

Chen, J., Fujii, K., Zhang, L., Roberts, T., and Fu, H. (2001). Raf-1 promotes cell survival by antagonizing apoptosis signal-regulating kinase 1 through a MEK-ERK independent mechanism. *Proc. Natl. Acad. Sci U S A.,* **98,** 7783-7788

Chen, J.S., and Mehta, K. (1999). Tissue transglutaminase: an enzyme with a split personality. *Int. J. Biochem. Cell Biol.,* **31,** 817-836

Chen, S., Lin, F., Iismaa, S., Lee, K.N., Birckbichler, P.J., and Graham, R.M. (1996). Alpha1-adrenergic receptor signaling via Gh is subtype specific and independent of its transglutaminase activity. *J. Biol. Chem.,* **271,** 32385-32391

Chen, X., Wang, J., Fu, B., and Yu, L. (1997). RGD-containing peptides trigger apoptosis in glomerular mesangial cells of adult human kidneys. *Biochem. Biophys. Res. Commun.,* **234,** 594-599

Cheng, J.J., Wung, B.S., Chao, Y.J., and Wang, D.L. (2001). Sequential activation of protein kinase C (PKC)-alpha and PKC-epsilon contributes to sustained Raf/ERK1/2 activation in endothelial cells under mechanical strain. *J. Biol. Chem.,* **276,** 31368-31375

Chernousov, M.A., Fogerty, F.J., Koteliansky, V.E., and Mosher, D.F. (1991). Role of the I-9 and III-1 modules of fibronectin in formation of an extracellular fibronectin matrix. *J. Biol. Chem.,* **266,** 10851-10858

Ciccocioppo, R., Di Sabatino, A., Ara, C., Biagi, F., Perilli, M., Amicosante, G., Cifone, M.G., and Corazza, G.R. (2003). Gliadin and tissue transglutaminase complexes in normal and coeliac duodenal mucosa. *Clin. Exp. Immunol.,* **134,** 516-524

Citron, B.A., SantaCruz, K.S., Davies, P.J., and Festoff, B.W. (2001). Intron-exon swapping of transglutaminase mRNA and neuronal Tau aggregation in Alzheimer's disease. *J. Biol. Chem.,* **276,** 3295-3301

Citron, B.A., Suo, Z., SantaCruz, K., Davies, P.J., Qin, F., and Festoff, B.W. (2002). Protein crosslinking, tissue transglutaminase, alternative splicing and neurodegeneration.*Neurochem. Int.*, **40,** 69-78

Clarke, D.D., Mycek, M.J., Neidle, A., and Waelsch, H. (1957). The incorporation of amines into proteins. *Arch. Biochem. Biophys.*, **79**, 338-354

Cocuzzi, E.T., and Chung, S.I. (1986). Cellular transglutaminase. Lung matrix-associated transglutaminase: characterization and activation with sulfhydryls. *J. Biol. Chem.*, **261,** 8122-8127

Cordella-Miele, E., Miele, L., and Mukherjee, A.B. (1990). A novel transglutaminase-mediated post-translational modification of phospholipase A2 dramatically increases its catalytic activity. *J. Biol. Chem.*, **265,** 17180-17188

Cordella-Miele, E., Miele, L., and Mukherjee, A.B. (1993). Identification of a specific region of low molecular weight phospholipases A2 (residues 21-40) as a potential target for structure-based design of inhibitors of these enzymes. *Proc. Natl. Acad. Sci. USA.*, **90,** 10290-10294

Cottrell, B.A., Strong, D.D., Watt, K.W., and Doolittle, R.F. (1979). Amino acid sequence studies on the alpha chain of human fibrinogen. Exact location of cross-linking acceptor sites. *Biochemistry,* **18,** 5405-1540

Critchley, D.R. (2000). Focal adhesions - the cytoskeletal connection. *Curr. Opin. Cell Biol.*, **12,** 133-139

Dallabrida, S.M., Falls, L.A., and Farrell, D.H. (2000). Factor XIIIa supports microvascular endothelial cell adhesion and inhibits capillary tube formation in fibrin. *Blood,*, **95,** 2586-2592

Dalton, B.A., McFarland, C.D., Underwood, P.A., and Steele, J.G. (1995). Role of the heparin binding domain of fibronectin in attachment and spreading of human bone-derived cells. *J. Cell Sci.*, **108,** 2083-2092

Damsky, C.H., Knudsen, K.A., Bradley, D., Buck, C.A., and Horwitz, A.F. (1985). Distribution of the cell substratum attachment (CSAT) antigen on myogenic and fibroblastic cells in culture. *J. Cell Biol.*, **100,** 1528-1539

Dardik, R., Shenkman, B., Tamarin, I., Eskaraev, R., Harsfalvi, J., Varon, D., and Inbal, A. (2002). Factor XIII mediates adhesion of platelets to endothelial cells through alpha(v)beta(3) and glycoprotein IIb/IIIa integrins. *Thromb. Res.*, **105,** 317-323

Davies, P.J., Cornwell, M.M., Johnson, J.D., Reggianni, A., Myers, M., and Murtaugh, M.P. (1984). Studies on the effects of dansylcadaverine and related compounds on receptor-mediated endocytosis in cultured cells. *Diabetes Care,* **1,** 35-41

Davies, P.J., Davies, D.R., Levitzki, A., Maxfield, F.R., Milhaud, P., Willingham, M.C., and Pastan, I.H. (1980). Transglutaminase is essential in receptor-mediated endocytosis of alpha 2-macroglobulin and polypeptide hormones. *Nature,* **283,** 162-167

Davis, E.C. (1994). Immunolocalization of microfibril and microfibril-associated proteins in the subendothelial matrix of the developing mouse aorta. *J. Cell Sci.,* 1994 Mar;107 (Pt 3):727-36.

De Laurenzi, V., and Melino, G. (2001). Gene disruption of tissue transglutaminase. *Mol. Cell Biol.,* **21,** 148-155

Decker, S., van Valen, F., and Vischer, P. (2002). Adhesion of osteosarcoma cells to the 70-kDa core region of thrombospondin-1 is mediated by the alpha 4 beta 1 integrin. *Biochem. Biophys. Res. Commun.,* **293,** 86-92

Dedhar, S., Ruoslahti, E., and Pierschbacher, M.D. (1987). A cell surface receptor complex for collagen type I recognizes the Arg-Gly-Asp sequence. *Cell Biol.,* **104,** 585-593

Delcros, J.G., Bard, S., Roch, A.M., Quash, G., Poupon, M.F., and Korach, S. (1986). Transglutaminase activity and putrescine-binding capacity in cloned cell lines with different metastatic potential. *FEBS Lett.,* **196,** 325-330

Denk, H., Bernklau, G., and Krepler, R. (1984). Effect of griseofulvin treatment and neoplastic transformation on transglutaminase activity in mouse liver. *Liver,* **4,** 208-213

Dieterich, W., Ehnis, T., Bauer, M., Donner, P., Volta, U., Riecken, E.O., and Schuppan, D. (1997). Identification of tissue transglutaminase as the autoantigen of celiac disease. *Nat. Med.,* **3,** 797-801

Doolittle, R.F., Watt, K.W., Cottrell, B.A., Strong, D.D., and Riley, M. (1979). The amino acid sequence of the alpha-chain of human fibrinogen. *Nature,* **280,** 464-468

Dubbink, H.J., Hoedemaeker, R.F., van der Kwast, T.H., Schroder, F.H., and Romijn, J.C. (1999). Human prostate-specific transglutaminase: a new prostatic marker with a unique distribution pattern. *Lab. Invest.,* **79,** 141-150

Dubbink, H.J., Verkaik, N.S., Faber, P.W., Trapman, J., Schroder, F.H., and Romijn, J.C. (1996). Tissue specific and androgen-regulated expression of human prostate-specific transglutaminase. *Biochem. J.,* **315,** 901-908

Duxbury, M.S., Ito, H., Benoit, E., Zinner, M.J., Ashley, S.W., Whang, E.E. (2003). RNA interference targeting focal adhesion kinase enhances pancreatic

adenocarcinoma gemcitabine chemosensitivity. *Biochem. Biophys. Res. Commun.*, **311,** 786-792

Dyr, J.E., Blomback, B., Hessel, B., and Kornalik, F. (1989). Conversion of fibrinogen to fibrin induced by preferential release of fibrinopeptide B. *Biochim. Biophys. Acta.*, **990,** 18-24

Eitan, S., Solomon, A., Lavie, V., Yoles, E., Hirschberg, D.L, Belkin, M., and Schwartz, M. (1994). Recovery of visual response of injured adult rat optic nerves treated with transglutaminase. *Science,* **264,** 1764-1768

Esterre, P., Risteli, L., and Ricard-Blum, S. (1998). Immunohistochemical study of type I collagen turn-over and of matrix metalloproteinases in chromoblastomycosis before and after treatment by terbinafine. *Pathol. Res. Pract.*, **194,** 847-853

Etzioni, A. (1999). Integrins-the glue of life. *Lancet.*, **353,** 341-343

Fellin, F.M., Barsigian, C., Rich, E., and Martinez, J. (1988). Binding and cross-linking of rabbit fibronectin by rabbit hepatocytes in suspension. *J. Biol. Chem.*, **263,** 1791-1797

Feng, J.F., Readon, M., Yadav, S.P., and Im, M.J. (1999). Calreticulin down-regulates both GTP binding and transglutaminase activities of transglutaminase II. *Biochemistry,* **38,** 10743-10749

Feng, J.F., Rhee, S.G., and Im, M.J. (1996). Evidence that phospholipase delta1 is the effector in the Gh (transglutaminase II)-mediated signaling. *J. Biol. Chem.*, **271,** 16451-16454

Fesus, L. (1998). Transglutaminase-catalyzed protein cross-linking in the molecular program of apoptosis and its relationship to neuronal processes. *Cell Mol. Neurobiol.*, **18,** 683-694

Fesus, L., Metsis, M.L., Muszbek, L., and Koteliansky, V.E. (1986). Transglutaminase-sensitive glutamine residues of human plasma fibronectin revealed by studying its proteolytic fragments. *Eur. J. Biochem.*, **154,** 371-374

Fesus, L., Thomazy, V., and Falus, A. (1987). Induction and activation of tissue transglutaminase during programmed cell death. *FEBS Lett.*, **224,** 104-108

Fesus, L., Thomazy, V., Autuori, F., Ceru, M.P., Tarcsa, E., and Piacentini, M. (1989). Apoptotic hepatocytes become insoluble in detergents and chaotropic agents as a result of transglutaminase action. *FEBS Lett.*, **245,** 150-154

Folk, J.E., and Cole, P.W. (1966). Mechanism of action of guinea pig liver transglutaminase. I. Purification and properties of the enzyme: identification of a functional cysteine essential for activity. *J. Biol. Chem.*, **241,** 5518-5525

Folk, J.E., and Finlayson, J.S. (1977). The ε(γ-glutamyl)lysine crosslink and the catalytic role of transglutaminase. *Adv. Prot. Chem.*, **31**, 1-133

Folk, J.E., Mullooly, J.P., and Cole, P.W. (1967). Mechanism of action of guinea pig liver transglutaminase. II. The role of metal in enzyme activation. *J. Biol. Chem.*, **242,** 1838-1844.

Fraij, B.M., and Gonzales, R.A. (1996). A third human tissue transglutaminase homologue as a result of alternative gene transcripts. *Biochim. Biophys. Acta,* **1306,** 63-74

Fraij, B.M., Birckbichler, P.J., Patterson, M.K. Jr., Lee, K.N., and Gonzales, R.A. (1992). A retinoic acid-inducible mRNA from human erythroleukemia cells encodes a novel tissue transglutaminase homologue. *J. Biol. Chem.*, **267,** 22616-22623

Francis, R.T., McDonagh, J., and Mann, K.G. (1986). Factor V is a substrate for the transamidase factor XIIIa. *J. Biol. Chem.*, **261,** 9787-9792

Freund, K.F., Doshi, K.P., Gaul, S.L., Claremon, D.A., Remy, D.C., Baldwin, J.J., Pitzenberger, S.M. and Stern, A.M. (1994). Transglutaminase inhibition by 2-[(2-oxopropyl)thio]imidazolium derivatives: mechanism of factor XIIIa inactivation. *Biochemistry,* **33,** 10109-10119

Friedrich, B., Koob, R., Kraemer, D., and Drenckhahn, D. (1989). Demonstration of immunoreactive forms of erythrocyte protein 4.2 in nonerythroid cells and tissues. *Eur. J. Cell. Biol.*, **48,** 121-127

Frisch, S.M., and Francis, H. (1994). Disruption of epithelial cell-matrix interactions induces apoptosis. *J. Cell. Biol.*, **124,** 619-626

Frisch, S.M., and Screaton, R.A. (2001). Anoikis mechanisms. *Curr. Opin. Cell Biol.*, **13,** 555-562

Frisch, S.M., Vuori, K., Ruoslahti, E., Chan-Hui, P.Y. (1996). Control of adhesion-dependent cell survival by focal adhesion kinase. *J. Cell Biol.*, **134,** 793-799

Fukuda, K., Kojiro, M., and Chiu, J.F. (1993). Cross-linked cytokeratin polypeptides in liver and hepatoma cells: possible association with the process of cell degeneration and death. *Hepatology,* **17,** 118-124

Gailit, J., and Clark, R.A. (1994). Wound repair in the context of extracellular matrix. *Curr. Opin. Cell Biol.*, **6,** 717-725

Gailit, J., and Ruoslahti, E. (1988). Regulation of the fibronectin receptor affinity by divalent cations. *J. Biol. Chem.*, **263,** 12927-12932

Garcia-Pardo A, Wayner EA, Carter WG, Ferreira OC Jr. (1990). Human B lymphocytes define an alternative mechanism of adhesion to fibronectin. The interaction of the alpha 4 beta 1 integrin with the LHGPEILDVPST sequence of the type III connecting segment is sufficient to promote cell attachment. *J. Immunol.*, **144,** 3361-3366

Garrington, T.P., and Johnson, G.L. (1999). Organization and regulation of mitogen-activated protein kinase signaling pathways. *Curr. Opin. Cell Biol.*, **11,** 211-218

Gaudry, C.A., Verderio, E., Aeschlimann, D., Cox, A., Smith, C., and Griffin, M. (1999a). Cell surface localization of tissue transglutaminase is dependent on a fibronectin-binding site in its N-terminal beta-sandwich domain. *J. Cell Biol.*, **274,** 30707-30714

Gaudry, C.A., Verderio, E., Jones, R.A., Smith, C., and Griffin, M. (1999b). Tissue transglutaminase is an important player at the surface of human endothelial cells: evidence for its externalization and its colocalization with the beta(1) integrin. *Exp. Cell. Res.*, **252,** 104-113

Gentile, V., Grant, F.J., Porta, R., and Baldini, A. (1995). Localization of the human prostate transglutaminase (type IV) gene (TGM4) to chromosome 3p21.33-p22 by fluorescence in situ hybridization. *Genomics,* **27,** 219-220

Gentile, V., Saydak, M., Chiocca, E.A., Akande, O., Birckbichler, P.I., Lee, K.X., Stein, J.P., and Davies, P.A.X. (1991). Isolation and characterization of cDNA clones to mouse macrophage and human endothelial cell tissue transglutaminases. *J. Biol. Chem.*, **266**, 478-483

Gentile, V., Sepe, C., Calvani, M., Melone, M.A., Cotrufo, R., Cooper, A.J., Blass, J.P., and Peluso, G. (1998). Tissue transglutaminase-catalyzed formation of high-molecular-weight aggregates in vitro is favored with long polyglutamine domains: a possible mechanism contributing to CAG-triplet diseases. *Arch. Biochem. Biophys.*, **352,** 314-321

Gentile, V., Thomazy, V., Piacentini, M., Fesus, L., and Davies, P.A.X. (1992). Expression of tissue transglutaminase in Balb-C 3T3 fibroblasts: effects on cellular morphology and adhesion. *J. Cell Biol.*, **119**, 463-474

Giancotti, F.G., and Ruoslahti, E. (1999). Integrin signaling. *Science.*, **285,** 1028-1032

Gilad, G.M., Varon, L.E., and Gilad, V.H. (1985). Calcium-dependent transglutaminase of rat sympathetic ganglion in development and after nerve injury. *J. Neurochem.*, **44,** 1385-1390

Gossen, M., and Bujard, H. (1992). Tight control of gene expression in mammalian cells by tetracycline-responsive promoters. *Proc. Natl. Acad. Sci. U S A.*, **89,** 5547-5551

Green, D.R., and Reed, J.C. (1998). Mitochondria and apoptosis. *Science,*, **281,** 1309-1312

Greenberg, C.S., Achyuthan, K.E., and Fenton, J.W. 2nd. (1987). Factor XIIIa formation promoted by complexing of alpha-thrombin, fibrin, and plasma factor XIII.
Blood,, Mar; 69(3): 867-71.

Greenberg, C.S., Birckbichler, P.J. and Rice, R.H. (1991). Transglutaminases: Multifunctional cross-linking enzymes that stabilise tissues. *FASEB. J.*, **5**, 3071-3077

Grenard, P., Bresson-Hadni, S., El Alaoui, S., Chevallier, M., Vuitton, D.A., and Ricard-Blum, S. (2001). Transglutaminase-mediated cross-linking is involved in the stabilization of extracellular matrix in human liver fibrosis. *J. Hepatol.*, **35,** 367-375

Grewal, S.S., York, R.D., and Stork, P.J. (1999). Extracellular-signal-regulated kinase signalling in neurons. *Curr. Opin. Neurobiol.*, **9,** 544-553

Griffin M, and Wilson J. (1984). Detection of epsilon(gamma-glutamyl) lysine. *Mol. Cell. Biochem.*, 1984; 58(1-2): 37-49.

Griffin, M., Barnes, R.N., Wynne, J., and Williams, C. (1978). The effects of bleomycin and copper bleomycin upon transglutaminase enzymes. *Biochem. Pharmacol.*, **27,** 1211-1219

Griffin, M., Casadio, R., and Bergamini, C.M. (2002). Transglutaminases: nature's biological glues. *Biochem. J.*, **368,** 377-396

Griffin, M., Smith, L.L., and Wynne, J. (1979). Changes in transglutaminase activity in an experimental model of pulmonary fibrosis induced by paraquat. *Br. J. Exp. Pathol.*, **60,** 653-661

Gronthos, S., Stewart, K., Graves, S.E., Hay, S., and Simmons, P.J. (1997). Integrin expression and function on human osteoblast-like cells. *J. Bone Miner. Res.*, **12,** 1189-1197

Gross, M., Whetzel, N.K., and Folk, J.E. (1975). The extended active site of guinea pig liver transglutaminase. *J. Biol. Chem.*, **250,** 4648-4655

Grossmann, J. (2002). Molecular mechanisms of "detachment-induced apoptosis--Anoikis". *Apoptosis*, **7,** 247-260

Grundmann, U., Amann, E., Zettlmeissl, G., and Kupper, H.A. (1986). Characterization of cDNA coding for human factor XIIIa.: *Proc. Natl. Acad. Sci. U S A,* **83,** 8024-8028

Guadiz, G., Sporn, L.A., and Simpson-Haidaris, P.J. (1997). Thrombin cleavage-independent deposition of fibrinogen in extracellular matrices. *Blood,* **90,** 2644-2653

Guan, J.L., and Hynes, R.O. (1990). Lymphoid cells recognize an alternatively spliced segment of fibronectin via the integrin receptor alpha 4 beta 1. *Cell,* **60,** 53-61

Haake, A.R., and Polakowska, R.R. (1993). Cell death by apoptosis in epidermal biology. *J. Invest. Dermatol.,* **101,** 107-112

Hada, M., Kaminski, M., Bockenstedt, P., and McDonagh, J. (1986). Covalent crosslinking of von Willebrand factor to fibrin. *Blood,* **68,** 95-101

Hadden, H.L., and Henke, C.A. (2000). Induction of lung fibroblast apoptosis by soluble fibronectin peptides. *Am. J. Respir. Crit. Care. Med.,* **162,** 1553-1560

Haigler, H.T., Maxfield, F.R., Willingham, M.C., and Pastan, I. (1980). Dansylcadaverine inhibits internalization of 125I-epidermal growth factor in BALB 3T3 cells. *J. Biol. Chem.,* **255,** 1239-1241

Halkier, T., and Magnusson, S. (1988). Contact activation of blood coagulation is inhibited by plasma factor M11c chain. *Thromb. Res.,* **51,** 313-324

Haller, H., Lindschau, C., Maasch, C., Olthoff, H., Kurscheid, D., and Luft, F.C. (1998). Integrin-induced protein kinase Calpha and Cepsilon translocation to focal adhesions mediates vascular smooth muscle cell spreading. *Circ. Res.,* **82,** 157-165

Han, J.A., and Park, S.C. (2000). Transglutaminase-dependent modulation of transcription factor Sp1 activity. *Mol. Cells,* **10,** 612-618

Hand, D., Elliott, B.M., and Griffin, M. (1988). Expression of the cytosolic and particulate forms of transglutaminase during chemically-induced rat liver carcinogenesis. *Biochim. Biophys. Acta.,* **970,** 137-145

Hand, D., Elliott, B.M., and Griffin, M. (1990). Characterisation of the cellular substrates for transglutaminase in normal liver and hepatocellular carcinoma. *Biochim. Biophys. Acta.,* **1033,** 57-64

Haroon, Z.A., Hettasch, J.M., Lai, T.S., Dewhirst, M.W., and Greenberg, C.S. (1999). Tissue transglutaminase is expressed, active, and directly involved in rat dermal wound healing and angiogenesis. *FASEB J.,* **13,** 1787-1795

Hasegawa, G., Suwa, M., Ichikawa, Y., Ohtsuka, T., Kumagai, S., Kikuchi, M., Sato, Y., and Saito, Y. (2003). A novel function of tissue-type transglutaminase: protein disulphide isomerase. *Biochem. J.*, **373,** 793-803

Hayette, S., Morle, L., Bozon, M., Ghanem, A., Risinger, M., Korsgren, C., Tanner, M. J. A., Fattoum, S., Cohen, C. M., and Delaunay, J. (1995). A point mutation in the protein 4.2 gene (allele 4.2 Tozeur) associated with hereditary haemolytic anaemia. *Br. J. Haematol.*, **89,** 762–770

Hayman, E.G., Pierschbacher, M.D., and Ruoslahti E. (1985). Detachment of cells from culture substrate by soluble fibronectin peptides. *J. Cell Biol.*, **100,** 1948-1954

Heath, D.J., Christian, P., and Griffin, M. (2002). Involvement of tissue transglutaminase in the stabilisation of biomaterial/tissue interfaces important in medical devices. *Biomaterials*, **23,** 1519-1526

Hennies, H.C., Kuster ,W., Wiebe, V., Krebsova, A., and Reis A. (1998). Genotype phenotype correlation in autosomal recessive lamellar ichthyosis. Am. J. Hum. Genet., **62,** 1052-1061

Hettasch, J.M., and Greenberg, C.S. (1994). Analysis of the catalytic activity of human factor XIIIa by site-directed mutagenesis. *J. Biol. Chem.*, **269,** 28309-28313

Hettasch, J.M., Peoples, K.A., and Greenberg, C.S. (1997). Analysis of factor XIII substrate specificity using recombinant human factor XIII and tissue transglutaminase chimeras. *J. Biol. Chem.*,. **272,** 25149-25156

Hibi, M., Lin, A., Smeal, T., Minden, A., and Karin, M. (1993). Identification of an oncoprotein- and UV-responsive protein kinase that binds and potentiates the c-Jun activation domain. *Genes Dev.*, **7,** 2135-2148

Hitomi, K., Kanehiro, S., Ikura, K., and Maki, M. (1999). Characterization of recombinant mouse epidermal-type transglutaminase (TGase 3): regulation of its activity by proteolysis and guanine nucleotides. *J. Biochem.*, **125,** 1048-1054

Hitomi, K., Presland, R.B., Nakayama, T., Fleckman, P., Dale, B.A., and Maki, M. (2003). Analysis of epidermal-type transglutaminase (transglutaminase 3) in human stratified epithelia and cultured keratinocytes using monoclonal antibodies. *J. Dermatol. Sci.*, **32,**95-103

Hocking, D.C., Sottile, J., and Langenbach, K.J. (2000). Stimulation of integrin-mediated cell contractility by fibronectin polymerization. *J. Biol. Chem.*, **275,** 10673-10682

Hohenadl, C., Mann, K., Mayer, U., Timpl, R., Paulsson, M., and Aeschlimann, D. (1995). Two adjacent N-terminal glutamines of BM-40 (osteonectin, SPARC) act as amine acceptor sites in transglutaminaseC-catalyzed modification. *J. Biol. Chem.*, **270,** 23415-23420

Hohl, D. (1993). Expression patterns of loricrin in dermatological disorders. *Am. J. Dermatopathol.*, **15,** 20-27

Hornyak, T.A., and Shafer, I.A. (1991). Role of calcium ion in the generation of factor XIII activity. *Biochemistry,* **30**, 6175-6182

Hornyak, T.J., Bishop, P.D., and Shafer, J.A. (1989). Alpha-thrombin-catalyzed activation of human platelet factor XIII: relationship between proteolysis and factor XIIIa activity. *Biochemistry,* **28,** 7326-7332

Horwitz, A., Duggan, K., Buck, C., Beckerle, M.C., and Burridge, K. (1986). Interaction of plasma membrane fibronectin receptor with talin--a transmembrane linkage. *Nature,* **320,** 531-533

Howe, A.K., and Juliano, R.L. (1998). Distinct mechanisms mediate the initial and sustained phases of integrin-mediated activation of the Raf/MEK/mitogen-activated protein kinase cascade. *J. Biol. Chem.,* 1998 Oct 16;273(42):27268-74.

Howe, A.K., Aplin, A.E., and Juliano, R.L. (2002). Anchorage-dependent ERK signaling--mechanisms and consequences. *Curr. Opin. Genet. Dev.,* **12,** 30-35

Huber, M., Rettler, I., Bernasconi, K., Wyss, M., and Hohl, D. (1995). Lamellar ichthyosis is genetically heterogeneous--cases with normal keratinocyte transglutaminase. *J. Invest. Dermatol.,* **105,** 653-654

Hungerford, J.E., Compton, M.T., Matter, M.L., Hoffstrom, B.G., and Otey, C.A. (1996). Inhibition of pp125FAK in cultured fibroblasts results in apoptosis. *J. Cell Biol.,* **135,** 1383-1390

Huser, M., Luckett, J., Chiloeches, A., Mercer, K., Iwobi, M., Giblett, S., Sun, X.M., Brown, J., Marais, R., and Pritchard, C. (2001) MEK kinase activity is not necessary for Raf-1 function. *EMBO. J.,* **20,**1940-1951

Hynes, R.O., and Zhao, Q. (2000). The evolution of cell adhesion. *J. Cell Biol.,* 2000 **150,** F89-F96

Hynes, RO. (1999). Cell adhesion: old and new questions. *Trends Cell Biol.,* **9,** M33-37

Ichinose, A., and Davie, E.W. (1988). Characterization of the gene for the a subunit of human factor XIII (plasma transglutaminase), a blood coagulation factor. *Proc. Natl. Acad. Sci. U S A,* **85,** 5829-5833

Ichinose, A., Bottenus, X.E., and Davie, E.W. (1990). Structure of transglutaminases. *J. Biol Chem.,* **265**, 13411-13414

Ichinose, A., Hendrickson, L.E., Fujikawa, K., and Davie, E.W. (1986). Amino acid sequence of the a subunit of human factor XIII. *Biochemistry,* 25, 6900-6906

Ichinose, A., McMullen, B.A., Fujikawa, K., and Davie, E.W. (1986). Amino acid sequence of the b subunit of human factor XIII, a protein composed of ten repetitive segments. *Biochemistry*, **25,** 4633-4638

Igishi, T., Fukuhara, S., Patel, V., Katz, B.Z., Yamada, K.M., and Gutkind, J.S. (1999). Divergent signaling pathways link focal adhesion kinase to mitogen-activated protein kinase cascades. Evidence for a role of paxillin in c-Jun NH(2)-terminal kinase activation. *J. Biol. Chem.*, **274,** 30738-30746

Iismaa, S.E., Chung, L.P., Wu, M.J., Teller, D.C., Yee, V.C., and Graham, R.M. (1997). The core domain of the tissue transglutaminase gh hydrolyzes GTP and ATP. *Biochem.*, 36, 11655-11664

Iismaa, S.E., Holman, S., Wouters, M.A., Lorand, L., Graham, R.M., and Husain, A. (2003). Evolutionary specialization of a tryptophan indole group for transition-state stabilization by eukaryotic transglutaminases. *Proc. Natl. Acad. Sci. U S A,* 2003 Oct 28; 100(22): 12636-41. Epub 2003 Oct 17.

Iismaa, S.E., Wu, M.J., Nanda, N., Church, W.B., and Graham, R.M. (2000). GTP binding and signaling by Gh/transglutaminase II involves distinct residues in a unique GTP-binding pocket. *J. Biol. Chem.*, **275,** 18259-18265

Ikura, K., Nasu, T., Yokota, H., Tsuchiya, Y., Sasaki, R., and Chiba, H. (1988). Amino acid sequence of guinea pig liver transglutaminase from its cDNA sequence. *Biochemistry,* **27**, 2898-2905

Ikura, K., Tsuchiya, Y., Sasaki, R., and Chiba, H. (1990). Expression of guinea-pig liver transglutaminase cDNA in Escherichia coli. Amino-terminal N alpha-acetyl group is not essential for catalytic function of transglutaminases. *Eur. J. Biochem.*, **187,** 705-711

Im, M.J., Russell, M.A., and Feng, J.F. (1997). Transglutaminase II: a new class of GTP-binding protein with new biological functions. *Cell Signal.*, **7,** 477-482

Ishiguro, K., Kadomatsu, K., Kojima, T., Muramatsu, H., Tsuzuki, S., Nakamura, E., Kusugami, K., Saito, H., and Muramatsu, T. (2000). Syndecan-4 deficiency impairs focal adhesion formation only under restricted conditions. *J. Biol. Chem.*, **275,** 5249-5252

Isobe, T., Takahashi, H., Ueki, S., Takagi, J., and Saito, Y. (1999). Activity-independent cell adhesion to tissue-type transglutaminase is mediated by alpha4beta1 integrin. *Eur. J. Cell Biol.*, **78,** 876-883

Izzard, C.S., and Lochner, L.R. (1980). Formation of cell-to-substrate contacts during fibroblast motility: an interference-reflexion study. *J. Cell Sci.*, **42,** 81-116

Jensen, P.H., Lorand, L., Ebbesen, P., and Gliemann, J. (1993). Type-2 plasminogen-activator inhibitor is a substrate for trophoblast transglutaminase and factor XIIIa. Transglutaminase-catalyzed cross-linking to cellular and extracellular structures. *Eur. J. Biochem.*, **214,** 141-146

Jeong, J., Han, I., Lim, Y., Kim, J., Park, I., Woods, A., Couchman, J.R., and Oh, E.S. (2001). Rat embryo fibroblasts require both the cell-binding and the heparin-binding domains of fibronectin for survival. *Biochem. J.*, **356,** 531-537

Jeong, J.M., Murthy, S.N., Rade,k J.T.,and Lorand, L. (1995). The fibronectin-binding domain of transglutaminase. *J. Biol. Chem.*, **270,** 5654-5658

Johnson, T.S., El-Koraie, A.F., Skill, N.J., Baddour, N.M., El Nahas, A.M., Njloma, M., Adam, A.G., and Griffin, M. (2003). Tissue transglutaminase and the progression of human renal scarring. *J. Am. Soc. Nephrol.*, **14,** 2052-2062

Johnson, T.S., Griffin, M., Thomas, G.L., Skill, J., Cox, A., Yang, B, Nicholas, B., Birekbichler, P.A., Muchaneta-Kubara, C., and El Nahas, A.M. (1997). The role of transglutaminase in the rat subtotal nephrectomy model of renal fibrosis. *J. Clin. Invest.*, **99**, 2950-2960

Johnson, T.S., Knight, C.R., El-Alaoui, S., Mian, S., Rees, R.C., Gentile, V., Davies, P.J., and Griffin, M. (1994). Transfection of tissue transglutaminase into a highly malignant hamster fibrosarcoma leads to a reduced incidence of primary tumour growth. *Oncogene,* **9**, 2935-2942

Johnson, T.S., Skill, N.J., El Nahas, A.M., Oldroyd, S.D., Thomas, G.L., Douthwaite, J.A., Haylor, J.L., and Griffin, M. (1999). Transglutaminase transcription and antigen translocation in experimental renal scarring. *J. Am. Soc. Nephrol.*, **10,** 2146-2157

Jones, R.A., Nicholas, B., Mian, S., Davies, P.J.A., and Griffin, M. (1997). Reduced expression of tissue transglutaminase in a human endothelial cell line leads to changes in cell spreading, cell adhesion and reduced polymerisation of fibronectin. *J. Cell Sci.*, **110**, 2461-2472

Jost, M., Huggett, T.M., Kari, C., and Rodeck, U. (2001). Matrix-independent survival of human keratinocytes through an EGF receptor/MAPK-kinase-dependent pathway. *Mol. Biol. Cell.*, **12,** 1519-1527

Juprelle-Soret, M., Wattiaux-De Coninck, S., and Wattiaux, R. (1988). Subcellular localization of transglutaminase. Effect of collagen. *Biochem. J.*, **250,** 421-427

Jurgensen, K., Aeschlimann, D., Cavin, V., Genge, M., and Hunziker, E.B. (1997). A new biological glue for cartilage-cartilage interfaces: tissue transglutaminase. *J. Bone Joint. Surg. Am.*, **79,** 185-193

Kaartinen, M.T., Pirhonen, A., Linnala-Kankkunen, A., and Maenpaa, P.H. (1997). Transglutaminase-catalyzed cross-linking of osteopontin is inhibited by osteocalcin. *J. Biol. Chem.*, **272,** 22736-22741

Kaetsu, H., Hashiguchi, T., Foster, D., and Ichinose, A. (1996). Expression and release of the a and b subunits for human coagulation factor XIII in Baby Hamster Kidney (BHK) cells. *J. Biochem.*, **119**, 961-969

Kahlem, P., Terre, C., Green, H., and Djian, P. (1996). Peptides containing glutamine repeats as substrates for transglutaminase-catalyzed cross-linking: relevance to diseases of the nervous system. *Proc. Natl. Acad. Sci. U S A,* **93,** 14580-14585

Kalinin, A.E., Kajava, A.V., and Steinert, P.M. (2002). Epithelial barrier function: assembly and structural features of the cornified cell envelope. *Bioessays,* **24,** 789-800

Kantlehner, M., Schaffner, P., Finsinger, D., Meyer, J., Jonczyk, A., Diefenbach, B., Nies, B., Holzemann, G., Goodman, S.L., and Kessler, H. (2000). Surface coating with cyclic RGD peptides stimulates osteoblast adhesion and proliferation as well as bone formation. *Chembiochem.*, **18,** 107-114

Kanzaki, A., Yasunaga, M., Okamoto, N., Inoue, T., Yawata, A., Wada, H., Andoh, A., Hodohara, K., Fujiyama, Y., Bamba, T., Harano, T., Harano, K., and Yawata, Y. (1995). Band 4.2 Shiga: 317 CGC-->TGC in compound heterozygotes with 142 GCT-->ACT results in band 4.2 deficiency and microspherocytosis. *Br. J. Haematol.*, 91, 333–340

Kapila, Y.L., Wang, S., and Johnson, P.W. (1999). Mutations in the heparin binding domain of fibronectin in cooperation with the V region induce decreases in pp125(FAK) levels plus proteoglycan-mediated apoptosis via caspases. *J. Biol. Chem.*, **274,** 30906-30913

Karpuj, M.V., Becher, M.W., and Steinman, L. (2002). Evidence for a role for transglutaminase in Huntington's disease and the potential therapeutic implications. *Neurochem. Int.*, **40,** 31-36

Karpuj, M.V., Garren, H., Slunt, H., Price, D.L., Gusella, J., Becher, M.W., and Steinman, L. (1999). Transglutaminase aggregates huntingtin into nonamyloidogenic polymers, and its enzymatic activity increases in Huntington's disease brain nuclei. *Proc. Natl. Acad. Sci. U S A,* **96,** 7388-7393

Katoh, S., Nakagawa, N., Yano, Y., Satoh, K., Kohno, H., Ohkubo, Y., Suzuki, T., and Kitani, K. (1996). Hepatocyte growth factor induces transglutaminase activity that negatively regulates the growth signal in primary cultured hepatocytes. *Exp. Cell Res.*, **222,** 255-261

Katz, B.Z., Zamir, E., Bershadsky, A., Kam, Z., Yamada, K.M., and Geiger, B. (2000). Physical state of the extracellular matrix regulates the structure and molecular composition of cell-matrix adhesions. *Mol. Biol. Cell,* **11,** 1047-1060

Kiesselbach, T.H., and Wagner, R.H. (1972). Demonstration of factor XIII in human megakaryocytes by a fluorescent antibody technique. *Ann. N Y. Acad. Sci.,* **202,** 318-328

Kim, H.C., Lewis, M.S., Gorman, J.J., Park, S.C., Girard, J.E., Folk, J.E., and Chung, S.I. (1990). Protransglutaminase E from guinea pig skin. Isolation and partial characterization. *J. Biol. Chem.,* **265,** 21971-21978

Kim, S.Y., Chung, S.L., and Steinert, P.M. (1995). Highly active soluble processed forms of the transglutaminase 1 enzyme in epidermal keratinocytes. *J. Biol. Chem.,* **270,** 18026-18035

Kim, S.Y., Jeitner, T.M., and Steinert, P.M. (2002). Transglutaminases in disease. *Neurochem. Int.,* **40,** 85-103

Kim, S.Y., Kim, I.G., Chung, S.I., and Steinert, P.M. (1994). The structure of the transglutaminase 1 enzyme. Deletion cloning reveals domains that regulate its specific activity and substrate specificity. *J. Biol. Chem.,* **269,** 27979-27986

Kinsella, M.G., and Wight, T.N. (1990). Formation of high molecular weight dermatan sulfate proteoglycan in bovine aortic endothelial cell cultures. Evidence for transglutaminase-catalyzed cross-linking to fibronectin. *J. Biol. Chem.,* **265,** 17891-17898

Kitchens, C.S., and Newcomb, T.F. (1979). Factor XIII. *Medicine (Baltimore),* **58,** 413-429

Kleman, J.P., Aeschlimann, D., Paulsson, M., and van der Rest, M. (1995). Transglutaminase catalyzed cross-linking of fibrils of collagen V/IX in A204 rhabdomyosarcoma cells. *Biochemistry,* **34,** 13768-13775

Knight, C.R., Rees, R.C., and Griffin, M. (1991). Apoptosis: a potential role for cytosolic transglutaminase and its importance in tumour progression. *Biochim. Biophys. Acta.,* **1096,** 312-318

Knight, R.L., Hand, D., Piacentini, M., and Griffin, M. (1993).Characterization of the transglutaminase-mediated large molecular weight polymer from rat liver; its relationship to apoptosis. *Eur. J. Cell Biol.,* **60,** 210-216

Koivunen, E., Wang, B., Dickinson, C.D., and Ruoslahti, E. (1994). Peptides in cell adhesion research. *Methods Enzymol.,* **245,** 346-369

Kojima, S., Nara, K., and Rifkin, D.B. (1993). Requirement for transglutaminase in the activation of latent transforming growth factor-beta in bovine endothelial cells. *J. Cell Biol.*, **121,** 439-448

Kolch, W. (2000). Meaningful relationships: the regulation of the Ras/Raf/MEK/ERK pathway by protein interactions. *Biochem, J.*, **351,** 289-305

Kolch, W., Heidecker, G., Kochs, G., Hummel, R., Vahidi, H., Mischak, H., Finkenzeller, G., Marme, D., and Rapp, U.R. (1993). Protein kinase C alpha activates RAF-1 by direct phosphorylation. *Nature,* **364,** 249-252

Korsgren, C., and Cohen, C.M. (1986). Purification and properties of human erythrocyte band 4.2. Association with the cytoplasmic domain of band 3. *J. Biol. Chem.*, **261,** 5536-5543

Korsgren, C., and Cohen, C.M. (1988), Associations of human erythrocyte band 4.2. Binding to ankyrin and to the cytoplasmic domain of band 3. *J. Biol. Chem.*, **263,** 10212-10218

Korsgren, C., and Cohen, C.M. (1991). Organization of the gene for human erythrocyte membrane protein 4.2: structural similarities with the gene for the subunit-a of factor XIII. *Proc. Natl. Acad. Sci. USA.*, **88,** 4840-4844

Korsgren, C., Lawler, J., Lambert, S., Speicher, D., and Cohen, C.M. (1990). Complete amino acid sequence and homologies of human erythrocyte membrane protein band 4.2. *Proc. Natl. Acad. Sci. USA,* **87,** 613-617

Laemmli, U.K. (1970). Cleavages of structural proteins during the assembly of the head of bacteriophages T4. *Nature,* **227,** 680-685

Lai, T.S., Bielawska, A., Peoples, K.A., Hannun, Y.A., and Greenberg, C.S. (1997). *J. Biol. Chem.*, **272,** 16295-16300

Le Gall, M., Chambard, J.C., Breittmayer, J.P., Grall, D., Pouyssegur, J., and Van Obberghen-Schilling, E. (2000). The p42/p44 MAP kinase pathway prevents apoptosis induced by anchorage and serum removal. *Mol. Biol. Cell.*, **11,** 1103-1112

Le, M., Gohr, C.M., and Rosenthal, A.K. (2001). Transglutaminase participates in the incorporation of latent TGFbeta into the extracellular matrix of aging articular chondrocytes. *Connect. Tissue Res.*, **42,** 245-253

- **Lee, J.C., Laydon, J.T., McDonnell, P.C., Gallagher, T.F., Kumar, S., Green, D., McNulty, D., Blumenthal, M.J., Heys, J.R., and Landvatter S.W.** (1994). A protein kinase involved in the regulation of inflammatory cytokine biosynthesis. *Nature,* **372,** 739-746

Lee, K.N., Arnold, S.A., Birckbichler, P.J., Patterson, M.K. Jr, Fraij, B.M., Takeuchi, Y., and Carter, H.A. (1993). Site-directed mutagenesis of human tissue transglutaminase: Cys-277 is essential for transglutaminase activity but not for GTPase activity. Biochem. Biophys. Acta., **1202,** 1-6

Lee, K.N., Birckbichlerk, P.J., and Patterson, M.K. Jr. (1989). GTP hydrolysis by guinea pig liver transglutaminases. *Biochem. Biophys. Res. Commun.*, **162,** 1370-1375

Lee, S.C., Kim, I.G., Marekov, L.N., O'Keefe, E.J., Parry, D.A., and Steinert, P.M. (1993). The structure of human trichohyalin. Potential multiple roles as a functional EF-hand-like calcium-binding protein, a cornified cell envelope precursor, and an intermediate filament-associated (cross-linking) protein. *J. Biol. Chem.*, **268,** 12164-12176

LeMosy, E.K., Erickson, H.P., Beyer, W.F. Jr, Radek, J.T., Jeong, J.M., Murthy, S.N., and Lorand, L. (1992). Visualization of purified fibronectin-transglutaminase complexes. *J. Biol. Chem.*, **267,** 7880-7885

Lesort, M., Attanavanish K., Zhang J.W., and Johnson, G.V.W. (1998). Distinct nuclear localization and activity of tissue transglutaminase. *J. Biol. Chem.*, **273**, 11991-11994

Lesort, M., Chun, W., Johnson, G.V., and Ferrante, R.J. (1999). Tissue transglutaminase is increased in Huntington's disease brain. *J. Neurochem.*, **73,** 2018-2027

Lesort, M., Tucholski, J., Miller, M.L., and Johnson, G.V. (2000). Tissue transglutaminase: a possible role in neurodegenerative diseases. *Prog. Neurobiol.* **61**, 439-63

Lewis, J.M., Cheresh, D.A., and Schwartz, M.A. (1996). Protein kinase C regulates alpha v beta 5-dependent cytoskeletal associations and focal adhesion kinase phosphorylation. *J. Cell Biol.*, **134,** 1323-1332

Lopaciuk, S., Lovette, K.M., McDonagh, J., Chuang, H.Y., and McDonagh, D. (1976). Subcellular distribution of fibrinogen and factor XIII in human blood platelets. *Thromb. Res.*, **8,** 453-465

Lorand, L. (1986). Activation of blood coagulation factor XIII. *Ann. N Y. Acad. Sci.*, **485,** 144-58

Lorand, L., and Conrad, S.M. (1984). Transglutaminases. *Mol. Cell Biochem.*, **58,** 9-35

Lorand, L., and Graham, R.M. (2003). Transglutaminases: crosslinking enzymes with pleiotropic functions. *Nat. Rev. Mol. Cell Biol.*, **4,** 140-156

Lorand, L., Dailey, J.E., and Turner, P.M. (1988). Fibronectin as a carrier for the transglutaminase from human erythrocytes. *Proc. Natl. Acad. Sci. U S A,* **85,** 1057-1059

Lorand, L., Losowsky, M.S., and Miloszewski, K.J. (1980). Human factor XIII: fibrin-stabilizing factor. *Prog. Hemost. Thromb.,*. **5,** 245-290

Lowry, O.H., Rosebrough, N.J., Farr, A.L. and Randall, R.J. (1951). Protein measurement with the Folin-Phenol reagents. *J. Biol. Chem.,* **193,** 265-275

Lu, S., Saydak, M., Gentile, V., Stein, J.P., and Davies, J.P.A. (1995). Isolation and characterization of the human tissue transglutaminase gene promoter. *J. Biol. Chem.,* **270**, 9748-9756

Lyman, S., Gilmore, A., Burridge, K., Gidwitz, S., and White, G.C. 2nd. (1997). Integrin-mediated activation of focal adhesion kinase is independent of focal adhesion formation or integrin activation. Studies with activated and inhibitory beta3 cytoplasmic domain mutants. *J. Biol. Chem.,* **272,** 22538-22547

Lyons, R.M., Keski-Oja, J., and Moses, H.L. (1988). Proteolytic activation of latent transforming growth factor-beta from fibroblast-conditioned medium. *J. Cell Biol.,* **106,** 1659-1665

Marais, R., Light, Y., Paterson, H.F., and Marshall, C.J. (1995). Ras recruits Raf-1 to the plasma membrane for activation by tyrosine phosphorylation. *EMBO J.,* **14,** 3136-3145

Martinet, N., Kim, H.C., Girard, J.E., Nigra, T.P., Strong, D.H., Chung, S.I., and Folk, J.E. (1988). Epidermal and hair follicle transglutaminases. Partial characterization of soluble enzymes in newborn mouse skin. *J. Biol. Chem.,* **263,** 4236-4241

Martinez, J., Chalupowicz, D.G., Roush, R.K., Sheth, A., and Barsigian, C. (1994). Transglutaminase-mediated processing of fibronectin by endothelial cell monolayers. *Biochemistry,* **33**, 2538-2545

Marvin, K.W., George, M.D., Fujimoto, W., Saunders, N.A., Bernacki, S.H., and Jetten, A.M. (1992). Cornifin, a cross-linked envelope precursor in keratinocytes that is down-regulated by retinoids. *Proc. Natl. Acad. Sci. U S A,* **89,** 11026-11030

Massague, J. (1990). The transforming growth factor-beta family. *Annu. Rev. Cell Biol.,* **6,** 597-641

Matschinsky, F.M. (1996). Banting Lecture 1995. A lesson in metabolic regulation inspired by the glucokinase glucose sensor paradigm. *Diabetes,* **45,** 223-241

Matsuki, M., Yamashita, F., Ishida-Yamamoto, A., Yamada, K., Kinoshita, C., Fushiki, S., Ueda, E., Morishima, Y., Tabata, K., Telci, U., Yasuno, H., Hashida, M., Iizuka, H., Ikawa, M., Okabe, M., Kondoh, G., Kinoshita, T., Takeda, J., and Yamanishi, K. (1998). Defective stratum corneum and early neonatal death in mice lacking the gene for transglutaminase 1 (keratinocyte transglutaminase). *Proc. Natl. Acad. Sci. U S A.*, **95,** 1044-1049

McCawley, L.J., and Matrisian, L.M. (2001). Matrix metalloproteinases: they're not just for matrix anymore! *Curr. Opin. Cell Biol.*, **13,** 534-540

McGill, G., Shimamura, A., Bates, R.C., Savage, R.E., and Fisher, D.E. (1997). Loss of matrix adhesion triggers rapid transformation-selective apoptosis in fibroblasts. *J. Cell Biol.*, **138,** 901-911

McKeown-Longo, P.J., and Mosher, D.F. (1983). Binding of plasma fibronectin to cell layers of human skin fibroblasts.*J. Cell Biol.*, **97,** 466-472

McKeown-Longo, P.J., and Mosher, D.F. (1984). Mechanism of formation of disulfide-bonded multimers of plasma fibronectin in cell layers of cultured human fibroblasts. *J. Biol. Chem.*, **259,** 12210-12215

Mearns, B., Nanda, N., Michalicek, J., Iismaa, S., and Graham, R. (2002). Impaired wound healing and altered fibroblast cytoskeletal dynamics in Gh knockout mice. *Minerva Biotecnologica* **14,** 218

Mehta, K. (1994). High levels of transglutaminase expression in doxorubicin-resistant human breast carcinoma cells. *Int. J. Cancer,* **58,** 400-406

Melino, G., Annicchiarico-Petruzzelli, M., Piredda, L., Candi, E., Gentile, V., Davies, P.J., and Piacentini, M. (1994). Tissue transglutaminase and apoptosis: sense and antisense transfection studies with human neuroblastoma cells. *Mol. Cell Biol.*, **14,** 6584-6596

Meredith, J.E. Jr, Fazeli, B., and Schwartz, M.A. (1993). The extracellular matrix as a cell survival factor. *Mol. Biol. Cell.*, **9,** 953-961

Michel, J.B. (2003). Anoikis in the cardiovascular system: known and unknown extracellular mediators. *Arterioscler. Thromb. Vasc. Biol.*, **23,** 2146-2154

Midwood, K.S., Williams, L.V., and Schwarzbauer, J.E. (2004). Tissue repair and the dynamics of the extracellular matrix. *Int. J. Biochem. Cell Biol.*, **36,** 1031-1037

Mikula, M., Schreiber, M., Husak, Z., Kucerova, L., Ruth, J., Wieser, R., Zatloukal, K., Beug, H., Wagner, E.F., and Baccarini, M. (2001). Embryonic lethality and fetal liver apoptosis in mice lacking the c-raf-1 gene. *EMBO. J.*, **20,** 1952-1962

Mirza, A., Liu, S.H., Frizell, E., Zhu, J., Maddukuri, S., Martinez, J., Davies, P., Schwarting, R., Norton, P., and Zern, M.A. (1997). A role for tissue transglutaminase in hepatic injury and fibrogenesis, and its regulation by NF-KB. *Am. J. Phys. Gastro. Liver Phys.*, **35**, G281-G288

Mishra, S., and Murphy, L.J. (2004). Tissue transglutaminase has intrinsic kinase activity: identification of transglutaminase 2 as an insulin-like growth factor-binding protein-3 kinase. *J. Biol. Chem.*, **279,** 23863-23868

Miyamoto, S., Katz, B.Z., Lafrenie, R.M., and Yamada, K.M. (1998). Fibronectin and integrins in cell adhesion, signaling, and morphogenesis. *Ann. N. Y. Acad. Sci.*, **857,** 119-129

Miyamoto, S., Teramoto, H., Coso, O.A., Gutkind, J.S., Burbelo, P.D., Akiyama, S.K., and Yamada, K.M. (1995). Integrin function: molecular hierarchies of cytoskeletal and signaling molecules. *J. Cell. Biol.*, **131,** 791-805

Molberg, O., Mcadam, S.N., Korner, R., Quarsten, H., Kristiansen, C., Madsen, L., Fugger, L., Scott, H., Noren, O., Roepstorff, P., Lundin, K.E., Sjostrom, H., and Sollid, L.M. (1998). Tissue transglutaminase selectively modifies gliadin peptides that are recognized by gut-derived T cells in celiac disease. *Nat. Med.*, **4,** 713-717

Monsonego, A., Shani, Y., Friedmann, I., Paas, Y., Eizenberg, O., and Schwartz, M. (1997). Expression of GTP-dependent and GTP-independent tissue-type transglutaminase in cytokine-treated rat brain astrocytes. *J. Biol. Chem.*, **272,** 3724-3732

Moore, W.T.J., Murtaugh, M.P., and Davies P.J.A. (1984). Retinoic acid-induced expression of tissue transglutaminase in mouse peritoneal macrophages. *J. Biol. Chem.*, **259**, 12794-12802

Mosher, D.F. (1984). Cross-linking of fibronectin to collagenous proteins. *Mol. Cell Biochem.*, **58,** 63-68

Mosher, D.F. (1984). Physiology of fibronectin. *Annu. Rev. Med.*, **35,** 561-575

Mosher, D.F., and Schad, P.E. (1979). Cross-linking of fibronectin to collagen by blood coagulation Factor XIIIa. *J. Clin. Invest.*, **64,** 781-787

Mosher, D.F., Fogerty, F.J., Chernousov, M.A., and Barry, E.L. (1991). Assembly of fibronectin into extracellular matrix. *Ann. N Y Acad. Sci.*, **614,** 167-180

Mostafavi-Pour, Z., Askari, A., Whittard, J.D., and Humphries, M.J. (2001). Identification of a novel heparin-binding site in the alternatively spliced IIICS region of fibronectin: roles of integrins and proteoglycans in cell adhesion to fibronectin splice variants. *Matrix Biol.*, **20,** 63-73

Mould, A.P., Komoriya, A., Yamada, K.M., and Humphries, M.J. (1991). The CS5 peptide is a second site in the IIICS region of fibronectin recognized by the integrin $\alpha 4\beta 1$. Inhibition of $\alpha 4\beta 1$ function by RGD peptide homologues. *J. Biol. Chem.*, **266,** 3579–3585

Mouro-Chanteloup, I., Delaunay, J., Gane, P., Nicolas, V., Johansen, M., Brown, E.J., Peters, L.L., Van Kim, C.L., Cartron, J.P., and Colin, Y. (2003). Evidence that the red cell skeleton protein 4.2 interacts with the Rh membrane complex member CD47.*Blood,* **101,** 338-344

Moyano, J.V., Carnemolla, B., Dominguez-Jimenez, C., Garcia-Gila, M., Albar, J.P., Sanchez-Aparicio, P., Leprini, A., Querze, G., Zardi, L., and Garcia-Pardo, A. (1997). Fibronectin type III5 repeat contains a novel cell adhesion sequence, KLDAPT, which binds activated alpha4beta1 and alpha4beta7 integrins. *J. Biol. Chem.*, **272,** 24832-24836

Mukherjee, D.C., Agrawal, A.K., Manjunath, R., and Mukherjee, A.B. (1983). Suppression of epididymal sperm antigenicity in the rabbit by uteroglobin and transglutaminase in vitro. *Science,* **219,** 989-991

Murtaugh, M.P., Mehta, K., Johnson, J., Myers, M., Juliano, R.L., and Davies, P.J. (1983). Induction of tissue transglutaminase in mouse peritoneal macrophages. *J. Biol. Chem.*, **258,** 11074-11081

Murthy, S.N., Iismaa, S., Begg, G., Freymann, D.M., Graham, R.M., and Lorand, L. (2002). Conserved tryptophan in the core domain of transglutaminase is essential for catalytic activity. *Proc. Natl. Acad. Sci. USA,* **99,** 2738-2742

Murthy, S.N., Wilson, J.H., Lukas, T.J., Kuret, J., and Lorand, L. (1998). Cross-linking sites of the human tau protein, probed by reactions with human transglutaminase. *J. Neurochem.*, **71,** 2607-1264

Muszbek, L., Yee, V.C., Hevessy, Z. (1999). Blood coagulation factor XIII: structure and function. *Thromb. Res.*, **94,** 271-305

Nakaoka, H., Perez, D.M., Baek, K.J., Das, T., Husain, A., Misono, K., Im, M.J., and Graham, R.M. (1994). Gh: a GTP-binding protein with transglutaminase activity and receptor signaling function. *Science*, **264**, 1593-1596

Nanda, N., Iismaa, S.E., Owens, W.A., Husain, A., Mackay, F., and Graham, R.M. (2001). Targeted inactivation of Gh/tissue transglutaminase II. *J. Biol. Chem.*, **276,** 20673-20678

Nara, K., Ito, S., Ito, T., Suzuki, Y., Ghoneim, M.A., Tachibana, S., and Hirose, S. (1994). Elastase inhibitor elafin is a new type of proteinase inhibitor which has a transglutaminase-mediated anchoring sequence termed "cementoin". *J. Biochem. (Tokyo),* **115,** 441-448

Naski, M.C., Lorand, L., and Shafer, J.A. (1991). Role of calcium ion in the generation of factor XIII activity. *Biochemistry,* **30,** 6175-6182

Nemes, Z., Marekov, L.N., Fesus, L., and Steinert, P.M. (1999). A novel function for transglutaminase 1: attachment of long-chain omega-hydroxyceramides to involucrin by ester bond formation. *Proc. Natl. Acad. Sci. US A,* **96,** 8402-8407

Nicholas, B., Smethurst, P., Verderio, E., Jones, R., and Griffin, M. (2003). Cross-linking of cellular proteins by tissue transglutaminase during necrotic cell death: a mechanism for maintaining tissue integrity. *Biochem. J.,* **371,** 413-422

Nunes, I., Gleizes, P.E., Metz, C.N., and Rifkin, D.B. (1997). Latent transforming growth factor-beta binding protein domains involved in activation and transglutaminase-dependent cross-linking of latent transforming growth factor-beta. *J. Cell Biol.* **136,** 1151-1163

Nurminskaya, M., Magee, C., Nurminsky, D., and Linsenmayer, T.F. (1998). Plasma transglutaminase in hypertrophic chondrocytes: expression and cell-specific intracellular activation produce cell death and externalization. *J. Cell Biol.,* **142,** 1135-1144

Oh, E.S., Woods, A., and Couchman J.R. (1997a). Multimerization of the cytoplasmic domain of syndecan-4 is required for its ability to activate protein kinase C. *J. Biol. Chem.,* **272,** 11805-11811

Oh, E.S., Woods, A., and Couchman, J.R. (1997b). Syndecan-4 proteoglycan regulates the distribution and activity of protein kinase C. *J. Cell Biol.,* **272,** 8133-8136

Oktay, M., Wary, K.K., Dans, M., Birge, R.B., and Giancotti, F.G. (1999). Integrin-mediated activation of focal adhesion kinase is required for signaling to Jun NH2-terminal kinase and progression through the G1 phase of the cell cycle. *J. Cell Biol.,* **145,** 1461-1469

Oliverio, S., Amendola, A., Di Sano, F., Farrace, M.G., Fesus, L., Nemes, Z., Piredda, L., Spinedi, A., and Piacentini, M. (1997). Tissue transglutaminase-dependent posttranslational modification of the retinoblastoma gene product in promonocytic cells undergoing apoptosis. *Mol. Cell Biol.,* **17,** 6040-5048.

Paonessa, G., Metafora, S., Tajana, G., Abrescia, P., De Santis, A., Gentile, V., and Porta R. (1984). Transglutaminase-mediated modifications of the rat sperm surface in vitro. *Science,* **226,** 852-855

Parameswaran, K.N., Cheng, X.F., Chen, E.C., Velasco, P.T. Wilson, J.H., and Lorand, L. (1997). Hydrolysis of the epsilon-gamma isopeptides by cytosolic

transglutaminases and by coagulation factor XIIIa. *J. Biol. Chem.*, **272**, 10311-10317

Park, E.S., Won, J.H., Han, K.J., Suh, P.G., Ryu, S.H., Lee, H.S., Yun, H.Y., Kwon, N.S., and Baek, K.J. (1998). Phospholipase C-delta1 and oxytocin receptor signalling: evidence of its role as an effector. *Biochem. J.*, **331,** 283-289

Paulsson, M., Aumailley, M., Deutzmann, R., Timpl, R., Beck, K., and Engel, J. (1987). Laminin-nidogen complex. Extraction with chelating agents and structural characterization. *Eur. J. Biochem.*, **166,** 11-19

Payne, D.M., Rossamando, A.J., Martino, P., Erickson, A.K., Her, J.H., Shabanowitz, J., Hunt, D.F., Weber, M.J., and Sturgill, T.W. (1991). Identification of a regulatory phosphorylation sites in p42/mitogen-activated protein kinase (MAP kinase). *EMBO J.*,, **10,** 885-892

Peng, X., Zhang, Y., Zhang, H., Graner, S., Williams, J.F., Levitt, M.L., and Lokshin, A. (1999). Interaction of tissue transglutaminase with nuclear transport protein importin-alpha3. *FEBS Lett.*, **446,** 35-39

Peters, L.L., Jindel, H.K., Gwynn, B., Korsgren, C., John, K.M., Lux, S.E., Mohandas, N., Cohen, C.M., Cho, M.R., Golan, D.E., and Brugnara, C. (1999). Mild spherocytosis and altered red cell ion transport in protein 4. 2-null mice. *J. Clin. Invest.*, **103,** 1527-1537

Petruzzelli, L., Takami, M., and Humes, H.D. (1999). Structure and function of cell adhesion molecules. *Am. J. Med.*, **106,** 467-476

Phillips, M.A., Stewart, B.E., Qin, Q., Chakravarty, R., Floyd, E.E., Jetten, A.M., and Rice, R.H. (1990). Primary structure of keratinocyte transglutaminase. *Proc. Nat. Acad. Sci. USA,* **87**, 9333-9337

Piacentini, M., and Colizzi, V. (1999). Tissue transglutaminase: apoptosis versus autoimmunity. *Immunol. Today,* **20,** 130-134

Piacentini, M., Farrace, M.G., Hassan, C., Serafini, B., and Autuori, F. (1999). 'Tissue' transglutaminase release from apoptotic cells into extracellular matrix during human liver fibrogenesis. *J. Pathol.*, **189,** 92-98

Pierschbacher, M.D., and Ruoslahti, E. (1984) Variants of the cell recognition site of fibronectin that retain attachment-promoting activity. *Proc. Natl. Acad. Sci. USA*, **19,** 5985-5988

Pisano, J.J., Finlayson, J.S., and Peyton, M.P. (1968). Cross-link in fibrin polymerized by factor 13: epsilon-(gamma-glutamyl)lysine. *Science,* **160,** 892-93

Polakowska, R.R., Eickbush, T., Falciano, V., Razvi, F., and Goldsmith, L.A. (1992). Organization and evolution of the human epidermal keratinocyte transglutaminase I gene. *Proc. Natl. Acad. Sci. U S A,* **89,** 4476-4480

Porta, R., Esposito, C., De Santis, A., Fusco, A., Iannone, M., and Metafora, S. (1986). Sperm maturation in human semen: role of transglutaminase-mediated reactions. *Biol. Reprod.,* **35,** 965-970

Porta, R., Gentile, V., Esposito, C., Marinello, L., and Auriccjio, S. (1990). Cereal dietary proteins with sites for cross-linking by transglutaminase. *Phytochemistry,* **29,** 2801-2804

Potapova, O., Haghighi, A., Bost, F., Liu, C., Birrer, M.J., Gjerset, R., Mercola, D. (1997). The Jun kinase/stress-activated protein kinase pathway functions to regulate DNA repair and inhibition of the pathway sensitizes tumor cells to cisplatin. *J. Biol. Chem.,* **272,** 14041-14044

Prince, C.W., Dickie, D., and Krumdieck, C.L. (1991). Osteopontin, a substrate for transglutaminase and factor XIII activity. *Biochem. Biophys. Res. Commun.,* **177,** 1205-1210

Puleo, D.A., and Bizios, R. (1991). RGDS tetrapeptide binds to osteoblasts and inhibits fibronectin-mediated adhesion. *Bone,* **12,** 271-276

Pytela, R., Pierschbacher, M.D., and Ruoslahti E. (1985a). A 125/115-kDa cell surface receptor specific for vitronectin interacts with the arginine-glycine-aspartic acid adhesion sequence derived from fibronectin. *Proc. Natl. Acad. Sci. U S A,* **82,** 5766-5770

Pytela, R., Pierschbacher, M.D., and Ruoslahti, E. (1985b). Identification and isolation of a 140 kd cell surface glycoprotein with properties expected of a fibronectin receptor. *Cell,* **40,** 191-198

Qian, R.Q., and Glanville, R.W. (1997). Alignment of fibrillin molecules in elastic microfibrils is defined by transglutaminase-derived cross-links. *Biochemistry,* **36,** 15841-15847

Radek, J.T., Jeong, J-M., Murthy, S.N.P., Ingham, K.C. and Lorand, L. (1993). Affinity of human erythrocyte transglutaminase for a 42-kDa gelatin-binding fragment of human plasma fibronectin. *Proc. Nad. Acad. Sci. USA,* **90,** 3152-3156

Raghunath, M., Bachi, T., Meuli, M., Altermatt, S., Gobet, R., Bruckner-Tuderman, L., and Steinmann, B. (1996a). Fibrillin and elastin expression in skin regenerating from cultured keratinocyte autografts: morphogenesis of microfibrils begins at the dermo-epidermal junction and precedes elastic fiber formation. *J. Invest. Dermatol.,* **106,** 1090-1095

Raghunath, M., Cankay, R., Kubitscheck, U., Fauteck, J.D., Mayne, R., Aeschlimann, D., and Schlotzer-Schrehardt, U. (1999). Transglutaminase activity in the eye: cross-linking in epithelia and connective tissue structures. *Invest. Ophthalmol.* Vis. Sci., **40,** 2780-2787

Raghunath, M., Hopfner, B., Aeschlimann, D., Luthi, U., Meuli, M., Altermatt, S., Gobet, R., Bruckner-Tuderman, L., and Steinmann, B. (1996b).Cross-linking of the dermo-epidermal junction of skin regenerating from keratinocyte autografts. Anchoring fibrils are a target for tissue transglutaminase. *J. Clin. Invest.*, **98,** 1174-1184

Rasmussen, L.K., Sorensen, E.S., Petersen, T.E., Gliemann, J., and Jensen, P.H. (1994). Identification of glutamine and lysine residues in Alzheimer amyloid beta A4 peptide responsible for transglutaminase-catalysed homopolymerization and cross-linking to alpha 2M receptor. *FEBS Lett.*, **338,** 161-166

Reed, G.L., Matsueda, G.R., and Haber, E. (1991). Fibrin-fibrin and alpha 2-antiplasmin-fibrin cross-linking by platelet factor XIII increases the resistance of platelet clots to fibrinolysis. *Trans. Assoc. Am. Physicians,* **104,** 21-28

Rice, R.H., and Green, H. (1977). The cornified envelope of terminally differentiated human epidermal keratinocytes consists of cross-linked protein. *Cell,* **11,** 417-22

Risinger, M.A., Dotimas, E.M., and Cohen, C.M. (1992). Human erythrocyte protein 4.2, a high copy number membrane protein, is N-myristylated. *J. Biol. Chem.*, **267,** 5680-5685

Risinger, M.A., Korsgren, C., and Cohen, C.M. (1996). Role of N-myristylation in targeting of band 4.2 (pallidin) in nonerythroid cells. *Exp. Cell Res.*, **229,** 421-431

Ritchie, H., Lawrie, L.C., Mosesson, M.W., and Booth, N.A. (2001). Characterization of crosslinking sites in fibrinogen for plasminogen activator inhibitor 2 (PAI-2). *Ann. N. Y. Acad. Sci.*, **936,** 215-218

Romberger, D.J. (1997). Fibronectin. *Int. J. Biochem. Cell. Biol.*, **29,** 939-943
Ruoslahti, E., and Pierschbacher, M.D. (1987). New perspectives in cell adhesion: RGD and integrins. *Science,* **238,** 491-497

Rybicki, A.C., Schwartz, R.S., Qiu, J.J., and Gilman, J.G. (1994). Molecular cloning of mouse erythrocyte protein 4.2: a membrane protein with strong homology with the transglutaminase supergene family. *Mamm. Genome,* **5,** 438-445

Sakata, Y., and Aoki, N. (1980). Cross-linking of alpha 2-plasmin inhibitor to fibrin by fibrin-stabilizing factor. *J. Clin. Invest.*, **65,** 290-297

Sanchez-Aparicio, P., Dominguez-Jimenez, C., and Garcia-Pardo, A. (1994). Activation of the alpha 4 beta 1 integrin through the beta 1 subunit induces recognition of the RGDS sequence in fibronectin. *J. Cell Biol.,* **126,** 271-279

Sane, D.C., Moser, T.L., and Greenberg, C.S. (1991). Vitronectin in the substratum of endothelial cells is cross-linked and phosphorylated. Biochem. *Biophys. Res. Commun.,* **174,** 465-469

Sane, D.C., Moser, T.L., Pippen, A.M.M., Parker, C.J, Achyuthan, K.E., and Greenberg, C.S. (1988). Vitronectin is substrate for transglutaminases. *Biochem. Biophys. Res. Commun.,* **57,** 115-120

Saoncella, S., Echtermeyer, F., Denhez, F., Nowlen, J.K., Mosher, D.F., Robinson, S.D., Hynes, R.O., and Goetinck, P.F. (1999). Syndecan-4 signals cooperatively with integrins in a Rho-dependent manner in the assembly of focal adhesions and actin stress fibers. *Proc. Natl. Acad. Sci. USA,* **96,** 2805-2810

Sardy, M., Karpati, S., Merkl, B., Paulsson, M., and Smyth N. (2002). Epidermal transglutaminase (TGase 3) is the autoantigen of dermatitis herpetiformis. *J. Exp. Med.,* **195,**747-757

Sarkar, N.K., Clarke D.D., and Waelsch, H. (1957). An enzymically catalyzed incorporation of amines into proteins. *Biochim. Biophys. Acta.,* **25,** 451-452

Schaller, M.D., Hildebrand, J.D., Shannon, J.D., Fox ,J.W., Vines, R.R., and Parsons, J.T. (1994). Autophosphorylation of the focal adhesion kinase, pp125FAK, directs SH2-dependent binding of pp60src. *Mol. Cell. Biol.,* **14,** 1680-1688

Schittny, J.C., Paulsson, M., Vallan, C., Burri, P.H., Kedei, N., and Aeschlimann, D. (1997). Protein cross-linking mediated by tissue transglutaminase correlates with the maturation of extracellular matrices during lung development. *Am. J. Respir. Cell Mol. Biol.,* **17,** 334-343

Schlaepfer, D.D., Hanks, S.K., Hunter, T., van der Geer, P. (1994). Integrin-mediated signal transduction linked to Ras pathway by GRB2 binding to focal adhesion kinase. *Nature,* **372,** 786-791

Schlaepfer, D.D., Hauck, C.R., and Sieg, D.J. (1999). Signaling through focal adhesion kinase. *Prog. Biophys. Mol. Biol.,* **71,** 435-478

Schroff, G., Neumann, C., and Sorg, C. (1981). Transglutaminase as a marker for subsets of murine macrophages. *Eur. J. Immunol.,* **11,** 637-642

Schwartz, M.L., Pizzo, S.V., Hill, R.L., and McKee, P.A. (1973). Human Factor XIII from plasma and platelets. Molecular weights, subunit structures, proteolytic activation, and cross-linking of fibrinogen and fibrin. *J. Biol. Chem.,* **248,** 1395-1407

Schwarzbauer, J.E. (1991). Alternative splicing of fibronectin: three variants, three functions. *Bioessays,* **13,** 527-533

Schwarzbauer, J.E., and Sechler, J.L. (1999). Fibronectin fibrillogenesis: a paradigm for extracellular matrix assembly. *Curr. Opin. Cell Biol.,* **5,** 622-627

Schwarzbauer, J.E., Spencer, C.S., and Wilson, C.L. (1989). Selective secretion of alternatively spliced fibronectin variants. *J. Cell Biol.,* **109,** 3445-3453

Sechler, J.L., and Schwarzbauer, J.E. (1998). Control of cell cycle progression by fibronectin matrix architecture. *J. Biol. Chem.,* **273,** 25533-25536

Sechler, J.L., Cumiskey, A.M., Gazzola, D.M., and Schwarzbauer, J.E. (2000). A novel RGD-independent fibronectin assembly pathway initiated by alpha4beta1 integrin binding to the alternatively spliced V region. *J. Cell Sci.,* **113,** 1491-1498

Seitz, J., Keppler, C., Huntemann, S., Rausch, U., and Aumuller, G. (1991). Purification and molecular characterisation of a secretory transglutaminase from coagulating gland of the rat. *Biochim. Biophys. Acta.,* **1078,** 139-146

Seitz, J., Keppler, C., Rausch, U., and Aumuller, G. (1990). Immunohistochemistry of secretory transglutaminase from rodent prostate. *Histochemistry,* **93,** 525-530

Seiving, B., Ohlsson, K., Linder, C., and Stenberg, P. (1991). Transglutaminase differentiation during maturation of human blood monocytes to macrophages. *Eur. J. Haematol.,* **46,** 263-271

Selkoe, D.J. (2002). Introducing transglutaminase into the study of Alzheimer's disease. A personal look back. *Neurochem. Int.,* **40,** 13-16

Sener, A., Dunlop, M.E., Gomis, R., Mathias, P.C., Malaisse-Lagae, F., and Malaisse, W.J. (1985). Role of transglutaminase in insulin release. Study with glycine and sarcosine methylesters. *Endocrinology,* **117,** 237-242

Shainoff, J.R., Urbanic, D.A., and DiBello, PM. (1991). Immunoelectrophoretic characterizations of the cross-linking of fibrinogen and fibrin by factor XIIIa and tissue transglutaminase. Identification of a rapid mode of hybrid alpha-/gamma-chain cross-linking that is promoted by the gamma-chain cross-linking. *J. Biol. Chem.,* **266,** 6429-6437

Sharma, A., Askari, J.A., Humphries, M.J., Jones, E.Y., and Stuart, D.I. (1999). Crystal structure of a heparin- and integrin-binding segment of human fibronectin.
EMBO J., **18,** 1468-1479

Shi, Q., and Boettiger, D. (2003). A novel mode for integrin-mediated signaling: tethering is required for phosphorylation of FAK Y397. *Mol. Biol. Cell.*, **14,** 4306-4315

Simon, M., and Green, H. (1988). The glutamine residues reactive in transglutaminase-catalyzed cross-linking of involucrin. *J. Biol. Chem.*, **263,** 18093-18098

Simon, M., Haftek, M., Sebbag, M., Montezin, M., Girbal-Neuhauser, E., Schmitt, D., and Serre, G. (1996). Evidence that filaggrin is a component of cornified cell envelopes in human plantar epidermis. *Biochem. J.*, **317,** 173-177

Sims, P.J., M.H. Ginsberg, E.F. Plow, and S.J. Shattil. (1991). Effect of platelet activation on the conformation of the plasma membrane glycoprotein IIb-IIIa complex. *J. Biol. Chem.* 266: 7345-7352

Singer, A.J., and Clark, R.A. (1999). Cutaneous wound healing. *N. Engl. J. Med.*, **341,** 738-746

Singh, U.S., Erickson, J.W., and Cerione, R.A. (1995). Identification and biochemical characterization of an 80 kilodalton GTP-binding/transglutaminase from rabbit liver nuclei. *Biochemistry,* **34,** 15863-15871

Slife, C.W, Dorsett, M.D. and Tillotson M.L. (1986). Sub-cellular location and identification of a large molecular weight substrate for the liver plasma membrane transglutaminase. *J. Biol. Chem.*, **261**, 3451-3456

Slife, C.W, Dorsett, M.D., Bouquett, G.T., Register, A., Taylor, E., and Conroy, S. (1985). Subcellular localization of a membrane-associated transglutaminase activity in rat liver. *Arch. Biochem. Biophys.*, **241**, 329-336

Small, K., Feng, J.F., Lorenz, J., Donnelly, E.T., Yu, A., Im, M.J., Dorn, G.W. 2nd., and Liggett, S.B. (1999). Cardiac specific overexpression of transglutaminase II (G(h)) results in a unique hypertrophy phenotype independent of phospholipase C activation. *J. Biol. Chem.*, **274,** 21291-21296

Smith, A., Ramos-Morales, F., Ashworth, A., and Collins, M. (1997). A role for JNK/SAPK in proliferation, but not apoptosis, of IL-3-dependent cells. *Curr. Biol.*, **7,** 893-896

Sohn, J., Kim, T.I., Yoon, Y.H., Kim, J.Y., and Kim, S.Y. (2003). Novel transglutaminase inhibitors reverse the inflammation of allergic conjunctivitis. *J. Clin. Invest.*, **111,** 121–128

Sorensen, E.S., Rasmussen, L.K., Moller, L., Jensen, P.H., Hojrup, P., and Petersen, T.E. (1994). Localization of transglutaminase-reactive glutamine residues in bovine osteopontin. *Biochem. J.*, **304,** 13-16

Sottile, J., Schwarzbauer, J., Selegue, J., and Mosher, D.F. (1991). Five type I modules of fibronectin form a functional unit that binds to fibroblasts and Staphylococcus aureus. *J. Biol. Chem.*, **266,** 12840-12843

Steinert P.M., and Marekov L.N. (1995). The proteins Elafin, Filaggrin, Keratin Intermediate Filaments, Loricrin and Small Proline-rich Proteins 1 and 2 are isodipeptide cross-linked components of the human epidermal cornified cell envelope. *J Biol. Chem.*, **270**, 17702-17711

Stephens, P., Grenard, P., Aeschlimann, P., Langley, M., Blain, E., Errington, R., Kipling, D., Thomas, D., and Aeschlimann, D. (2004). Crosslinking and G-protein functions of transglutaminase 2 contribute differentially to fibroblast wound healing responses. *J. Cell Sci.*, **117,** 3389-3403

Stephens, P.E., Ortlepp, S., Perkins, V.C., Robinson, M.K., and Kirby, H. (2000). Expression of a soluble functional form of the integrin alpha4beta1 in mammalian cells. *Cell Adhes. Commun.*, **7,** 377-390

Sung, L.A., Chien, S., Chang, L.S., Lambert, K., Bliss, S.A., Bouhassira, E.E., Nagel, R.L., Schwartz, R.S., and Rybicki, A.C. (1990). Molecular Molecular cloning of human protein 4.2: a major component of the erythrocyte membrane. *Proc. Natl. Acad. Sc. USA.* **87,** 955-959

Szondy, Z., Sarang, Z., Molnar, P., Nemeth, T., Piacentini, M., Mastroberardino, P.G., Falasca, L., Aeschlimann, D., Kovacs, J., Kiss, I., Szegezdi, E., Lakos, G., Rajnavolgyi, E., Birckbichler, P.J., Melino, G., and Fesus, L. (2003). Transglutaminase 2-/- mice reveal a phagocytosis-associated crosstalk between macrophages and apoptotic cells. *Proc. Natl. Acad. Sci. U S A.*, **100,** 7812-7817

Ta, B.M., Gallagher, G.T., Chakravarty, R., and Rice, R.H. (1990). Keratinocyte transglutaminase in human skin and oral mucosa: cytoplasmic localization and uncoupling of differentiation markers. *J. Cell Sci.*, **95,** 631-8

Taipale, J., Miyazono, K., Heldin, C.H., and Keski-Oja, J. (1994). Latent transforming growth factor-beta 1 associates to fibroblast extracellular matrix via latent TGF-beta binding protein. *J. Cell Biol.*, **124,** 171-181

Takagi, T., and Doolittle, R.F. (1974). Amino acid sequence studies on factor XIII and the peptide released during its activation by thrombin. *Biochemistry,* **13**, 750-756

Takahashi, H., Isobe, T., Horibe, S., Takagi, J., Yokosaki, Y., Sheppard, D., and Saito, Y. (2000). Tissue transglutaminase, coagulation factor XIII, and the pro-polypeptide of von Willebrand factor are all ligands for the integrins alpha 9beta 1 and alpha 4beta 1. *J. Biol. Chem.* **275,** 23589-23595

Takahashi, R., Takahashi, Y., and Putnam, F.W. (1986). Primary structure of blood coagulation factor XIIIa (fibrinoligase, transglutaminase) from human placenta. *Proc. Nat. Acad. Sci.*, **83**, 8019-8023

Takaku, K., Futamura, M., Saitoh, S., and Takeuchi, Y. (1995). Tissue-type transglutaminase is not a tumor-related marker. *J. Biochem. (Tokyo),* **118,** 1268-1270

Tamaki, T., and Aoki, N. (1981). Cross-linking of alpha 2-plasmin inhibitor and fibronectin to fibrin by fibrin-stabilizing factor. *Biochem. Biophys. Acta.*, **661.** 280-286

Tang, D.G., Tarrien, M., Dobrzynski, P., and Honn, K.V. (1995). Melanoma cell spreading on fibronectin induced by 12(S)-HETE involves both protein kinase C- and protein tyrosine kinase-dependent focal adhesion formation and tyrosine phosphorylation of focal adhesion kinase (pp125FAK). *J. Cell Physiol.*,**165,** 291-306

Thacher, S.M., and Rice, R.H. (1985). Keratinocyte-specific transglutaminase of cultured human epidermal-cells - relation to cross-linked envelope formation and terminal differentiation. *Cell,* **40**, 685-695

Thomazy, V., and Fesus, L. (1989). Differential expression of tissue transglutaminase in human cells. An immuno-histochemical study. *Cell Tissue Res.*, **255**, 215-221

Tournier, C., Hess, P., Yang, D.D., Xu, J., Turner, T.K., Nimnual, A., Bar-Sagi, D., Jones, S.N., Flavell, R.A., Davis, R.J. (2000). Requirement of JNK for stress-induced activation of the cytochrome c-mediated death pathway. *Science,* **288,** 870-874

Towbin R., Dumbar J.S. and Bove K. (1979). Antrochoanal polyps. *AJR Am. J. Roentgenol.*, **132**, 27-31

Trask, B.C., Broekelmann, T., Ritty, T.M., Trask, T.M., Tisdale, C., and Mecham, R.P. (2001). Posttranslational modifications of microfibril associated glycoprotein-1 (MAGP-1). *Biochemistry,* **40,** 4372-4380

Trier, J.S. (1991). Celiac sprue. *N. Engl. J. Med.*, **325,** 1709-1719

Tsuchida, M., Manthei, E.R., Alam, T., Knechtle, S.J., and Hamawy, M.M. (2000). Regulation of T cell receptor- and CD28-induced tyrosine phosphorylation of the focal adhesion tyrosine kinases Pyk2 and Fak by protein kinase C. A role for protein tyrosine phosphatases. *J. Biol. Chem.*, **275,** 1344-1350

Tumova, S., Woods, A., and Couchman, J.R. (2000).Heparan sulfate proteoglycans on the cell surface: versatile coordinators of cellular functions. *Int. J. Biochem. Cell Biol.*, **32,** 269-288

Turner, P.M., and Lorand, L. (1989). Complexation of fibronectin with tissue transglutaminase. *Biochemistry,* **28,** 628-635

Tyrrell, D.J., Sale, W.S. and Slife, C.W. (1988a). Fibronectin is a component of the sodium dodecyl sulfate-insoluble transglutaminase substrate. *J. Biol. Chem.,* **263,** 8464-8469

Tyrrell, D.J., Sale, W.S. and Slife, C.W. (1988b). Isolation of a sodium dodecyl sulfate-insoluble transglutaminase substrate from liver plasma membranes. *J. Biol. Chem.,* **263,** 1946-1951

Tyrrell, D.J., Sale, W.S., and Slife, C.W. (1986). Localization of a liver transglutaminase and a large molecular weight transglutaminase substrate to a distinct plasma membrane domain. *J. Biol. Chem.,* **261**,14833-14836

Tyrrell, D.J., Sale, W.S., and Slife, C.W. (1988). Isolation of a sodium dodecyl sulfate-insoluble transglutaminase substrate from liver plasma membranes. *J. Biol. Chem.,* **263,** 1946-1951

Upchurch, H.F., Conway, E., Patterson, M.K. Jr., Birckbichler, P.J., and Maxwell MD. (1987). Cellular transglutaminase has affinity for extracellular matrix. *In Vitro Cell Dev. Biol.,* **23,** 795-800

Upchurch, H.F., Conway, E., Patterson, M.K.Jr. and Maxwell, M.D. (1991). Localization of cellular transglutaminase on the extracellular matrix after wounding: characteristics of the matrix bound enzyme. *J. Cell. Phys.,* **149,** 375-383

van de Wal, Y., Kooy, Y., van Veelen, P., Pena, S., Mearin, L., Papadopoulos, G., and Koning, F. (1998). Selective deamidation by tissue transglutaminase strongly enhances gliadin-specific T cell reactivity. *J. Immunol.,* **161,** 1585-1588

van de Water, B., Nagelkerke, J.F., and Stevens, J.L. (1999). Dephosphorylation of focal adhesion kinase (FAK) and loss of focal contacts precede caspase-mediated cleavage of FAK during apoptosis in renal epithelial cells. *J. Biol. Chem.,* **274,** 13328-13337

Verderio, E., Gaudry, C., Gross, S., Smith, C., Downes, S., and Griffin, M. (1999). Regulation of cell surface tissue transglutaminase: effects on matrix storage of latent transforming growth factor-beta binding protein-1. *J. Histochem. Cytochem.,* **47,** 1417-1432

Verderio, E., Nicholas, B., Gross, S. and Griffin, M. (1998). Regulated expression of tissue transgiutaminase in Swiss 3T3 fibroblasts: effects on the processing of fibronectin, cell attachement and cell death. *Exp. Cell Res.,* **239,** 119-138

Verderio, E., Okoye, A., and Griffin M (2000). Inhibition of integrin mediated cell adhesion to fibronectin is bypassed by extracellular tissue transglutaminase. *6th International conference on transglutaminase and protein crosslinking.*

Verderio, E., Telci, D., Okoye, A., Baccarini, M, and Griffin, M. (2002). A tissue transglutaminase FN complex supports a novel RGD independent cell adhesion. *The BSCB Annual Spring Meeting on Cell Regulation through Molecular Machines*

Vezza, R., Habib, A., and FitzGerald, GA. Differential signaling by the thromboxane receptor isoforms via the novel GTP-binding protein, Gh. *J. Biol. Chem.*, **274,** 12774-12779

Vitale, M., Di Matola, T., Fenzi, G., Illario, M., and Rossi, G. (1998). Fibronectin is required to prevent thyroid cell apoptosis through an integrin-mediated adhesion mechanism. *J. Clin. Endocrinol. Metab.*, **83,** 3673-3680

Wang, R.N., and Rosenberg, L. (1999). Maintenance of beta-cell function and survival following islet isolation requires re-establishment of the islet-matrix relationship. *J. Endocrinol.*, **163,** 181-190

Wary, K.K., Mainiero, F., Isakoff, S.J., Marcantonio, E.E., and Giancotti, F.G. (1996). The adaptor protein Shc couples a class of integrins to the control of cell cycle progression. *Cell*, **87,** 733-743

Wary, K.K., Mariotti, A., Zurzolo, C., and Giancotti, F.G. (1998). A requirement for caveolin-1 and associated kinase Fyn in integrin signaling and anchorage-dependent cell growth. *Cell*, **94,** 625-634

Wayner, E.A., Garcia-Pardo, A., Humphries, M.J., McDonald, J.A., and Carter, W.G. (1989). Identification and characterization of the T lymphocyte adhesion receptor for an alternative cell attachment domain (CS-1) in plasma fibronectin. *J. Cell Biol.*, **109,** 1321-1330

Weisberg, L.J., Shiu, D.T., Conkling, P.R., and Shuman, M.A. (1987). Identification of normal human peripheral blood monocytes and liver as sites of synthesis of coagulation factor XIII a-chain. *Blood,*, **70,** 579-582

Weiss, M.S., Metzner, H.J. and Hilgenfeld, R. (1998). Two non-proline cis peptide bonds may be important for factor XIII function. *FEBS Lett.*, **423,** 291-266

Weraarchakul-Boonmark, N., Jeong, J.M., Murthy, S.N., Engel, J.D., and Lorand, L. (1992). Cloning and expression of chicken erythrocyte transglutaminase. *Proc. Natl. Acad. Sci. USA*, **89,** 9804-9808

Widmann, C., Gibson, S., and Johnson, G.L. (1998). Caspase-dependent cleavage of signaling proteins during apoptosis. A turn-off mechanism for anti-apoptotic signals. *J. Biol. Chem.*, **273,** 7141-7147

Widmann, C., Gibson, S., Jarpe, M.B., and Johnson, G.L. (1999). Mitogen-activated protein kinase: conservation of a three-kinase module from yeast to human. *Physiol. Rev.*, **79,** 143-180

Wilcox-Adelman SA, Denhez F, Goetinck PF. (2002). Syndecan-4 modulates focal adhesion kinase phosphorylation. *J. Biol. Chem.*, **277,** 32970-32977

Williams-Ashman, H.G. (1984). Transglutaminase and the clotting of mammalian seminal fluids. *Mol. Cell. Biochem.*, **58**, 51-61

Wilson, E.M., and French, F.S. (1980). Biochemical homology between rat dorsal prostate and coagulating gland. Purification of a major androgen-induced protein. J. *Biol. Chem.*, **255,** 10946-10953

Woods, A. (2001). Syndecans: transmembrane modulators of adhesion and matrix assembly. *J. Clin. Invest.*, **107,** 935-941

Woods, A., and Couchman, J.R. (1994). Syndecan 4 heparan sulfate proteoglycan is a selectively enriched and widespread focal adhesion component. *Mol. Biol. Cell,* **5,** 183-192

Woods, A., and Couchman, J.R. (1998). Syndecans: synergistic activators of cell adhesion. *Trends Cell Biol.*, **8,** 189-192

Woods, A., and Couchman, J.R. (2000). Integrin modulation by lateral association. *J. Biol. Chem.*, **275,** 24233-24236

Woods, A., Couchman, J.R. (1994). Syndecan 4 heparan sulfate proteoglycan is a selectively enriched and widespread focal adhesion component. *Mol. Biol. Cell.*, **5,** 183-192

Woods, A., Couchman, J.R., Johansson, S., and Hook, M. (1986). Adhesion and cytoskeletal organisation of fibroblasts in response to fibronectin fragments. *EMBO J.*, **5,** 665-670

Woods, A., Longley, R.L., Tumova, S., and Couchman, J.R. (2000). Syndecan-4 binding to the high affinity heparin-binding domain of fibronectin drives focal adhesion formation in fibroblasts. *Arch. Biochem. Biophys.*, **374,** 66-72

Xia, Z., Dickens, M., Raingeaud, J., Davis, R.J., and Greenberg, M.E. (1995). Opposing effects of ERK and JNK-p38 MAP kinases on apoptosis. *Science,* **270,** 1326-1331

Xu, L.H., Owens, L.V., Sturge, G.C., Yang, X., Liu, E.T., Craven, R.J., and Cance, W.G. (1996). Attenuation of the expression of the focal adhesion kinase induces apoptosis in tumor cells. *Cell Growth Differ.*, **7,** 413-418

Yaffe, M.B., Beegen, H., and Eckert, R.L. (1992). Biophysical characterization of involucrin reveals a molecule ideally suited to function as an intermolecular cross-bridge of the keratinocyte cornified envelope. *J. Biol. Chem.*, **267,** 12233-12238

Yang, J.T., Rayburn, H., and Hynes, R.O. (1993). Embryonic mesodermal defects in alpha 5 integrin-deficient mice. *Development*, **119,** 1093-1105

Yee, V.C., Pedersen, L.C., Bishop, P.D., Stenkamp, R.E., and Teller, D.C. (1995). Structural evidence that the activation peptide is not released upon thrombin cleavage of factor XIII. *Thromb. Res.*, **78,** 389-397

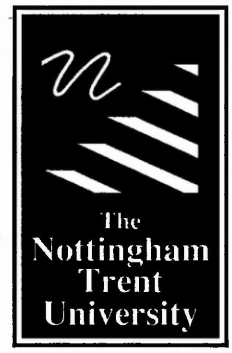
Zamir, E., and Geiger, B. (2001). Molecular complexity and dynamics of cell-matrix adhesions. *J. Cell Sci.*, **114,** 3583-9350

Zatloukal, K., Fesus, L., Denk, H., Tarcsa, E., Spurej, G., and Bock, G. (1992). High amount of epsilon-(gamma-glutamyl)lysine cross-links in Mallory bodies. *Lab. Invest.*, **66,** 774-777

Zhang, Z., Vezza, R., Plappert, T., McNamara, P., Lawson, J.A., Austin, S., Pratico, D., Sutton, M.S., and FitzGerald, G.A. (2003). COX-2-dependent cardiac failure in Gh/tTG transgenic mice. *Circ. Res.*, **92,** 1153-1161

Zhu, H.J, and Burgess, A.W. (2001). Regulation of transforming growth factor-beta signaling. *Mol .Cell Biol. Res. Commun.*, **4,** 321-330

Zimmermann, P., and David, G. (1999). The syndecans, tuners of transmembrane signaling. *FASEB J.*, **13,** S91-S100



Libraries &
Learning
Resources

The Boots Library: 0115 848 6343
Clifton Campus Library: 0115 848 6612
Brackenhurst Library: 01636 817049